# 5 Overconstrained *T3*-type TPMs with uncoupled motions

*T3*-type translational parallel robots with *uncoupled motions* with various degrees of overconstraint may be obtained by using three simple or complex limbs. In these solutions, each operational velocity given by Eq. (1.19) depends, in the general case, on just one actuated joint velocity: $v_i = v_i(\dot{q}_i)$, $i = 1,2,3$. The Jacobian matrix in Eq. (1.19) is a diagonal matrix.

They can be actuated by linear or rotating actuators which can be mounted on the fixed base or on a moving link. In the solutions presented in this section, the actuators are associated with a revolute joint mounted on the fixed base.

Equation (1.16) indicates that *overconstrained* solutions of *T3* translational parallel robots with coupled motions and $q$ independent loops meet the condition $\sum_1^p f_i < 3 + 6q$. Various solutions fulfil this condition along with $S_F = 3$, $(R_F) = (\boldsymbol{v}_1, \boldsymbol{v}_2, \boldsymbol{v}_3)$ and $N_F \geq 1$.

They may have identical limbs or limbs with different structures. We limit our presentation in this section to the solutions with just three identical limbs. A large set of solutions with an additional unactuated limb can also be obtained by combining an unactuated limb presented in Figs. 7.1–7.11 – Part 1 with three other limbs with $4 \leq M_{Gi} = S_{Gi} \leq 6$ that integrate velocities $\boldsymbol{v}_1$, $\boldsymbol{v}_2$ and $\boldsymbol{v}_3$ in the basis of their operational space and fulfil the uncoupled motions condition.

## 5.1 Basic solutions with rotating actuators

In the *basic* solutions of overconstrained TPMs with *rotating actuators* and uncoupled motions $F \leftarrow G_1\text{–}G_2\text{–}G_3$, the moving platform $n \equiv n_{Gi}$ ($i = 1, 2, 3$) is connected to the reference platform $1 \equiv 1_{Gi} \equiv 0$ by three limbs with three, four or five degrees of connectivity. No idle mobilities exist in these basic solutions.



G. Gogu, *Structural Synthesis of Parallel Robots: Part 2: Translational Topologies with Two and Three Degrees of Freedom,* Solid Mechanics and Its Applications 159, 471–614.

The various types of limbs with three degrees of connectivity are systematized in Fig. 5.1. They combine one (Fig. 5.1a, b), two (Fig. 5.1c–f) or three (Fig. 5.1g) *Pa*-type parallelogram loops. Other parallelogram loops of types $Pa^t$ (Fig. 5.1h), $Pa^{tcc}$ (Fig. 5.1i) or $Pa^{cc}$ (Fig. 5.1j, k) may also be combined in these limbs. We recall that the parallelogram loop $Pa^{cc}$-type has two degrees of mobility, $Pa^t$-type has three degrees of mobility and $Pa^{tcc}$-type has four degrees of mobility.

The various types of limbs with four degrees of connectivity are systematized in Figs. 5.2–5.4. They are simple (Fig. 5.2) or complex (Figs. 5.3 and 5.4) kinematic chains. The following types of closed loops are integrated in the complex limbs: one (Figs. 5.3a–f and 5.4a–d) or two (Figs. 5.3g, h and 5.4e, f) *Pa*-type parallelogram loops, one (Fig. 5.3i) or two (Fig. 5.3j) *Rb*-type rhombus loops, one $Pa^{cc}$-type parallelogram loop (Fig. 5.3o) or various other types of *Pn2* or *Pn3* planar loops with two (Fig. 5.3k, l) or three degrees of mobility (Fig. 5.3m, n). The planar loops with two degrees of freedom *Pn2*-type illustrated in Fig. 5.3k, l are of types $R||R||R||R||R$ and $R \perp P \perp^{||} R \perp P \perp^{||} R$. The planar loops with three degrees of freedom *Pn3*-type illustrated in Fig. 5.3m, n are of types $R||R||R||R||R||R$ and $R \perp P \perp^{||} R||R \perp P \perp^{||} R$. Other planar loops of types *Pn2* and *Pn3* can also be used (see Table 5.1).

The various types of limbs with five degrees of connectivity are systematized in Fig. 5.5. They are complex limbs which combine one (Fig. 5.5a) or two (Fig. 5.5b) *Rb*-type rhombus loops, one *Pn2* (Fig. 5.5c, d) or *Pn3*-type (Fig. 5.5e, f) planar loop or one *Pa*-type parallelogram loop (Fig. 5.5g–i). Any planar loops of types *Pn2* and *Pn3* presented in Table 5.1 can be used.

Various solutions of translational parallel robots with uncoupled motions and no idle mobilities can be obtained by using three limbs with identical or different topologies presented in Figs. 5.1–5.5. We only show solutions with identical limb type as illustrated in Figs. 5.6–5.48. The limb topology and connecting conditions in these solutions are systematized in Tables 5.2–5.5 and their structural parameters in Tables 5.6–5.12.

The directions of the three actuated revolute joints adjacent to the fixed base can be reciprocally orthogonal or parallel to two coplanar and perpendicular directions.

Basic solutions of *T3*-type TPMs with decoupled motions and different limb topologies can be obtained by using two limbs from Figs. 5.1–5.5 and one limb from Figs. 3.1–3.5, Figs. 3.60–3.70 and Figs. 4.1, 4.2 or 4.29.

Basic solutions of *T3*-type TPMs with coupled motions and different limb topologies can be obtained by using one limb from Figs. 5.1–5.5 and two limbs from Figs. 3.1–3.5, Figs. 3.60–3.70 and Figs. 4.1, 4.2 or 4.29.

**Table 5.1.** Topology of the planar loops with two and three degrees of mobility that can be used in the limbs of TPM with uncoupled motions

| No. | *Pn2*-type loops with two degrees of freedom | *Pn3*-type loops with three degrees of freedom |
|---|---|---|
| 1 | $R\|\|R\|\|R\|\|R\|\|R$ | $R\|\|R\|\|R\|\|R\|\|R\|\|R$ |
| 2 | $P\perp R\|\|R\|\|R\|\|R$ | $P\perp R\|\|R\|\|R\|\|R\|\|R$ |
| 3 | $R\perp P\perp^{\|\|}R\|\|R\|\|R$ | $R\perp P\perp^{\|\|}R\|\|R\|\|R\|\|R$ |
| 4 | $R\|\|R\perp P\perp^{\|\|}R\|\|R$ | $R\|\|R\perp P\perp^{\|\|}R\|\|R\|\|R$ |
| 5 | $P\perp P\perp^{\perp}R\|\|R\|\|R$ | $P\perp P\perp^{\perp}R\|\|R\|\|R\|\|R$ |
| 6 | $R\perp P\perp^{\perp}P\perp^{\perp}R\|\|R$ | $R\perp P\perp^{\perp}P\perp^{\perp}R\|\|R\|\|R$ |
| 7 | $P\perp R\perp^{\perp}P\perp R\|\|R$ | $P\perp R\perp^{\perp}P\perp^{\|\|}R\|\|R\|\|R$ |
| 8 | $R\perp P\perp^{\|\|}R\perp P\perp^{\|\|}R$ | $R\perp P\perp^{\|\|}R\perp P\perp^{\|\|}R\|\|R$ |
| 9 | $P\perp R\|\|R\perp P\perp^{\|\|}R$ | $P\perp R\|\|R\perp P\perp^{\|\|}R\|\|R$ |
| 10 | $P\perp R\|\|R\|\|R\perp P$ | $P\perp R\|\|R\|\|R\perp P\perp^{\|\|}R$ |
| 11 | $P\perp P\perp^{\perp}R\|\|R\perp P$ | $R\|\|R\perp P\perp^{\perp}P\perp^{\perp}R\|\|R$ |
| 12 | | $P\perp R\|\|R\|\|R\|\|R\perp P$ |
| 13 | | $R\perp P\perp^{\|\|}R\|\|R\perp P\perp^{\|\|}R$ |
| 14 | | $P\perp P\perp^{\perp}R\|\|R\|\|R\perp P$ |

**Table 5.2.** Limb topology and connecting conditions of the overconstrained TPM with uncoupled motions and no idle mobilities presented in Figs. 5.6–5.15

| No. | TPM type | Limb topology | Connecting conditions |
|---|---|---|---|
| 1 | 3-$\underline{Pa}PP$ (Fig. 5.6a) | $\underline{Pa}\|\|P\perp^{\perp}P$ (Fig. 5.1a) | The rotation axes of the actuated revolute joints are reciprocally orthogonal |
| 2 | 3-$\underline{Pa}PP$ (Fig. 5.6b) | $\underline{Pa}\|\|P\perp^{\perp}P$ (Fig. 5.1a) | The rotation axes of the actuated revolute joints are parallel to two orthogonal directions |
| 3 | 3-$\underline{Pa}PP$ (Fig. 5.7a) | $\underline{Pa}\perp P\perp^{\|\|}P$ (Fig. 5.1b) | Idem No. 1 |
| 4 | 3-$\underline{Pa}PP$ (Fig. 5.7b) | $\underline{Pa}\perp P\perp^{\|\|}P$ (Fig. 5.1b) | Idem No. 2 |
| 5 | 3-$\underline{Pa}PaP$ (Fig. 5.8a) | $\underline{Pa}\perp Pa\perp^{\|\|}P$ (Fig. 5.1c) | Idem No. 1 |
| 6 | 3-$\underline{Pa}PaP$ (Fig. 5.8b) | $\underline{Pa}\perp Pa\perp^{\|\|}P$ (Fig. 5.1c) | Idem No. 2 |
| 7 | 3-$\underline{Pa}PaP$ (Fig. 5.9a) | $\underline{Pa}\perp Pa\perp^{\perp}P$ (Fig. 5.1d) | Idem No. 1 |
| 8 | 3-$\underline{Pa}PaP$ (Fig. 5.9b) | $\underline{Pa}\perp Pa\perp^{\perp}P$ (Fig. 5.1d) | Idem No. 2 |
| 9 | 3-$\underline{Pa}PPa$ (Fig. 5.10a) | $\underline{Pa}\|\|P\perp Pa$ (Fig. 5.1e) | Idem No. 1 |
| 10 | 3-$\underline{Pa}PPa$ (Fig. 5.10b) | $\underline{Pa}\|\|P\perp Pa$ (Fig. 5.1e) | Idem No. 2 |
| 11 | 3-$\underline{Pa}PPa$ (Fig. 5.11a) | $\underline{Pa}\perp P\perp^{\perp}Pa$ (Fig. 5.1f) | Idem No. 1 |
| 12 | 3-$\underline{Pa}PPa$ (Fig. 5.11b) | $\underline{Pa}\perp P\perp^{\perp}Pa$ (Fig. 5.1f) | Idem No. 2 |
| 13 | 3-$\underline{Pa}PaPa$ (Fig. 5.12) | $\underline{Pa}\perp Pa\|\|Pa$ (Fig. 5.1g) | Idem No. 1 |
| 14 | 3-$\underline{Pa}PaPa$ (Fig. 5.13) | $\underline{Pa}\perp Pa\|\|Pa$ (Fig. 5.1g) | Idem No. 2 |
| 15 | 3-$\underline{Pa}Pa^{t}P$ (Fig. 5.14a) | $\underline{Pa}\|\|Pa^{t}\|\|P$ (Fig. 5.1h) | Idem No. 1 |
| 16 | 3-$\underline{Pa}Pa^{t}P$ (Fig. 5.14b) | $\underline{Pa}\|\|Pa^{t}\|\|P$ (Fig. 5.1h) | Idem No. 2 |
| 17 | 3-$\underline{Pa}Pa^{tcc}$ (Fig. 5.15a) | $\underline{Pa}\|\|Pa^{tcc}$ (Fig. 5.1i) | Idem No. 1 |
| 18 | 3-$\underline{Pa}Pa^{tcc}$ (Fig. 5.15b) | $\underline{Pa}\|\|Pa^{tcc}$ (Fig. 5.1i) | Idem No. 2 |

**Table 5.3.** Limb topology and connecting conditions of the overconstrained TPM with uncoupled motions and no idle mobilities presented in Figs. 5.16–5.24

| No. | TPM type | Limb topology | Connecting conditions |
|---|---|---|---|
| 1 | $3\text{-}\underline{Pa}^{cc}P$ (Fig. 5.16a) | $\underline{Pa}^{cc} \perp P$ (Fig. 5.1j) | The rotation axes of the actuated revolute joints are reciprocally orthogonal |
| 2 | $3\text{-}\underline{Pa}^{cc}P$ (Fig. 5.16b) | $\underline{Pa}^{cc} \perp P$ (Fig. 5.1j) | The rotation axes of the actuated revolute joints are parallel to two orthogonal coplanar directions |
| 3 | $3\text{-}\underline{Pa}^{cc}Pa$ (Fig. 5.17a) | $\underline{Pa}^{cc} \perp Pa$ (Fig. 5.1k) | Idem No. 1 |
| 4 | $3\text{-}\underline{Pa}^{cc}Pa$ (Fig. 5.17b) | $\underline{Pa}^{cc} \perp Pa$ (Fig. 5.1k) | Idem No. 2 |
| 5 | $3\text{-}\underline{R}RPP$ (Fig. 5.18a) | $\underline{R} \parallel R \perp P \perp^{\parallel} P$ (Fig. 5.2a) | Idem No. 1 |
| 6 | $3\text{-}\underline{R}RPP$ (Fig. 5.18b) | $\underline{R} \parallel R \perp P \perp^{\parallel} P$ (Fig. 5.2a) | Idem No. 2 |
| 7 | $3\text{-}\underline{R}CP$ (Fig. 5.19a) | $\underline{R} \parallel C \perp P$ (Fig. 5.2c) | Idem No. 1 |
| 8 | $3\text{-}\underline{R}CP$ (Fig. 5.19b) | $\underline{R} \parallel C \perp P$ (Fig. 5.2c) | Idem No. 2 |
| 9 | $3\text{-}\underline{Pa}RRP$ (Fig. 5.20a) | $\underline{Pa} \perp R \parallel R \perp^{\parallel} P$ (Fig. 5.3a) | Idem No. 1 |
| 10 | $3\text{-}\underline{Pa}RRP$ (Fig. 5.20b) | $\underline{Pa} \perp R \parallel R \perp^{\parallel} P$ (Fig. 5.3a) | Idem No. 2 |
| 11 | $3\text{-}\underline{Pa}RRP$ (Fig. 5.21a) | $\underline{Pa} \perp R \parallel R \perp^{\perp} P$ (Fig. 5.3b) | Idem No. 1 |
| 12 | $3\text{-}\underline{Pa}RRP$ (Fig. 5.21b) | $\underline{Pa} \perp R \parallel R \perp^{\perp} P$ (Fig. 5.3b) | Idem No. 2 |
| 13 | $3\text{-}\underline{Pa}RPR$ (Fig. 5.22a) | $\underline{Pa} \perp R \perp P \perp^{\parallel} R$ (Fig. 5.3c) | Idem No. 1 |
| 14 | $3\text{-}\underline{Pa}RPR$ (Fig. 5.22b) | $\underline{Pa} \perp R \perp P \perp^{\parallel} R$ (Fig. 5.3c) | Idem No. 2 |
| 15 | $3\text{-}\underline{Pa}RRR$ (Fig. 5.23a) | $\underline{Pa} \perp R \parallel R \parallel R$ (Fig. 5.3d) | Idem No. 1 |
| 16 | $3\text{-}\underline{Pa}RRR$ (Fig. 5.23b) | $\underline{Pa} \perp R \parallel R \parallel R$ (Fig. 5.3d) | Idem No. 2 |
| 17 | $3\text{-}\underline{Pa}PRR$ (Fig. 5.24a) | $\underline{Pa} \parallel P \perp R \parallel R$ (Fig. 5.3e) | Idem No. 1 |
| 18 | $3\text{-}\underline{Pa}PRR$ (Fig. 5.24b) | $\underline{Pa} \parallel P \perp R \parallel R$ (Fig. 5.3e) | Idem No. 2 |

**Table 5.4.** Limb topology and connecting conditions of the overconstrained TPM with uncoupled motions and no idle mobilities presented in Figs. 5.25–5.37

| No. | TPM type | Limb topology | Connecting conditions |
|---|---|---|---|
| 1 | $3\text{-}\underline{Pa}PRR$ (Fig. 5.25a) | $\underline{Pa} \perp P \perp^{\perp} R \| R$ (Fig. 5.3f) | The rotation axes of the actuated revolute joints are reciprocally orthogonal |
| 2 | $3\text{-}\underline{Pa}PRR$ (Fig. 5.25b) | $\underline{Pa} \perp P \perp^{\perp} R \| R$ (Fig. 5.3f) | The rotation axes of the actuated revolute joints are parallel to two orthogonal coplanar directions |
| 3 | $3\text{-}\underline{Pa}PaRR$ (Fig. 5.26a) | $\underline{Pa} \perp Pa \| R \| R$ (Fig. 5.3g) | Idem No. 1 |
| 4 | $3\text{-}\underline{Pa}PaRR$ (Fig. 5.26b) | $\underline{Pa} \perp Pa \| R \| R$ (Fig. 5.3g) | Idem No. 2 |
| 5 | $3\text{-}\underline{Pa}RRPa$ (Fig. 5.27a) | $\underline{Pa} \perp R \| R \| Pa$ (Fig. 5.3h) | Idem No. 1 |
| 6 | $3\text{-}\underline{Pa}RRPa$ (Fig. 5.27b) | $\underline{Pa} \perp R \| R \| Pa$ (Fig. 5.3h) | Idem No. 2 |
| 7 | $3\text{-}\underline{Pa}RRbR$ (Fig. 5.28) | $\underline{Pa} \perp R \| Rb \| R$ (Fig. 5.3i) | Idem No. 2 |
| 8 | $3\text{-}\underline{Pa}RRbRbR$ (Fig. 5.29) | $\underline{Pa} \perp R \| Rb \| Rb \| R$ (Fig. 5.3j) | Idem No. 2 |
| 9 | $3\text{-}\underline{Pa}Pn2R$ (Figs. 5.30, 5.31) | $\underline{Pa} \perp Pn2 \| R$ (Fig. 5.3k, l) | Idem No. 2 |
| 10 | $3\text{-}\underline{Pa}Pn3$ (Figs. 5.32, 5.33) | $\underline{Pa} \perp Pn3$ (Fig. 5.3m, n) | Idem No. 2 |
| 11 | $3\text{-}\underline{Pa^{cc}}RR$ (Fig. 5.34a) | $\underline{Pa^{cc}} \perp R \| R$ (Fig. 5.3o) | Idem No. 1 |
| 12 | $3\text{-}\underline{Pa^{cc}}RR$ (Fig. 5.34b) | $\underline{Pa^{cc}} \perp R \| R$ (Fig. 5.3o) | Idem No. 2 |
| 13 | $3\text{-}\underline{R}RPaP$ (Fig. 5.35a) | $\underline{R} \| R \perp Pa \perp^{\perp} P$ (Fig. 5.4a) | Idem No. 1 |
| 14 | $3\text{-}\underline{R}RPaP$ (Fig. 5.35b) | $\underline{R} \| R \perp Pa \perp^{\perp} P$ (Fig. 5.4a) | Idem No. 2 |
| 15 | $3\text{-}\underline{R}RPaP$ (Fig. 5.36a) | $\underline{R} \| R \perp Pa \perp^{\|} P$ (Fig. 5.4b) | Idem No. 1 |
| 16 | $3\text{-}\underline{R}RPaP$ (Fig. 5.36b) | $\underline{R} \| R \perp Pa \perp^{\|} P$ (Fig. 5.4b) | Idem No. 2 |
| 17 | $3\text{-}\underline{R}CPa$ (Fig. 5.37a) | $\underline{R} \| C \perp Pa$ (Fig. 5.4c) | Idem No. 1 |
| 18 | $3\text{-}\underline{R}CPa$ (Fig. 5.37b) | $\underline{R} \| C \perp Pa$ (Fig. 5.4c) | Idem No. 2 |

**Table 5.5.** Limb topology and connecting conditions of the overconstrained TPM with uncoupled motions and no idle mobilities presented in Figs. 5.38–5.48

| No. | TPM type | Limb topology | Connecting conditions |
|---|---|---|---|
| 1 | $3\text{-}\underline{R}RPPa$ (Fig. 5.38a) | $\underline{R}\|\|R\perp P\perp^{\perp} Pa$ (Fig. 5.4d) | The rotation axes of the actuated revolute joints are reciprocally orthogonal |
| 2 | $3\text{-}\underline{R}RPPa$ (Fig. 5.38b) | $\underline{R}\|\|R\perp P\perp^{\perp} Pa$ (Fig. 5.4d) | The rotation axes of the actuated revolute joints are parallel to two orthogonal coplanar directions |
| 3 | $3\text{-}\underline{R}RPaPa$ (Fig. 5.39a) | $\underline{R}\|\|R\perp Pa\|\|Pa$ (Fig. 5.4e) | Idem No. 1 |
| 4 | $3\text{-}\underline{R}RPaPa$ (Fig. 5.39b) | $\underline{R}\|\|R\perp Pa\|\|Pa$ (Fig. 5.4e) | Idem No. 2 |
| 5 | $3\text{-}\underline{R}RPaPa$ (Fig. 5.40a) | $\underline{R}\|\|R\perp Pa\|\|Pa$ (Fig. 5.4f) | Idem No. 1 |
| 6 | $3\text{-}\underline{R}RPaPa$ (Fig. 5.40a) | $\underline{R}\|\|R\perp Pa\|\|Pa$ (Fig. 5.4f) | Idem No. 2 |
| 7 | $3\text{-}\underline{R}RRRbR$ (Fig. 5.41) | $\underline{R}\|\|R\perp R\|\|Rb\|\|R$ (Fig. 5.5a) | Idem No. 1 |
| 8 | $3\text{-}\underline{R}RRRbRbR$ (Fig. 5.42) | $\underline{R}\|\|R\perp R\|\|Rb\|\|Rb\|\|R$ (Fig. 5.5b) | Idem No. 1 |
| 9 | $3\text{-}\underline{R}RPn2R$ (Figs. 5.43, 5.44) | $\underline{R}\|\|R\perp Pn2\|\|R$ (Fig. 5.5c, d) | Idem No. 1 |
| 10 | $3\text{-}\underline{R}RPn3$ (Figs. 5.45, 5.46) | $\underline{R}\|\|R\perp Pn3$ (Fig. 5.5e, f) | Idem No. 1 |
| 11 | $3\text{-}\underline{R}RRRPa$ (Fig. 5.47a) | $\underline{R}\|\|R\perp R\|\|R\|\|Pa$ (Fig. 5.5g) | Idem No. 1 |
| 13 | $3\text{-}\underline{R}RPaRR$ (Fig. 5.48a) | $\underline{R}\|\|R\perp Pa\|\|R\|\|R$ (Fig. 5.5h) | Idem No. 1 |
| 13 | $3\text{-}\underline{R}RPaRR$ (Fig. 5.48b) | $\underline{R}\|\|R\perp Pa\|\|R\|\|R$ (Fig. 5.5i) | Idem No. 2 |

**Table 5.6.** Bases of the operational velocities spaces of the limbs isolated from the parallel mechanisms presented in Figs. 5.6–5.48

| No. | Parallel mechanism | Basis ($R_{G1}$) | ($R_{G2}$) | ($R_{G3}$) |
|---|---|---|---|---|
| 1 | Figs. 5.6–5.17 | $(\boldsymbol{v}_1, \boldsymbol{v}_2, \boldsymbol{v}_3)$ | $(\boldsymbol{v}_1, \boldsymbol{v}_2, \boldsymbol{v}_3)$ | $(\boldsymbol{v}_1, \boldsymbol{v}_2, \boldsymbol{v}_3)$ |
| 2 | Figs. 5.18a, 5.36a, 5.37a, 5.38a, 5.39a, | $(\boldsymbol{v}_1, \boldsymbol{v}_2, \boldsymbol{v}_3, \boldsymbol{\omega}_\delta)$ | $(\boldsymbol{v}_1, \boldsymbol{v}_2, \boldsymbol{v}_3, \boldsymbol{\omega}_\alpha)$ | $(\boldsymbol{v}_1, \boldsymbol{v}_2, \boldsymbol{v}_3, \boldsymbol{\omega}_\beta)$ |
| 3 | Figs. 5.18b, 5.36b, 5.37b, 5.38b, 5.39b, | $(\boldsymbol{v}_1, \boldsymbol{v}_2, \boldsymbol{v}_3, \boldsymbol{\omega}_\delta)$ | $(\boldsymbol{v}_1, \boldsymbol{v}_2, \boldsymbol{v}_3, \boldsymbol{\omega}_\delta)$ | $(\boldsymbol{v}_1, \boldsymbol{v}_2, \boldsymbol{v}_3, \boldsymbol{\omega}_\beta)$ |
| 4 | Figs. 5.19a, 5.35a, 5.40a | $(\boldsymbol{v}_1, \boldsymbol{v}_2, \boldsymbol{v}_3, \boldsymbol{\omega}_\beta)$ | $(\boldsymbol{v}_1, \boldsymbol{v}_2, \boldsymbol{v}_3, \boldsymbol{\omega}_\delta)$ | $(\boldsymbol{v}_1, \boldsymbol{v}_2, \boldsymbol{v}_3, \boldsymbol{\omega}_\alpha)$ |
| 5 | Figs. 5.19b, 5.35b, 5.40b | $(\boldsymbol{v}_1, \boldsymbol{v}_2, \boldsymbol{v}_3, \boldsymbol{\omega}_\beta)$ | $(\boldsymbol{v}_1, \boldsymbol{v}_2, \boldsymbol{v}_3, \boldsymbol{\omega}_\alpha)$ | $(\boldsymbol{v}_1, \boldsymbol{v}_2, \boldsymbol{v}_3, \boldsymbol{\omega}_\alpha)$ |
| 6 | Figs. 5.20–5.34 | $(\boldsymbol{v}_1, \boldsymbol{v}_2, \boldsymbol{v}_3, \boldsymbol{\omega}_\alpha)$ | $(\boldsymbol{v}_1, \boldsymbol{v}_2, \boldsymbol{v}_3, \boldsymbol{\omega}_\beta)$ | $(\boldsymbol{v}_1, \boldsymbol{v}_2, \boldsymbol{v}_3, \boldsymbol{\omega}_\delta)$ |
| 7 | Figs. 5.41, 5.42, 5.47, 5.48a | $(\boldsymbol{v}_1, \boldsymbol{v}_2, \boldsymbol{v}_3, \boldsymbol{\omega}_\alpha, \boldsymbol{\omega}_\delta)$ | $(\boldsymbol{v}_1, \boldsymbol{v}_2, \boldsymbol{v}_3, \boldsymbol{\omega}_\alpha, \boldsymbol{\omega}_\beta)$ | $(\boldsymbol{v}_1, \boldsymbol{v}_2, \boldsymbol{v}_3, \boldsymbol{\omega}_\beta, \boldsymbol{\omega}_\delta)$ |
| 8 | Figs. 5.43, 5.44, 5.45, 5.46, 5.48b | $(\boldsymbol{v}_1, \boldsymbol{v}_2, \boldsymbol{v}_3, \boldsymbol{\omega}_\alpha, \boldsymbol{\omega}_\beta)$ | $(\boldsymbol{v}_1, \boldsymbol{v}_2, \boldsymbol{v}_3, \boldsymbol{\omega}_\beta, \boldsymbol{\omega}_\delta)$ | $(\boldsymbol{v}_1, \boldsymbol{v}_2, \boldsymbol{v}_3, \boldsymbol{\omega}_\alpha, \boldsymbol{\omega}_\delta)$ |

**Table 5.7.** Structural parameters[a] of translational parallel mechanisms in Figs. 5.6–5.14

| No. | Structural parameter | Solution *3-PaPP* (Figs. 5.6, 5.7) | *3-PaPaP* (Figs. 5.8, 5.9) *3-PaPPa* (Figs. 5.10, 5.11) *3-PaPa$^t$P* (Figs. 5.14) | *3-PaPaPa* (Figs. 5.12, 5.13) |
|---|---|---|---|---|
| 1 | $m$ | 14 | 20 | 26 |
| 2 | $p_1$ | 6 | 9 | 12 |
| 3 | $p_2$ | 6 | 9 | 12 |
| 4 | $p_3$ | 6 | 9 | 12 |
| 5 | $p$ | 18 | 27 | 36 |
| 6 | $q$ | 5 | 8 | 11 |
| 7 | $k_1$ | 0 | 0 | 0 |
| 8 | $k_2$ | 3 | 3 | 3 |
| 9 | $k$ | 3 | 3 | 3 |
| 10 | $(R_{Gi})$ $(i = 1,2,3)$ | See Table 5.6 | See Table 5.6 | See Table 5.6 |
| 11 | $S_{G1}$ | 3 | 3 | 3 |
| 12 | $S_{G2}$ | 3 | 3 | 3 |
| 13 | $S_{G3}$ | 3 | 3 | 3 |
| 14 | $r_{G1}$ | 3 | 6 | 9 |
| 15 | $r_{G2}$ | 3 | 6 | 9 |
| 16 | $r_{G3}$ | 3 | 6 | 9 |
| 17 | $M_{G1}$ | 3 | 3 | 3 |
| 18 | $M_{G2}$ | 3 | 3 | 3 |
| 19 | $M_{G3}$ | 3 | 3 | 3 |
| 20 | $(R_F)$ | $(\boldsymbol{v}_1,\boldsymbol{v}_2,\boldsymbol{v}_3)$ | $(\boldsymbol{v}_1,\boldsymbol{v}_2,\boldsymbol{v}_3)$ | $(\boldsymbol{v}_1,\boldsymbol{v}_2,\boldsymbol{v}_3)$ |
| 21 | $S_F$ | 3 | 3 | 3 |
| 22 | $r_l$ | 9 | 18 | 27 |
| 23 | $r_F$ | 15 | 24 | 33 |
| 24 | $M_F$ | 3 | 3 | 3 |
| 25 | $N_F$ | 15 | 24 | 33 |
| 26 | $T_F$ | 0 | 0 | 0 |
| 27 | $\sum_{j=1}^{p_1} f_j$ | 6 | 9 | 12 |
| 28 | $\sum_{j=1}^{p_2} f_j$ | 6 | 9 | 12 |
| 29 | $\sum_{j=1}^{p_3} f_j$ | 6 | 9 | 12 |
| 30 | $\sum_{j=1}^{p} f_j$ | 18 | 27 | 36 |

[a]See footnote of Table 2.1 for the nomenclature of structural parameters

**Table 5.8.** Structural parameters[a] of translational parallel mechanisms in Figs. 5.15–5.18

| No. | Structural parameter | Solution *3-PaPa^tcc* (Fig. 5.15) *3-Pa^ccPa* (Fig. 5.17) | *3-Pa^ccP* (Fig. 5.16) | *3-RRPP* (Fig. 5.18) |
|---|---|---|---|---|
| 1 | $m$ | 17 | 11 | 11 |
| 2 | $p_1$ | 8 | 5 | 4 |
| 3 | $p_2$ | 8 | 5 | 4 |
| 4 | $p_3$ | 8 | 5 | 4 |
| 5 | $p$ | 24 | 15 | 12 |
| 6 | $q$ | 8 | 5 | 2 |
| 7 | $k_1$ | 0 | 0 | 3 |
| 8 | $k_2$ | 3 | 3 | 0 |
| 9 | $k$ | 3 | 3 | 3 |
| 10 | $(R_{Gi})$ $(i = 1,2,3)$ | See Table 5.6 | See Table 5.6 | See Table 5.6 |
| 11 | $S_{G1}$ | 3 | 3 | 4 |
| 12 | $S_{G2}$ | 3 | 3 | 4 |
| 13 | $S_{G3}$ | 3 | 3 | 4 |
| 14 | $r_{G1}$ | 7 | 4 | 0 |
| 15 | $r_{G2}$ | 7 | 4 | 0 |
| 16 | $r_{G3}$ | 7 | 4 | 0 |
| 17 | $M_{G1}$ | 3 | 3 | 4 |
| 18 | $M_{G2}$ | 3 | 3 | 4 |
| 19 | $M_{G3}$ | 3 | 3 | 4 |
| 20 | $(R_F)$ | $(\mathbf{v}_1, \mathbf{v}_2, \mathbf{v}_3)$ | $(\mathbf{v}_1, \mathbf{v}_2, \mathbf{v}_3)$ | $(\mathbf{v}_1, \mathbf{v}_2, \mathbf{v}_3)$ |
| 21 | $S_F$ | 3 | 3 | 3 |
| 22 | $r_l$ | 21 | 12 | 0 |
| 23 | $r_F$ | 27 | 18 | 9 |
| 24 | $M_F$ | 3 | 3 | 3 |
| 25 | $N_F$ | 21 | 12 | 3 |
| 26 | $T_F$ | 0 | 0 | 0 |
| 27 | $\sum_{j=1}^{p_1} f_j$ | 10 | 7 | 4 |
| 28 | $\sum_{j=1}^{p_2} f_j$ | 10 | 7 | 4 |
| 29 | $\sum_{j=1}^{p_3} f_j$ | 10 | 7 | 4 |
| 30 | $\sum_{j=1}^{p} f_j$ | 30 | 21 | 12 |

[a]See footnote of Table 2.1 for the nomenclature of structural parameters

**Table 5.9.** Structural parameters[a] of translational parallel mechanisms in Figs. 5.19–5.27

| No. | Structural parameter | Solution 3-*RCP* (Fig. 5.19) | 3-*PaRRP* (Figs. 5.20, 5.21) 3-*PaRPR* (Fig. 5.22) 3-*PaRRR* (Fig. 5.23) 3-*PaPRR* (Figs. 5.24, 5.25) | 3-*PaPaRR* (Fig. 5.26) 3-*PaRRPa* (Fig. 5.27) |
|---|---|---|---|---|
| 1 | $m$ | 8 | 17 | 23 |
| 2 | $p_1$ | 3 | 7 | 10 |
| 3 | $p_2$ | 3 | 7 | 10 |
| 4 | $p_3$ | 3 | 7 | 10 |
| 5 | $p$ | 9 | 21 | 30 |
| 6 | $q$ | 2 | 5 | 8 |
| 7 | $k_1$ | 3 | 0 | 0 |
| 8 | $k_2$ | 0 | 3 | 3 |
| 9 | $k$ | 3 | 3 | 3 |
| 10 | $(R_{Gi})$ $(i = 1,2,3)$ | See Table 5.6 | See Table 5.6 | See Table 5.6 |
| 11 | $S_{G1}$ | 4 | 4 | 4 |
| 12 | $S_{G2}$ | 4 | 4 | 4 |
| 13 | $S_{G3}$ | 4 | 4 | 4 |
| 14 | $r_{G1}$ | 0 | 3 | 6 |
| 15 | $r_{G2}$ | 0 | 3 | 6 |
| 16 | $r_{G3}$ | 0 | 3 | 6 |
| 17 | $M_{G1}$ | 4 | 4 | 4 |
| 18 | $M_{G2}$ | 4 | 4 | 4 |
| 19 | $M_{G3}$ | 4 | 4 | 4 |
| 20 | $(R_F)$ | $(\boldsymbol{v}_1, \boldsymbol{v}_2, \boldsymbol{v}_3)$ | $(\boldsymbol{v}_1, \boldsymbol{v}_2, \boldsymbol{v}_3)$ | $(\boldsymbol{v}_1, \boldsymbol{v}_2, \boldsymbol{v}_3)$ |
| 21 | $S_F$ | 3 | 3 | 3 |
| 22 | $r_l$ | 0 | 9 | 18 |
| 23 | $r_F$ | 9 | 18 | 27 |
| 24 | $M_F$ | 3 | 3 | 3 |
| 25 | $N_F$ | 3 | 12 | 21 |
| 26 | $T_F$ | 0 | 0 | 0 |
| 27 | $\sum_{j=1}^{p_1} f_j$ | 4 | 7 | 10 |
| 28 | $\sum_{j=1}^{p_2} f_j$ | 4 | 7 | 10 |
| 29 | $\sum_{j=1}^{p_3} f_j$ | 4 | 7 | 10 |
| 30 | $\sum_{j=1}^{p} f_j$ | 12 | 21 | 30 |

[a]See footnote of Table 2.1 for the nomenclature of structural parameters

**Table 5.10.** Structural parameters[a] of translational parallel mechanisms in Figs. 5.28–5.34

| No. | Structural parameter | Solution 3-<u>*Pa*</u>*RRbR* (Fig. 5.28) 3-<u>*Pa*</u>*Pn2R* (Figs. 5.30, 5.31) 3-<u>*Pa*</u>*Pn3* (Figs. 5.32, 5.33) | 3-<u>*Pa*</u>*RRbRbR* (Fig. 5.29) | 3-<u>*Pa*$^{cc}$</u>*RR* (Fig. 5.34) |
|---|---|---|---|---|
| 1 | $m$ | 23 | 29 | 14 |
| 2 | $p_1$ | 10 | 13 | 6 |
| 3 | $p_2$ | 10 | 13 | 6 |
| 4 | $p_3$ | 10 | 13 | 6 |
| 5 | $p$ | 30 | 39 | 18 |
| 6 | $q$ | 8 | 11 | 5 |
| 7 | $k_1$ | 0 | 0 | 0 |
| 8 | $k_2$ | 3 | 3 | 3 |
| 9 | $k$ | 3 | 3 | 3 |
| 10 | $(R_{Gi})$ $(i = 1,2,3)$ | See Table 5.6 | See Table 5.6 | See Table 5.6 |
| 11 | $S_{G1}$ | 4 | 4 | 4 |
| 12 | $S_{G2}$ | 4 | 4 | 4 |
| 13 | $S_{G3}$ | 4 | 4 | 4 |
| 14 | $r_{G1}$ | 6 | 9 | 4 |
| 15 | $r_{G2}$ | 6 | 9 | 4 |
| 16 | $r_{G3}$ | 6 | 9 | 4 |
| 17 | $M_{G1}$ | 4 | 4 | 4 |
| 18 | $M_{G2}$ | 4 | 4 | 4 |
| 19 | $M_{G3}$ | 4 | 4 | 4 |
| 20 | $(R_F)$ | $(\mathbf{v}_1,\mathbf{v}_2,\mathbf{v}_3)$ | $(\mathbf{v}_1,\mathbf{v}_2,\mathbf{v}_3)$ | $(\mathbf{v}_1,\mathbf{v}_2,\mathbf{v}_3)$ |
| 21 | $S_F$ | 3 | 3 | 3 |
| 22 | $r_l$ | 18 | 27 | 12 |
| 23 | $r_F$ | 27 | 36 | 21 |
| 24 | $M_F$ | 3 | 3 | 3 |
| 25 | $N_F$ | 21 | 30 | 9 |
| 26 | $T_F$ | 0 | 0 | 0 |
| 27 | $\sum_{j=1}^{p_1} f_j$ | 10 | 13 | 8 |
| 28 | $\sum_{j=1}^{p_2} f_j$ | 10 | 13 | 8 |
| 29 | $\sum_{j=1}^{p_3} f_j$ | 10 | 13 | 8 |
| 30 | $\sum_{j=1}^{p} f_j$ | 30 | 39 | 24 |

[a]See footnote of Table 2.1 for the nomenclature of structural parameters

**Table 5.11.** Structural parameters[a] of translational parallel mechanisms in Figs. 5.35–5.40

| No. | Structural parameter | Solution *3-RRPaP* (Figs. 5.35, 5.36) *3-RRPPa* (Fig. 5.38) | *3-RCPa* (Fig. 5.37) | *3-RRPaPa* (Figs. 5.39, 5.40) |
|---|---|---|---|---|
| 1 | $m$ | 17 | 14 | 23 |
| 2 | $p_1$ | 7 | 6 | 10 |
| 3 | $p_2$ | 7 | 6 | 10 |
| 4 | $p_3$ | 7 | 6 | 10 |
| 5 | $p$ | 21 | 18 | 30 |
| 6 | $q$ | 5 | 5 | 8 |
| 7 | $k_1$ | 0 | 0 | 0 |
| 8 | $k_2$ | 3 | 3 | 3 |
| 9 | $k$ | 3 | 3 | 3 |
| 10 | $(R_{Gi})$ $(i = 1,2,3)$ | See Table 5.6 | See Table 5.6 | See Table 5.6 |
| 11 | $S_{G1}$ | 4 | 4 | 4 |
| 12 | $S_{G2}$ | 4 | 4 | 4 |
| 13 | $S_{G3}$ | 4 | 4 | 4 |
| 14 | $r_{G1}$ | 3 | 3 | 6 |
| 15 | $r_{G2}$ | 3 | 3 | 6 |
| 16 | $r_{G3}$ | 3 | 3 | 6 |
| 17 | $M_{G1}$ | 4 | 4 | 4 |
| 18 | $M_{G2}$ | 4 | 4 | 4 |
| 19 | $M_{G3}$ | 4 | 4 | 4 |
| 20 | $(R_F)$ | $(\boldsymbol{v}_1, \boldsymbol{v}_2, \boldsymbol{v}_3)$ | $(\boldsymbol{v}_1, \boldsymbol{v}_2, \boldsymbol{v}_3)$ | $(\boldsymbol{v}_1, \boldsymbol{v}_2, \boldsymbol{v}_3)$ |
| 21 | $S_F$ | 3 | 3 | 3 |
| 22 | $r_l$ | 9 | 9 | 18 |
| 23 | $r_F$ | 18 | 18 | 27 |
| 24 | $M_F$ | 3 | 3 | 3 |
| 25 | $N_F$ | 12 | 12 | 21 |
| 26 | $T_F$ | 0 | 0 | 0 |
| 27 | $\sum_{j=1}^{p_1} f_j$ | 8 | 7 | 10 |
| 28 | $\sum_{j=1}^{p_2} f_j$ | 8 | 7 | 10 |
| 29 | $\sum_{j=1}^{p_3} f_j$ | 8 | 7 | 10 |
| 30 | $\sum_{j=1}^{p} f_j$ | 24 | 21 | 30 |

[a]See footnote of Table 2.1 for the nomenclature of structural parameters

**Table 5.12.** Structural parameters[a] of translational parallel mechanisms in Figs. 5.41–5.48

| No. | Structural parameter | Solution<br>*3-RRRRbR* (Fig. 5.41)<br>*3-RRPn2R* (Figs. 5.43, 5.44)<br>*3-RRPn3* (Figs. 5.45, 5.46)<br>*3-RRRRPa* (Fig. 5.47)<br>*3-RRPaRR* (Fig. 5.48) | <br>*3-RRRRbRbR*<br>(Fig. 5.42) |
|---|---|---|---|
| 1 | $m$ | 20 | 26 |
| 2 | $p_1$ | 8 | 11 |
| 3 | $p_2$ | 8 | 11 |
| 4 | $p_3$ | 8 | 11 |
| 5 | $p$ | 24 | 33 |
| 6 | $q$ | 5 | 8 |
| 7 | $k_1$ | 0 | 0 |
| 8 | $k_2$ | 3 | 3 |
| 9 | $k$ | 3 | 3 |
| 10 | $(R_{Gi})$ $(i = 1,2,3)$ | See Table 5.6 | See Table 5.6 |
| 11 | $S_{G1}$ | 5 | 5 |
| 12 | $S_{G2}$ | 5 | 5 |
| 13 | $S_{G3}$ | 5 | 5 |
| 14 | $r_{G1}$ | 3 | 6 |
| 15 | $r_{G2}$ | 3 | 6 |
| 16 | $r_{G3}$ | 3 | 6 |
| 17 | $M_{G1}$ | 5 | 5 |
| 18 | $M_{G2}$ | 5 | 5 |
| 19 | $M_{G3}$ | 5 | 5 |
| 20 | $(R_F)$ | $(\boldsymbol{v}_1, \boldsymbol{v}_2, \boldsymbol{v}_3)$ | $(\boldsymbol{v}_1, \boldsymbol{v}_2, \boldsymbol{v}_3)$ |
| 21 | $S_F$ | 3 | 3 |
| 22 | $r_l$ | 9 | 18 |
| 23 | $r_F$ | 21 | 30 |
| 24 | $M_F$ | 3 | 3 |
| 25 | $N_F$ | 9 | 18 |
| 26 | $T_F$ | 0 | 0 |
| 27 | $\sum_{j=1}^{p_1} f_j$ | 8 | 11 |
| 28 | $\sum_{j=1}^{p_2} f_j$ | 8 | 11 |
| 29 | $\sum_{j=1}^{p_3} f_j$ | 8 | 11 |
| 30 | $\sum_{j=1}^{p} f_j$ | 24 | 33 |

[a]See footnote of Table 2.1 for the nomenclature of structural parameters

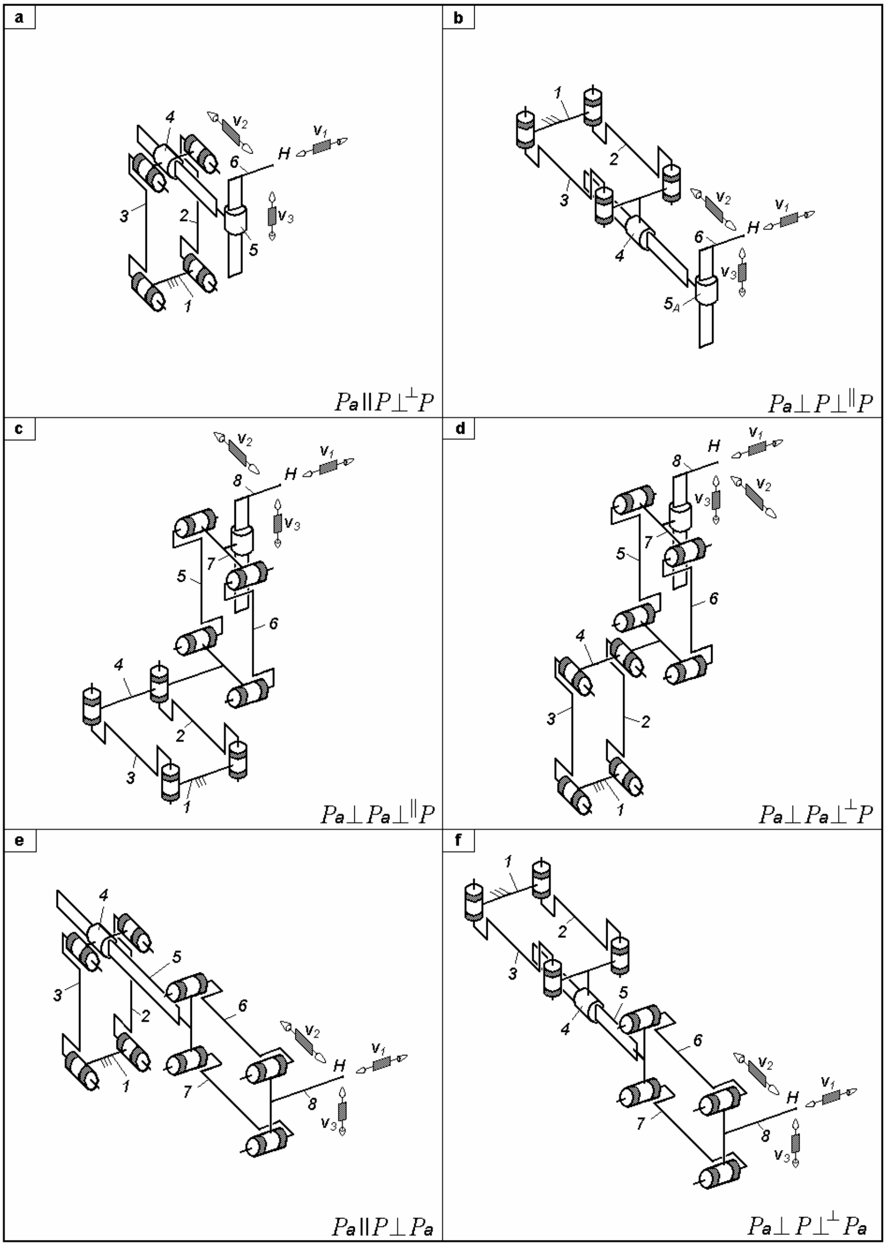


**Fig. 5.1.** Complex limbs for overconstrained TPMs with uncoupled motions defined by $M_G = S_G = 3$, $(R_G) = (\boldsymbol{v}_1, \boldsymbol{v}_2, \boldsymbol{v}_3)$ and actuated by rotating motors mounted on the fixed base and combined in a parallelogram loop of type *Pa* (**a**–**i**) or $Pa^{cc}$ (**j** and **k**)

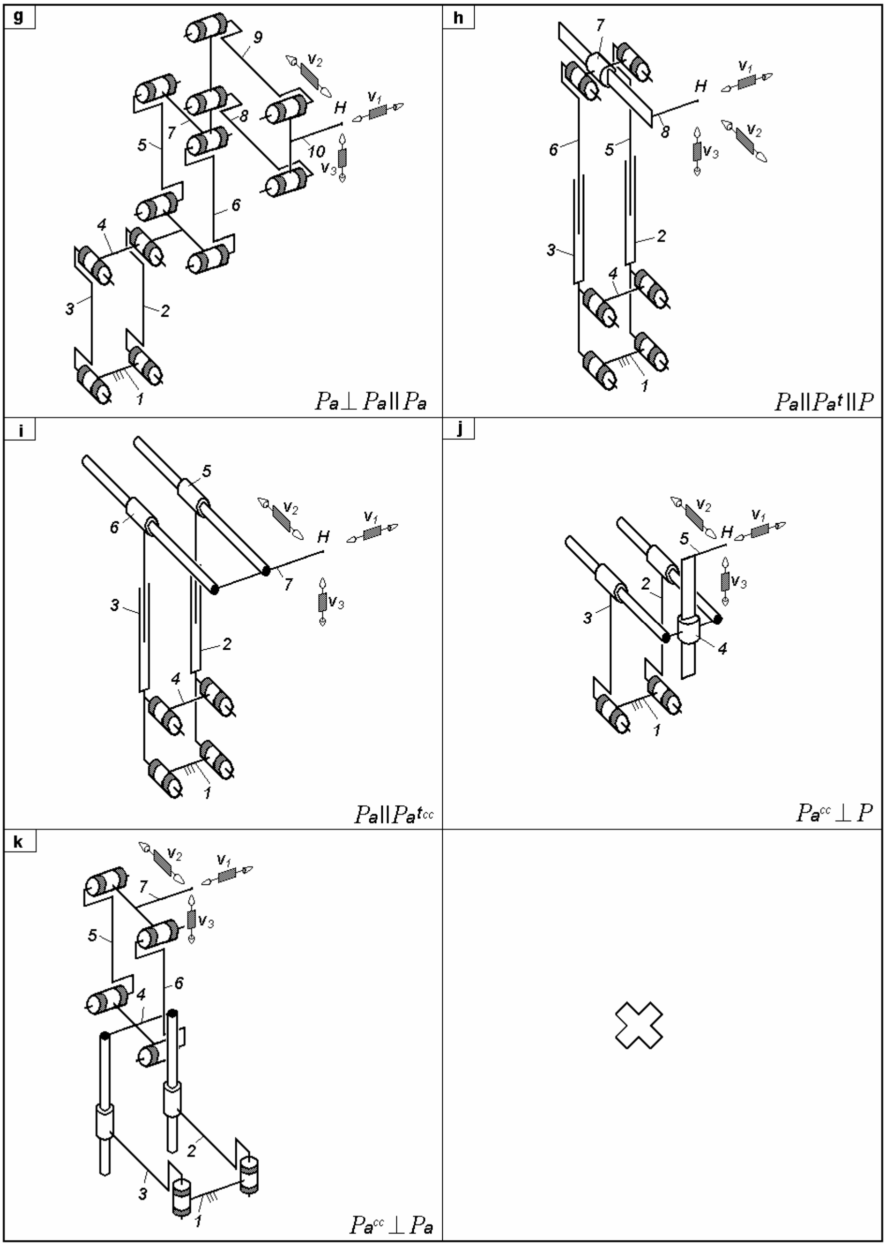


**Fig. 5.1.** (cont.)

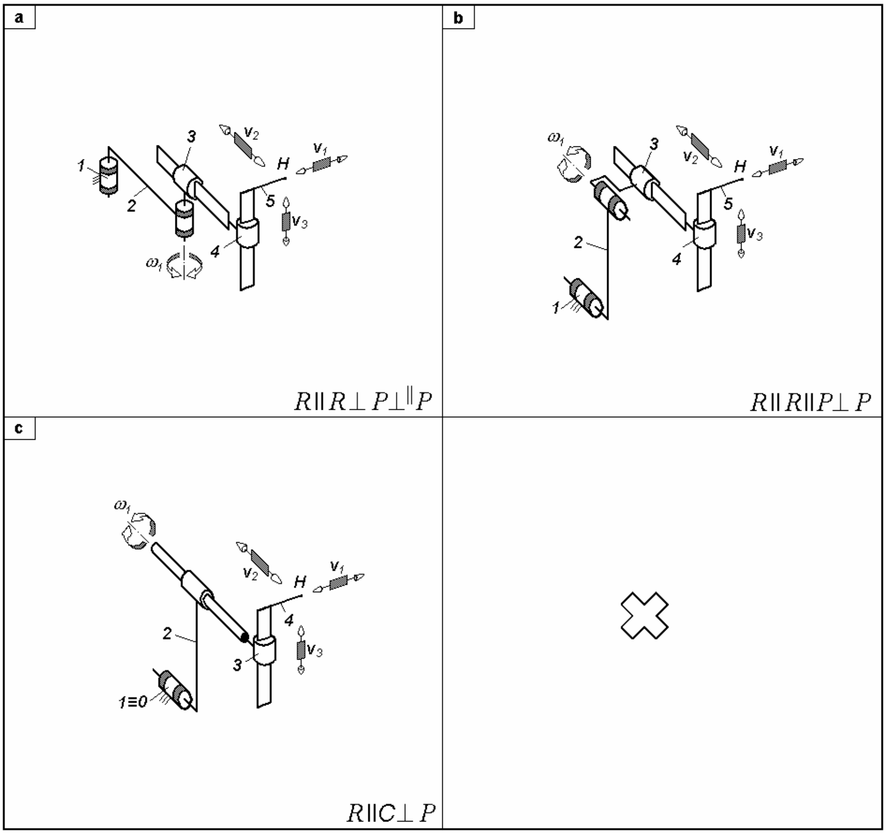


**Fig. 5.2.** Simple limbs for overconstrained TPMs with uncoupled motions defined by $M_G = S_G = 4$, $(R_G) = (\boldsymbol{v}_1, \boldsymbol{v}_2, \boldsymbol{v}_3, \boldsymbol{\omega}_1)$ and actuated by rotating motors mounted on the fixed base

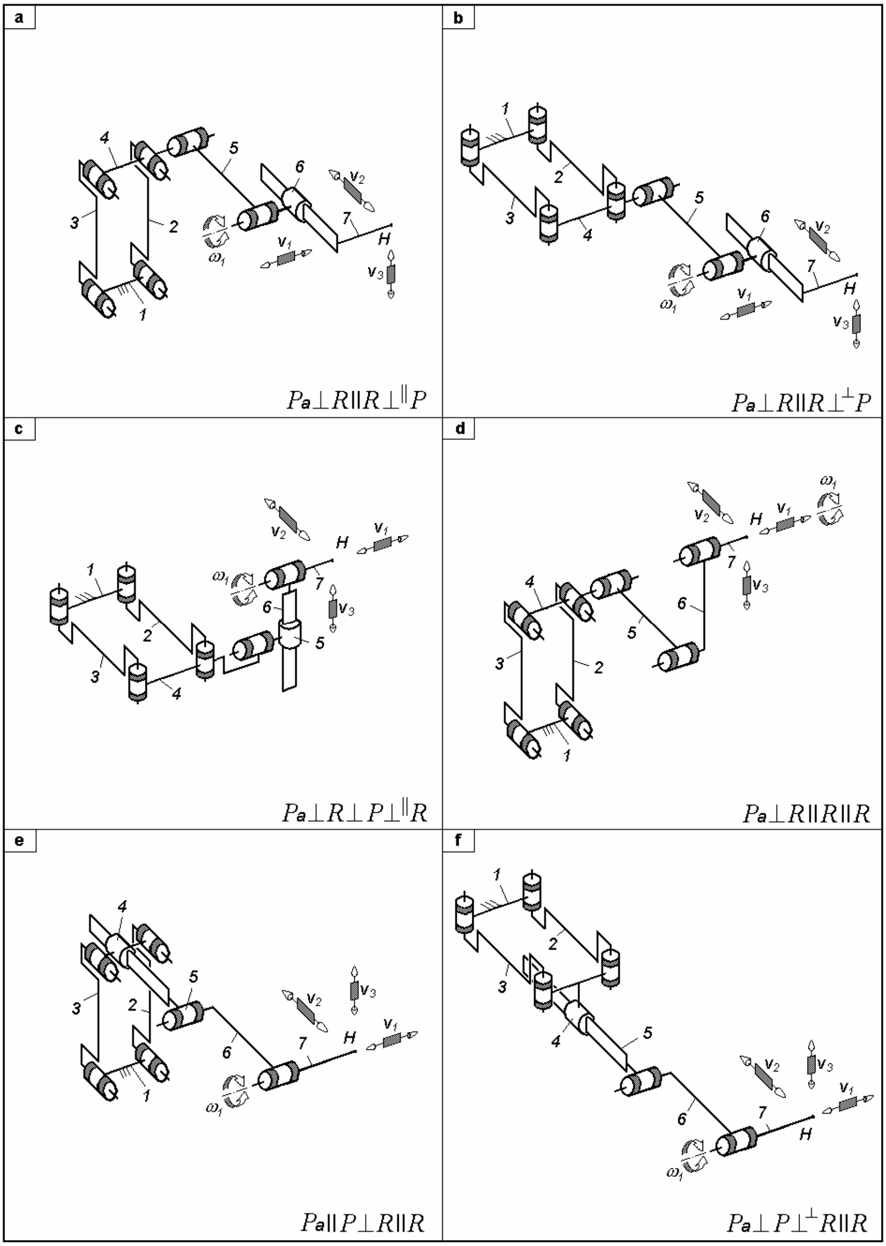


**Fig. 5.3.** Complex limbs for overconstrained TPMs with uncoupled motions defined by $M_G = S_G = 4$, $(R_G) = (\boldsymbol{v}_1, \boldsymbol{v}_2, \boldsymbol{v}_3, \boldsymbol{\omega}_1)$ and actuated by rotating motors mounted on the fixed base and combined in a parallelogram loop of type *Pa* (**a–n**) or $Pa^{cc}$ (**o**)

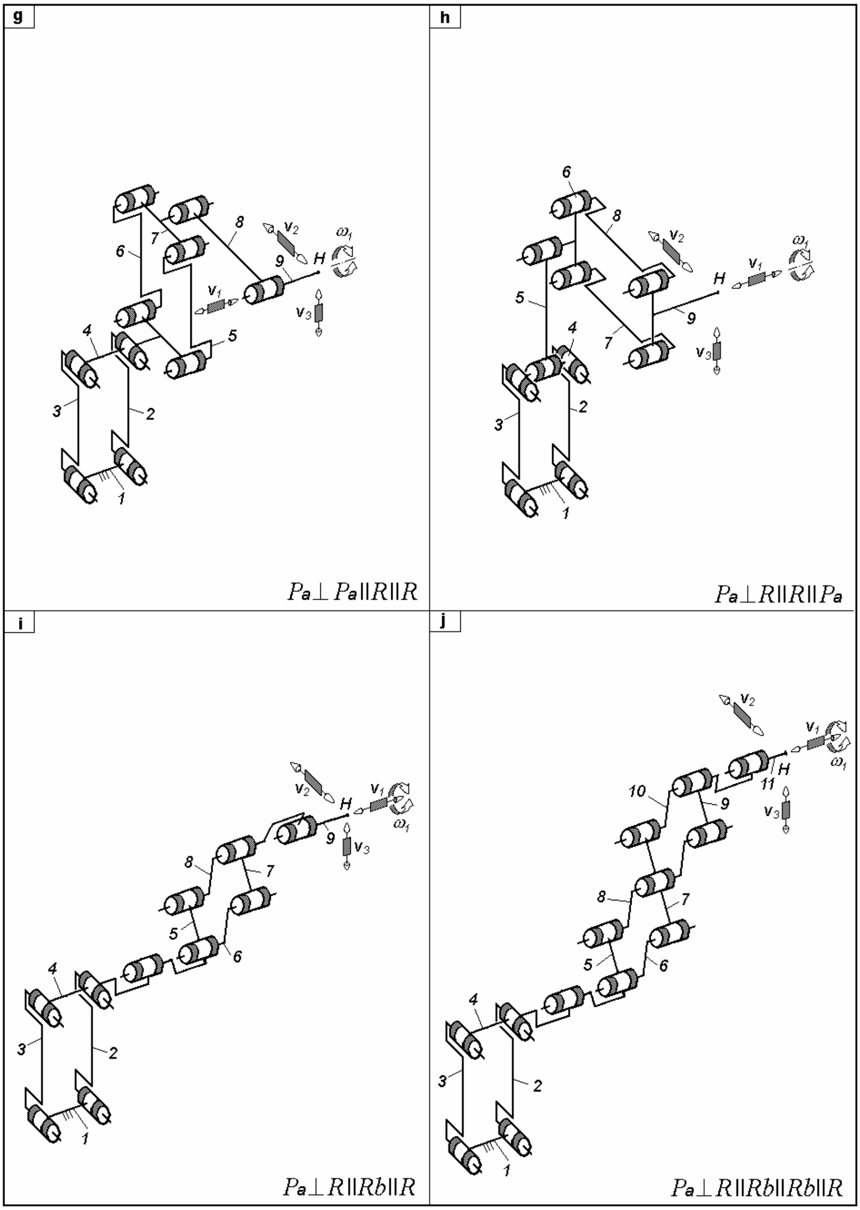


**Fig. 5.3.** (cont.)

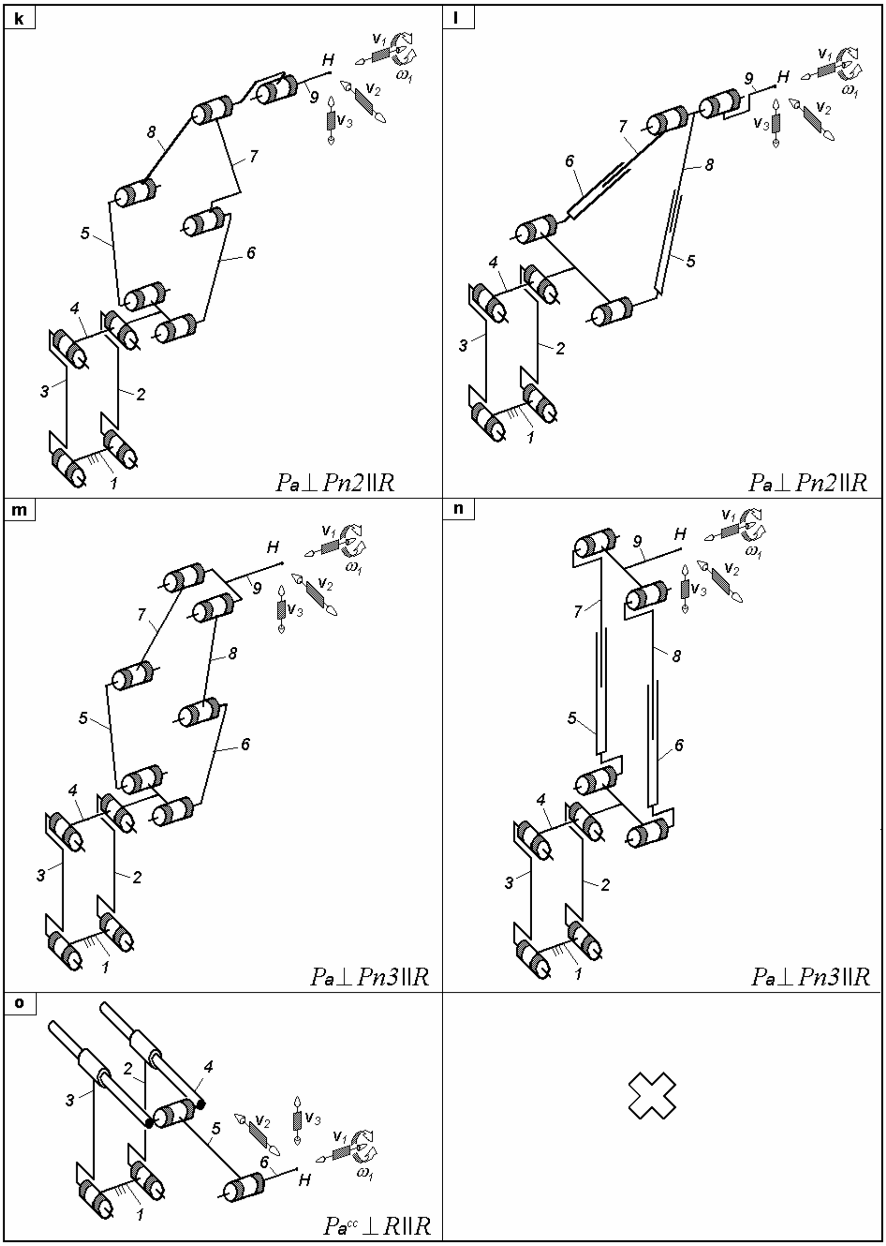
k
H
9
8
7
5
6
4
3
2
1
v1
ω1
v2
v3
Pa⊥Pn2||R
l
Pa⊥Pn2||R
m
Pa⊥Pn3||R
n
Pa⊥Pn3||R
o
Pacc⊥R||R

**Fig. 5.3.** (cont.)

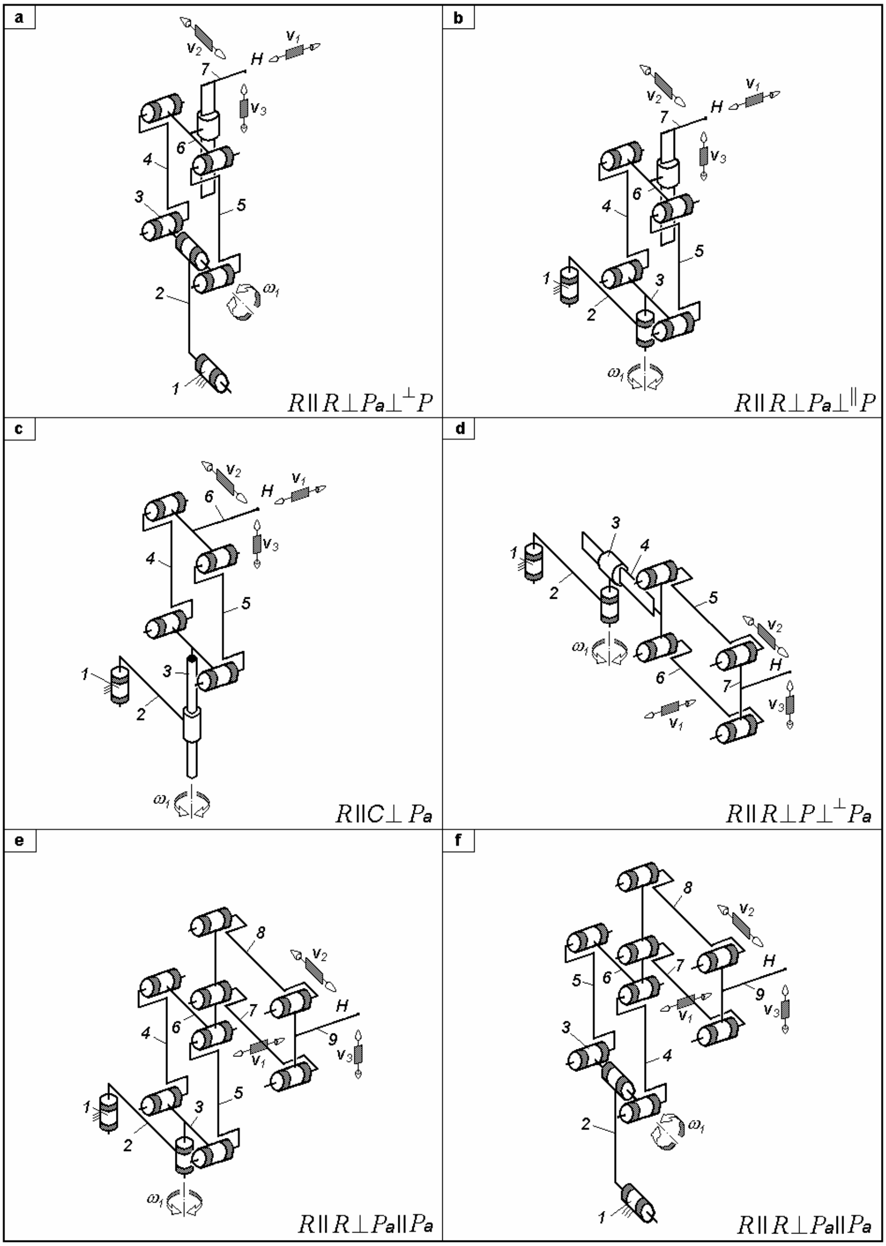


**Fig. 5.4.** Complex limbs for overconstrained TPMs with uncoupled motions defined by $M_G = S_G = 4$, $(R_G) = (\boldsymbol{v}_1, \boldsymbol{v}_2, \boldsymbol{v}_3, \boldsymbol{\omega}_1)$ and actuated by rotating motors mounted on the fixed base

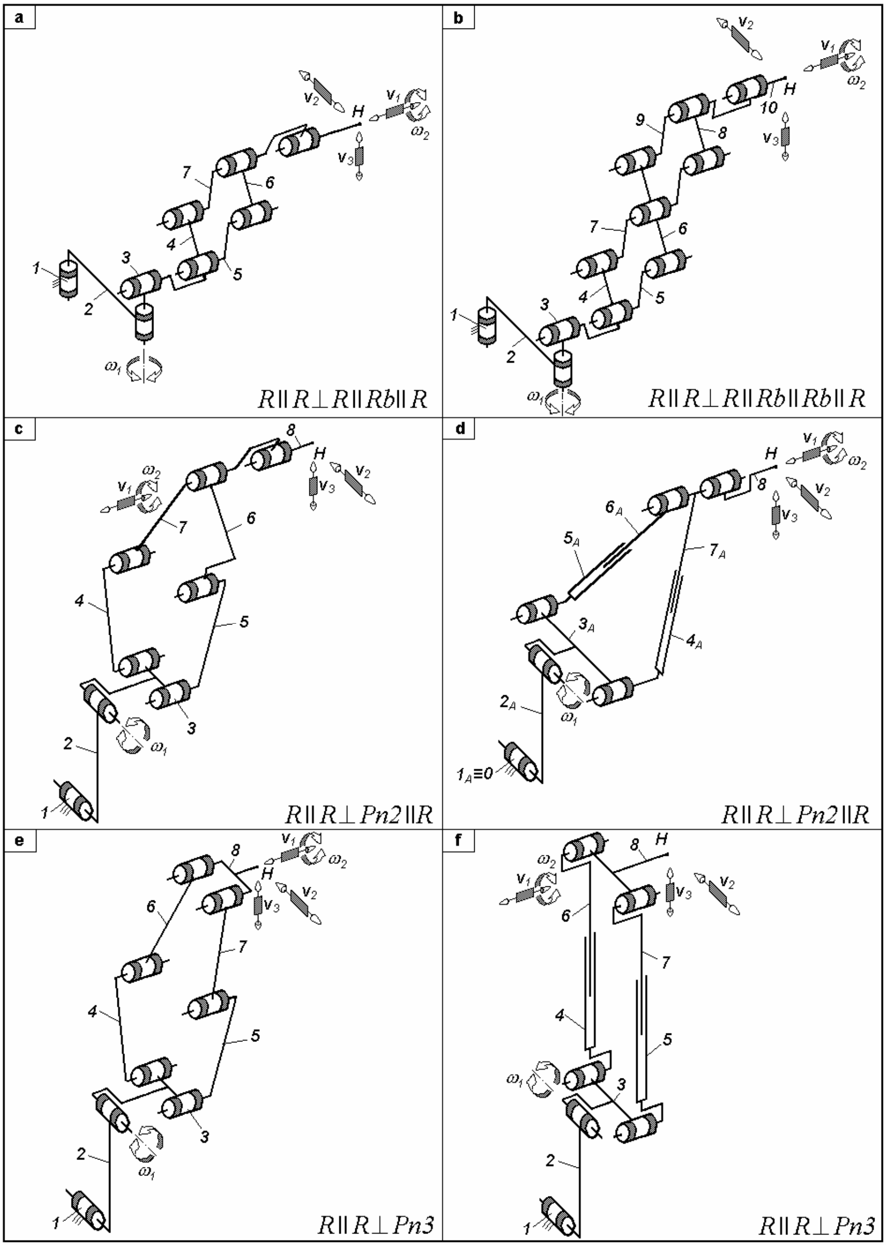


**Fig. 5.5.** Complex limbs for overconstrained TPMs with uncoupled motions defined by $M_G = S_G = 5$, $(R_G) = (\boldsymbol{v}_1, \boldsymbol{v}_2, \boldsymbol{v}_3, \boldsymbol{\omega}_1, \boldsymbol{\omega}_2)$ and actuated by rotating motors mounted on the fixed base

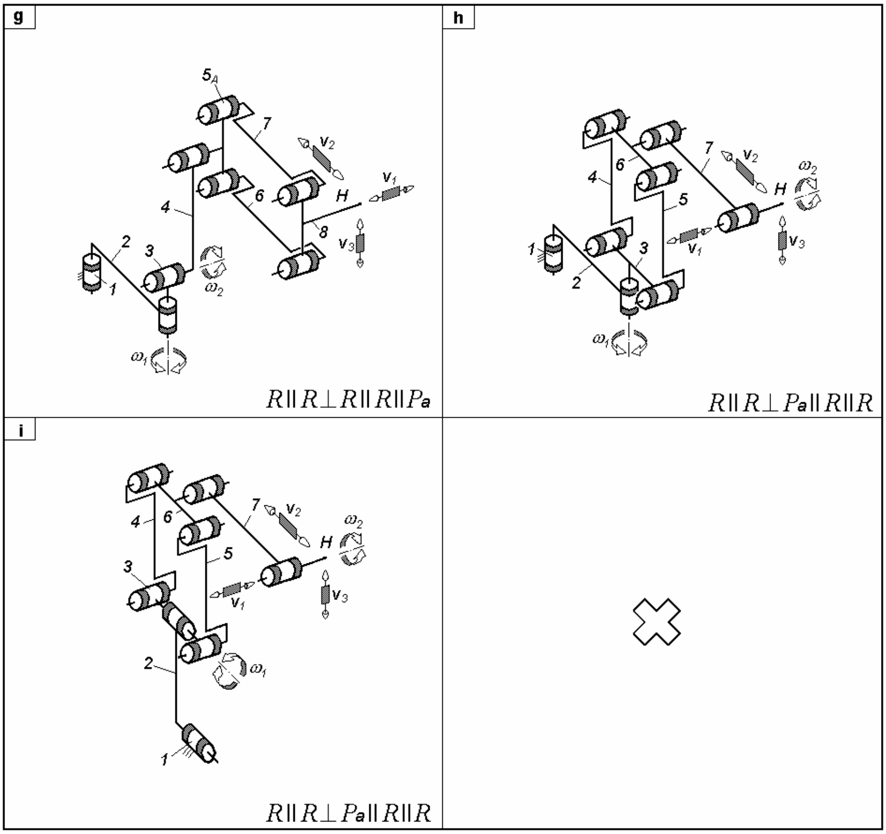
g
5A
7
v2
v1
H
6
4
8
v3
2
3
1
ω2
ω1
R||R⊥R||R||Pa
h
7
v2
6
ω2
4
H
5
1
3
v1
v3
2
ω1
R||R⊥Pa||R||R
i
4
6
7
v2
ω2
H
5
3
v1
v3
2
ω1
1
R||R⊥Pa||R||R

**Fig. 5.5.** (cont)

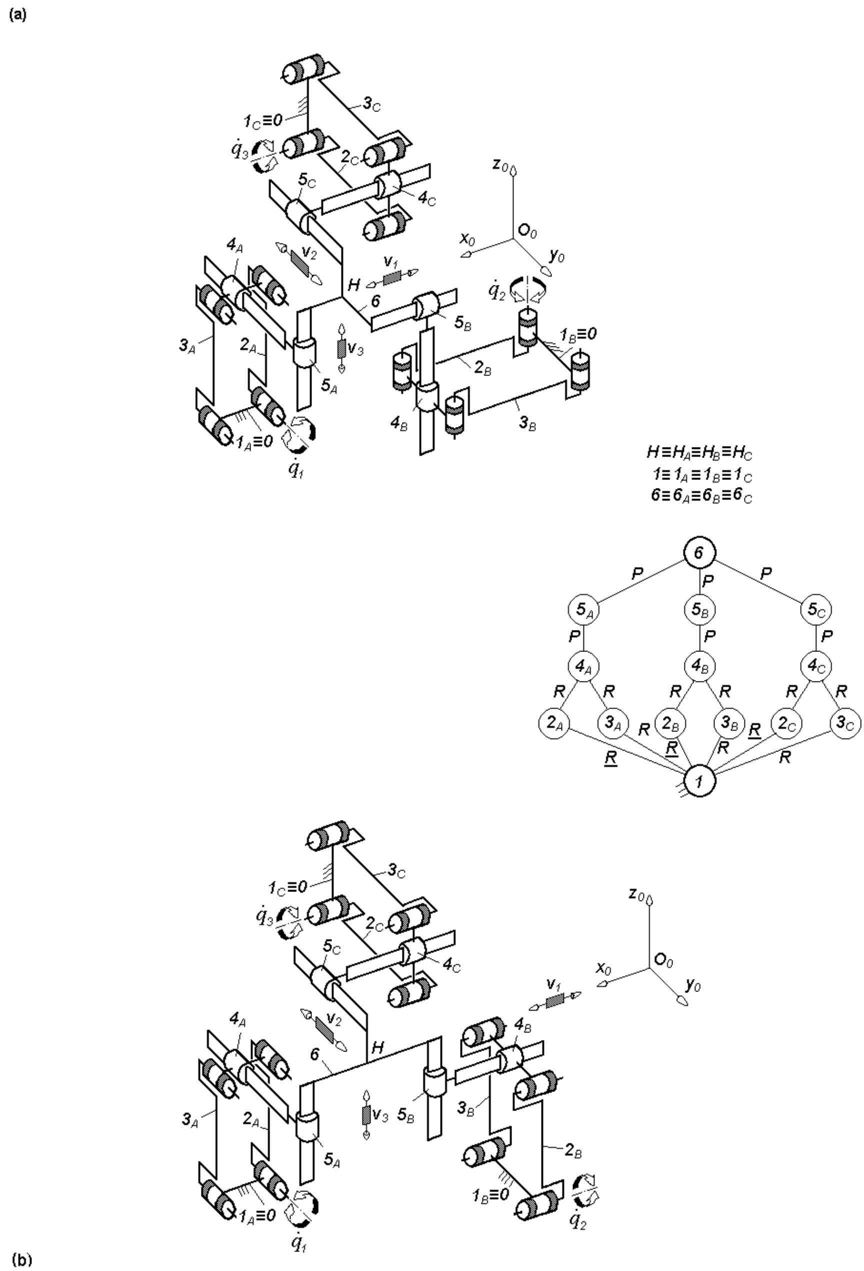


**Fig. 5.6.** *3-<u>Pa</u>PP*-type overconstrained TPMs with uncoupled motions and rotating actuators mounted on the fixed base, defined by $M_F = S_F = 3$, $(R_F) = (\boldsymbol{v}_1, \boldsymbol{v}_2, \boldsymbol{v}_3)$, $T_F = 0$, $N_F = 15$, limb topology $\underline{Pa}||P \perp^{\perp} P$

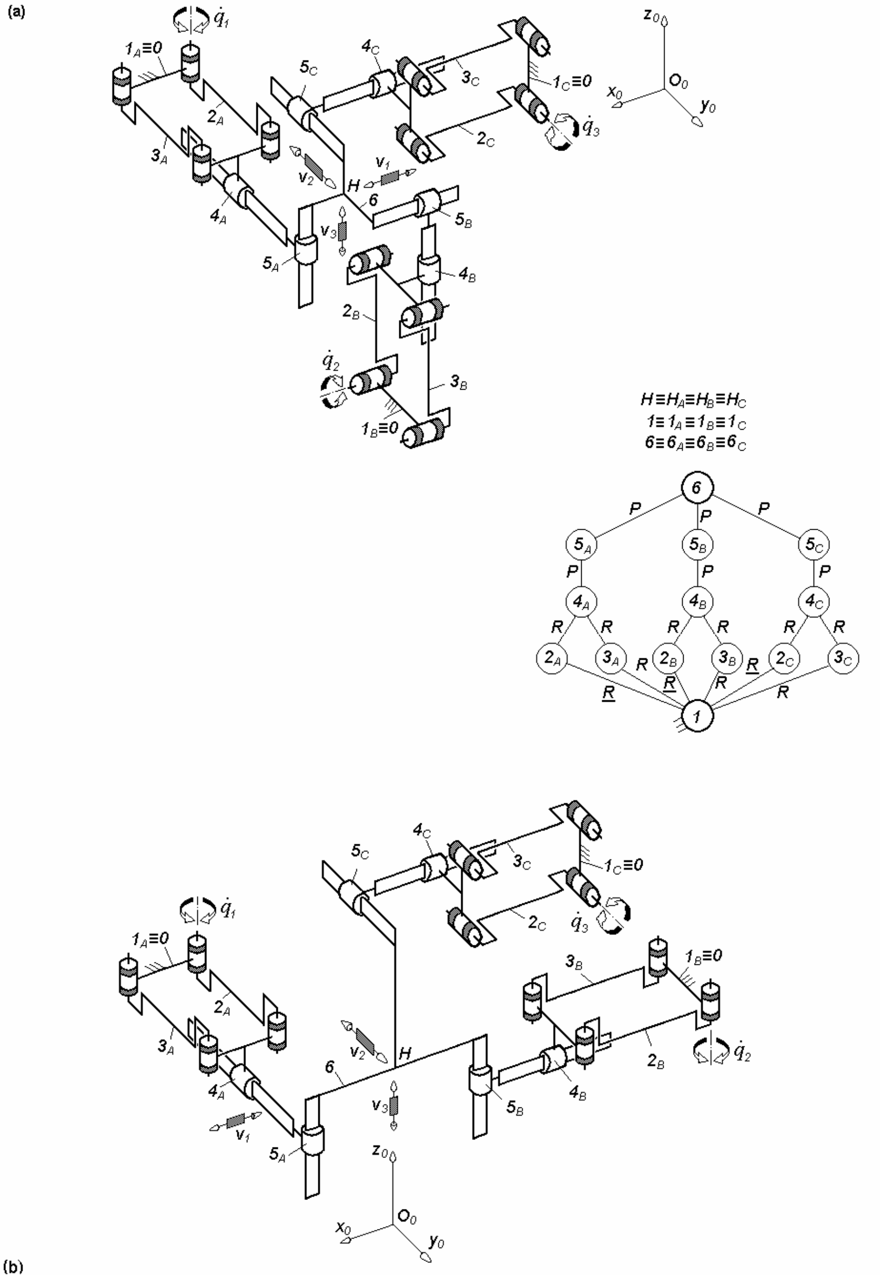


**Fig. 5.7.** *3-<u>Pa</u>PP*-type overconstrained TPMs with uncoupled motions and rotating actuators mounted on the fixed base, defined by $M_F = S_F = 3$, $(R_F) = (\boldsymbol{v}_1, \boldsymbol{v}_2, \boldsymbol{v}_3)$, $T_F = 0$, $N_F = 15$, limb topology $\underline{Pa} \perp P \perp^{||} P$

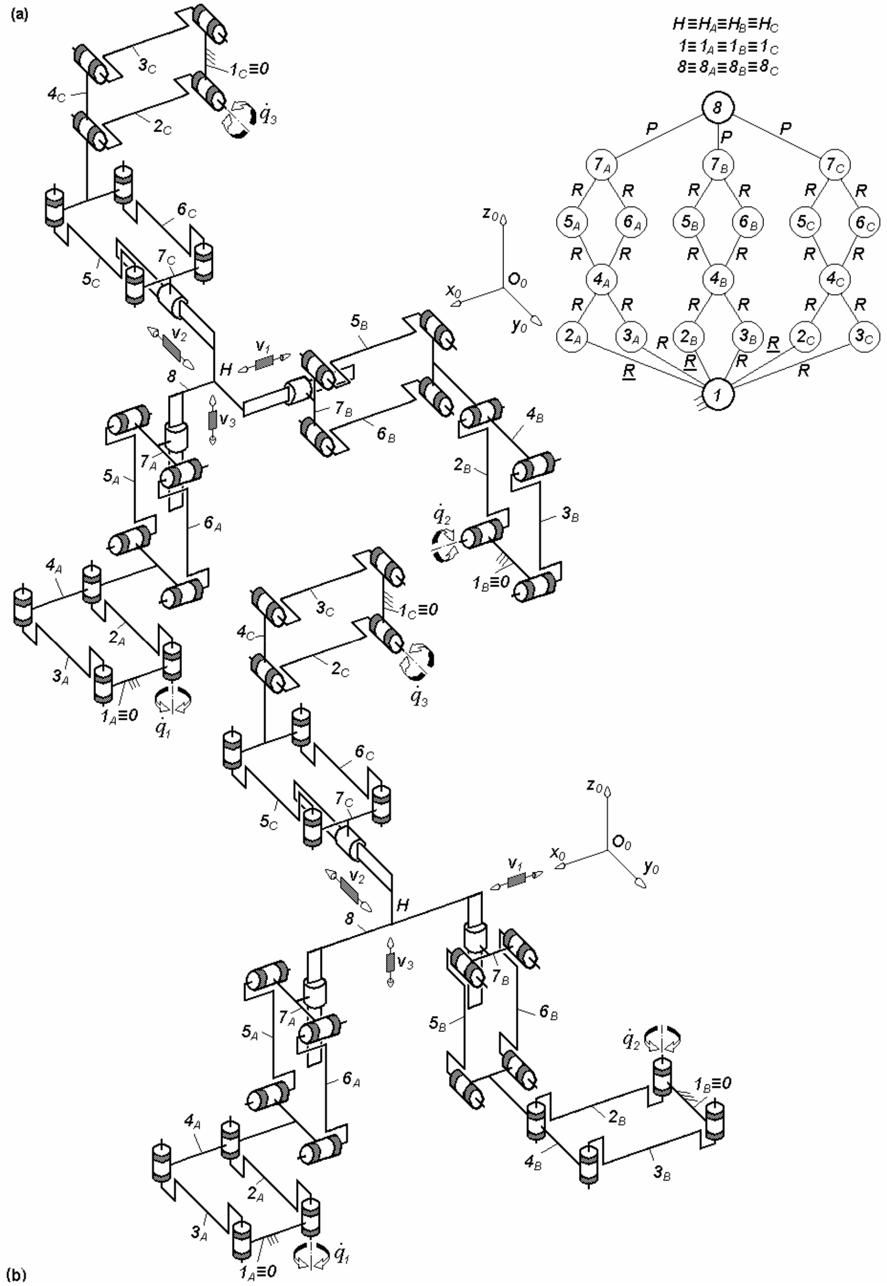


**Fig. 5.8.** *3-*$\underline{Pa}$*PaP*-type overconstrained TPMs with uncoupled motions and rotating actuators mounted on the fixed base, defined by $M_F = S_F = 3$, $(R_F) = (\boldsymbol{v}_1, \boldsymbol{v}_2, \boldsymbol{v}_3)$, $T_F = 0$, $N_F = 24$, limb topology $\underline{Pa} \perp Pa \perp^{||} P$

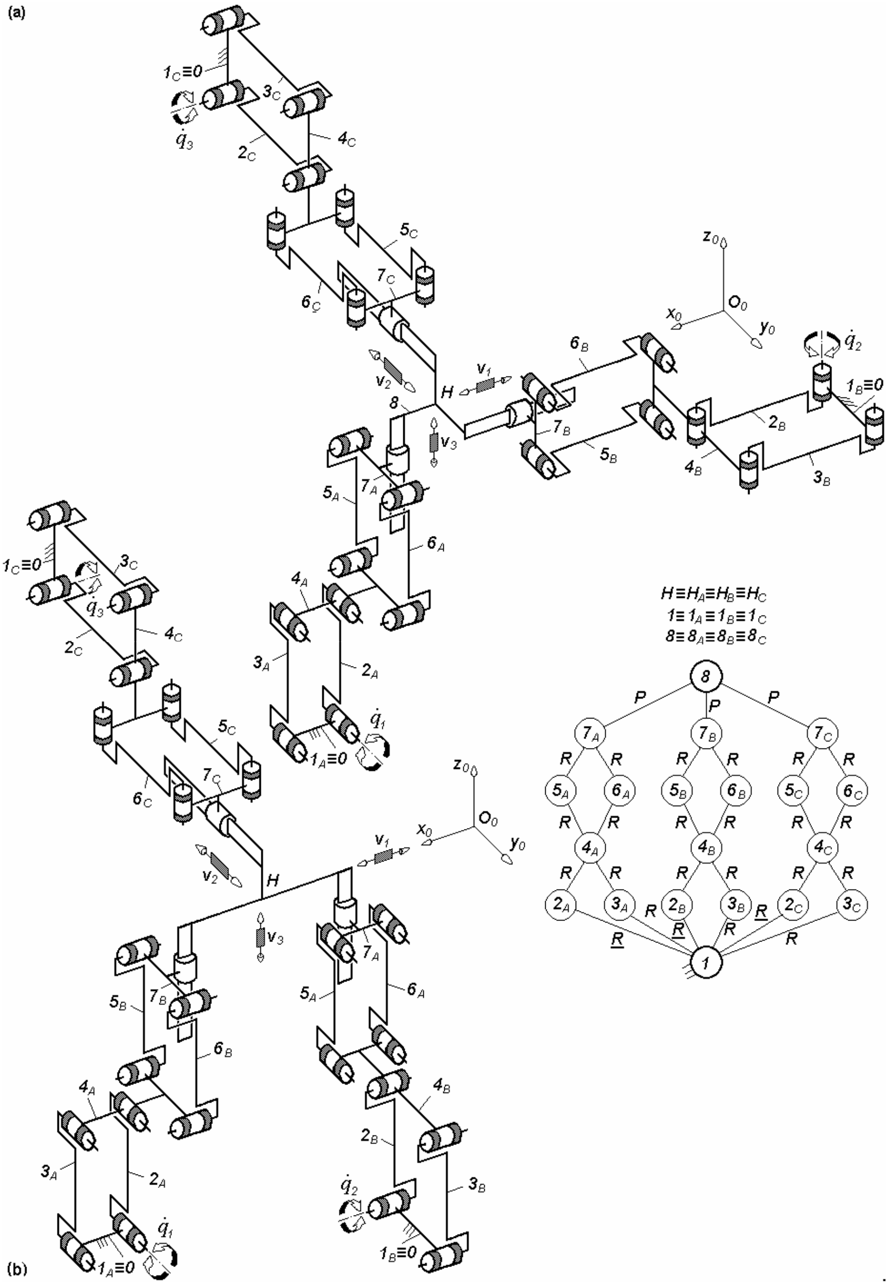


**Fig. 5.9.** *3-<u>Pa</u>PaP*-type overconstrained TPMs with uncoupled motions and rotating actuators mounted on the fixed base, defined by $M_F = S_F = 3$, $(R_F) = (\boldsymbol{v}_1, \boldsymbol{v}_2, \boldsymbol{v}_3)$, $T_F = 0$, $N_F = 24$, limb topology $\underline{Pa} \perp Pa \perp^{\perp} P$

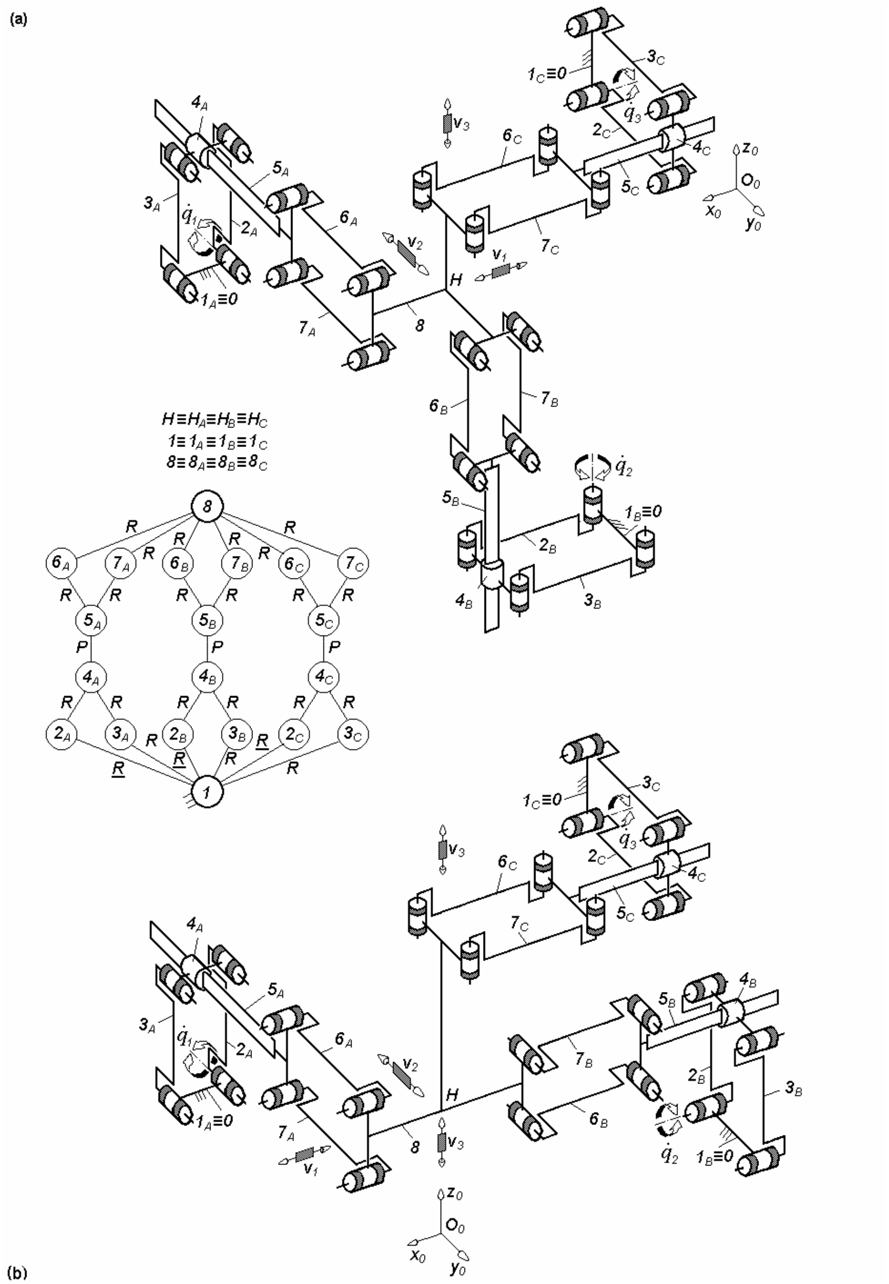


**Fig. 5.10.** *3-<u>Pa</u>PPa*-type overconstrained TPMs with uncoupled motions and rotating actuators mounted on the fixed base, defined by $M_F = S_F = 3$, $(R_F) = (\boldsymbol{v}_1, \boldsymbol{v}_2, \boldsymbol{v}_3)$, $T_F = 0$, $N_F = 24$, limb topology <u>*Pa*</u>||*P* ⊥ *Pa*

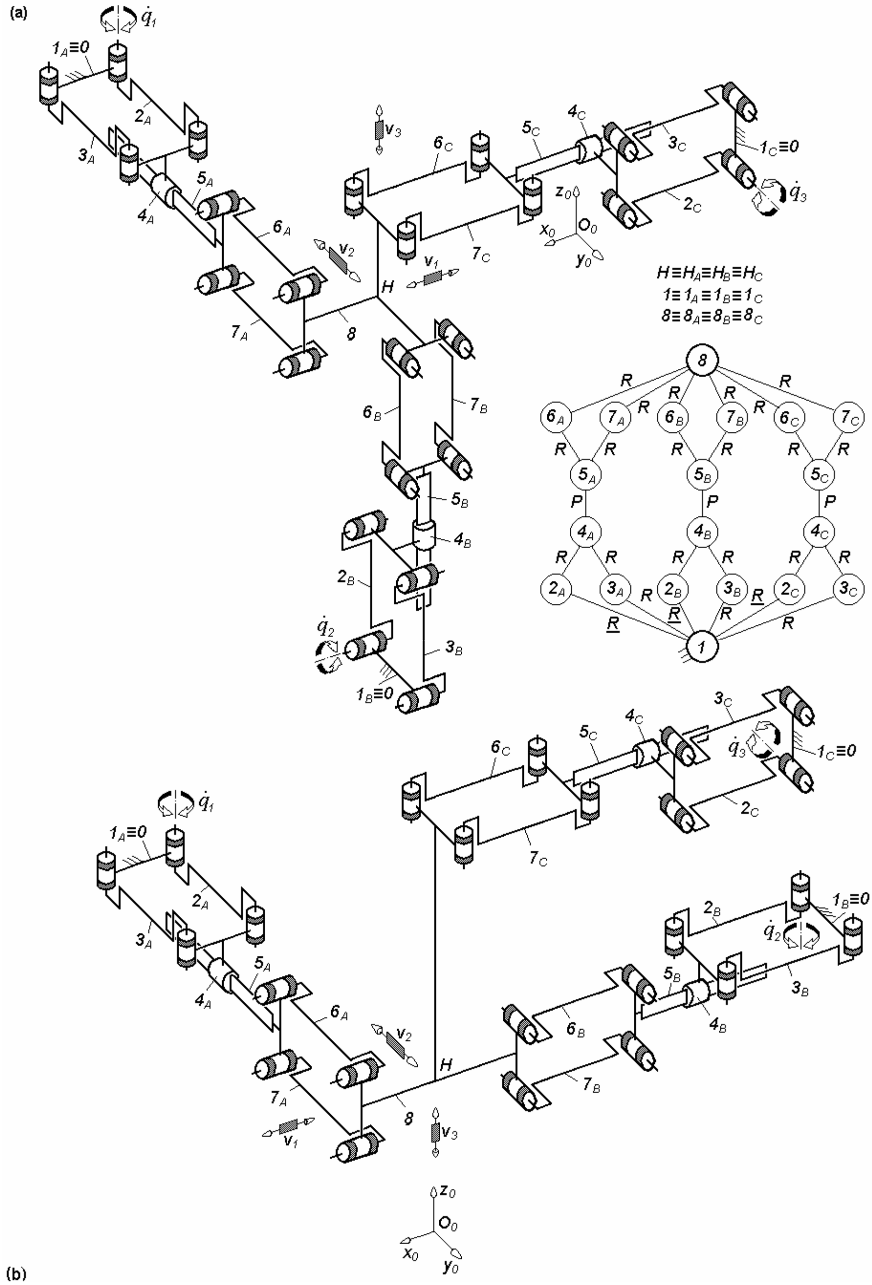


**Fig. 5.11.** *3-*<u>*Pa*</u>*PPa*-type overconstrained TPMs with uncoupled motions and rotating actuators mounted on the fixed base, defined by $M_F = S_F = 3$, $(R_F) = (\boldsymbol{v}_1, \boldsymbol{v}_2, \boldsymbol{v}_3)$, $T_F = 0$, $N_F = 24$, limb topology <u>*Pa*</u> $\perp P \perp^{\perp} Pa$

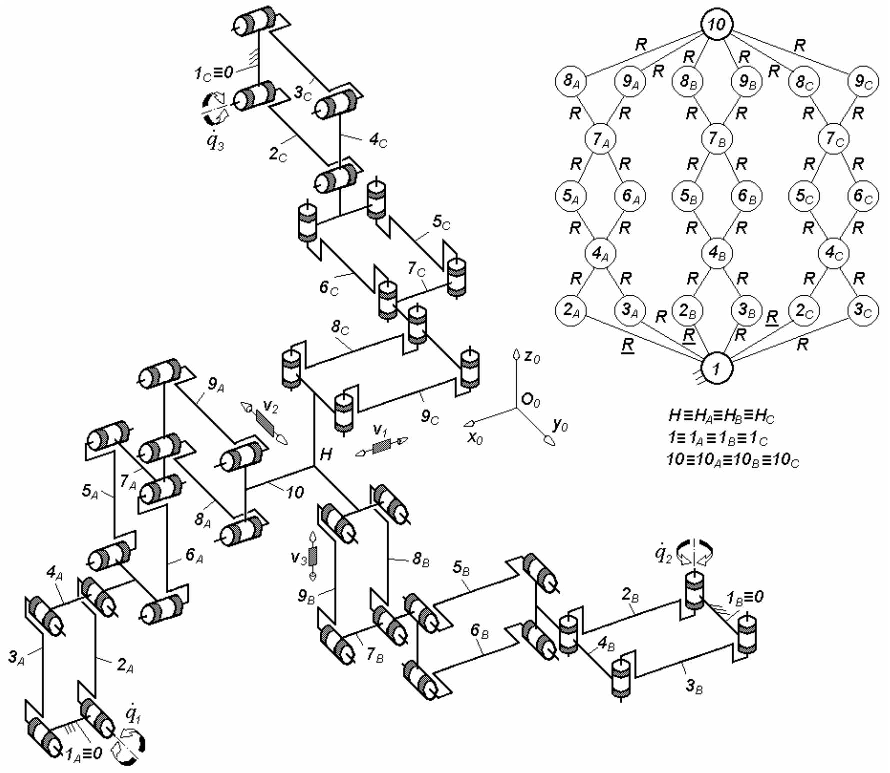


**Fig. 5.12.** *3-PaPaPa*-type overconstrained TPMs with uncoupled motions and rotating actuators mounted on the fixed base with the axes parallel to three reciprocally orthogonal directions, defined by $M_F = S_F = 3$, $(R_F) = (\boldsymbol{v}_1, \boldsymbol{v}_2, \boldsymbol{v}_3)$, $T_F = 0$, $N_F = 33$, limb topology $\underline{Pa} \perp Pa || Pa$

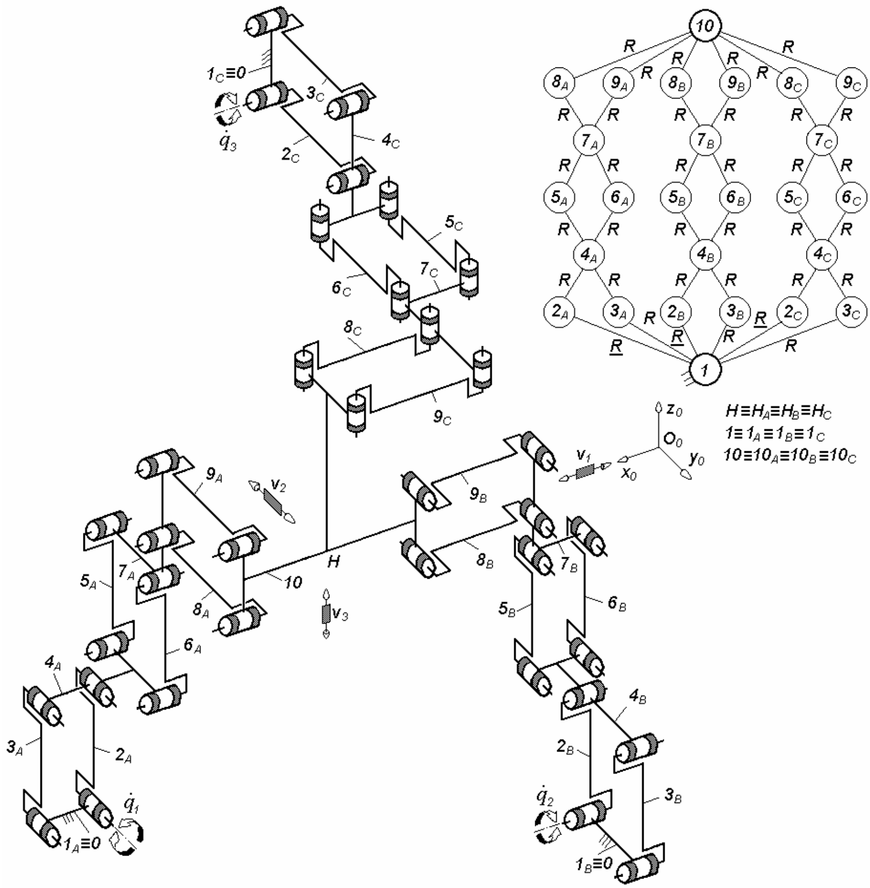


**Fig. 5.13.** *3-<u>Pa</u>PaPa*-type overconstrained TPMs with uncoupled motions and rotating actuators mounted on the fixed base with the axes parallel to two planar orthogonal directions, defined by $M_F = S_F = 3$, $(R_F) = (\boldsymbol{v}_1, \boldsymbol{v}_2, \boldsymbol{v}_3)$, $T_F = 0$, $N_F = 33$, limb topology $\underline{Pa} \perp Pa||Pa$

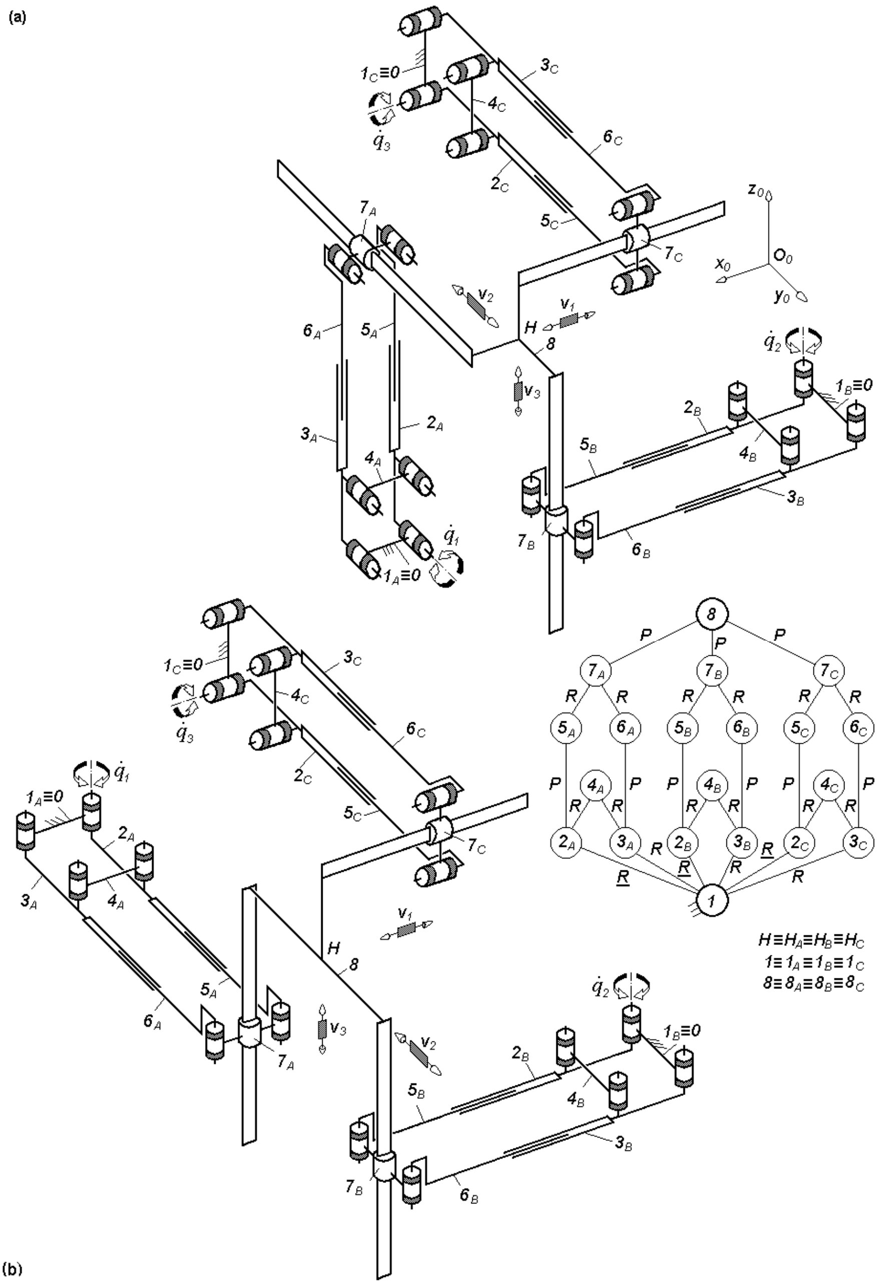


**Fig. 5.14.** $3\text{-}\underline{Pa}Pa^tP$-type overconstrained TPMs with uncoupled motions and rotating actuators mounted on the fixed base, defined by $M_F = S_F = 3$, $(R_F) = (\boldsymbol{v}_1, \boldsymbol{v}_2, \boldsymbol{v}_3)$, $T_F = 0$, $N_F = 24$, limb topology $\underline{Pa}||Pa^t||P$

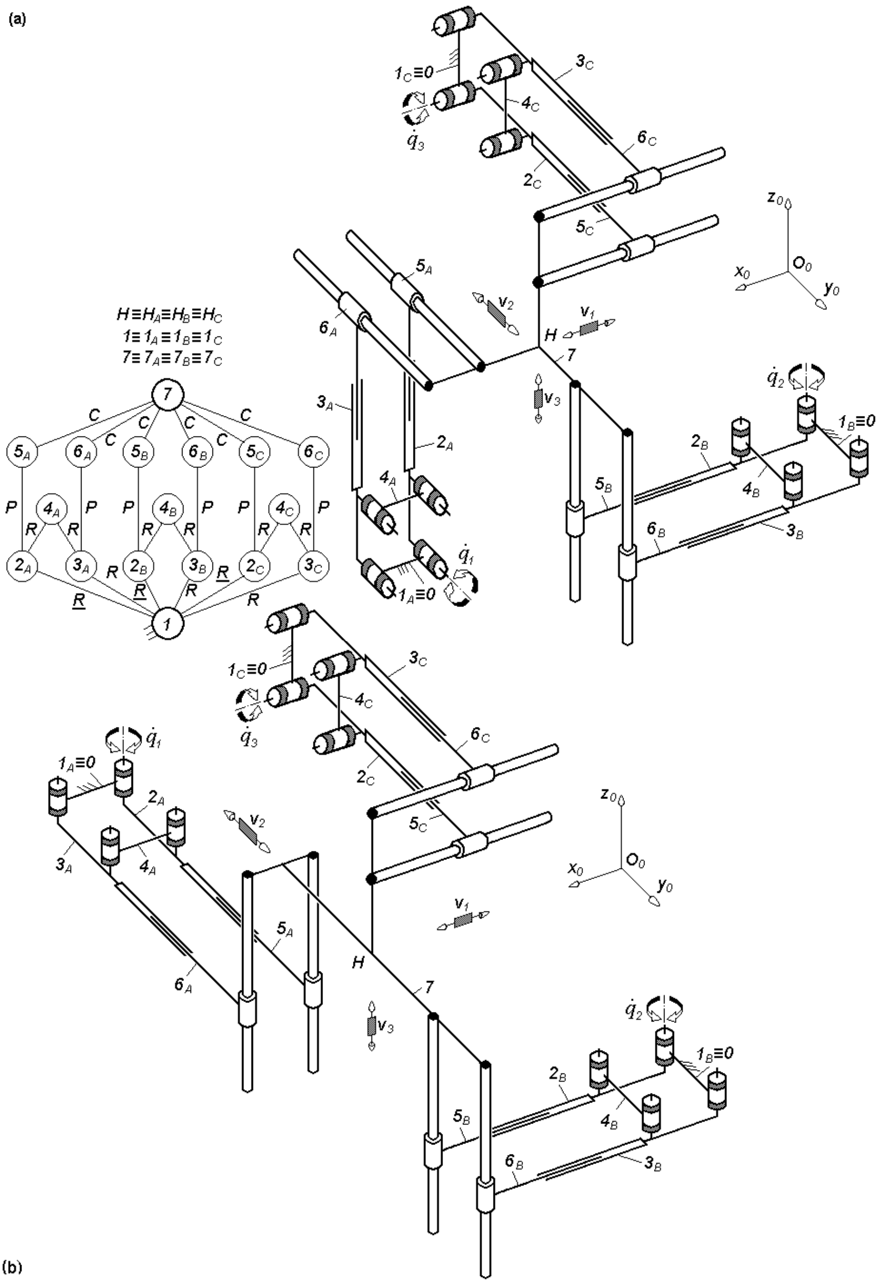


**Fig. 5.15.** $3\text{-}\underline{Pa}Pa^{tcc}$-type overconstrained TPMs with uncoupled motions and rotating actuators mounted on the fixed base, defined by $M_F = S_F = 3$, $(R_F) = (\boldsymbol{v}_1, \boldsymbol{v}_2, \boldsymbol{v}_3)$, $T_F = 0$, $N_F = 21$, limb topology $\underline{Pa}||Pa^{tcc}$

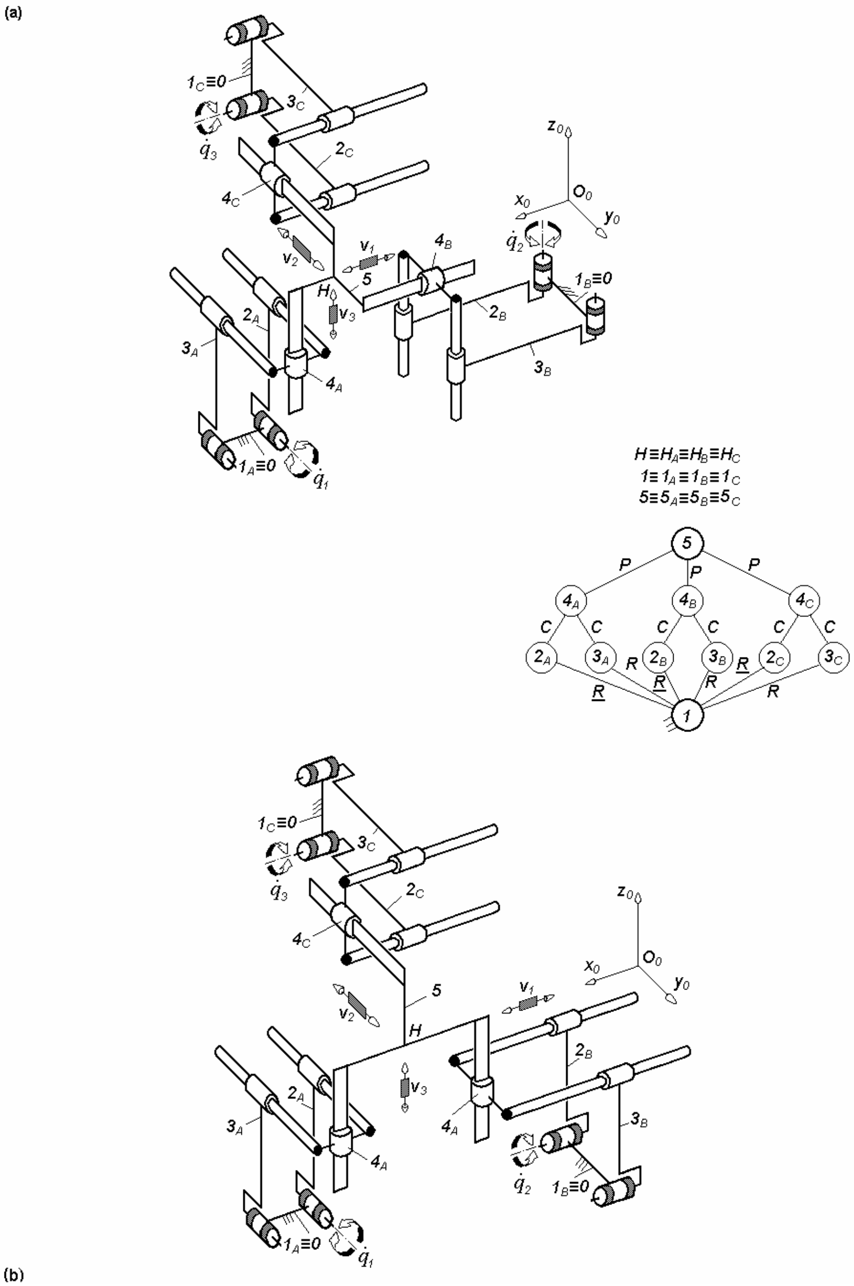


**Fig. 5.16.** $3\text{-}\underline{Pa}^{cc}P$-type overconstrained TPMs with uncoupled motions and rotating actuators mounted on the fixed base, defined by $M_F = S_F = 3$, $(R_F) = (\boldsymbol{v}_1, \boldsymbol{v}_2, \boldsymbol{v}_3)$, $T_F = 0$, $N_F = 12$, limb topology $\underline{Pa}^{cc} \perp P$

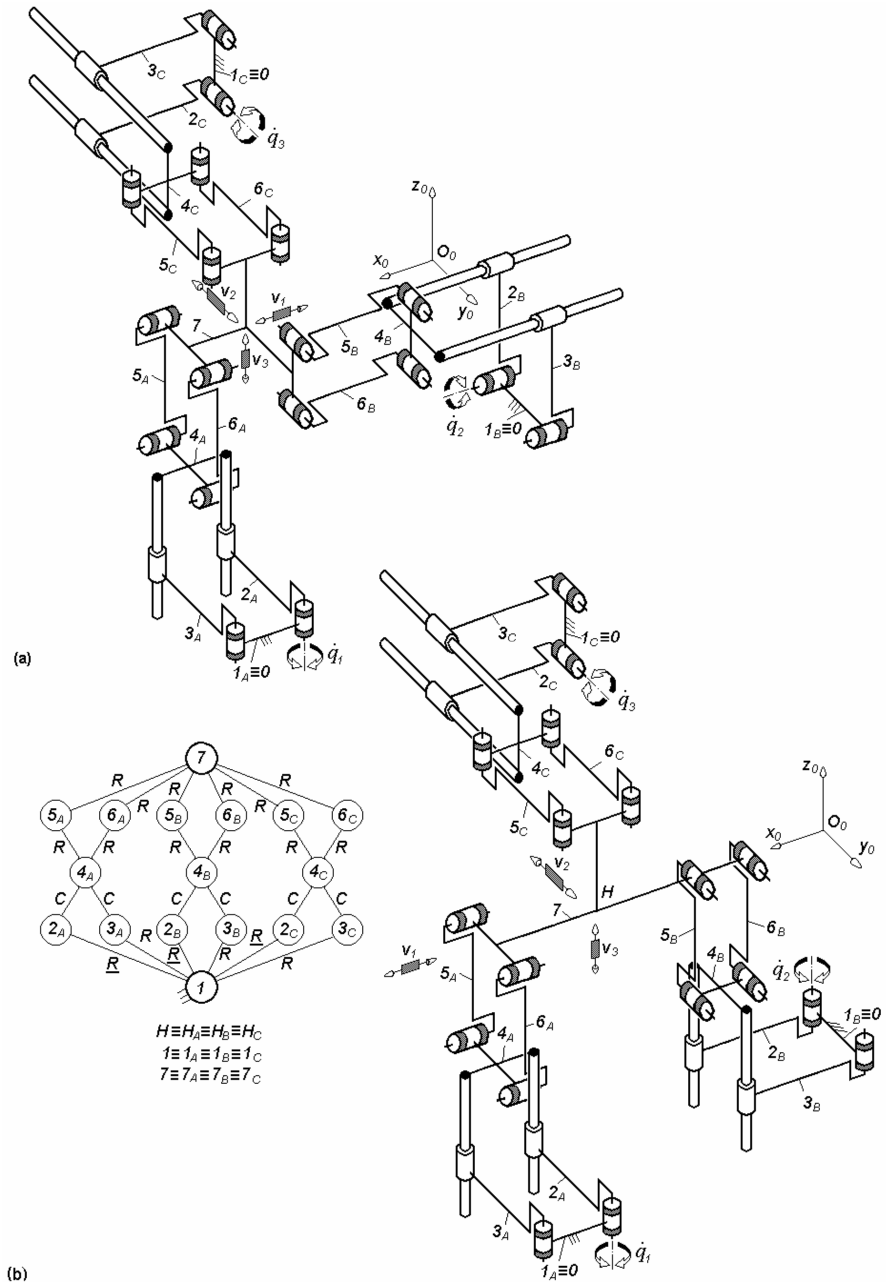


**Fig. 5.17.** 3-$\underline{Pa}^{cc}Pa$-type overconstrained TPMs with uncoupled motions and rotating actuators mounted on the fixed base, defined by $M_F = S_F = 3$, $(R_F) = (\mathbf{v}_1, \mathbf{v}_2, \mathbf{v}_3)$, $T_F = 0$, $N_F = 21$, limb topology $\underline{Pa^{cc}} \perp Pa$

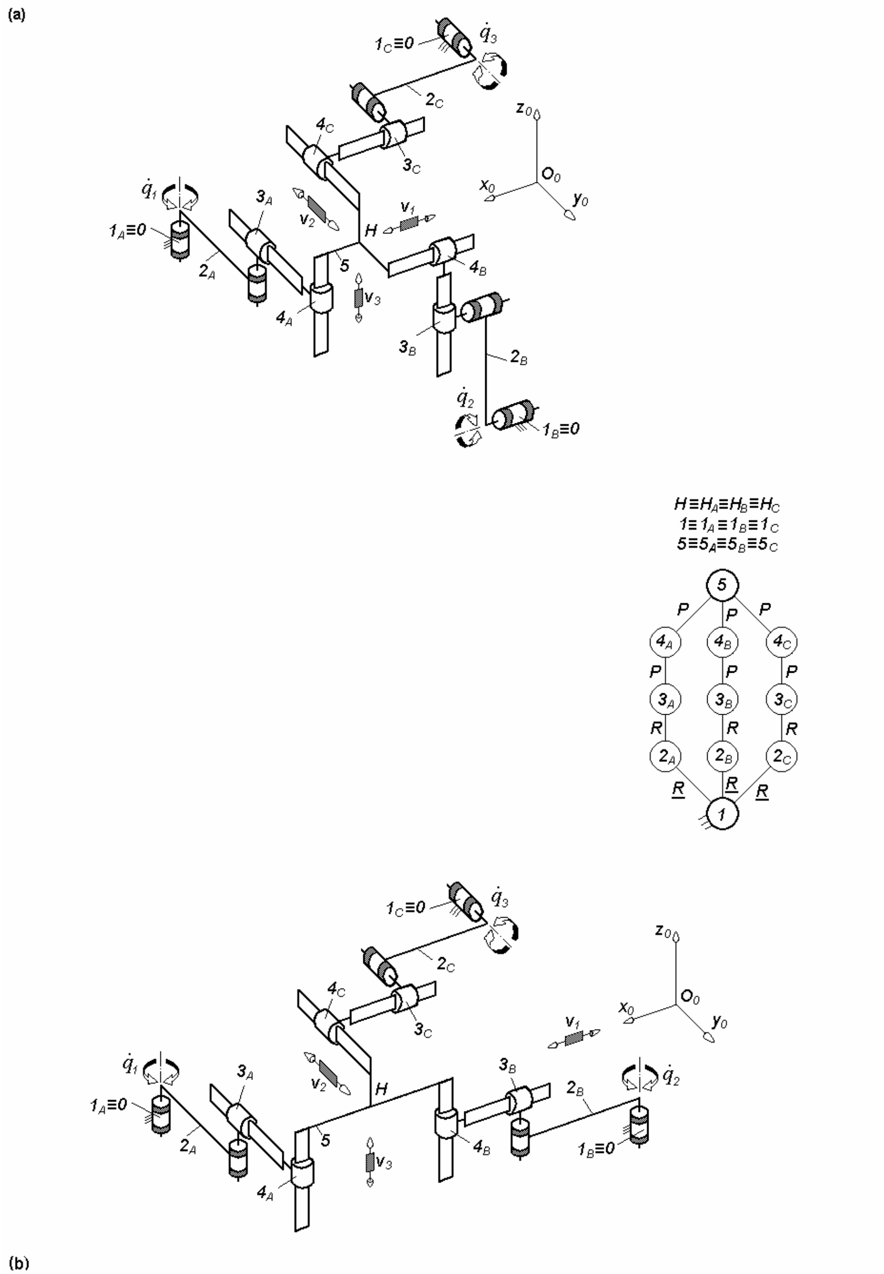


**Fig. 5.18.** *3-$\underline{R}RPP$*-type overconstrained TPMs with uncoupled motions and rotating actuators mounted on the fixed base, defined by $M_F = S_F = 3$, $(R_F) = (\boldsymbol{v}_1, \boldsymbol{v}_2, \boldsymbol{v}_3)$, $T_F = 0$, $N_F = 3$, limb topology $\underline{R} \| R \perp P \perp^{\|} P$

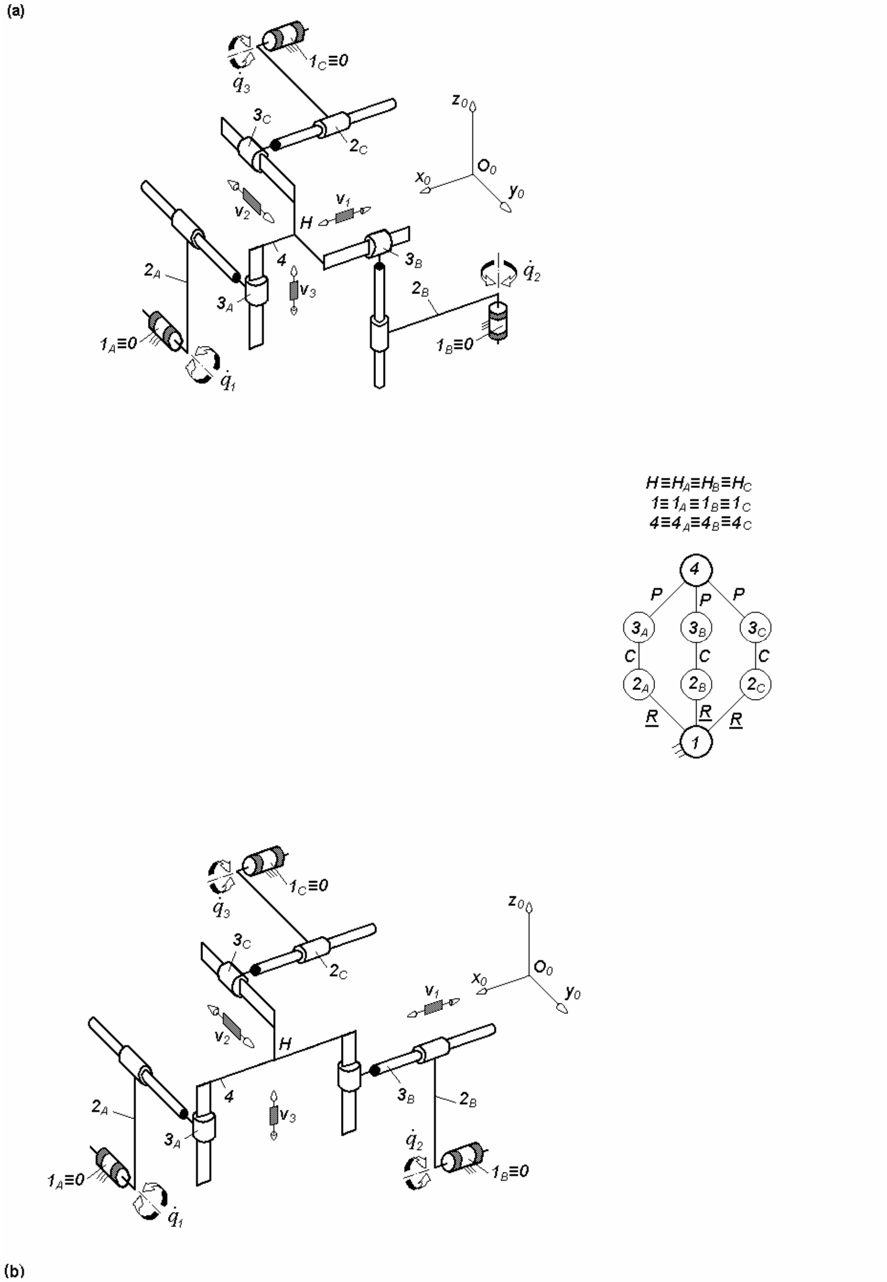


**Fig. 5.19.** *3-<u>R</u>CP*-type overconstrained TPMs with uncoupled motions and rotating actuators mounted on the fixed base, defined by $M_F = S_F = 3$, $(R_F) = (\mathbf{v}_1, \mathbf{v}_2, \mathbf{v}_3)$, $T_F = 0$, $N_F = 3$, limb topology $\underline{R}||C \perp P$

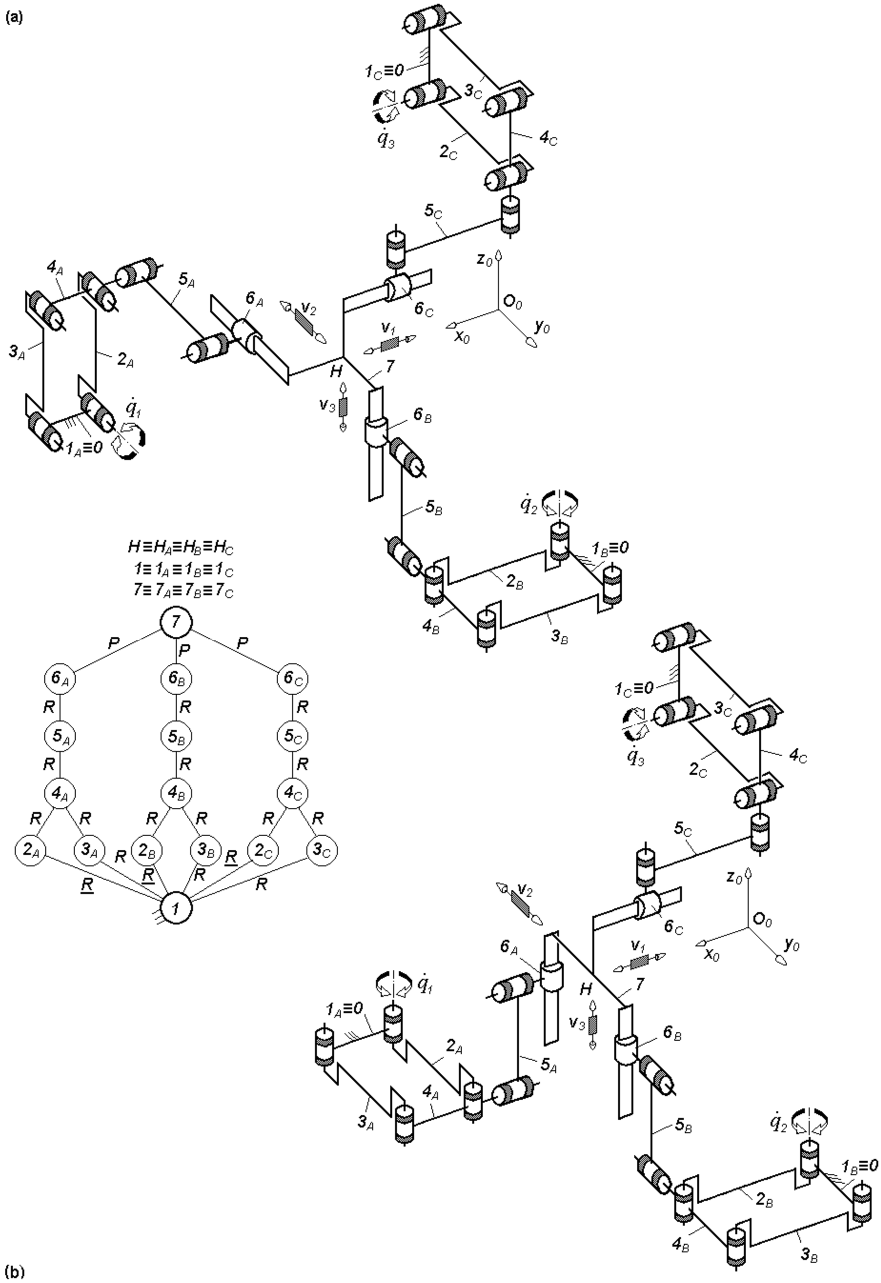


**Fig. 5.20.** *3-<u>Pa</u>RRP*-type overconstrained TPMs with uncoupled motions and rotating actuators mounted on the fixed base, defined by $M_F = S_F = 3$, $(R_F) = (\boldsymbol{v}_1, \boldsymbol{v}_2, \boldsymbol{v}_3)$, $T_F = 0$, $N_F = 12$, limb topology $\underline{Pa} \perp R||R \perp^{||} P$

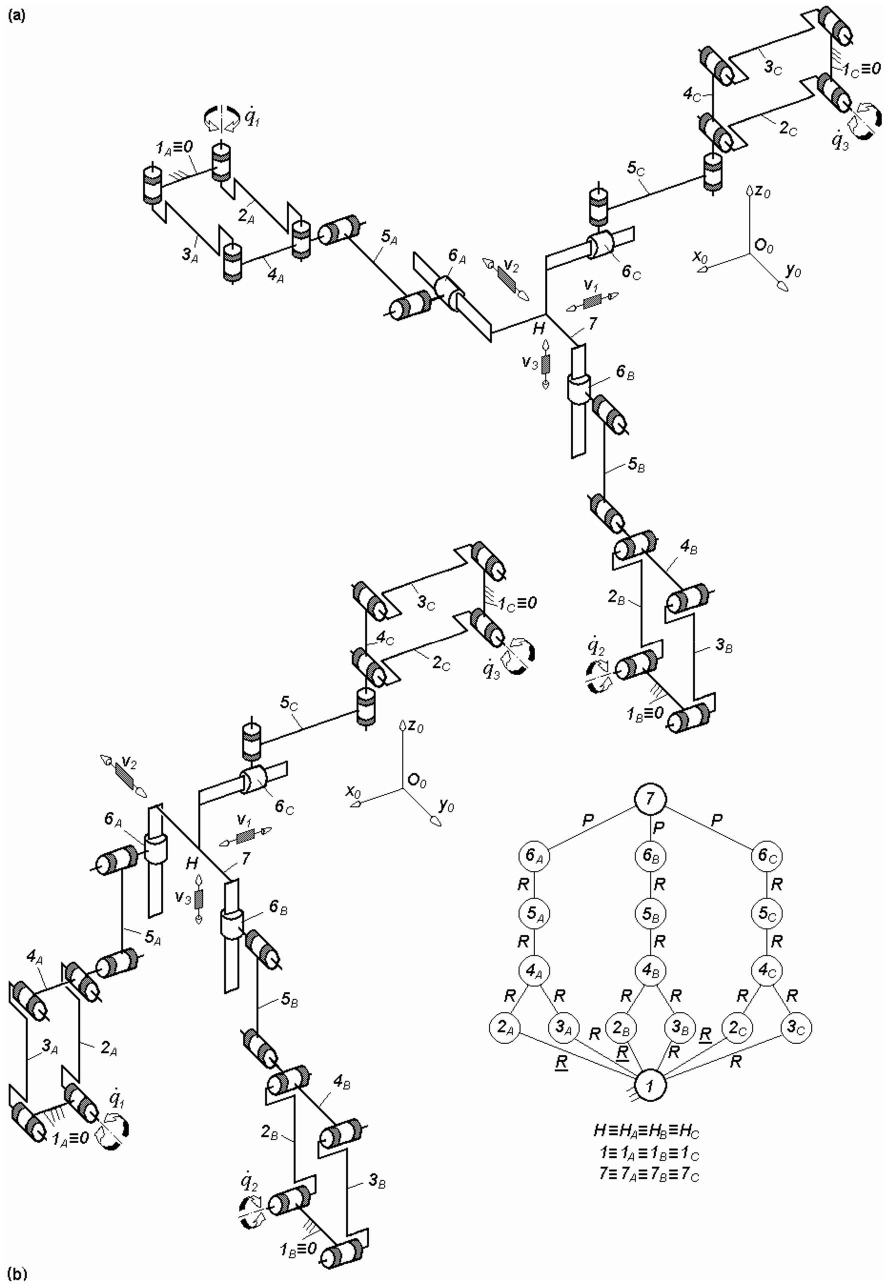


**Fig. 5.21.** *3-<u>Pa</u>RRP*-type overconstrained TPMs with uncoupled motions and rotating actuators mounted on the fixed base, defined by $M_F = S_F = 3$, $(R_F) = (\boldsymbol{v}_1, \boldsymbol{v}_2, \boldsymbol{v}_3)$, $T_F = 0$, $N_F = 12$, limb topology $\underline{Pa} \perp R || R \perp^{\perp} P$

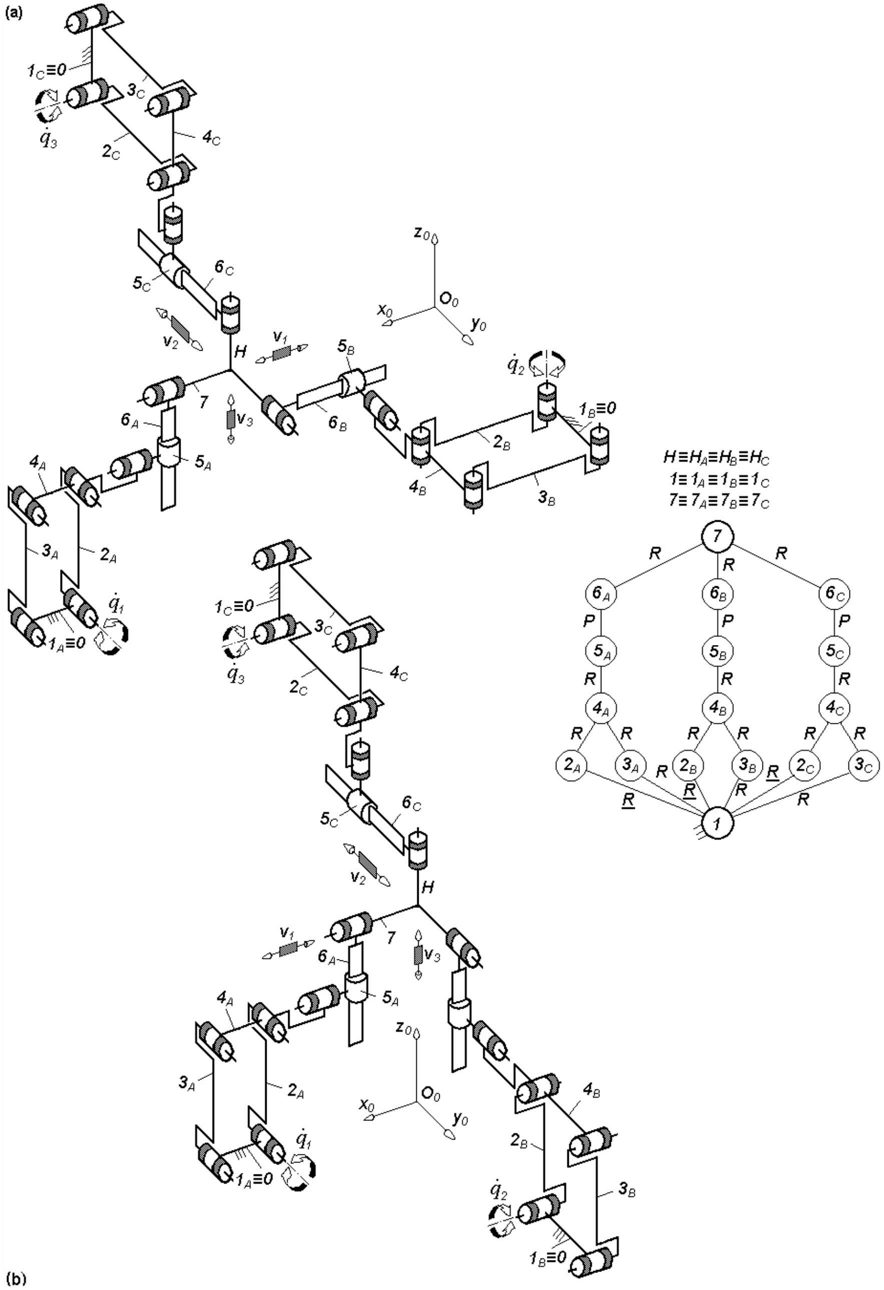


**Fig. 5.22.** *3-PaRPR*-type overconstrained TPMs with uncoupled motions and rotating actuators mounted on the fixed base, defined by $M_F = S_F = 3$, $(R_F) = (\boldsymbol{v}_1, \boldsymbol{v}_2, \boldsymbol{v}_3)$, $T_F = 0$, $N_F = 12$, limb topology $\underline{Pa} \perp R \perp P \perp^{||} R$

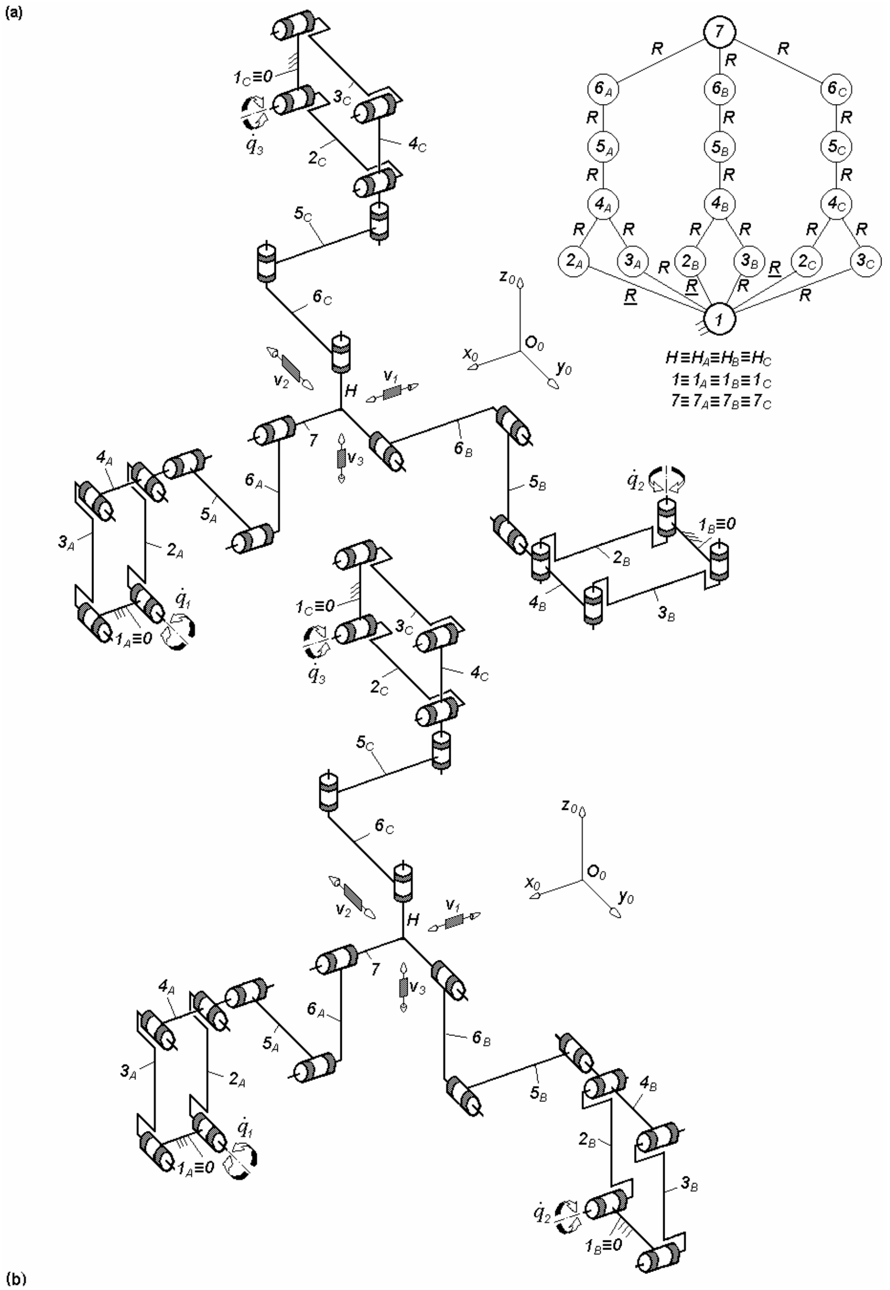


**Fig. 5.23.** *3-<u>Pa</u>RRR*-type overconstrained TPMs with uncoupled motions and rotating actuators mounted on the fixed base, defined by $M_F = S_F = 3$, $(R_F) = (\boldsymbol{v}_1, \boldsymbol{v}_2, \boldsymbol{v}_3)$, $T_F = 0$, $N_F = 12$, limb topology $\underline{Pa} \perp R||R||R$

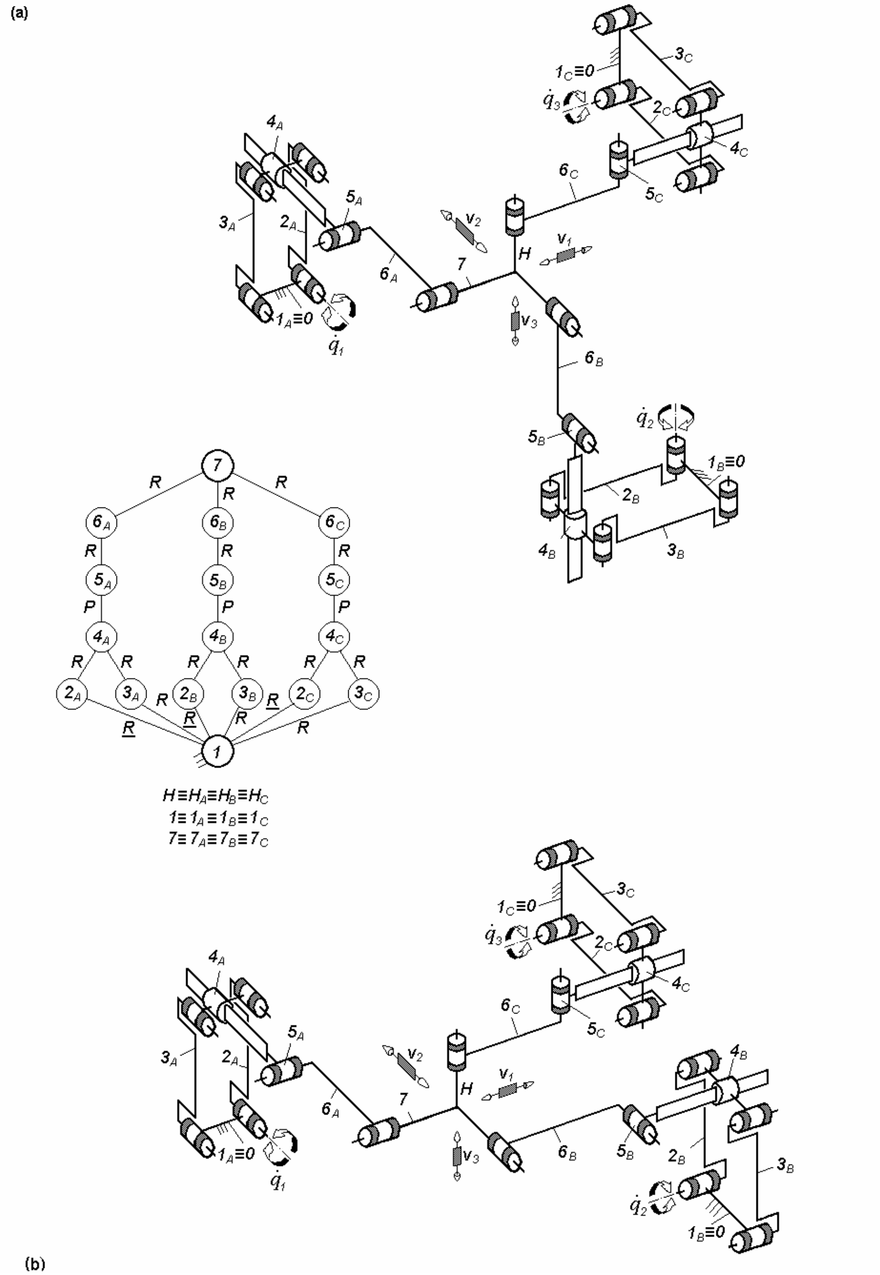


**Fig. 5.24.** *3-<u>Pa</u>PRR*-type overconstrained TPMs with uncoupled motions and rotating actuators mounted on the fixed base, defined by $M_F = S_F = 3$, $(R_F) = (\boldsymbol{v}_1, \boldsymbol{v}_2, \boldsymbol{v}_3)$, $T_F = 0$, $N_F = 12$, limb topology $\underline{Pa}||P \perp R||R$

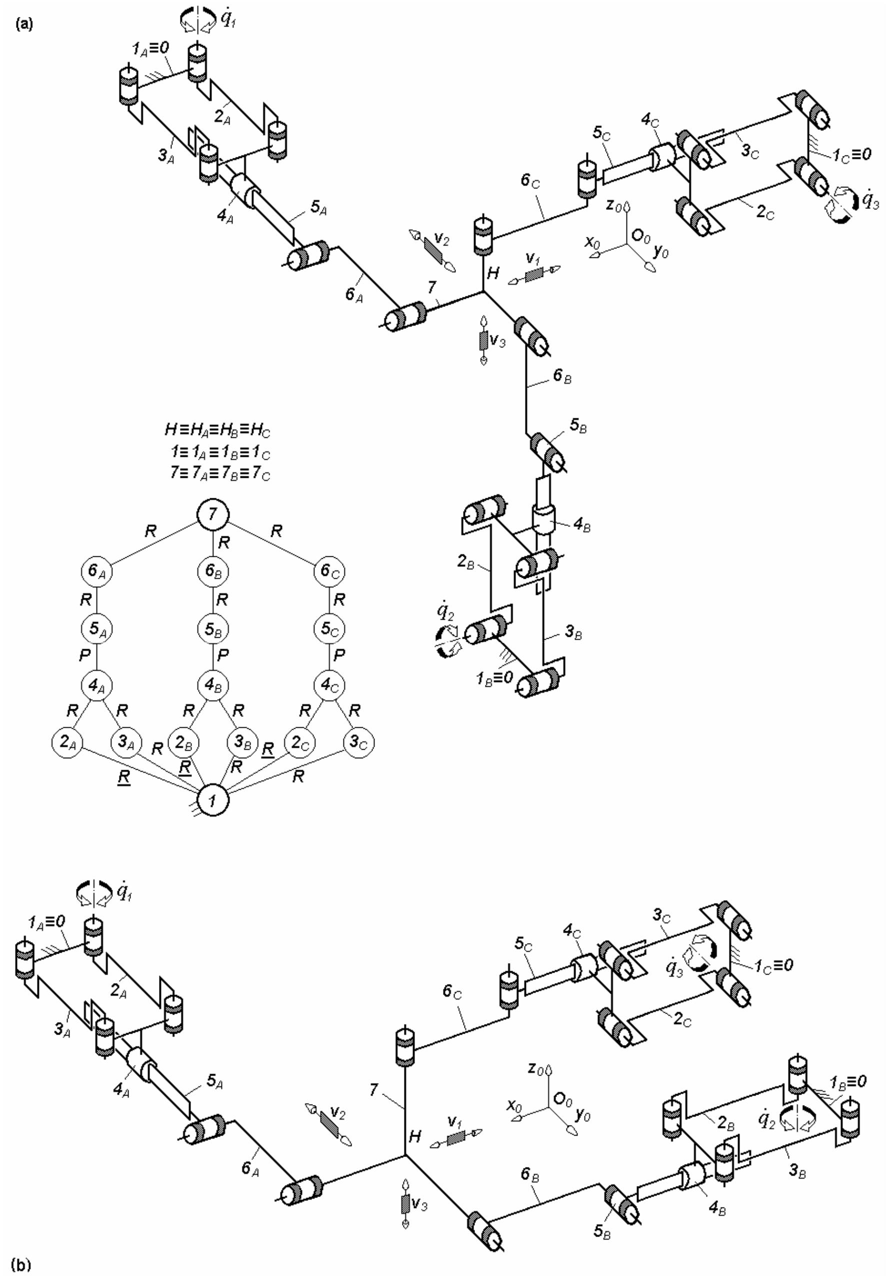


**Fig. 5.25.** *3-<u>Pa</u>PRR*-type overconstrained TPMs with uncoupled motions and rotating actuators mounted on the fixed base defined by $M_F = S_F = 3$, $(R_F) = (\boldsymbol{v}_1, \boldsymbol{v}_2, \boldsymbol{v}_3)$, $T_F = 0$, $N_F = 12$, limb topology $\underline{Pa} \perp P \perp^{\perp} R||R$

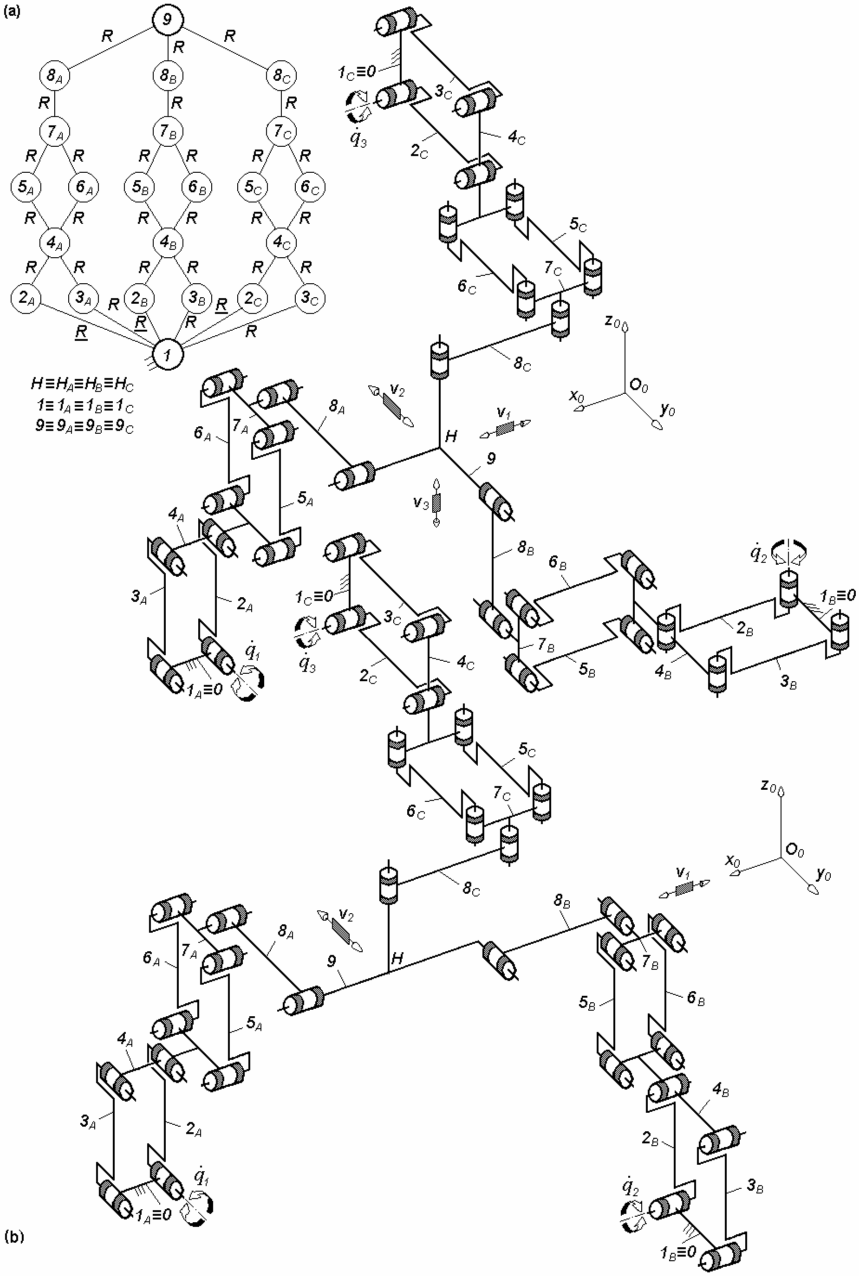


**Fig. 5.26.** *3-<u>Pa</u>PaRR*-type overconstrained TPMs with uncoupled motions and rotating actuators mounted on the fixed base, defined by $M_F = S_F = 3$, $(R_F) = (\boldsymbol{v}_1, \boldsymbol{v}_2, \boldsymbol{v}_3)$, $T_F = 0$, $N_F = 21$, limb topology $\underline{Pa} \perp Pa||R||R$

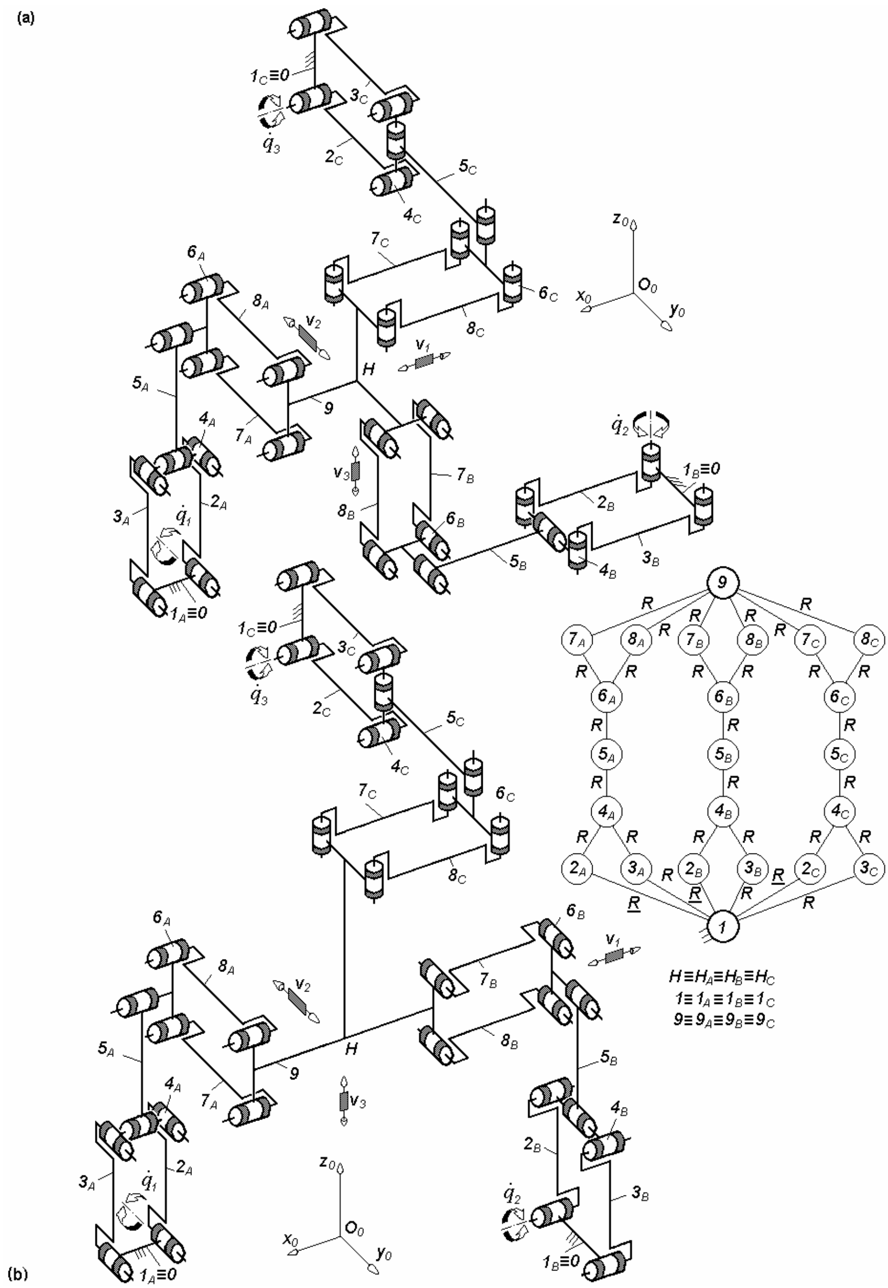


**Fig. 5.27.** *3-<u>Pa</u>RRPa*-type overconstrained TPMs with uncoupled motions and rotating actuators mounted on the fixed base, defined by $M_F = S_F = 3$, $(R_F) = (\boldsymbol{v}_1, \boldsymbol{v}_2, \boldsymbol{v}_3)$, $T_F = 0$, $N_F = 21$, limb topology <u>*Pa*</u>$\perp R||R||Pa$

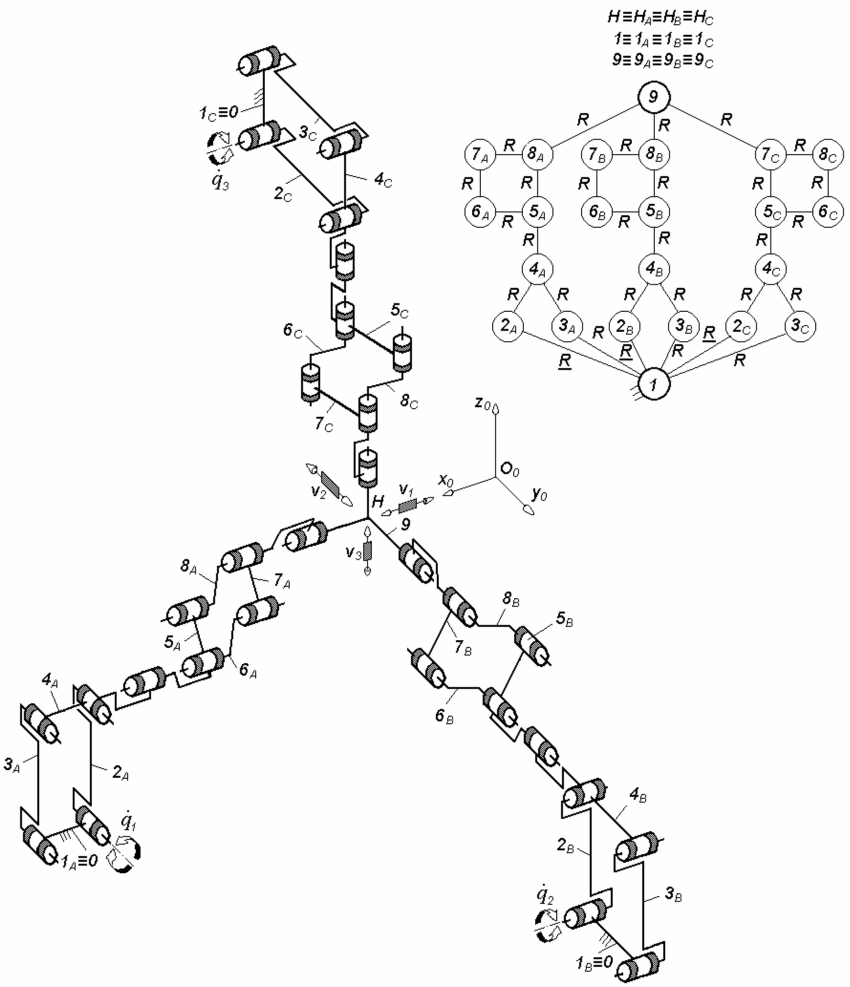


**Fig. 5.28.** *3-<u>Pa</u>RRbR*-type overconstrained TPMs with uncoupled motions and rotating actuators mounted on the fixed base, defined by $M_F = S_F = 3$, $(R_F) = (\mathbf{v}_1, \mathbf{v}_2, \mathbf{v}_3)$, $T_F = 0$, $N_F = 21$, limb topology <u>*Pa*</u>$\perp R||Rb||R$

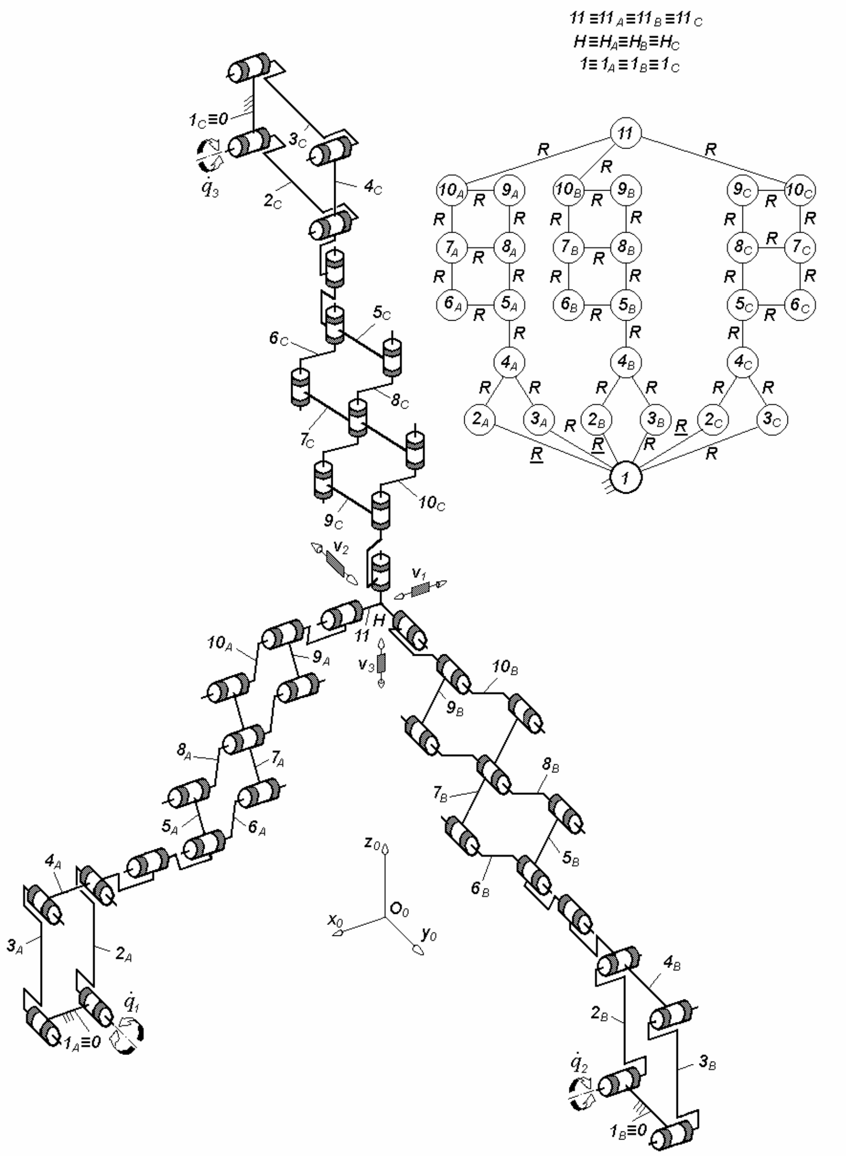

**Fig. 5.29.** *3-PaRRbRbR*-type overconstrained TPMs with uncoupled motions and rotating actuators mounted on the fixed base, defined by $M_F = S_F = 3$, $(R_F) = (\mathbf{v}_1, \mathbf{v}_2, \mathbf{v}_3)$, $T_F = 0$, $N_F = 30$, limb topology $\underline{Pa} \perp R||Rb||Rb||R$

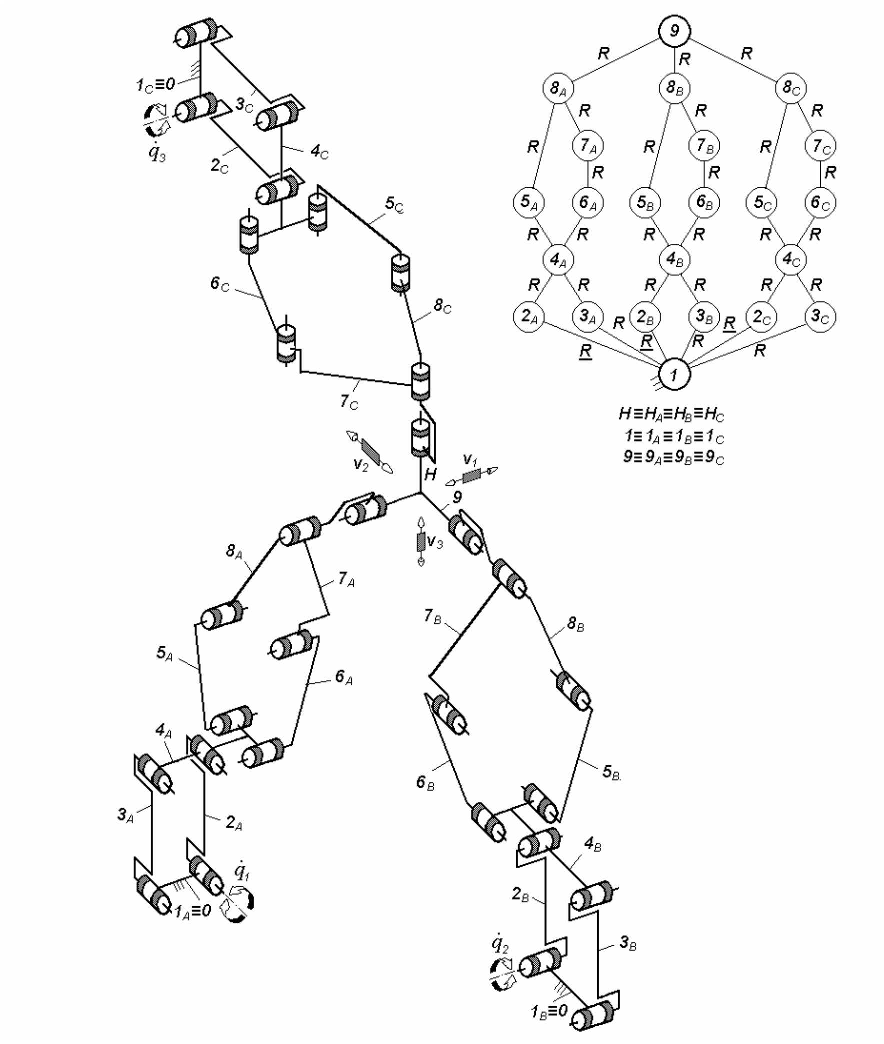


**Fig. 5.30.** *3-PaPn2R*-type overconstrained TPMs with uncoupled motions and rotating actuators mounted on the fixed base, defined by $M_F = S_F = 3$, $(R_F) = (\boldsymbol{v}_1, \boldsymbol{v}_2, \boldsymbol{v}_3)$, $T_F = 0$, $N_F = 21$, limb topology $\underline{Pa} \perp Pn2 || R$

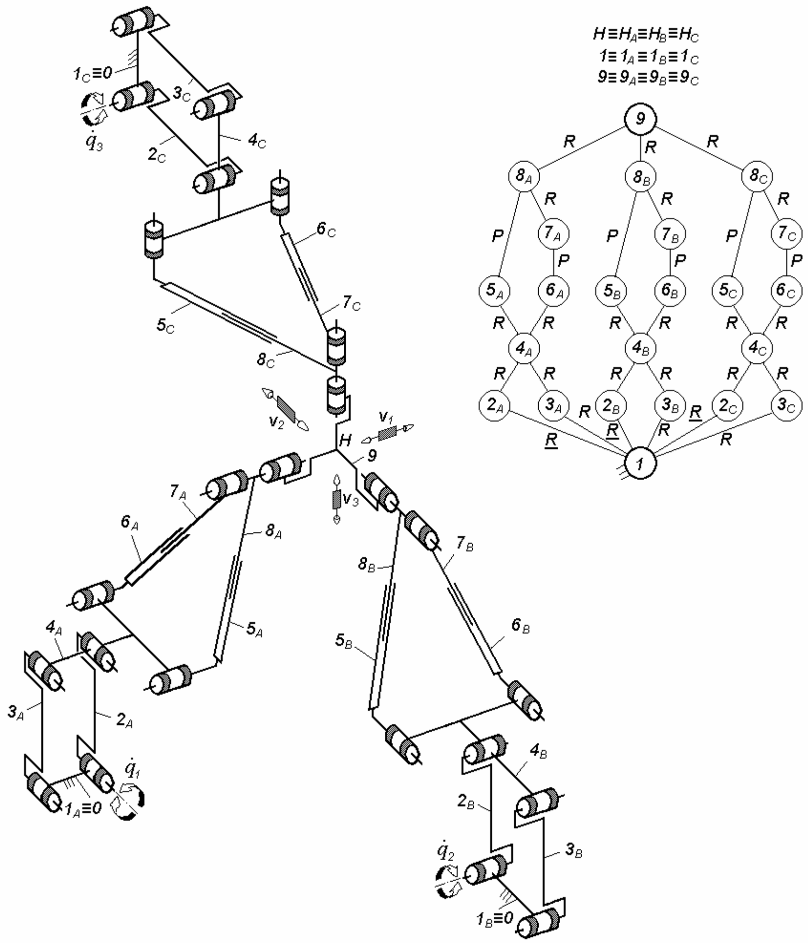

**Fig. 5.31.** *3-PaPn2R*-type overconstrained TPMs with uncoupled motions and rotating actuators mounted on the fixed base, defined by $M_F = S_F = 3$, $(R_F) = (\boldsymbol{v}_1, \boldsymbol{v}_2, \boldsymbol{v}_3)$, $T_F = 0$, $N_F = 21$, limb topology $\underline{Pa} \perp Pn2 || R$

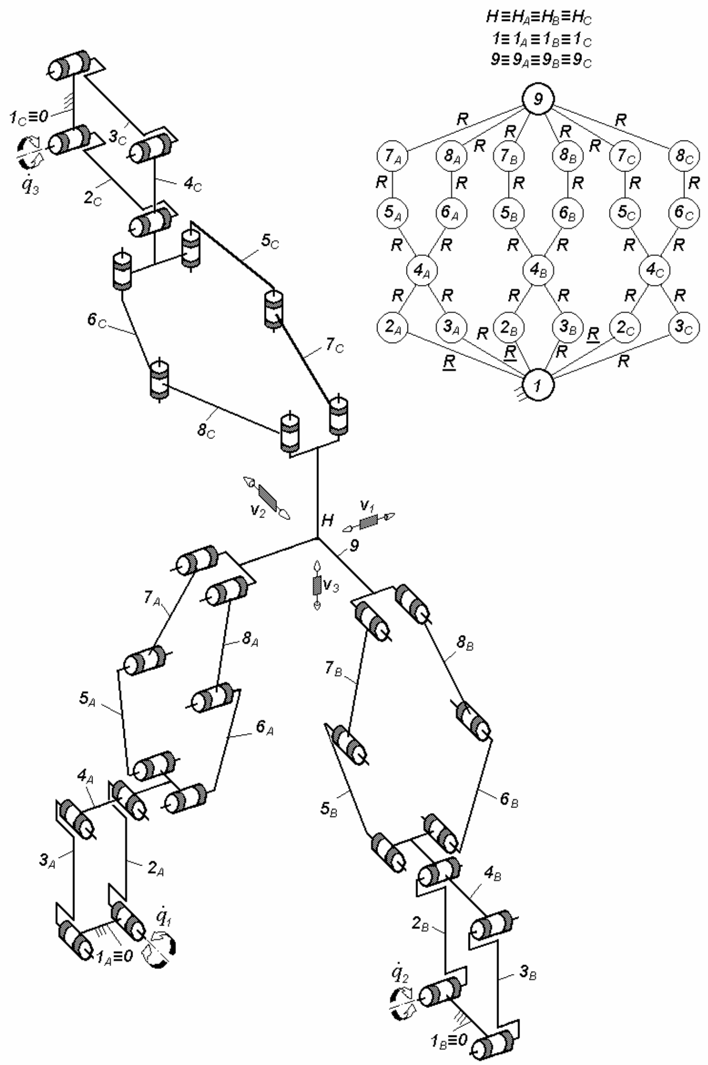


**Fig. 5.32.** *3-PaPn3*-type overconstrained TPMs with uncoupled motions and rotating actuators mounted on the fixed base, defined by $M_F = S_F = 3$, $(R_F) = (\boldsymbol{v}_1, \boldsymbol{v}_2, \boldsymbol{v}_3)$, $T_F = 0$, $N_F = 21$, limb topology $\underline{Pa} \perp Pn3$

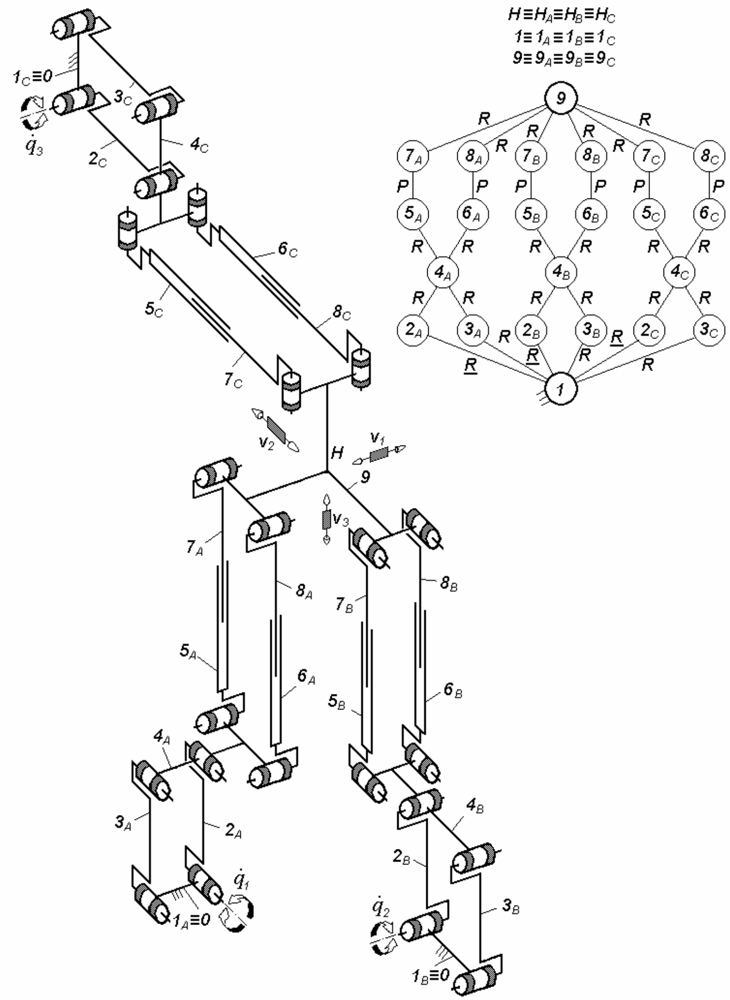

**Fig. 5.33.** *3-<u>Pa</u>Pn3*-type overconstrained TPMs with uncoupled motions and rotating actuators mounted on the fixed base, defined by $M_F = S_F = 3$, $(R_F) = (\boldsymbol{v}_1, \boldsymbol{v}_2, \boldsymbol{v}_3)$, $T_F = 0$, $N_F = 21$, limb topology $\underline{Pa} \perp Pn3$

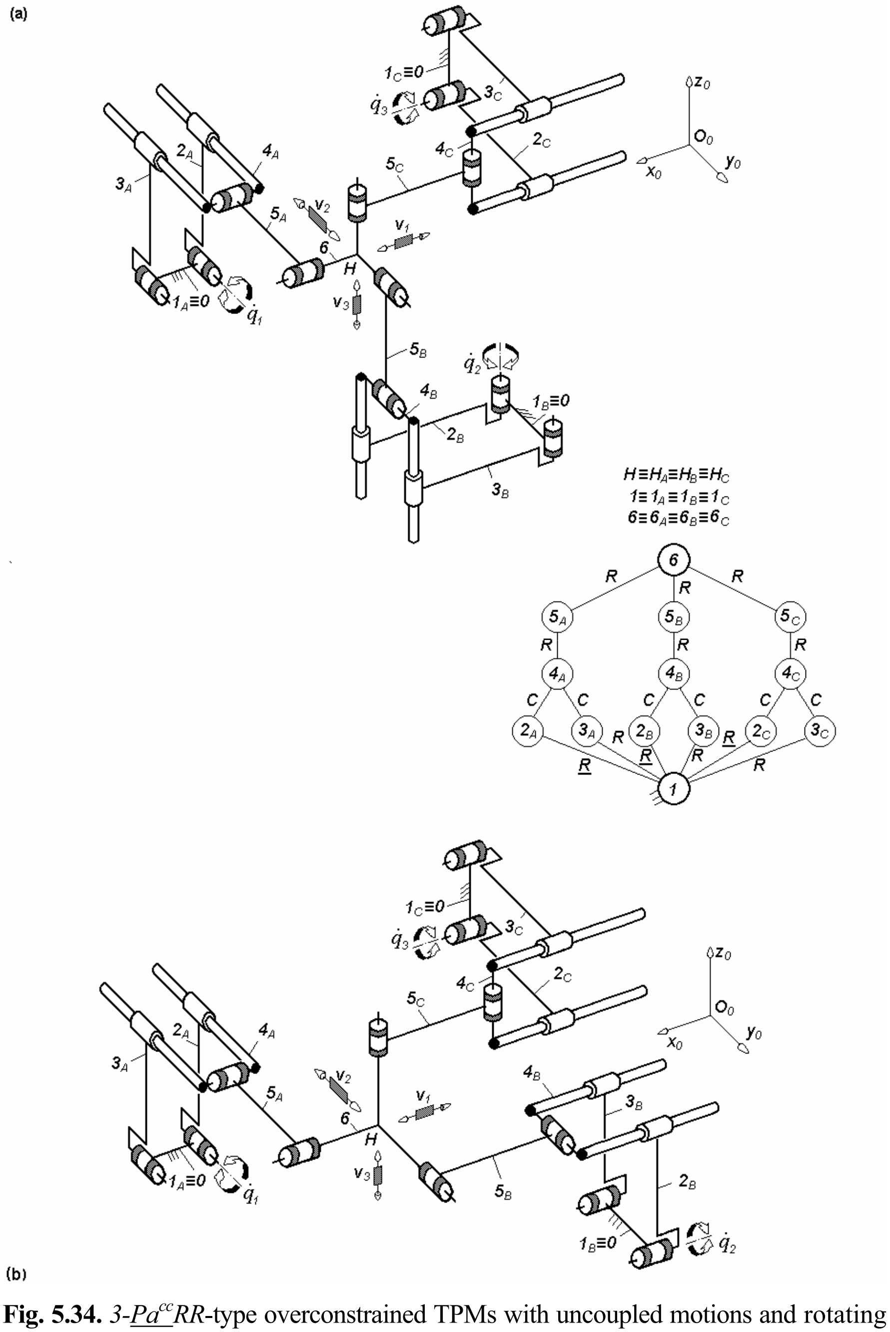


**Fig. 5.34.** *3-*$\underline{Pa^{cc}}RR$-type overconstrained TPMs with uncoupled motions and rotating actuators mounted on the fixed base, defined by $M_F = S_F = 3$, $(R_F) = (\boldsymbol{v}_1, \boldsymbol{v}_2, \boldsymbol{v}_3)$, $T_F = 0$, $N_F = 9$, limb topology $\underline{Pa^{cc}} \perp R||R$

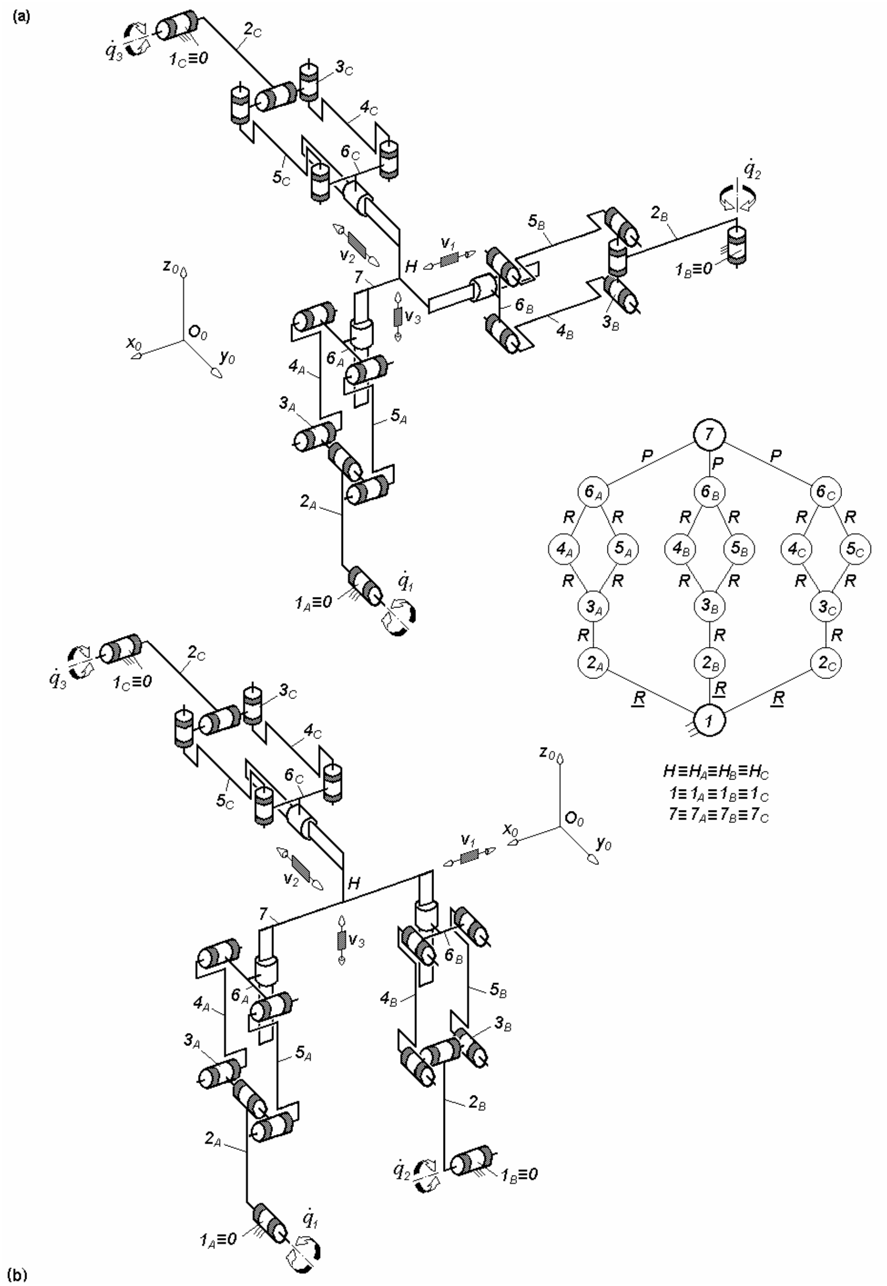


**Fig. 5.35.** *3-RRPaP*-type overconstrained TPMs with uncoupled motions and rotating actuators mounted on the fixed base, defined by $M_F = S_F = 3$, $(R_F) = (\boldsymbol{v}_1, \boldsymbol{v}_2, \boldsymbol{v}_3)$, $T_F = 0$, $N_F = 12$, limb topology $\underline{R}||R \perp Pa \perp^{\perp} P$

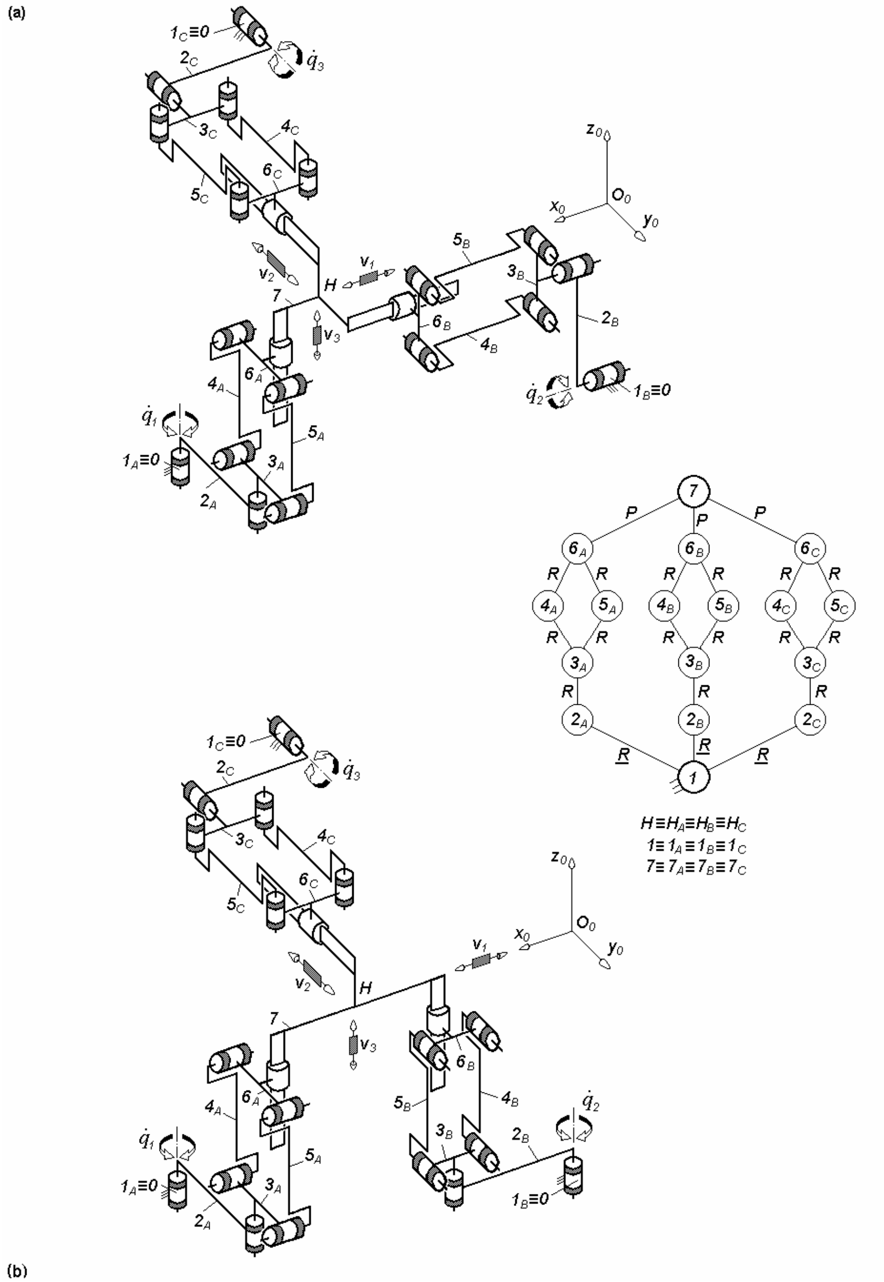


**Fig. 5.36.** *3-RRPaP*-type overconstrained TPMs with uncoupled motions and rotating actuators mounted on the fixed base, defined by $M_F = S_F = 3$, $(R_F) = (\mathbf{v}_1, \mathbf{v}_2, \mathbf{v}_3)$, $T_F = 0$, $N_F = 12$, limb topology $\underline{R}||R \perp Pa \perp^{||} P$

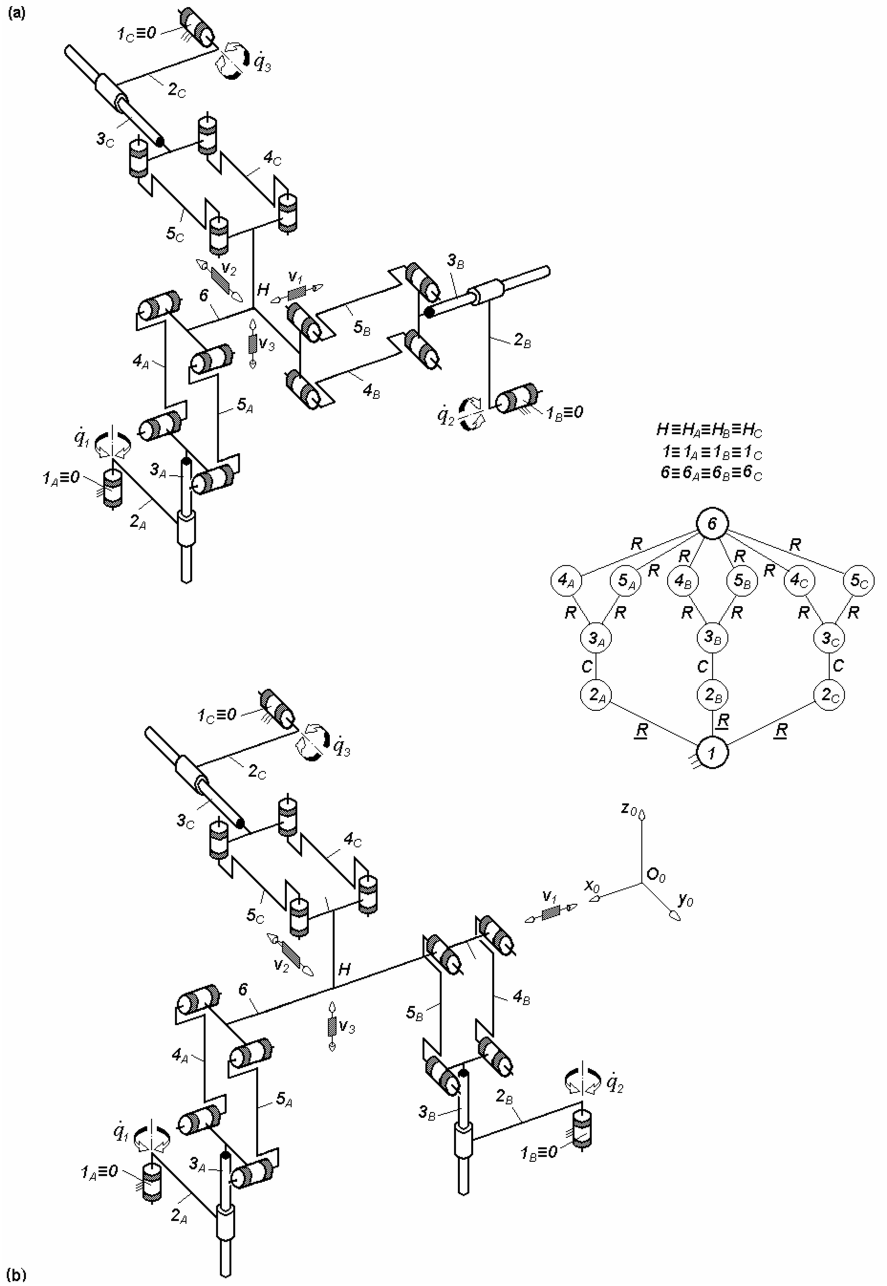


**Fig. 5.37.** *3-<u>R</u>CPa*-type overconstrained TPMs with uncoupled motions and rotating actuators mounted on the fixed base defined by $M_F = S_F = 3$, $(R_F) = (\boldsymbol{v}_1, \boldsymbol{v}_2, \boldsymbol{v}_3)$, $T_F = 0$, $N_F = 12$, limb topology $\underline{R}||C \perp Pa$

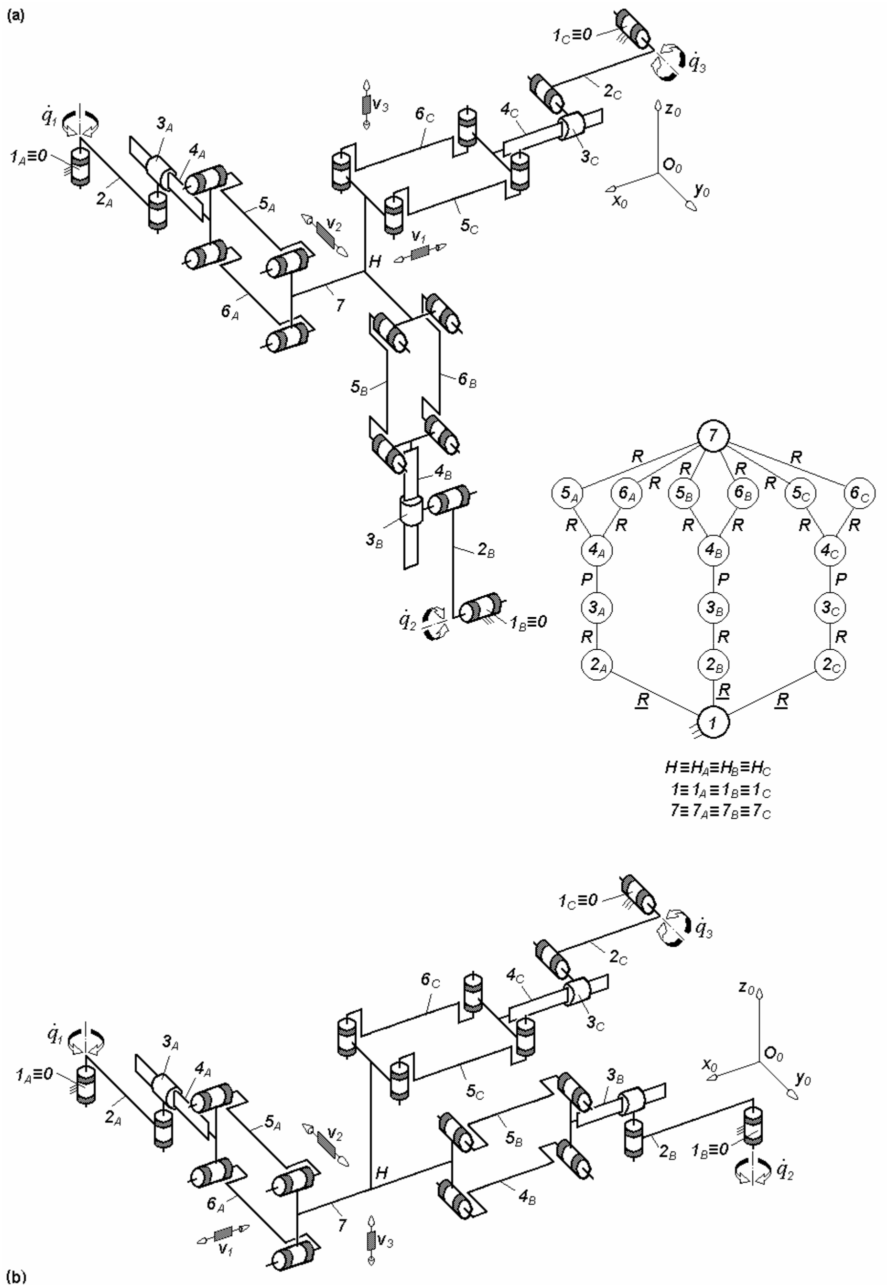


**Fig. 5.38.** 3-$\underline{R}RPPa$-type overconstrained TPMs with uncoupled motions and rotating actuators mounted on the fixed base defined by $M_F = S_F = 3$, $(R_F) = (\boldsymbol{v}_1, \boldsymbol{v}_2, \boldsymbol{v}_3)$, $T_F = 0$, $N_F = 12$, limb topology $\underline{R}||R \perp P \perp^{\perp} Pa$

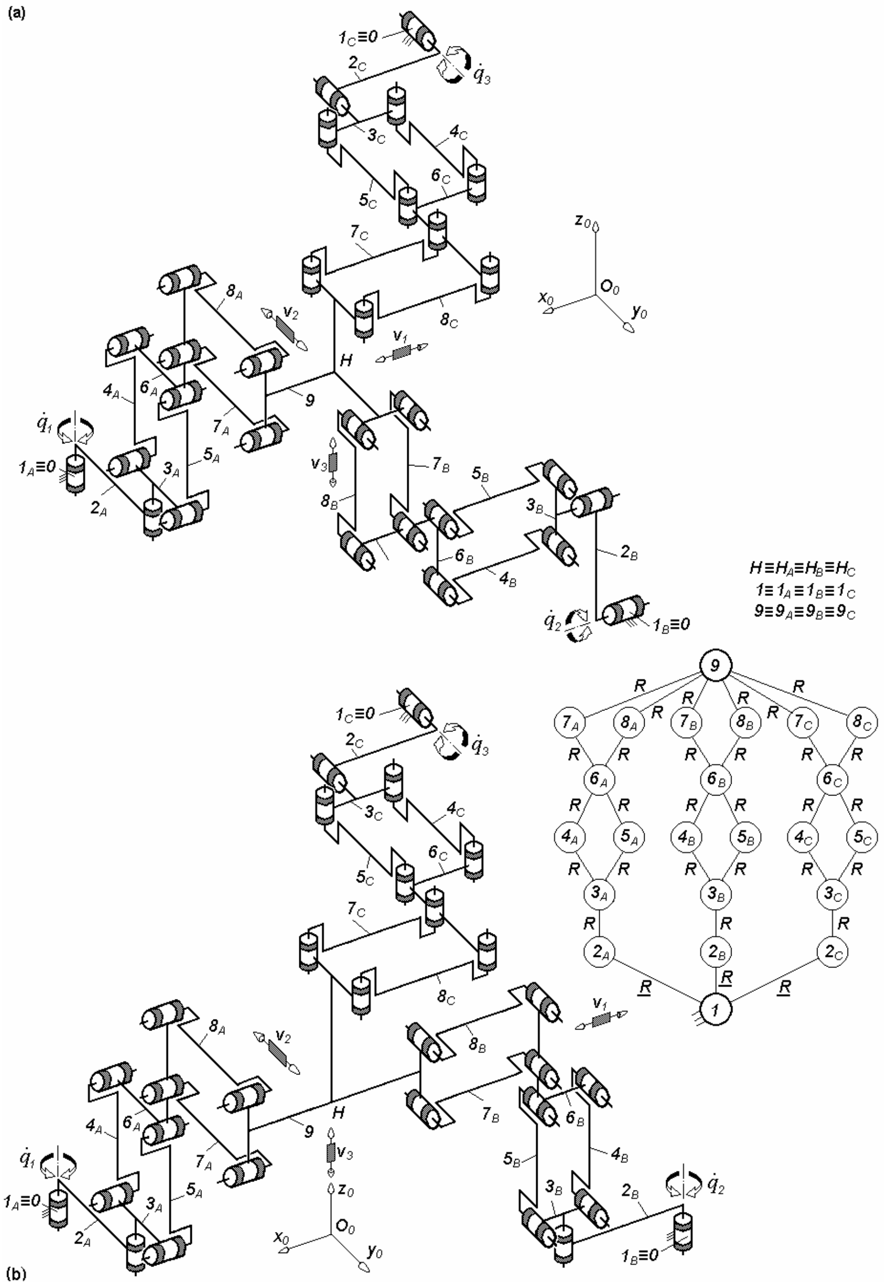


**Fig. 5.39.** *3-RRPaPa*-type overconstrained TPMs with uncoupled motions and rotating actuators mounted on the fixed base, defined by $M_F = S_F = 3$, $(R_F) = (\boldsymbol{v}_1, \boldsymbol{v}_2, \boldsymbol{v}_3)$, $T_F = 0$, $N_F = 21$, limb topology $\underline{R}||R \perp Pa||Pa$

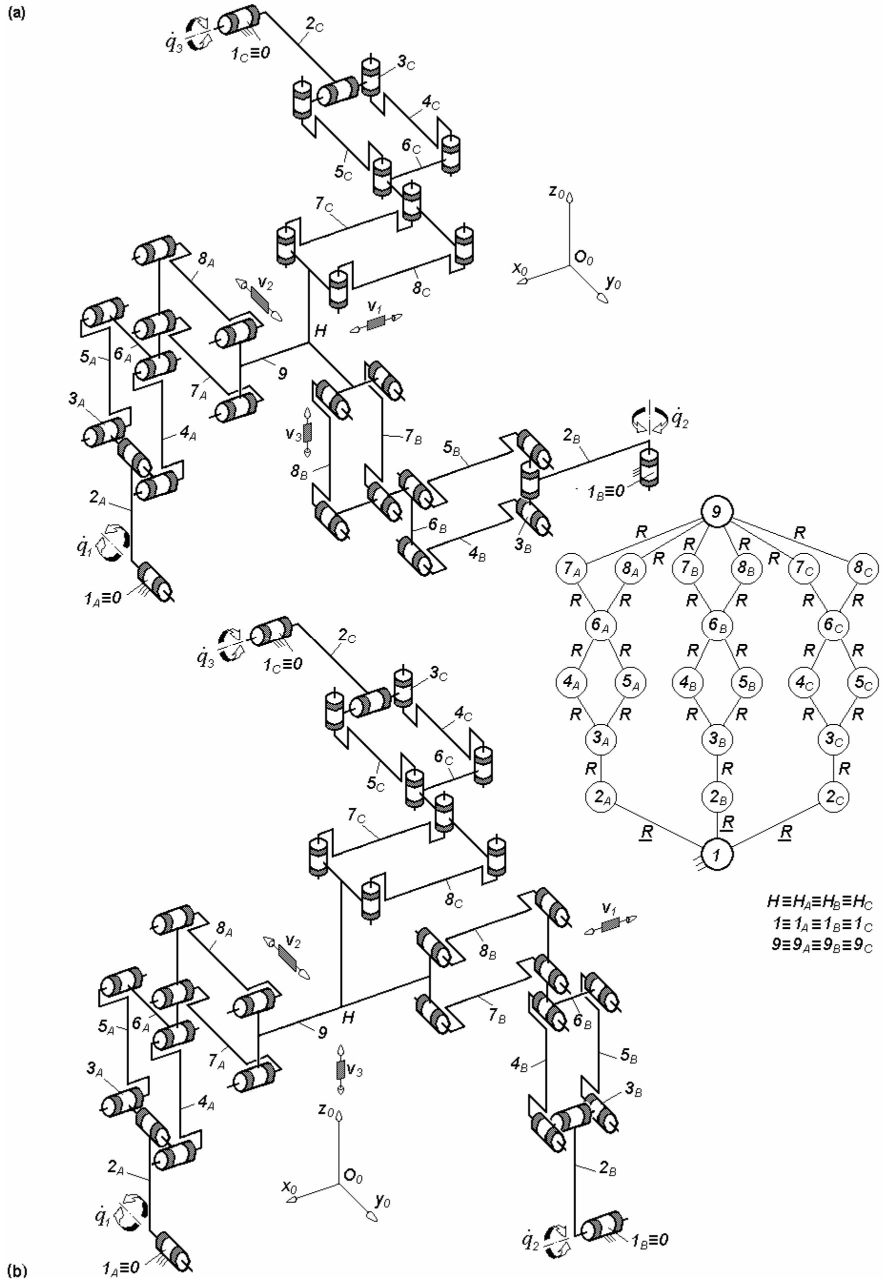


**Fig. 5.40.** *3-RRPaPa*-type overconstrained TPMs with uncoupled motions and rotating actuators mounted on the fixed base, defined by $M_F = S_F = 3$, $(R_F) = (\boldsymbol{v}_1, \boldsymbol{v}_2, \boldsymbol{v}_3)$, $T_F = 0$, $N_F = 21$, limb topology $\underline{R}||R \perp Pa||Pa$

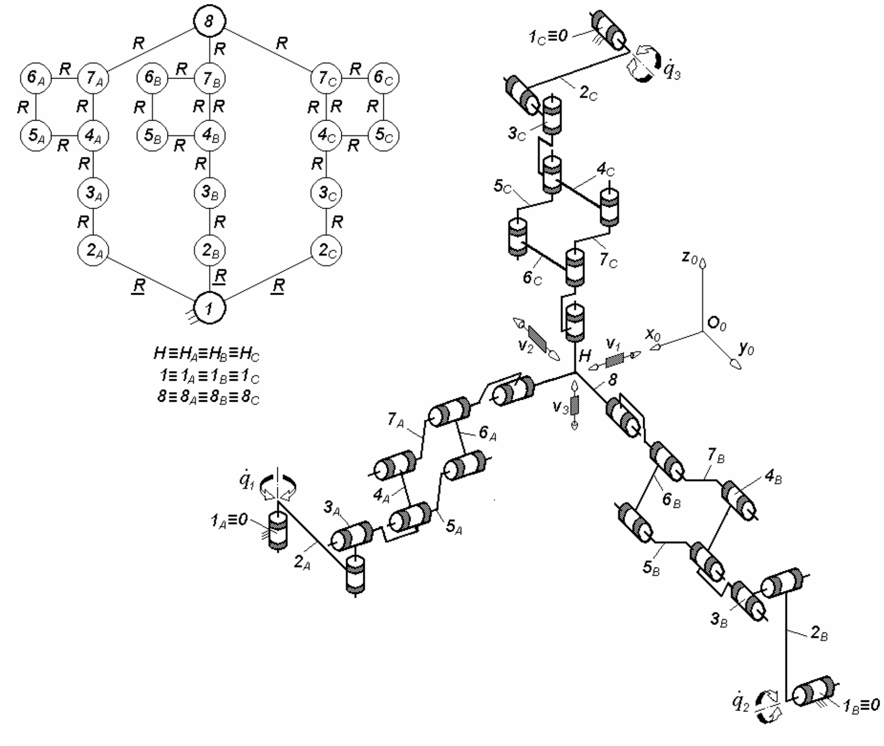


**Fig. 5.41.** *3-RRRRbR*-type overconstrained TPMs with uncoupled motions and rotating actuators mounted on the fixed base, defined by $M_F = S_F = 3$, $(R_F) = (\boldsymbol{v}_1, \boldsymbol{v}_2, \boldsymbol{v}_3)$, $T_F = 0$, $N_F = 9$ limb topology $\underline{R}||R \perp R||Rb||R$

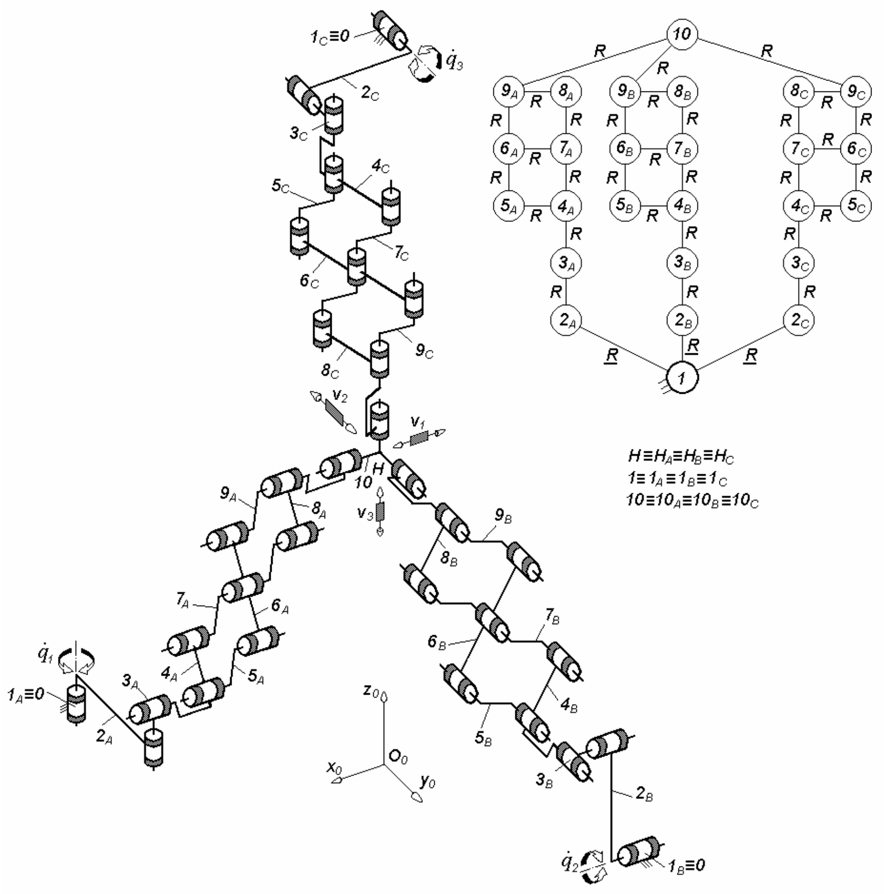


**Fig. 5.42.** *3-RRRRbRbR*-type overconstrained TPMs with uncoupled motions and rotating actuators mounted on the fixed base, defined by $M_F = S_F = 3$, $(R_F) = (\boldsymbol{v}_1, \boldsymbol{v}_2, \boldsymbol{v}_3)$, $T_F = 0$, $N_F = 18$, limb topology $\underline{R}||R \perp R||Rb||Rb||R$

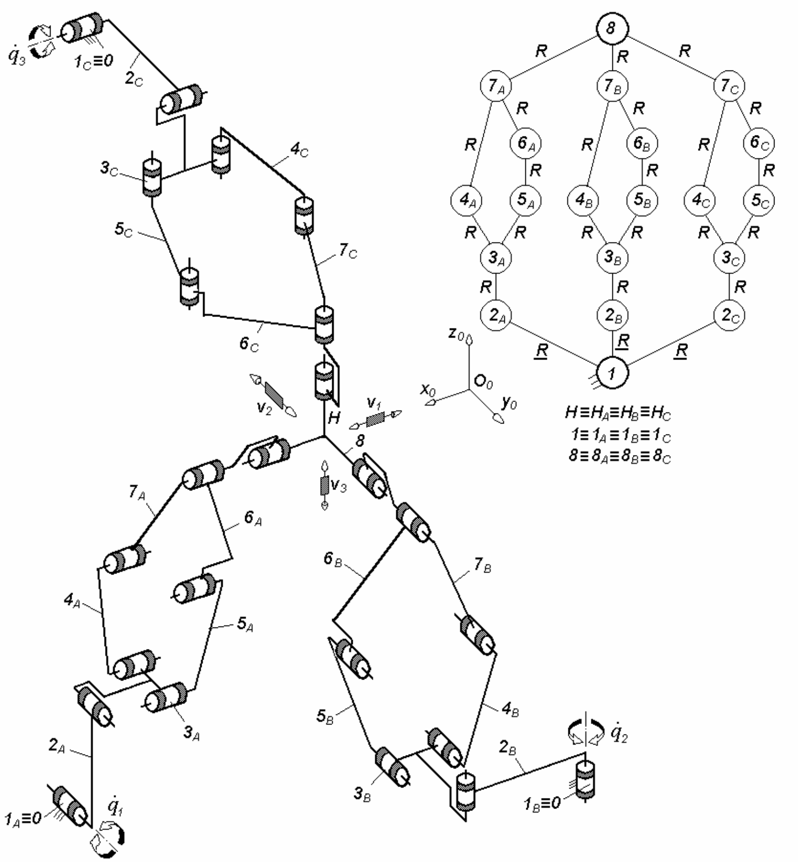


**Fig. 5.43.** *3-RRPn2R*-type overconstrained TPMs with uncoupled motions and rotating actuators mounted on the fixed base, defined by $M_F = S_F = 3$, $(R_F) = (\boldsymbol{v}_1, \boldsymbol{v}_2, \boldsymbol{v}_3)$, $T_F = 0$, $N_F = 9$, limb topology $\underline{R}||R \perp Pn2||R$

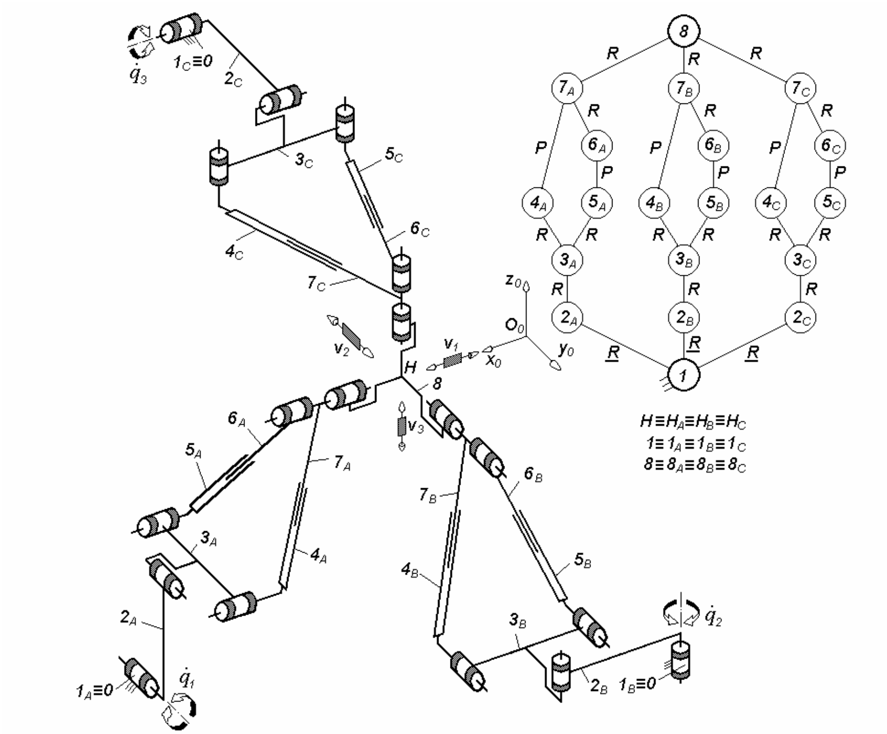


**Fig. 5.44.** *3-<u>R</u>RPn2R*-type overconstrained TPMs with uncoupled motions and rotating actuators mounted on the fixed base, defined by $M_F = S_F = 3$, $(R_F) = (\boldsymbol{v}_1, \boldsymbol{v}_2, \boldsymbol{v}_3)$, $T_F = 0$, $N_F = 9$, limb topology $\underline{R}||R \perp Pn2||R$

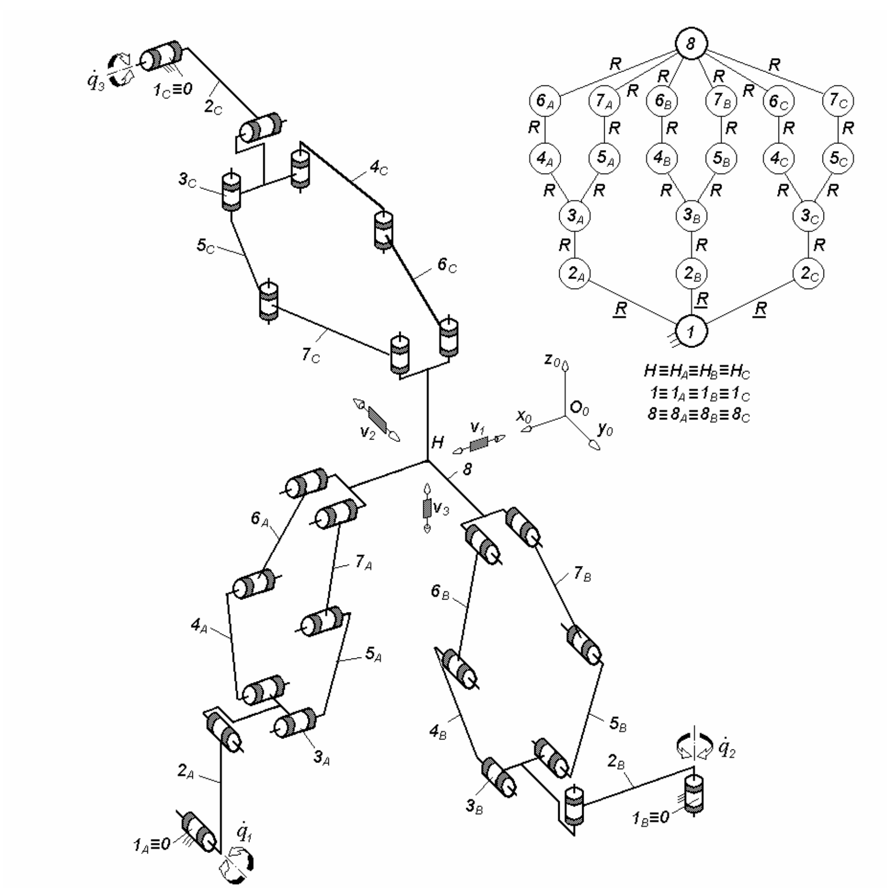


**Fig. 5.45.** *3-RRPn3*-type overconstrained TPMs with uncoupled motions and rotating actuators mounted on the fixed base, defined by $M_F = S_F = 3$, $(R_F) = (\mathbf{v}_1, \mathbf{v}_2, \mathbf{v}_3)$, $T_F = 0$, $N_F = 9$, limb topology $\underline{R}||R \perp Pn3$

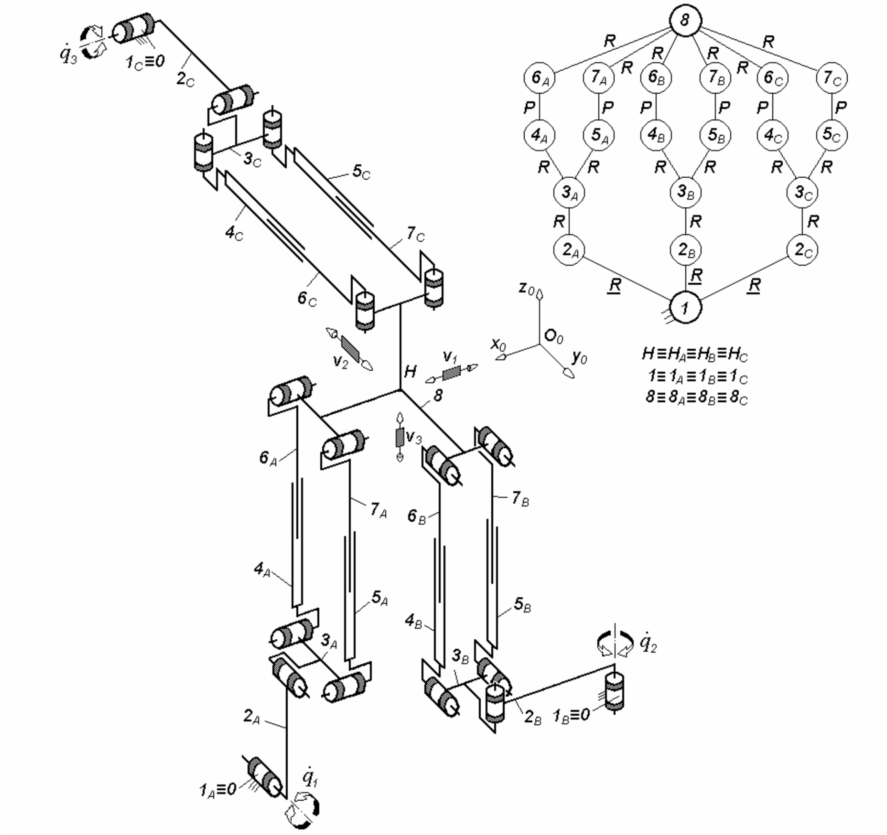


**Fig. 5.46.** *3-RRPn3*-type overconstrained TPMs with uncoupled motions and rotating actuators mounted on the fixed base, defined by $M_F = S_F = 3$, $(R_F) = (\boldsymbol{v}_1, \boldsymbol{v}_2, \boldsymbol{v}_3)$, $T_F = 0$, $N_F = 9$, limb topologies $\underline{R}||R \perp Pn3$

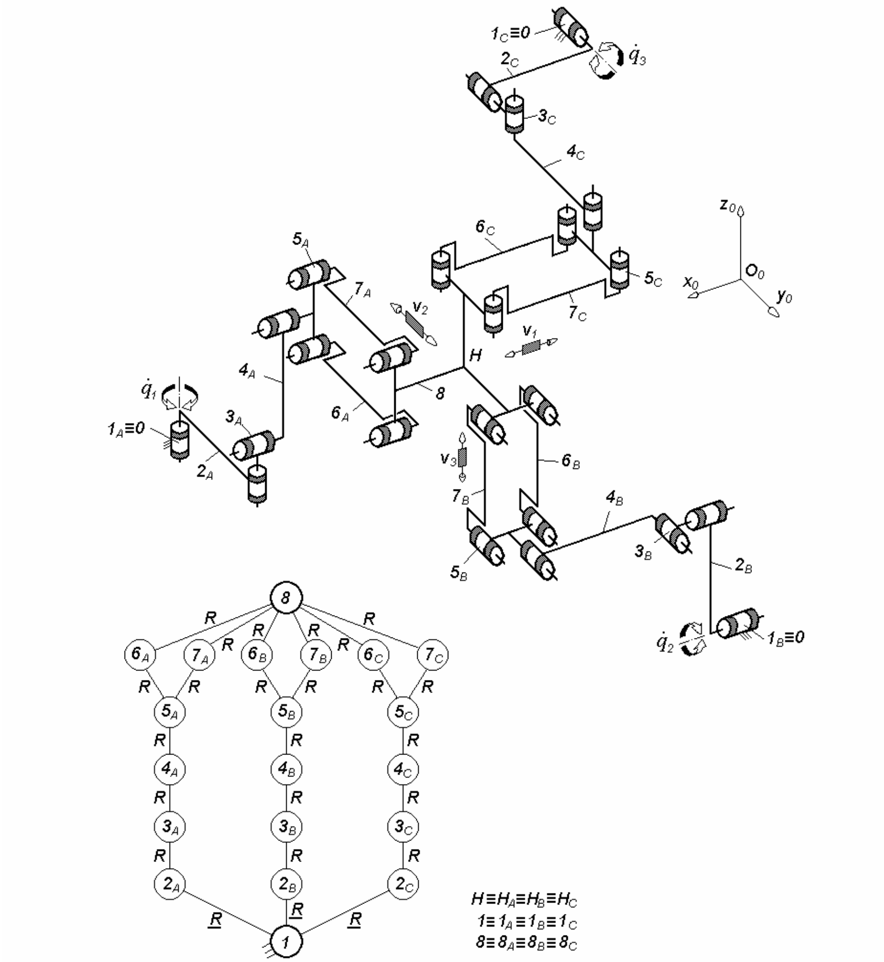


**Fig. 5.47.** *3-<u>R</u>RRRPa*-type overconstrained TPM with uncoupled motions and rotating actuators mounted on the fixed base, defined by $M_F = S_F = 3$, $(R_F) = (\mathbf{v}_1, \mathbf{v}_2, \mathbf{v}_3)$, $T_F = 0$, $N_F = 9$, limb topology $\underline{R}||R \perp R||R||Pa$

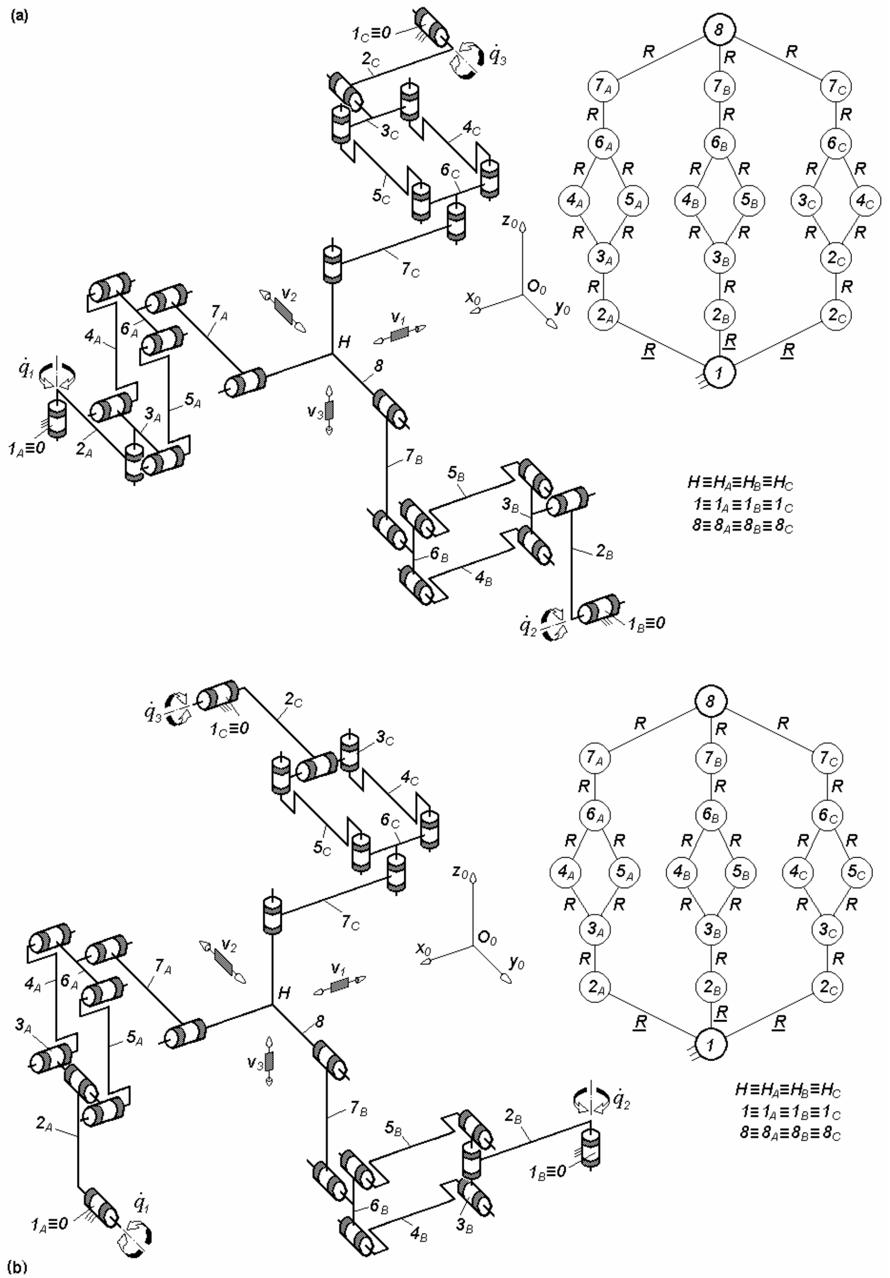


**Fig. 5.48.** *3-RRPaRR*-type overconstrained TPMs with uncoupled motions and rotating actuators mounted on the fixed base, defined by $M_F = S_F = 3$, $(R_F) = (\boldsymbol{v}_1, \boldsymbol{v}_2, \boldsymbol{v}_3)$, $T_F = 0$, $N_F = 9$, limb topology $\underline{R}||R\perp Pa||R||R$

## 5.2 Derived solutions with rotating actuators

Solutions with lower degrees of overconstraint can be derived from the basic solutions in Figs. 5.6–5.48 by using joints with *idle mobilities*. A large set of solutions can be obtained by introducing one or two rotational idle mobilities outside the closed loops that can be integrated in the limbs and up to three idle mobilities (two rotations and one translation) in each planar loop. The joints combining idle mobilities are denoted by an asterisk. We recall that the idle mobilities combined in a parallelogram loop (see Fig. 6.3 – Part 1) are systematized in Table 3.12. Two idle rotational mobilities are introduced in the spherical joint of the parallelogram loops denoted by $Pa^{ccs}$ and $Pa^{scc}$ which combines two cylindrical, one revolute and one spherical joint. In the cylindrical joint denoted by *C**, the rotation is the idle mobility.

For example, the solution *3-<u>Pa</u>PC**-type in Fig. 5.49 is derived from the basic solution *3-<u>Pa</u>PP* in Fig. 5.6 by replacing the last prismatic joint *P* in each limb by a cylindrical joint *C** which combines a rotational idle mobility.

Examples of solutions with identical limbs and three to twenty one degrees of overconstraint derived from the basic solutions in Figs. 5.6–5.48 are illustrated in Figs. 5.49–5.108. The limb topology and the number of overconstraints in these solutions are systematized in Table 5.13 and the structural parameters in Tables 5.14–5.26.

**Table 5.13.** Limb topology and the number of overconstraints $N_F$ of the derived TPMs with idle mobilities and rotating actuators mounted on the fixed base presented in Figs. 5.49–5.108

| No. | Basic TPM type | $N_F$ | Derived TPM type | $N_F$ | Limb topology |
|---|---|---|---|---|---|
| 1 | $3\text{-}\underline{Pa}PP$ (Fig. 5.6) | *15* | $3\text{-}\underline{Pa}PC^*$ (Fig. 5.49) | *12* | $\underline{Pa}\|P\perp C^*$ |
| 2 | | | $3\text{-}\underline{Pa}^{ss}PP$ (Fig. 5.50) | *3* | $\underline{Pa}^{ss}\|P\perp P$ |
| 3 | $3\text{-}\underline{Pa}PP$ (Fig. 5.7) | *15* | $3\text{-}\underline{Pa}PC^*$ (Fig. 5.51) | *12* | $\underline{Pa}\perp P\perp^{\|}C^*$ |
| 4 | | | $3\text{-}\underline{Pa}^{ss}PP$ $\underline{Pa}^{ss}\perp P\perp^{\|}P$ (Fig. 5.52) | *3* | $\underline{Pa}^{ss}\perp P\perp^{\|}P$ |
| 5 | $3\text{-}\underline{Pa}PaP$ (Fig. 5.8a) | *24* | $3\text{-}\underline{Pa}Pa^{ss}P$ (Fig. 5.53a) | *12* | $\underline{Pa}\perp Pa^{ss}\perp^{\|}P$ |
| 6 | | | $3\text{-}\underline{Pa}Pa^{cs}P$ (Fig. 5.53b) | *15* | $\underline{Pa}\perp Pa^{cs}\perp^{\|}P$ |
| 7 | | | $3\text{-}\underline{Pa}^{ss}PaP$ (Fig. 5.54a) | *12* | $\underline{Pa}^{ss}\perp Pa\perp^{\|}P$ |
| 8 | | | $3\text{-}\underline{Pa}Pa^{cs}PR^*R^*$ (Fig. 5.54b) | *9* | $\underline{Pa}\perp Pa^{cs}\perp^{\|}P\perp^{\perp}R^*\perp^{\|}R^*$ |
| 9 | $3\text{-}\underline{Pa}PaP$ (Fig. 5.9) | *24* | $3\text{-}\underline{Pa}Pa^{ss}P$ (Fig. 5.55a) | *12* | $\underline{Pa}\perp Pa^{ss}\perp^{\perp}P$ |
| 10 | | | $3\text{-}\underline{Pa}Pa^{cs}P$ (Fig. 5.55b) | *15* | $\underline{Pa}\perp Pa^{cs}\perp^{\perp}P$ |
| 11 | | | $3\text{-}\underline{Pa}^{ss}PaP$ (Fig. 5.56a) | *12* | $\underline{Pa}^{ss}\perp Pa\perp^{\perp}P$ |
| 12 | | | $3\text{-}\underline{Pa}Pa^{cs}PR^*R^*$ (Fig. 5.56b) | *9* | $\underline{Pa}\perp Pa^{cs}\perp^{\perp}P\perp^{\perp}R^*\perp^{\|}R^*$ |
| 13 | $3\text{-}\underline{Pa}PPa$ (Fig. 5.10) | *24* | $3\text{-}\underline{Pa}PPa^{ss}$ (Fig. 5.57a) | *12* | $\underline{Pa}\|P\perp Pa^{ss}$ |
| 14 | | | $3\text{-}\underline{Pa}^{cs}PPa$ (Fig. 5.57b) | *15* | $\underline{Pa}^{cs}\|P\perp Pa$ |
| 15 | | | $3\text{-}\underline{Pa}^{ss}PPa$ (Fig. 5.58a) | *12* | $\underline{Pa}^{ss}\|P\perp Pa$ |
| 16 | | | $3\text{-}\underline{Pa}PPa^{cs}R^*R^*$ (Fig. 5.58b) | *9* | $\underline{Pa}\|P\perp Pa^{cs}\perp^{\|}R^*\perp^{\perp}R^*$ |
| 17 | $3\text{-}\underline{Pa}PPa$ (Fig. 5.11) | *24* | $3\text{-}\underline{Pa}PPa^{ss}$ (Fig. 5.59a) | *12* | $\underline{Pa}\perp P\perp^{\perp}Pa^{ss}$ |
| 18 | | | $3\text{-}\underline{Pa}^{cs}PPa$ (Fig. 5.59b) | *15* | $\underline{Pa}^{cs}\perp P\perp^{\perp}Pa$ |
| 19 | | | $3\text{-}\underline{Pa}^{ss}PPa$ (Fig. 5.60a) | *12* | $\underline{Pa}^{ss}\perp P\perp^{\perp}Pa$ |

**Table 5.13.** (cont.)

| | | | | | |
|---|---|---|---|---|---|
| 20 | | | $3\text{-}\underline{Pa}PPa^{cs}R^*R^*$<br>(Fig. 5.60b) | *9* | $\underline{Pa}\perp P\perp^{\perp}Pa^{cs}\perp^{\|\|}R^*\perp^{\perp}R^*$ |
| 21 | $3\text{-}\underline{Pa}PaPa$<br>(Fig. 5.12) | *33* | $3\text{-}\underline{Pa}PaPa^{ss}$<br>(Fig. 5.61) | *21* | $\underline{Pa}\perp Pa\|\|Pa^{ss}$ |
| 22 | | | $3\text{-}\underline{Pa}^{ss}PaPa^{ss}$<br>(Fig. 5.62) | *9* | $\underline{Pa}^{ss}\perp Pa\|\|Pa^{ss}$ |
| 23 | | | $3\text{-}\underline{Pa}PaPa^{cs}$<br>(Fig. 5.63) | *24* | $\underline{Pa}\perp Pa\|\|Pa^{cs}$ |
| 24 | | | $3\text{-}\underline{Pa}^{cs}PaPa^{cs}R^*R^*$<br>(Fig. 5.64) | *9* | $\underline{Pa}^{cs}\perp Pa\|\|Pa^{cs}\perp^{\|\|}R^*\perp^{\perp}R^*$ |
| 25 | $3\text{-}\underline{Pa}Pa^{t}P$<br>(Fig. 5.14) | *24* | $3\text{-}\underline{Pa}Pa^{t}C^*$<br>(Fig. 5.65) | *21* | $\underline{Pa}\|\|Pa^{t}\|\|C^*$ |
| 26 | | | $3\text{-}\underline{Pa}Pa^{tss}P$<br>(Fig. 5.66a) | *12* | $\underline{Pa}\|\|Pa^{tss}\|\|P$ |
| 27 | | | $3\text{-}\underline{Pa}Pa^{tcs}PR^*$<br>(Fig. 5.66b) | *12* | $\underline{Pa}\|\|Pa^{tcs}\|\|P\perp^{\perp}R^*$ |
| 28 | $3\text{-}\underline{Pa}Pa^{tcc}$<br>(Fig. 5.15) | *21* | $3\text{-}\underline{Pa}^{ss}Pa^{tcc}$<br>(Fig. 5.67a) | *12* | $\underline{Pa}^{ss}\|\|Pa^{tcc}$ |
| 29 | | | $3\text{-}\underline{Pa}^{cs}Pa^{tcc}$<br>(Fig. 5.67b) | *12* | $\underline{Pa}^{cs}\|\|Pa^{tcc}$ |
| 30 | | | $3\text{-}\underline{Pa}^{ss}Pa^{tcc}R^*R^*$<br>(Fig. 5.68a) | *6* | $\underline{Pa}^{ss}\|\|Pa^{tcc}\perp R^*\perp^{\|\|}R^*$ |
| 31 | | | $3\text{-}\underline{Pa}^{cs}Pa^{tcc}R^*R^*$<br>(Fig. 5.68b) | *6* | $\underline{Pa}^{cs}\|\|Pa^{tcc}\perp R^*\perp^{\|\|}R^*$ |
| 32 | $3\text{-}\underline{Pa}^{cc}P$<br>(Fig. 5.16) | *12* | $3\text{-}\underline{Pa}^{cc}C^*R^*$<br>(Fig. 5.69) | *6* | $\underline{Pa}^{cc}\perp C^*\perp R^*$ |
| 33 | | | $3\text{-}\underline{Pa}^{ccs}P$<br>(Fig. 5.70) | *6* | $\underline{Pa}^{ccs}\perp P$ |
| 34 | $3\text{-}\underline{Pa}^{cc}Pa$<br>(Fig. 5.17) | *21* | $3\text{-}\underline{Pa}^{ccs}Pa$<br>(Fig. 5.71) | *15* | $\underline{Pa}^{ccs}\perp Pa$ |
| 35 | | | $3\text{-}\underline{Pa}^{cc}Pa^{ss}R^*$<br>(Fig. 5.72) | *6* | $\underline{Pa}^{cc}\perp Pa^{ss}\|\|R^*$ |
| 36 | $3\text{-}\underline{Pa}RRP$<br>(Fig. 5.20) | *12* | $3\text{-}\underline{Pa}^{ss}RP$<br>(Fig. 5.73 | *3* | $\underline{Pa}^{ss}\perp R\perp^{\|\|}P$ |
| 37 | $3\text{-}\underline{Pa}RRP$<br>(Fig. 5.21) | *12* | $3\text{-}\underline{Pa}^{ss}RP$<br>(Fig. 5.74) | *3* | $\underline{Pa}^{ss}\perp R\perp^{\perp}P$ |
| 38 | | | $3\text{-}\underline{Pa}RRC^*$<br>(Fig. 5.75) | *9* | $\underline{Pa}\perp R\|\|R\perp^{\perp}C^*$ |
| 39 | $3\text{-}\underline{Pa}RPR$<br>(Fig. 5.22) | *12* | $3\text{-}\underline{Pa}RPRR^*$<br>(Fig. 5.76) | *9* | $\underline{Pa}\perp R\perp P\perp^{\|\|}R\perp R^*$ |
| 40 | | | $3\text{-}\underline{Pa}^{ss}PR$<br>(Fig. 5.77) | *3* | $\underline{Pa}^{ss}\text{-}P\perp^{\perp}R$ |
| 41 | $3\text{-}\underline{Pa}RRR$<br>(Fig. 5.23) | *12* | $3\text{-}\underline{Pa}RRRR^*$<br>(Fig. 5.78) | *9* | $\underline{Pa}\perp R\|\|R\|\|R\perp R^*$ |

**Table 5.13.** (cont.)

| | | | | | |
|---|---|---|---|---|---|
| 42 | | | $3\text{-}\underline{Pa}^{ss}RR$ (Fig. 5.79) | *3* | $\underline{Pa}^{ss} \perp R \| R$ |
| 43 | $3\text{-}\underline{Pa}PRR$ (Fig. 5.24) | *12* | $3\text{-}\underline{Pa}PRRR*$ (Fig. 5.80) | *9* | $\underline{Pa} \| P \perp R \| R \perp R*$ |
| 44 | | | $3\text{-}\underline{Pa}^{cs}PRR$ (Fig. 5.81) | *3* | $\underline{Pa}^{cs} \| P \perp R \| R$ |
| 45 | $3\text{-}\underline{Pa}PRR$ (Fig. 5.25) | *12* | $3\text{-}\underline{Pa}PRRR$ (Fig. 5.82) | *9* | $\underline{Pa} \perp P \perp^{\perp} R \| R \perp R*$ |
| 46 | | | $3\text{-}\underline{Pa}^{cs}PRR$ (Fig. 5.83) | *3* | $\underline{Pa}^{cs} \perp P \perp^{\perp} R \| R$ |
| 47 | $3\text{-}\underline{Pa}PaRR$ (Fig. 5.26) | *21* | $3\text{-}\underline{Pa}PaRRR*$ (Fig. 5.84) | *18* | $\underline{Pa} \perp Pa \| R \| R \perp^{\perp} R*$ |
| 48 | | | $3\text{-}\underline{Pa}^{cs}Pa^{cs}RR$ (Fig. 5.85) | *3* | $\underline{Pa}^{cs} \perp Pa^{cs} \| R \| R$ |
| 49 | $3\text{-}\underline{Pa}RRPa$ (Fig. 5.27) | *21* | $3\text{-}\underline{Pa}^{ss}RPa$ (Fig. 5.86) | *12* | $\underline{Pa}^{ss} \perp R \| Pa$ |
| 50 | | | $3\text{-}\underline{Pa}^{ss}RPa^{cs}$ (Fig. 5.87) | *3* | $\underline{Pa}^{ss} \perp R \| Pa^{cs}$ |
| 51 | $3\text{-}\underline{Pa}RRbR$ (Fig. 5.28) | *21* | $3\text{-}\underline{Pa}^{ss}RbR$ (Fig. 5.88) | *12* | $\underline{Pa}^{ss} \perp Rb \| R$ |
| 52 | | | $3\text{-}\underline{Pa}^{ss}Rb^{cs}R$ (Fig. 5.89) | *3* | $\underline{Pa}^{ss} \perp Rb^{cs} \| R$ |
| 53 | $3\text{-}\underline{Pa}RRbRbR$ (Fig. 5.29) | *30* | $3\text{-}\underline{Pa}^{ss}RbRbR$ (Fig. 5.90) | *21* | $\underline{Pa}^{ss} \perp Rb \| Rb \| R$ |
| 54 | | | $3\text{-}\underline{Pa}^{ss}Rb^{cs}Rb^{cs}R$ (Fig. 5.91) | *3* | $\underline{Pa}^{ss} \perp Rb^{cs} \| Rb^{cs} \| R$ |
| 55 | $3\text{-}\underline{Pa}Pn2R$ (Fig. 5.30) | *21* | $3\text{-}\underline{Pa}Pn2RR*$ (Fig. 5.92) | *18* | $\underline{Pa} \perp Pn2 \| R \perp R*$ |
| 56 | | | $3\text{-}\underline{Pa}^{cs}Pn2^{cs}R$ (Fig. 5.93) | *3* | $\underline{Pa}^{cs} \perp Pn2^{cs} \| R$ |
| 57 | $3\text{-}\underline{Pa}Pn2R$ (Fig. 5.31) | *21* | $3\text{-}\underline{Pa}Pn2RR*$ (Fig. 5.94) | *18* | $\underline{Pa} \perp Pn2 \| R \perp R*$ |
| 58 | | | $3\text{-}\underline{Pa}^{cs}Pn2^{cs}R$ (Fig. 5.95) | *3* | $\underline{Pa}^{cs} \perp Pn2^{cs} \| R$ |
| 59 | $3\text{-}\underline{Pa}Pn3$ (Fig. 5.32) | *21* | $3\text{-}\underline{Pa}Pn3R*$ (Fig. 5.96) | *18* | $\underline{Pa} \perp Pn3 \perp R*$ |
| 60 | | | $3\text{-}\underline{Pa}^{cs}Pn3^{cs}$ (Fig. 5.97) | *3* | $\underline{Pa}^{cs} \perp Pn3^{cs}$ |
| 61 | $3\text{-}\underline{Pa}Pn3$ (Fig. 5.33) | *21* | $3\text{-}\underline{Pa}Pn3R*$ (Fig. 5.98) | *18* | $\underline{Pa} \perp Pn3 \perp R*$ |
| 62 | | | $3\text{-}\underline{Pa}^{cs}Pn3^{cs}$ (Fig. 5.99) | *3* | $\underline{Pa}^{cs} \perp Pn3^{cs}$ |
| 63 | $3\text{-}\underline{Pa}^{cc}RR$ (Fig. 5.34) | *9* | $3\text{-}\underline{Pa}^{cc}RRR*$ (Fig. 5.100) | *6* | $\underline{Pa}^{cc} \perp R \| R \perp R*$ |

**Table 5.13.** (cont.)

| | | | | | |
|---|---|---|---|---|---|
| 64 | | | *3-<u>Pa</u>$^{scc}$RR* (Fig. 5.101) | *3* | *<u>Pa</u>$^{scc}$* $\perp$ *R*\|\|*R* |
| 65 | *3-<u>R</u>RPaP* (Fig. 5.35) | *12* | *3-<u>R</u>Pa$^{ss}$P* (Fig. 5.102) | *3* | *<u>R</u>* $\perp$ *Pa$^{ss}$* $\perp$ *P* |
| 66 | *3-<u>R</u>RPPa* (Fig. 5.38) | *12* | *3-<u>R</u>RC*Pa* (Fig. 5.103) | *9* | *<u>R</u>*\|\|*R* $\perp$ *C** $\perp^{\perp}$ *Pa* |
| 67 | | | *3-<u>R</u>RPPa$^{cs}$* (Fig. 5.104) | *3* | *<u>R</u>*\|\|*R* $\perp$ *P* $\perp^{\perp}$ *Pa$^{cs}$* |
| 68 | *3-<u>R</u>RPaPa* (Fig. 5.39) | *21* | *3-<u>R</u>RPaPa$^{cs}$* (Fig. 5.105) | *12* | *<u>R</u>*\|\|*R* $\perp$ *Pa*\|\|*Pa$^{cs}$* |
| 69 | | | *3-<u>R</u>RPa$^{ss}$Pa* (Fig. 5.106) | *9* | *<u>R</u>*\|\|*R* $\perp$ *Pa$^{ss}$*\|\|*Pa* |
| 70 | | | *3-<u>R</u>Pa$^{ss}$Pa* (Fig. 5.107) | *12* | *<u>R</u>* $\perp$ *Pa$^{ss}$*\|\|*Pa* |
| 71 | | | *3-<u>R</u>RPaPa$^{ss}$* (Fig. 5.108) | *9* | *<u>R</u>*\|\|*R* $\perp$ *Pa*\|\|*Pa$^{ss}$* |

**Table 5.14.** Bases of the operational velocities spaces of the limbs isolated from the parallel mechanisms presented in Figs. 5.49–5.108

| No. | Parallel mechanism | Basis ($R_{G1}$) | ($R_{G2}$) | ($R_{G3}$) |
|---|---|---|---|---|
| 1 | Figs. 5.49a, 5.51a, 5.57a, 5.59a, 5.61, 5.104a, 5.105a | $(\boldsymbol{v}_1, \boldsymbol{v}_2, \boldsymbol{v}_3, \boldsymbol{\omega}_\delta)$ | $(\boldsymbol{v}_1, \boldsymbol{v}_2, \boldsymbol{v}_3, \boldsymbol{\omega}_\alpha)$ | $(\boldsymbol{v}_1, \boldsymbol{v}_2, \boldsymbol{v}_3, \boldsymbol{\omega}_\beta)$ |
| 2 | Figs. 5.49b, 5.51b, 5.104b, 5.105b | $(\boldsymbol{v}_1, \boldsymbol{v}_2, \boldsymbol{v}_3, \boldsymbol{\omega}_\delta)$ | $(\boldsymbol{v}_1, \boldsymbol{v}_2, \boldsymbol{v}_3, \boldsymbol{\omega}_\delta)$ | $(\boldsymbol{v}_1, \boldsymbol{v}_2, \boldsymbol{v}_3, \boldsymbol{\omega}_\beta)$ |
| 3 | Figs. 5.50, 5.52, 5.54a, 5.56a, 5.58a, 5.60a, 5.66a, 5.73, 5.74, 5.77, 5.79, 5.81, 5.83, 5.85, 5.86, 5.87, 5.88-5.91, 5.93, 5.95, 5.97, 5.99, 5.101 | $(\boldsymbol{v}_1, \boldsymbol{v}_2, \boldsymbol{v}_3, \boldsymbol{\omega}_\alpha)$ | $(\boldsymbol{v}_1, \boldsymbol{v}_2, \boldsymbol{v}_3, \boldsymbol{\omega}_\beta)$ | $(\boldsymbol{v}_1, \boldsymbol{v}_2, \boldsymbol{v}_3, \boldsymbol{\omega}_\delta)$ |
| 4 | Figs. 5.53a, 5.55a, 5.65a, 5.102a, 5.107a | $(\boldsymbol{v}_1, \boldsymbol{v}_2, \boldsymbol{v}_3, \boldsymbol{\omega}_\beta)$ | $(\boldsymbol{v}_1, \boldsymbol{v}_2, \boldsymbol{v}_3, \boldsymbol{\omega}_\delta)$ | $(\boldsymbol{v}_1, \boldsymbol{v}_2, \boldsymbol{v}_3, \boldsymbol{\omega}_\alpha)$ |
| 5 | Figs. 5.53b, 5.55b, 5.57b, 5.59b, 5.63 5.67, 5.70, 5.71 | $(\boldsymbol{v}_1, \boldsymbol{v}_2, \boldsymbol{v}_3)$ | $(\boldsymbol{v}_1, \boldsymbol{v}_2, \boldsymbol{v}_3)$ | $(\boldsymbol{v}_1, \boldsymbol{v}_2, \boldsymbol{v}_3)$ |
| 6 | Figs. 5.54b, 5.56b, 5.58b, 5.60b, 5.64 5.68, 5.69b, 5.103 5.106, 5.108 | $(\boldsymbol{v}_1, \boldsymbol{v}_2, \boldsymbol{v}_3, \boldsymbol{\omega}_\beta, \boldsymbol{\omega}_\delta)$ | $(\boldsymbol{v}_1, \boldsymbol{v}_2, \boldsymbol{v}_3, \boldsymbol{\omega}_\alpha, \boldsymbol{\omega}_\delta)$ | $(\boldsymbol{v}_1, \boldsymbol{v}_2, \boldsymbol{v}_3, \boldsymbol{\omega}_\alpha, \boldsymbol{\omega}_\beta)$ |
| 7 | Figs. 5.62, 5.69a | $(\boldsymbol{v}_1, \boldsymbol{v}_2, \boldsymbol{v}_3, \boldsymbol{\omega}_\alpha, \boldsymbol{\omega}_\delta)$ | $(\boldsymbol{v}_1, \boldsymbol{v}_2, \boldsymbol{v}_3, \boldsymbol{\omega}_\alpha, \boldsymbol{\omega}_\beta)$ | $(\boldsymbol{v}_1, \boldsymbol{v}_2, \boldsymbol{v}_3, \boldsymbol{\omega}_\beta, \boldsymbol{\omega}_\delta)$ |
| 8 | Fig. 5.65b | $(\boldsymbol{v}_1, \boldsymbol{v}_2, \boldsymbol{v}_3, \boldsymbol{\omega}_\delta)$ | $(\boldsymbol{v}_1, \boldsymbol{v}_2, \boldsymbol{v}_3, \boldsymbol{\omega}_\delta)$ | $(\boldsymbol{v}_1, \boldsymbol{v}_2, \boldsymbol{v}_3, \boldsymbol{\omega}_\alpha)$ |
| 9 | Fig. 5.66b | $(\boldsymbol{v}_1, \boldsymbol{v}_2, \boldsymbol{v}_3, \boldsymbol{\omega}_\beta)$ | $(\boldsymbol{v}_1, \boldsymbol{v}_2, \boldsymbol{v}_3, \boldsymbol{\omega}_\alpha)$ | $(\boldsymbol{v}_1, \boldsymbol{v}_2, \boldsymbol{v}_3, \boldsymbol{\omega}_\beta)$ |
| 10 | Figs. 5.72, 5.75, 5.76, 5.78, 5.80, 5.82, 5.84, 5.92, 5.94, 5.96, 5.98, 5.100 | $(\boldsymbol{v}_1, \boldsymbol{v}_2, \boldsymbol{v}_3, \boldsymbol{\omega}_\alpha, \boldsymbol{\omega}_\beta)$ | $(\boldsymbol{v}_1, \boldsymbol{v}_2, \boldsymbol{v}_3, \boldsymbol{\omega}_\beta, \boldsymbol{\omega}_\delta)$ | $(\boldsymbol{v}_1, \boldsymbol{v}_2, \boldsymbol{v}_3, \boldsymbol{\omega}_\alpha, \boldsymbol{\omega}_\delta)$ |
| 11 | Figs. 5.102b, 5.107b | $(\boldsymbol{v}_1, \boldsymbol{v}_2, \boldsymbol{v}_3, \boldsymbol{\omega}_\beta)$ | $(\boldsymbol{v}_1, \boldsymbol{v}_2, \boldsymbol{v}_3, \boldsymbol{\omega}_\alpha)$ | $(\boldsymbol{v}_1, \boldsymbol{v}_2, \boldsymbol{v}_3, \boldsymbol{\omega}_\alpha)$ |

**Table 5.15.** Structural parameters[a] of translational parallel mechanisms in Figs. 5.49–5.52

| No. | Structural parameter | Solution *3-PaPC** (Figs. 5.49, 5.51) | *3-Pa^ss PP* (Figs. 5.50, 5.52) |
|---|---|---|---|
| 1 | $m$ | 14 | 14 |
| 2 | $p_1$ | 6 | 6 |
| 3 | $p_2$ | 6 | 6 |
| 4 | $p_3$ | 6 | 6 |
| 5 | $p$ | 18 | 18 |
| 6 | $q$ | 5 | 5 |
| 7 | $k_1$ | 0 | 0 |
| 8 | $k_2$ | 3 | 3 |
| 9 | $k$ | 3 | 3 |
| 10 | $(R_{Gi})$ $(i = 1,2,3)$ | See Table 5.14 | See Table 5.14 |
| 11 | $S_{G1}$ | 4 | 4 |
| 12 | $S_{G2}$ | 4 | 4 |
| 13 | $S_{G3}$ | 4 | 4 |
| 14 | $r_{G1}$ | 3 | 6 |
| 15 | $r_{G2}$ | 3 | 6 |
| 16 | $r_{G3}$ | 3 | 6 |
| 17 | $M_{G1}$ | 4 | 4 |
| 18 | $M_{G2}$ | 4 | 4 |
| 19 | $M_{G3}$ | 4 | 4 |
| 20 | $(R_F)$ | $(\boldsymbol{v}_1, \boldsymbol{v}_2, \boldsymbol{v}_3)$ | $(\boldsymbol{v}_1, \boldsymbol{v}_2, \boldsymbol{v}_3)$ |
| 21 | $S_F$ | 3 | 3 |
| 22 | $r_l$ | 9 | 18 |
| 23 | $r_F$ | 18 | 27 |
| 24 | $M_F$ | 3 | 3 |
| 25 | $N_F$ | 12 | 3 |
| 26 | $T_F$ | 0 | 0 |
| 27 | $\sum_{j=1}^{p_1} f_j$ | 7 | 10 |
| 28 | $\sum_{j=1}^{p_2} f_j$ | 7 | 10 |
| 29 | $\sum_{j=1}^{p_3} f_j$ | 7 | 10 |
| 30 | $\sum_{j=1}^{p} f_j$ | 21 | 30 |

[a]See footnote of Table 2.1 for the nomenclature of structural parameters

**Table 5.16.** Structural parameters[a] of translational parallel mechanisms in Figs. 5.53–5.60

| No. | Structural parameter | Solution 3-*PaPa*$^{ss}$*P* (Figs. 5.53a, 5.55a) 3-*Pa*$^{ss}$*PaP* (Figs. 5.54a, 5.56a) 3-*PaPPa*$^{ss}$ (Figs. 5.57a, 5.59a) 3-*Pa*$^{ss}$*PPa* (Figs. 5.58a, 5.60a) | 3-*PaPa*$^{cs}$*P* (Figs. 5.53b, 5.55b) 3-*Pa*$^{cs}$*PPa* (Figs. 5.57b, 5.59b) | 3-*PaPa*$^{cs}$*PR*R** (Figs. 5.54b, 5.56b) 3-*PaPPa*$^{cs}$*R*R** (Figs. 5.58b, 5.60b) |
|---|---|---|---|---|
| 1 | $m$ | 20 | 20 | 26 |
| 2 | $p_1$ | 9 | 9 | 11 |
| 3 | $p_2$ | 9 | 9 | 11 |
| 4 | $p_3$ | 9 | 9 | 11 |
| 5 | $p$ | 27 | 27 | 33 |
| 6 | $q$ | 8 | 8 | 8 |
| 7 | $k_1$ | 0 | 0 | 0 |
| 8 | $k_2$ | 3 | 3 | 3 |
| 9 | $k$ | 3 | 3 | 3 |
| 10 | $(R_{Gi})$ $(i = 1,2,3)$ | See Table 5.14 | See Table 5.14 | See Table 5.14 |
| 11 | $S_{G1}$ | 4 | 3 | 5 |
| 12 | $S_{G2}$ | 4 | 3 | 5 |
| 13 | $S_{G3}$ | 4 | 3 | 5 |
| 14 | $r_{G1}$ | 9 | 9 | 9 |
| 15 | $r_{G2}$ | 9 | 9 | 9 |
| 16 | $r_{G3}$ | 9 | 9 | 9 |
| 17 | $M_{G1}$ | 4 | 3 | 5 |
| 18 | $M_{G2}$ | 4 | 3 | 5 |
| 19 | $M_{G3}$ | 4 | 3 | 5 |
| 20 | $(R_F)$ | $(\boldsymbol{v}_1,\boldsymbol{v}_2,\boldsymbol{v}_3)$ | $(\boldsymbol{v}_1,\boldsymbol{v}_2,\boldsymbol{v}_3)$ | $(\boldsymbol{v}_1,\boldsymbol{v}_2,\boldsymbol{v}_3)$ |
| 21 | $S_F$ | 3 | 3 | 3 |
| 22 | $r_l$ | 27 | 27 | 27 |
| 23 | $r_F$ | 36 | 33 | 39 |
| 24 | $M_F$ | 3 | 3 | 3 |
| 25 | $N_F$ | 12 | 15 | 9 |
| 26 | $T_F$ | 0 | 0 | 0 |
| 27 | $\sum_{j=1}^{p_1} f_j$ | 13 | 12 | 14 |
| 28 | $\sum_{j=1}^{p_2} f_j$ | 13 | 12 | 14 |
| 29 | $\sum_{j=1}^{p_3} f_j$ | 13 | 12 | 14 |
| 30 | $\sum_{j=1}^{p} f_j$ | 39 | 36 | 42 |

[a]See footnote of Table 2.1 for the nomenclature of structural parameters

**Table 5.17.** Structural parameters[a] of translational parallel mechanisms in Figs. 5.61–5.63

| No. | Structural parameter | Solution 3-<u>Pa</u>PaPa^ss (Fig. 5.61) | 3-<u>Pa</u>^ss PaPa^ss (Fig. 5.62) | 3-<u>Pa</u>PaPa^cs (Fig. 5.63) |
|---|---|---|---|---|
| 1 | $m$ | 26 | 26 | 26 |
| 2 | $p_1$ | 12 | 12 | 12 |
| 3 | $p_2$ | 12 | 12 | 12 |
| 4 | $p_3$ | 12 | 12 | 12 |
| 5 | $p$ | 36 | 36 | 36 |
| 6 | $q$ | 11 | 11 | 11 |
| 7 | $k_1$ | 0 | 0 | 0 |
| 8 | $k_2$ | 3 | 3 | 3 |
| 9 | $k$ | 3 | 3 | 3 |
| 10 | $(R_{Gi})$ $(i = 1,2,3)$ | See Table 5.14 | See Table 5.14 | See Table 5.14 |
| 11 | $S_{G1}$ | 4 | 5 | 3 |
| 12 | $S_{G2}$ | 4 | 5 | 3 |
| 13 | $S_{G3}$ | 4 | 5 | 3 |
| 14 | $r_{G1}$ | 12 | 15 | 12 |
| 15 | $r_{G2}$ | 12 | 15 | 12 |
| 16 | $r_{G3}$ | 12 | 15 | 12 |
| 17 | $M_{G1}$ | 4 | 5 | 3 |
| 18 | $M_{G2}$ | 4 | 5 | 3 |
| 19 | $M_{G3}$ | 4 | 5 | 3 |
| 20 | $(R_F)$ | $(\boldsymbol{v}_1,\boldsymbol{v}_2,\boldsymbol{v}_3)$ | $(\boldsymbol{v}_1,\boldsymbol{v}_2,\boldsymbol{v}_3)$ | $(\boldsymbol{v}_1,\boldsymbol{v}_2,\boldsymbol{v}_3)$ |
| 21 | $S_F$ | 3 | 3 | 3 |
| 22 | $r_l$ | 36 | 45 | 36 |
| 23 | $r_F$ | 45 | 57 | 42 |
| 24 | $M_F$ | 3 | 3 | 3 |
| 25 | $N_F$ | 21 | 9 | 24 |
| 26 | $T_F$ | 0 | 0 | 0 |
| 27 | $\sum_{j=1}^{p_1} f_j$ | 16 | 20 | 15 |
| 28 | $\sum_{j=1}^{p_2} f_j$ | 16 | 20 | 15 |
| 29 | $\sum_{j=1}^{p_3} f_j$ | 16 | 20 | 15 |
| 30 | $\sum_{j=1}^{p} f_j$ | 48 | 60 | 45 |

[a]See footnote of Table 2.1 for the nomenclature of structural parameters

**Table 5.18.** Structural parameters[a] of translational parallel mechanisms in Figs. 5.64–5.66

| No. | Structural parameter | Solution 3-<u>Pa</u>$^{cs}$PaPa$^{cs}$R*R* (Fig. 5.64) | 3-<u>Pa</u>Pa$^{t}$C* (Fig. 5.65) | 3-<u>Pa</u>Pa$^{tss}$P (Fig. 5.66a) | 3-<u>Pa</u>Pa$^{tcs}$PR* (Fig. 5.66b) |
|---|---|---|---|---|---|
| 1 | $m$ | 32 | 20 | 20 | 23 |
| 2 | $p_1$ | 14 | 9 | 9 | 10 |
| 3 | $p_2$ | 14 | 9 | 9 | 10 |
| 4 | $p_3$ | 14 | 9 | 9 | 10 |
| 5 | $p$ | 42 | 27 | 27 | 30 |
| 6 | $q$ | 11 | 8 | 8 | 8 |
| 7 | $k_1$ | 0 | 0 | 0 | 0 |
| 8 | $k_2$ | 3 | 3 | 3 | 3 |
| 9 | $k$ | 3 | 3 | 3 | 3 |
| 10 | $(R_{Gi})$ $(i = 1,2,3)$ | See Table 5.14 | See Table 5.14 | See Table 5.14 | See Table 5.14 |
| 11 | $S_{G1}$ | 5 | 4 | 4 | 4 |
| 12 | $S_{G2}$ | 5 | 4 | 4 | 4 |
| 13 | $S_{G3}$ | 5 | 4 | 4 | 4 |
| 14 | $r_{G1}$ | 15 | 6 | 9 | 9 |
| 15 | $r_{G2}$ | 15 | 6 | 9 | 9 |
| 16 | $r_{G3}$ | 15 | 6 | 9 | 9 |
| 17 | $M_{G1}$ | 5 | 4 | 4 | 4 |
| 18 | $M_{G2}$ | 5 | 4 | 4 | 4 |
| 19 | $M_{G3}$ | 5 | 4 | 4 | 4 |
| 20 | $(R_F)$ | $(\boldsymbol{v}_1,\boldsymbol{v}_2,\boldsymbol{v}_3)$ | $(\boldsymbol{v}_1,\boldsymbol{v}_2,\boldsymbol{v}_3)$ | $(\boldsymbol{v}_1,\boldsymbol{v}_2,\boldsymbol{v}_3)$ | $(\boldsymbol{v}_1,\boldsymbol{v}_2,\boldsymbol{v}_3)$ |
| 21 | $S_F$ | 3 | 3 | 3 | 3 |
| 22 | $r_l$ | 45 | 18 | 27 | 27 |
| 23 | $r_F$ | 57 | 27 | 36 | 36 |
| 24 | $M_F$ | 3 | 3 | 3 | 3 |
| 25 | $N_F$ | 9 | 21 | 12 | 12 |
| 26 | $T_F$ | 0 | 0 | 0 | 0 |
| 27 | $\sum_{j=1}^{p_1} f_j$ | 20 | 10 | 13 | 13 |
| 28 | $\sum_{j=1}^{p_2} f_j$ | 20 | 10 | 13 | 13 |
| 29 | $\sum_{j=1}^{p_3} f_j$ | 20 | 10 | 13 | 13 |
| 30 | $\sum_{j=1}^{p} f_j$ | 60 | 30 | 39 | 39 |

[a]See footnote of Table 2.1 for the nomenclature of structural parameters

**Table 5.19.** Structural parameters[a] of translational parallel mechanisms in Figs. 5.67 and 5.68

| No. | Structural parameter | Solution 3-<u>Pa</u>$^{ss}$Pa$^{tcc}$ (Fig. 5.67a) | 3-<u>Pa</u>$^{cs}$Pa$^{tcc}$ (Fig. 5.67b) | <u>Pa</u>$^{ss}$Pa$^{tcc}$R*R* (Fig. 5.68a) | 3-<u>Pa</u>$^{cs}$Pa$^{tcc}$R*R* (Fig. 5.68b) |
|---|---|---|---|---|---|
| 1 | $m$ | 17 | 17 | 23 | 23 |
| 2 | $p_1$ | 8 | 8 | 10 | 10 |
| 3 | $p_2$ | 8 | 8 | 10 | 10 |
| 4 | $p_3$ | 8 | 8 | 10 | 10 |
| 5 | $p$ | 24 | 24 | 30 | 30 |
| 6 | $q$ | 8 | 8 | 8 | 8 |
| 7 | $k_1$ | 0 | 0 | 0 | 0 |
| 8 | $k_2$ | 3 | 3 | 3 | 3 |
| 9 | $k$ | 3 | 3 | 3 | 3 |
| 10 | $(R_{Gi})$ $(i = 1,2,3)$ | See Table 5.14 | See Table 5.14 | See Table 5.14 | See Table 5.14 |
| 11 | $S_{G1}$ | 3 | 3 | 5 | 5 |
| 12 | $S_{G2}$ | 3 | 3 | 5 | 5 |
| 13 | $S_{G3}$ | 3 | 3 | 5 | 5 |
| 14 | $r_{G1}$ | 10 | 10 | 10 | 10 |
| 15 | $r_{G2}$ | 10 | 10 | 10 | 10 |
| 16 | $r_{G3}$ | 10 | 10 | 10 | 10 |
| 17 | $M_{G1}$ | 4 | 3 | 6 | 5 |
| 18 | $M_{G2}$ | 4 | 3 | 6 | 5 |
| 19 | $M_{G3}$ | 4 | 3 | 6 | 5 |
| 20 | $(R_F)$ | $(\boldsymbol{v}_1, \boldsymbol{v}_2, \boldsymbol{v}_3)$ | $(\boldsymbol{v}_1, \boldsymbol{v}_2, \boldsymbol{v}_3)$ | $(\boldsymbol{v}_1, \boldsymbol{v}_2, \boldsymbol{v}_3)$ | $(\boldsymbol{v}_1, \boldsymbol{v}_2, \boldsymbol{v}_3)$ |
| 21 | $S_F$ | 3 | 3 | 3 | 3 |
| 22 | $r_l$ | 30 | 30 | 30 | 30 |
| 23 | $r_F$ | 36 | 36 | 42 | 42 |
| 24 | $M_F$ | 6 | 3 | 6 | 3 |
| 25 | $N_F$ | 12 | 12 | 6 | 6 |
| 26 | $T_F$ | 3 | 0 | 3 | 0 |
| 27 | $\sum_{j=1}^{p_1} f_j$ | 14 | 13 | 16 | 15 |
| 28 | $\sum_{j=1}^{p_2} f_j$ | 14 | 13 | 16 | 15 |
| 29 | $\sum_{j=1}^{p_3} f_j$ | 14 | 13 | 16 | 15 |
| 30 | $\sum_{j=1}^{p} f_j$ | 42 | 39 | 48 | 45 |

[a]See footnote of Table 2.1 for the nomenclature of structural parameters

**Table 5.20.** Structural parameters[a] of translational parallel mechanisms in Figs. 5.69–5.72

| No. | Structural parameter | Solution 3-$\underline{Pa}^{cc}C^*R^*$ (Fig. 5.69) | 3-$\underline{Pa}^{ccs}P$ (Fig. 5.70) | 3-$\underline{Pa}^{ccs}Pa$ (Fig. 5.71) | 3-$\underline{Pa}^{cc}Pa^{ss}R^*$ (Fig. 5.72) |
|---|---|---|---|---|---|
| 1 | $m$ | 14 | 11 | 17 | 20 |
| 2 | $p_1$ | 6 | 5 | 8 | 9 |
| 3 | $p_2$ | 6 | 5 | 8 | 9 |
| 4 | $p_3$ | 6 | 5 | 8 | 9 |
| 5 | $p$ | 18 | 15 | 24 | 27 |
| 6 | $q$ | 5 | 5 | 8 | 8 |
| 7 | $k_1$ | 0 | 0 | 0 | 0 |
| 8 | $k_2$ | 3 | 3 | 3 | 3 |
| 9 | $k$ | 3 | 3 | 3 | 3 |
| 10 | $(R_{Gi})$ $(i = 1,2,3)$ | See Table 5.14 | See Table 5.14 | See Table 5.14 | See Table 5.14 |
| 11 | $S_{G1}$ | 5 | 3 | 3 | 5 |
| 12 | $S_{G2}$ | 5 | 3 | 3 | 5 |
| 13 | $S_{G3}$ | 5 | 3 | 3 | 5 |
| 14 | $r_{G1}$ | 4 | 6 | 9 | 10 |
| 15 | $r_{G2}$ | 4 | 6 | 9 | 10 |
| 16 | $r_{G3}$ | 4 | 6 | 9 | 10 |
| 17 | $M_{G1}$ | 5 | 3 | 3 | 5 |
| 18 | $M_{G2}$ | 5 | 3 | 3 | 5 |
| 19 | $M_{G3}$ | 5 | 3 | 3 | 5 |
| 20 | $(R_F)$ | $(\boldsymbol{v}_1,\boldsymbol{v}_2,\boldsymbol{v}_3)$ | $(\boldsymbol{v}_1,\boldsymbol{v}_2,\boldsymbol{v}_3)$ | $(\boldsymbol{v}_1,\boldsymbol{v}_2,\boldsymbol{v}_3)$ | $(\boldsymbol{v}_1,\boldsymbol{v}_2,\boldsymbol{v}_3)$ |
| 21 | $S_F$ | 3 | 3 | 3 | 3 |
| 22 | $r_l$ | 12 | 18 | 27 | 30 |
| 23 | $r_F$ | 24 | 24 | 33 | 42 |
| 24 | $M_F$ | 3 | 3 | 3 | 3 |
| 25 | $N_F$ | 6 | 6 | 15 | 6 |
| 26 | $T_F$ | 0 | 0 | 0 | 0 |
| 27 | $\sum_{j=1}^{p_1} f_j$ | 9 | 9 | 12 | 15 |
| 28 | $\sum_{j=1}^{p_2} f_j$ | 9 | 9 | 12 | 15 |
| 29 | $\sum_{j=1}^{p_3} f_j$ | 9 | 9 | 12 | 15 |
| 30 | $\sum_{j=1}^{p} f_j$ | 27 | 27 | 36 | 45 |

[a]See footnote of Table 2.1 for the nomenclature of structural parameters

**Table 5.21.** Structural parameters[a] of translational parallel mechanisms in Figs. 5.73–5.80

| No. | Structural parameter | Solution 3-$\underline{Pa}^{ss}RP$ (Figs. 5.73, 5.74) 3-$\underline{Pa}^{ss}PR$ (Fig. 5.77) 3-$\underline{Pa}^{ss}RR$ (Fig. 5.79) | 3-$\underline{Pa}RRC$* (Fig. 5.75) | 3-$\underline{Pa}RPRR$* (Fig. 5.76) 3-$\underline{Pa}RRRR$* (Fig. 5.78) 3-$\underline{Pa}PRRR$* (Fig. 5.80) |
|---|---|---|---|---|
| 1 | $m$ | 14 | 17 | 20 |
| 2 | $p_1$ | 6 | 7 | 8 |
| 3 | $p_2$ | 6 | 7 | 8 |
| 4 | $p_3$ | 6 | 7 | 8 |
| 5 | $p$ | 18 | 21 | 24 |
| 6 | $q$ | 5 | 5 | 5 |
| 7 | $k_1$ | 0 | 0 | 0 |
| 8 | $k_2$ | 3 | 3 | 3 |
| 9 | $k$ | 3 | 3 | 3 |
| 10 | $(R_{Gi})$ $(i = 1,2,3)$ | See Table 5.14 | See Table 5.14 | See Table 5.14 |
| 11 | $S_{G1}$ | 4 | 5 | 5 |
| 12 | $S_{G2}$ | 4 | 5 | 5 |
| 13 | $S_{G3}$ | 4 | 5 | 5 |
| 14 | $r_{G1}$ | 6 | 3 | 3 |
| 15 | $r_{G2}$ | 6 | 3 | 3 |
| 16 | $r_{G3}$ | 6 | 3 | 3 |
| 17 | $M_{G1}$ | 4 | 5 | 5 |
| 18 | $M_{G2}$ | 4 | 5 | 5 |
| 19 | $M_{G3}$ | 4 | 5 | 5 |
| 20 | $(R_F)$ | $(\boldsymbol{v}_1,\boldsymbol{v}_2,\boldsymbol{v}_3)$ | $(\boldsymbol{v}_1,\boldsymbol{v}_2,\boldsymbol{v}_3)$ | $(\boldsymbol{v}_1,\boldsymbol{v}_2,\boldsymbol{v}_3)$ |
| 21 | $S_F$ | 3 | 3 | 3 |
| 22 | $r_l$ | 18 | 9 | 9 |
| 23 | $r_F$ | 27 | 21 | 21 |
| 24 | $M_F$ | 3 | 3 | 3 |
| 25 | $N_F$ | 3 | 9 | 9 |
| 26 | $T_F$ | 0 | 0 | 0 |
| 27 | $\sum_{j=1}^{p_1} f_j$ | 10 | 8 | 8 |
| 28 | $\sum_{j=1}^{p_2} f_j$ | 10 | 8 | 8 |
| 29 | $\sum_{j=1}^{p_3} f_j$ | 10 | 8 | 8 |
| 30 | $\sum_{j=1}^{p} f_j$ | 30 | 24 | 24 |

[a]See footnote of Table 2.1 for the nomenclature of structural parameters

**Table 5.22.** Structural parameters[a] of translational parallel mechanisms in Figs. 5.81–5.85

| No. | Structural parameter | Solution 3-<u>Pa</u>$^{cs}$PRR (Figs. 5.81, 5.83) | 3-<u>Pa</u>PRRR* (Fig. 5.82) | 3-<u>Pa</u>PaRRR* (Fig. 5.84) | 3-<u>Pa</u>$^{cs}$Pa$^{cs}$RR (Fig. 5.85) |
|---|---|---|---|---|---|
| 1 | $m$ | 17 | 20 | 26 | 23 |
| 2 | $p_1$ | 7 | 8 | 11 | 10 |
| 3 | $p_2$ | 7 | 8 | 11 | 10 |
| 4 | $p_3$ | 7 | 8 | 11 | 10 |
| 5 | $p$ | 21 | 24 | 33 | 30 |
| 6 | $q$ | 5 | 5 | 8 | 8 |
| 7 | $k_1$ | 0 | 0 | 0 | 0 |
| 8 | $k_2$ | 3 | 3 | 3 | 3 |
| 9 | $k$ | 3 | 3 | 3 | 3 |
| 10 | $(R_{Gi})$ $(i = 1,2,3)$ | See Table 5.14 | See Table 5.14 | See Table 5.14 | See Table 5.14 |
| 11 | $S_{G1}$ | 4 | 5 | 5 | 4 |
| 12 | $S_{G2}$ | 4 | 5 | 5 | 4 |
| 13 | $S_{G3}$ | 4 | 5 | 5 | 4 |
| 14 | $r_{G1}$ | 6 | 3 | 6 | 12 |
| 15 | $r_{G2}$ | 6 | 3 | 6 | 12 |
| 16 | $r_{G3}$ | 6 | 3 | 6 | 12 |
| 17 | $M_{G1}$ | 4 | 5 | 5 | 4 |
| 18 | $M_{G2}$ | 4 | 5 | 5 | 4 |
| 19 | $M_{G3}$ | 4 | 5 | 5 | 4 |
| 20 | $(R_F)$ | $(\boldsymbol{v}_1,\boldsymbol{v}_2,\boldsymbol{v}_3)$ | $(\boldsymbol{v}_1,\boldsymbol{v}_2,\boldsymbol{v}_3)$ | $(\boldsymbol{v}_1,\boldsymbol{v}_2,\boldsymbol{v}_3)$ | $(\boldsymbol{v}_1,\boldsymbol{v}_2,\boldsymbol{v}_3)$ |
| 21 | $S_F$ | 3 | 3 | 3 | 3 |
| 22 | $r_l$ | 18 | 9 | 18 | 36 |
| 23 | $r_F$ | 27 | 21 | 30 | 45 |
| 24 | $M_F$ | 3 | 3 | 3 | 3 |
| 25 | $N_F$ | 3 | 9 | 18 | 3 |
| 26 | $T_F$ | 0 | 0 | 0 | 0 |
| 27 | $\sum_{j=1}^{p_1} f_j$ | 10 | 8 | 11 | 16 |
| 28 | $\sum_{j=1}^{p_2} f_j$ | 10 | 8 | 11 | 16 |
| 29 | $\sum_{j=1}^{p_3} f_j$ | 10 | 8 | 11 | 16 |
| 30 | $\sum_{j=1}^{p} f_j$ | 30 | 24 | 33 | 48 |

[a]See footnote of Table 2.1 for the nomenclature of structural parameters

**Table 5.23.** Structural parameters[a] of translational parallel mechanisms in Figs. 5.86–5.91

| No. | Structural parameter | Solution 3-$\underline{Pa}^{ss}RPa$ (Fig. 5.86) 3-$\underline{Pa}^{ss}RbR$ (Fig. 5.88) | 3-$\underline{Pa}^{ss}RPa^{cs}$ (Fig. 5.87) 3-$\underline{Pa}^{ss}Rb^{cs}R$ (Fig. 5.89) | 3-$\underline{Pa}^{ss}RbRbR$ (Fig. 5.90) | 3-$\underline{Pa}^{ss}Rb^{cs}Rb^{cs}R$ (Fig. 5.91) |
|---|---|---|---|---|---|
| 1 | $m$ | 20 | 20 | 26 | 26 |
| 2 | $p_1$ | 9 | 9 | 12 | 12 |
| 3 | $p_2$ | 9 | 9 | 12 | 12 |
| 4 | $p_3$ | 9 | 9 | 12 | 12 |
| 5 | $p$ | 27 | 27 | 36 | 36 |
| 6 | $q$ | 8 | 8 | 11 | 11 |
| 7 | $k_1$ | 0 | 0 | 0 | 0 |
| 8 | $k_2$ | 3 | 3 | 3 | 3 |
| 9 | $k$ | 3 | 3 | 3 | 3 |
| 10 | $(R_{Gi})$ $(i = 1,2,3)$ | See Table 5.14 | See Table 5.14 | See Table 5.14 | See Table 5.14 |
| 11 | $S_{G1}$ | 4 | 4 | 4 | 4 |
| 12 | $S_{G2}$ | 4 | 4 | 4 | 4 |
| 13 | $S_{G3}$ | 4 | 4 | 4 | 4 |
| 14 | $r_{G1}$ | 9 | 12 | 12 | 18 |
| 15 | $r_{G2}$ | 9 | 12 | 12 | 18 |
| 16 | $r_{G3}$ | 9 | 12 | 12 | 18 |
| 17 | $M_{G1}$ | 4 | 4 | 4 | 4 |
| 18 | $M_{G2}$ | 4 | 4 | 4 | 4 |
| 19 | $M_{G3}$ | 4 | 4 | 4 | 4 |
| 20 | $(R_F)$ | $(\boldsymbol{v}_1,\boldsymbol{v}_2,\boldsymbol{v}_3)$ | $(\boldsymbol{v}_1,\boldsymbol{v}_2,\boldsymbol{v}_3)$ | $(\boldsymbol{v}_1,\boldsymbol{v}_2,\boldsymbol{v}_3)$ | $(\boldsymbol{v}_1,\boldsymbol{v}_2,\boldsymbol{v}_3)$ |
| 21 | $S_F$ | 3 | 3 | 3 | 3 |
| 22 | $r_l$ | 27 | 36 | 36 | 54 |
| 23 | $r_F$ | 36 | 45 | 45 | 63 |
| 24 | $M_F$ | 3 | 3 | 3 | 3 |
| 25 | $N_F$ | 12 | 3 | 21 | 3 |
| 26 | $T_F$ | 0 | 0 | 0 | 0 |
| 27 | $\sum_{j=1}^{p_1} f_j$ | 13 | 16 | 16 | 22 |
| 28 | $\sum_{j=1}^{p_2} f_j$ | 13 | 16 | 16 | 22 |
| 29 | $\sum_{j=1}^{p_3} f_j$ | 13 | 16 | 16 | 22 |
| 30 | $\sum_{j=1}^{p} f_j$ | 39 | 48 | 48 | 66 |

[a]See footnote of Table 2.1 for the nomenclature of structural parameters

**Table 5.24.** Structural parameters[a] of translational parallel mechanisms in Figs. 5.92–5.101

| No. | Structural parameter | Solution 3-*<u>Pa</u>Pn2RR** (Figs. 5.92, 5.94) 3-*<u>Pa</u>Pn3R** (Figs. 5.96, 5.98) | 3-*<u>Pa</u>$^{cs}$Pn2$^{cs}$R* (Figs. 5.93, 5.95) 3-*<u>Pa</u>$^{cs}$Pn3$^{cs}$* (Figs. 5.97, 5.99) | 3-*<u>Pa</u>$^{cc}$RRR** (Fig. 5.100) | 3-*<u>Pa</u>$^{scc}$RR* (Fig. 5.101) |
|---|---|---|---|---|---|
| 1 | $m$ | 26 | 23 | 17 | 14 |
| 2 | $p_1$ | 11 | 10 | 7 | 6 |
| 3 | $p_2$ | 11 | 10 | 7 | 6 |
| 4 | $p_3$ | 11 | 10 | 7 | 6 |
| 5 | $p$ | 33 | 30 | 21 | 18 |
| 6 | $q$ | 8 | 8 | 5 | 5 |
| 7 | $k_1$ | 0 | 0 | 0 | 0 |
| 8 | $k_2$ | 3 | 3 | 3 | 3 |
| 9 | $k$ | 3 | 3 | 3 | 3 |
| 10 | $(R_{Gi})$ $(i = 1,2,3)$ | See Table 5.14 | See Table 5.14 | See Table 5.14 | See Table 5.14 |
| 11 | $S_{G1}$ | 5 | 4 | 5 | 4 |
| 12 | $S_{G2}$ | 5 | 4 | 5 | 4 |
| 13 | $S_{G3}$ | 5 | 4 | 5 | 4 |
| 14 | $r_{G1}$ | 6 | 12 | 4 | 6 |
| 15 | $r_{G2}$ | 6 | 12 | 4 | 6 |
| 16 | $r_{G3}$ | 6 | 12 | 4 | 6 |
| 17 | $M_{G1}$ | 5 | 4 | 5 | 4 |
| 18 | $M_{G2}$ | 5 | 4 | 5 | 4 |
| 19 | $M_{G3}$ | 5 | 4 | 5 | 4 |
| 20 | $(R_F)$ | $(\boldsymbol{v}_1, \boldsymbol{v}_2, \boldsymbol{v}_3)$ | $(\boldsymbol{v}_1, \boldsymbol{v}_2, \boldsymbol{v}_3)$ | $(\boldsymbol{v}_1, \boldsymbol{v}_2, \boldsymbol{v}_3)$ | $(\boldsymbol{v}_1, \boldsymbol{v}_2, \boldsymbol{v}_3)$ |
| 21 | $S_F$ | 3 | 3 | 3 | 3 |
| 22 | $r_l$ | 18 | 36 | 12 | 18 |
| 23 | $r_F$ | 30 | 45 | 24 | 27 |
| 24 | $M_F$ | 3 | 3 | 3 | 3 |
| 25 | $N_F$ | 18 | 3 | 6 | 3 |
| 26 | $T_F$ | 0 | 0 | 0 | 0 |
| 27 | $\sum_{j=1}^{p_1} f_j$ | 11 | 16 | 9 | 10 |
| 28 | $\sum_{j=1}^{p_2} f_j$ | 11 | 16 | 9 | 10 |
| 29 | $\sum_{j=1}^{p_3} f_j$ | 11 | 16 | 9 | 10 |
| 30 | $\sum_{j=1}^{p} f_j$ | 33 | 48 | 27 | 30 |

[a]See footnote of Table 2.1 for the nomenclature of structural parameters

**Table 5.25.** Structural parameters[a] of translational parallel mechanisms in Figs. 5.102–5.104

| No. | Structural parameter | Solution 3-*<u>R</u>Pa^ss P* (Fig. 5.102) | 3-*<u>R</u>RC*Pa* (Fig. 5.103) | 3-*<u>R</u>RPPa^cs* (Fig. 5.104) |
|---|---|---|---|---|
| 1 | $m$ | 14 | 17 | 17 |
| 2 | $p_1$ | 6 | 7 | 7 |
| 3 | $p_2$ | 6 | 7 | 7 |
| 4 | $p_3$ | 6 | 7 | 7 |
| 5 | $p$ | 18 | 21 | 21 |
| 6 | $q$ | 5 | 5 | 5 |
| 7 | $k_1$ | 0 | 0 | 0 |
| 8 | $k_2$ | 3 | 3 | 3 |
| 9 | $k$ | 3 | 3 | 3 |
| 10 | $(R_{Gi})$ $(i = 1,2,3)$ | See Table 5.14 | See Table 5.14 | See Table 5.14 |
| 11 | $S_{G1}$ | 4 | 5 | 4 |
| 12 | $S_{G2}$ | 4 | 5 | 4 |
| 13 | $S_{G3}$ | 4 | 5 | 4 |
| 14 | $r_{G1}$ | 6 | 3 | 6 |
| 15 | $r_{G2}$ | 6 | 3 | 6 |
| 16 | $r_{G3}$ | 6 | 3 | 6 |
| 17 | $M_{G1}$ | 4 | 5 | 4 |
| 18 | $M_{G2}$ | 4 | 5 | 4 |
| 19 | $M_{G3}$ | 4 | 5 | 4 |
| 20 | $(R_F)$ | $(\boldsymbol{v}_1, \boldsymbol{v}_2, \boldsymbol{v}_3)$ | $(\boldsymbol{v}_1, \boldsymbol{v}_2, \boldsymbol{v}_3)$ | $(\boldsymbol{v}_1, \boldsymbol{v}_2, \boldsymbol{v}_3)$ |
| 21 | $S_F$ | 3 | 3 | 3 |
| 22 | $r_l$ | 18 | 9 | 18 |
| 23 | $r_F$ | 27 | 21 | 27 |
| 24 | $M_F$ | 3 | 3 | 3 |
| 25 | $N_F$ | 3 | 9 | 3 |
| 26 | $T_F$ | 0 | 0 | 0 |
| 27 | $\sum_{j=1}^{p_1} f_j$ | 10 | 8 | 10 |
| 28 | $\sum_{j=1}^{p_2} f_j$ | 10 | 8 | 10 |
| 29 | $\sum_{j=1}^{p_3} f_j$ | 10 | 8 | 10 |
| 30 | $\sum_{j=1}^{p} f_j$ | 30 | 24 | 30 |

[a]See footnote of Table 2.1 for the nomenclature of structural parameters

**Table 5.26.** Structural parameters[a] of translational parallel mechanisms in Figs. 5.105–5.108

| No. | Structural parameter | Solution<br>*3-RRPaPa^cs* (Fig. 5.105) | *3-RRPa^ss Pa* (Fig. 5.106)<br>*3-RRPaPa^ss* (Fig. 5.108) | *3-RPa^ss Pa* (Fig. 5.107) |
|---|---|---|---|---|
| 1 | $m$ | 23 | 23 | 20 |
| 2 | $p_1$ | 10 | 10 | 9 |
| 3 | $p_2$ | 10 | 10 | 9 |
| 4 | $p_3$ | 10 | 10 | 9 |
| 5 | $p$ | 30 | 30 | 27 |
| 6 | $q$ | 8 | 8 | 8 |
| 7 | $k_1$ | 0 | 0 | 0 |
| 8 | $k_2$ | 3 | 3 | 3 |
| 9 | $k$ | 3 | 3 | 3 |
| 10 | $(R_{Gi})$ $(i = 1,2,3)$ | See Table 5.14 | See Table 5.14 | See Table 5.14 |
| 11 | $S_{G1}$ | 4 | 5 | 4 |
| 12 | $S_{G2}$ | 4 | 5 | 4 |
| 13 | $S_{G3}$ | 4 | 5 | 4 |
| 14 | $r_{G1}$ | 9 | 9 | 9 |
| 15 | $r_{G2}$ | 9 | 9 | 9 |
| 16 | $r_{G3}$ | 9 | 9 | 9 |
| 17 | $M_{G1}$ | 4 | 5 | 4 |
| 18 | $M_{G2}$ | 4 | 5 | 4 |
| 19 | $M_{G3}$ | 4 | 5 | 4 |
| 20 | $(R_F)$ | $(\boldsymbol{v}_1,\boldsymbol{v}_2,\boldsymbol{v}_3)$ | $(\boldsymbol{v}_1,\boldsymbol{v}_2,\boldsymbol{v}_3)$ | $(\boldsymbol{v}_1,\boldsymbol{v}_2,\boldsymbol{v}_3)$ |
| 21 | $S_F$ | 3 | 3 | 3 |
| 22 | $r_l$ | 27 | 27 | 27 |
| 23 | $r_F$ | 36 | 39 | 36 |
| 24 | $M_F$ | 3 | 3 | 3 |
| 25 | $N_F$ | 12 | 9 | 12 |
| 26 | $T_F$ | 0 | 0 | 0 |
| 27 | $\sum_{j=1}^{p_1} f_j$ | 13 | 14 | 13 |
| 28 | $\sum_{j=1}^{p_2} f_j$ | 13 | 14 | 13 |
| 29 | $\sum_{j=1}^{p_3} f_j$ | 13 | 14 | 13 |
| 30 | $\sum_{j=1}^{p} f_j$ | 39 | 42 | 39 |

[a]See footnote of Table 2.1 for the nomenclature of structural parameters

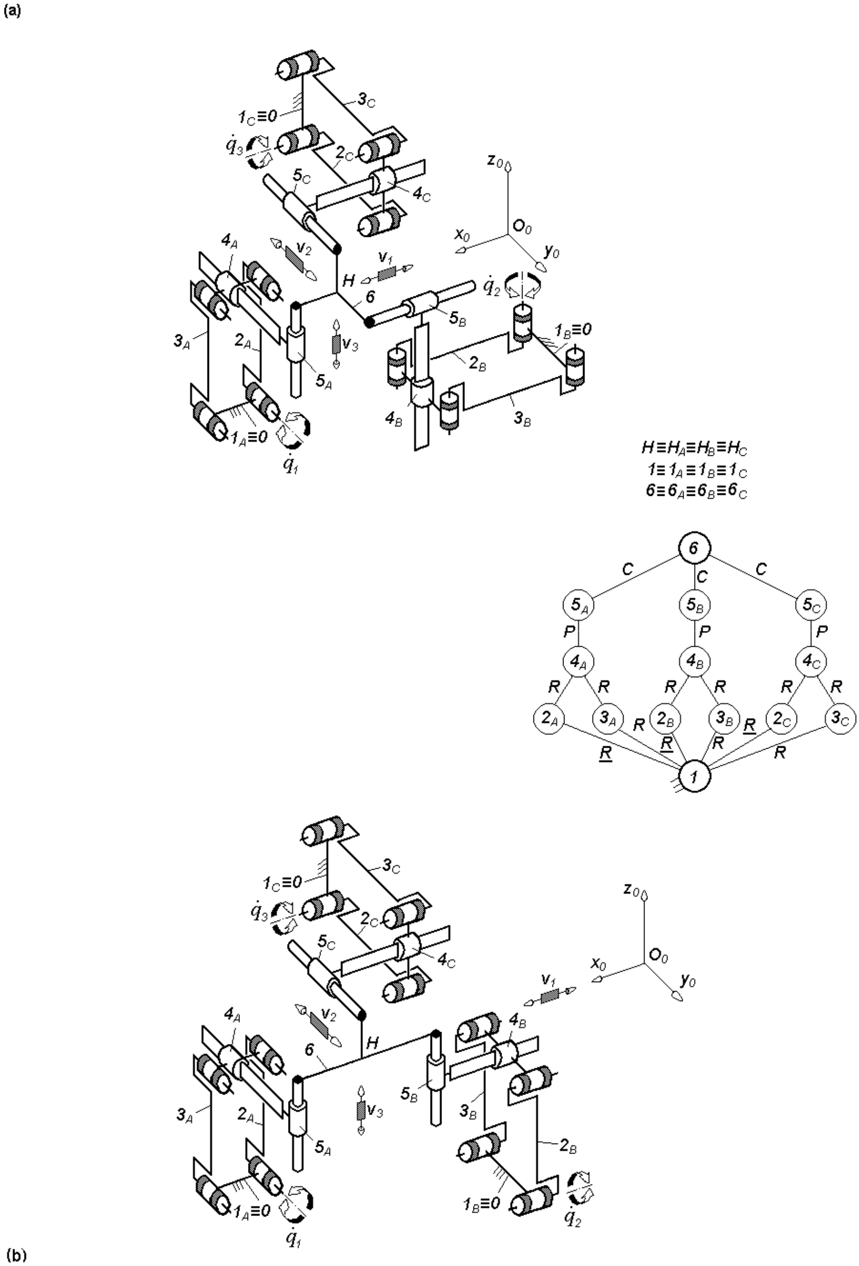


**Fig. 5.49.** *3-PaPC**-type overconstrained TPMs with uncoupled motions and rotating actuators mounted on the fixed base, defined by $M_F = S_F = 3$, $(R_F) = (\boldsymbol{v}_1, \boldsymbol{v}_2, \boldsymbol{v}_3)$, $T_F = 0$, $N_F = 12$, limb topology $\underline{Pa}||P \perp C^*$

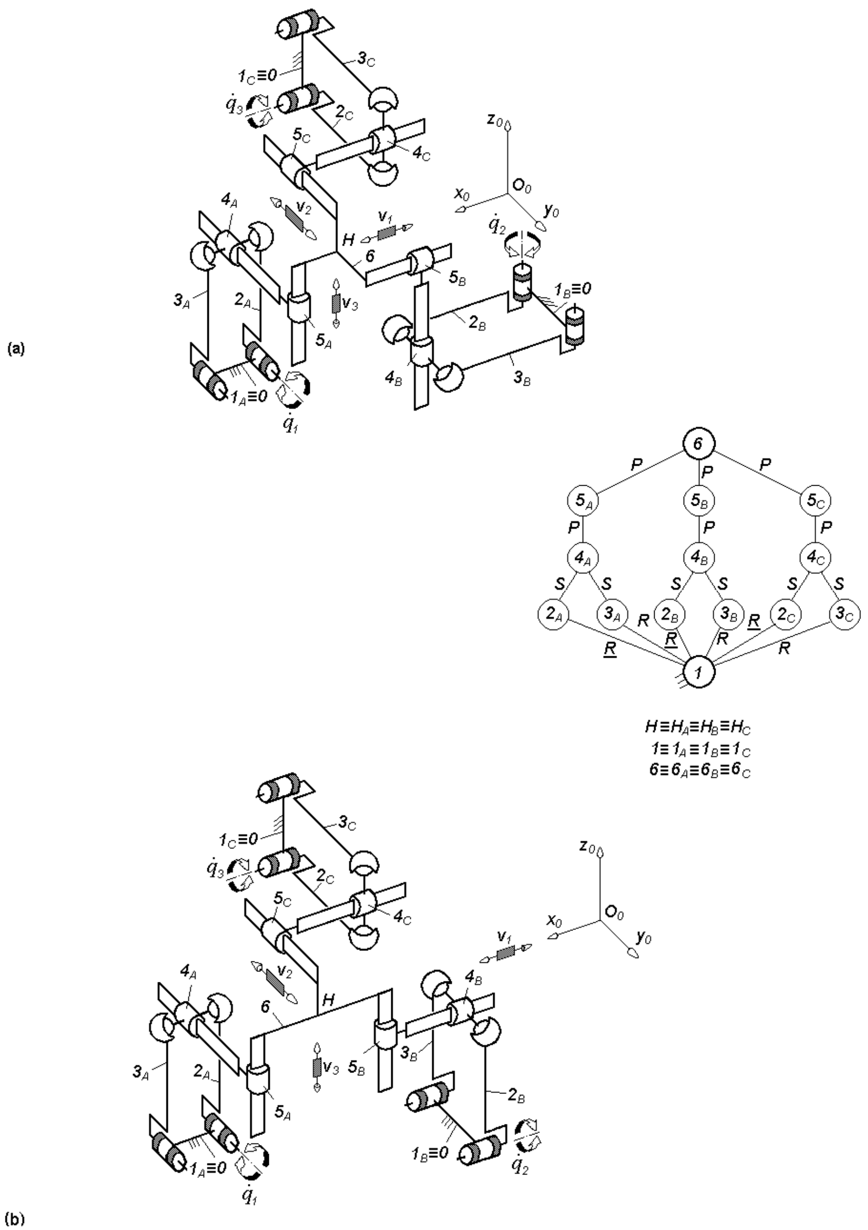


**Fig. 5.50.** 3-$\underline{Pa}^{ss}PP$-type ($\underline{Pa}^{ss}||P \perp P$) overconstrained TPMs with uncoupled motions and rotating actuators mounted on the fixed base, defined by $M_F = S_F = 3$, $(R_F) = (\mathbf{v}_1, \mathbf{v}_2, \mathbf{v}_3)$, $T_F = 0$, $N_F = 3$, limb topology $\underline{Pa}^{ss}||P \perp P$

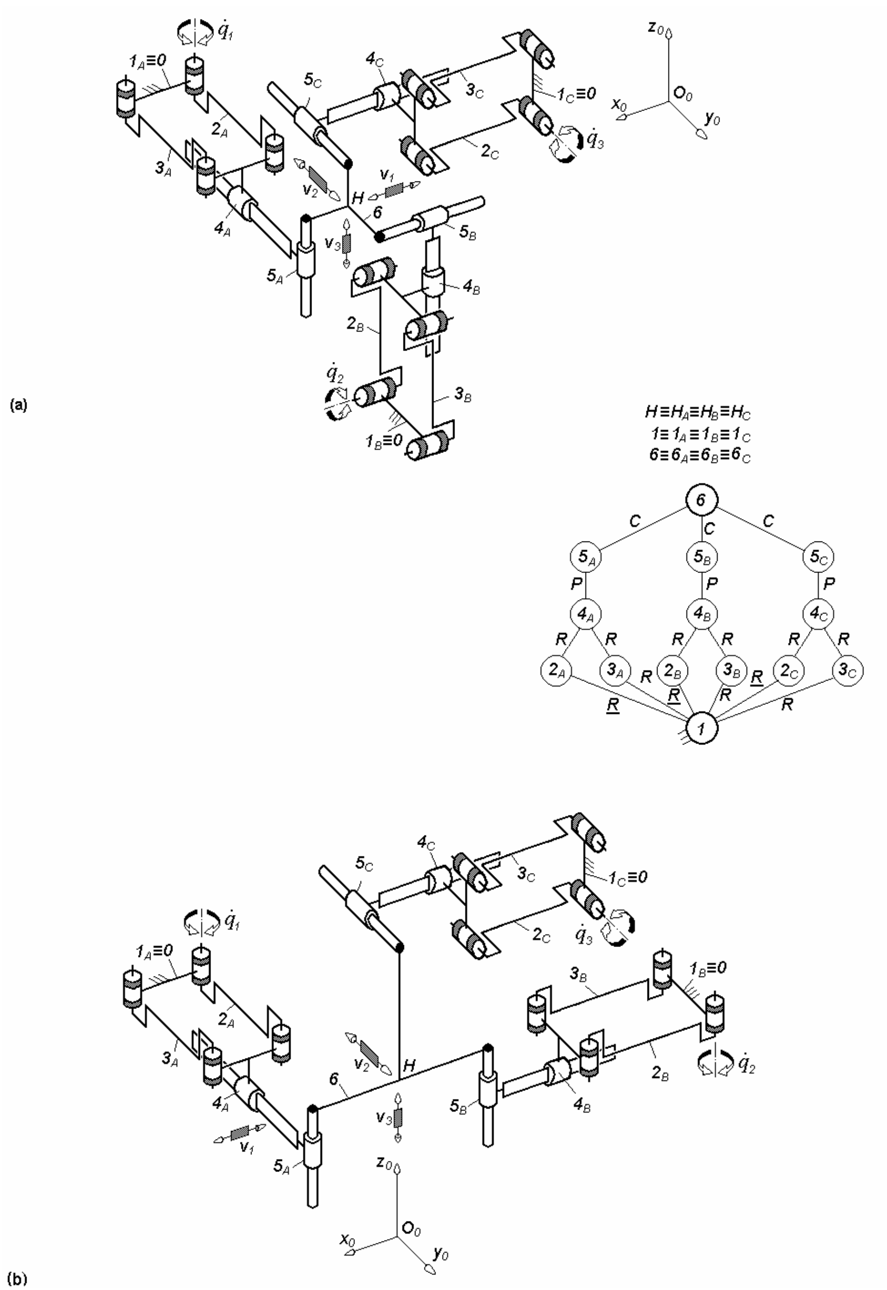


**Fig. 5.51.** *3-<u>Pa</u>PC**-type overconstrained TPMs with uncoupled motions and rotating actuators mounted on the fixed base, defined by $M_F = S_F = 3$, $(R_F) = (\boldsymbol{v}_1, \boldsymbol{v}_2, \boldsymbol{v}_3)$, $T_F = 0$, $N_F = 12$, limb topology $\underline{Pa} \perp P \perp^{\parallel} C^*$

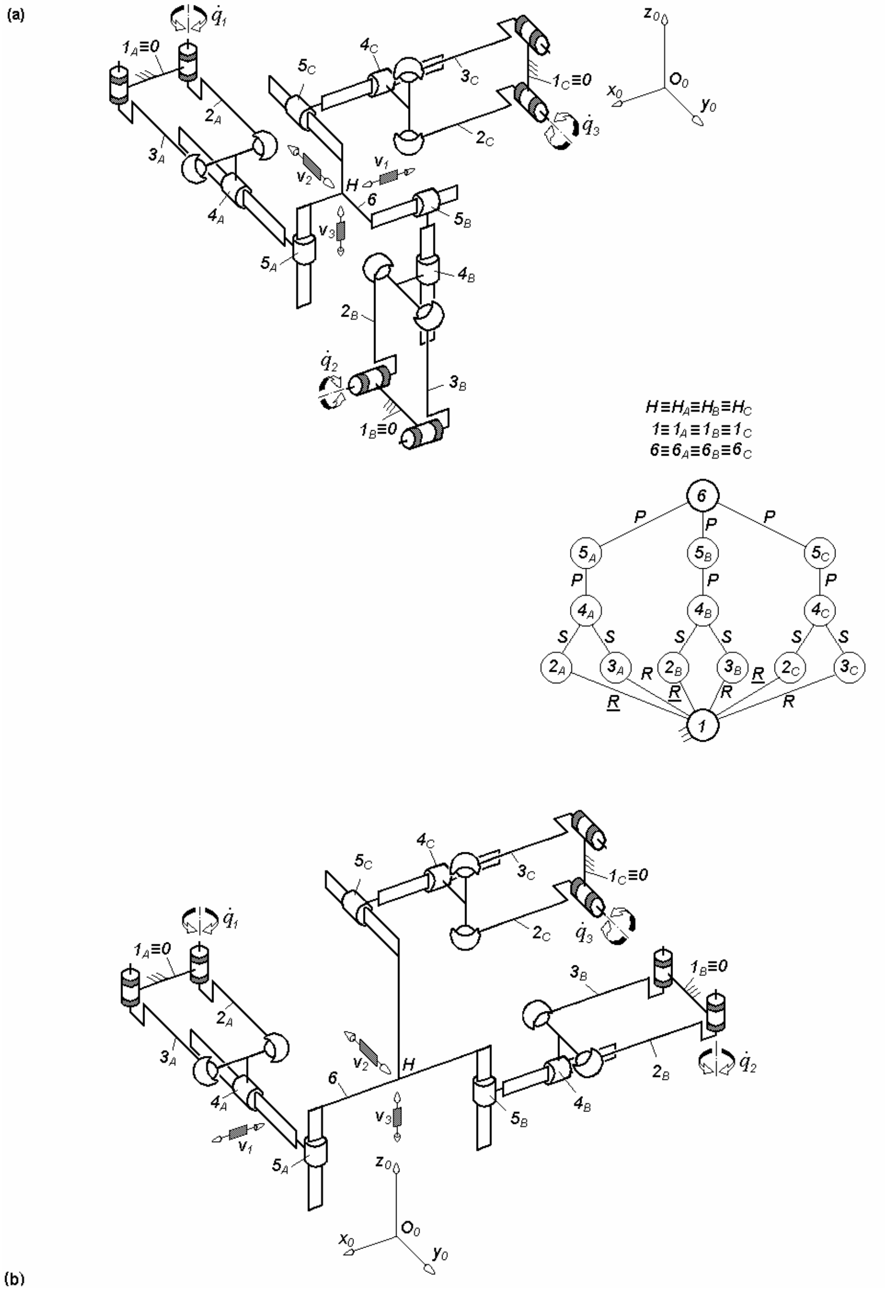


**Fig. 5.52.** *3-<u>Pa</u>$^{ss}$PP*-type overconstrained TPMs with uncoupled motions and rotating actuators mounted on the fixed base, defined by $M_F = S_F = 3$, $(R_F) = (\boldsymbol{v}_1, \boldsymbol{v}_2, \boldsymbol{v}_3)$, $T_F = 0$, $N_F = 3$, limb topology $\underline{Pa}^{ss} \perp P \perp^{||} P$

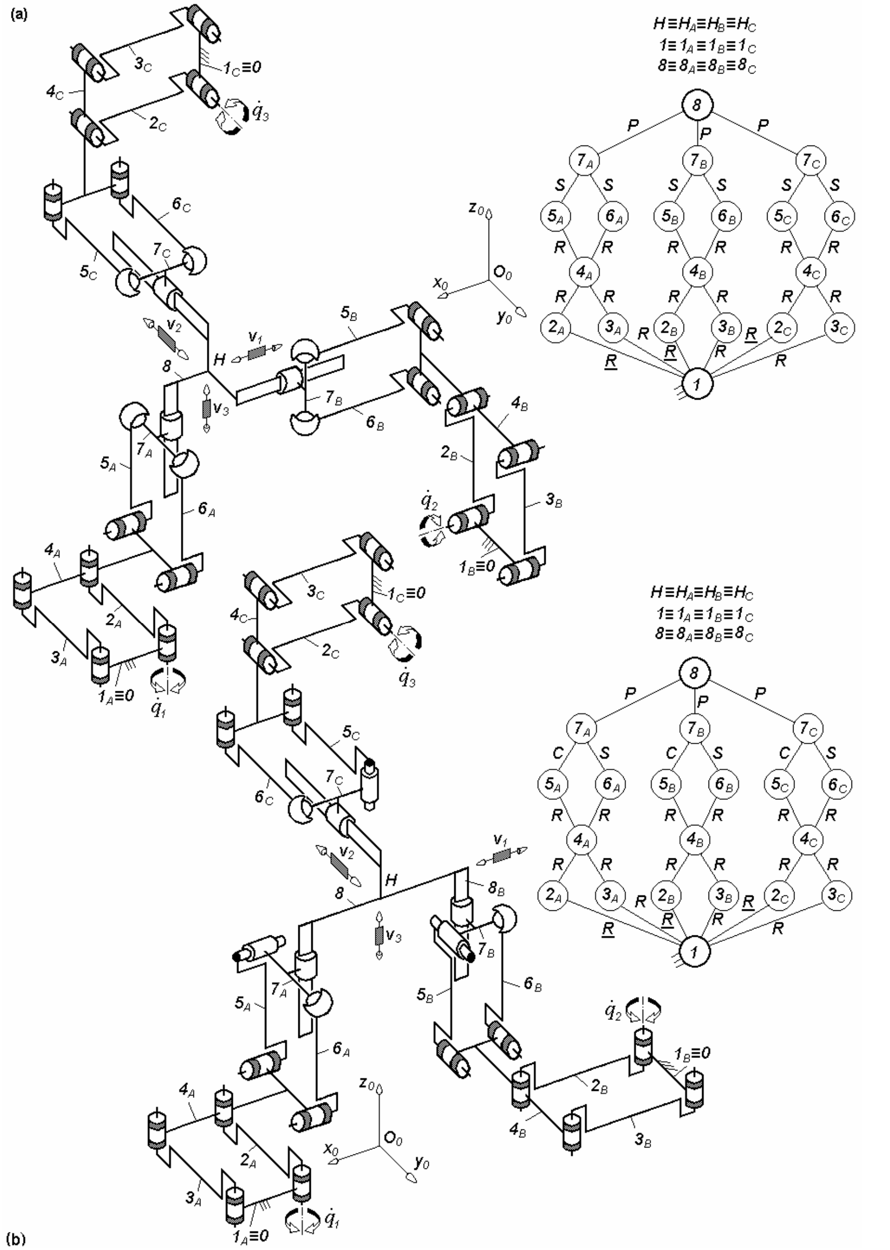


**Fig. 5.53.** Overconstrained TPMs with uncoupled motions of types $3\text{-}\underline{Pa}Pa^{ss}P$ (**a**) and $3\text{-}\underline{Pa}Pa^{cs}P$ (**b**) defined by $M_F = S_F = 3$, $(R_F) = (\boldsymbol{v}_1, \boldsymbol{v}_2, \boldsymbol{v}_3)$, $T_F = 0$, $N_F = 12$ (**a**), $N_F = 15$ (**b**), limb topology $\underline{Pa} \perp Pa^{ss} \perp^{\parallel} P$ (**a**) and $\underline{Pa} \perp Pa^{cs} \perp^{\parallel} P$ (**b**)

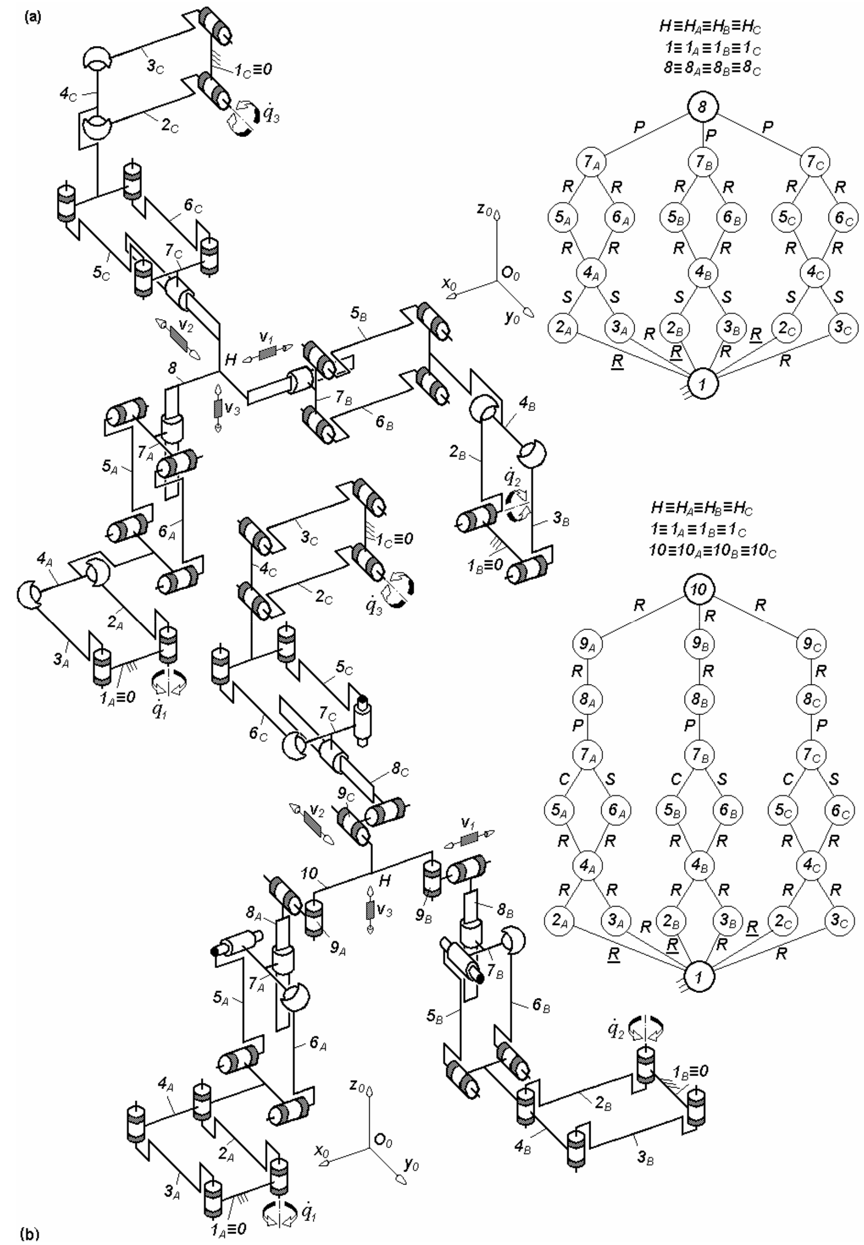


**Fig. 5.54.** Overconstrained TPMs with uncoupled motions of types *3-*$\underline{Pa}^{ss}PaP$ (**a**) and *3-*$\underline{Pa}Pa^{cs}PR^*R^*$ (**b**) defined by $M_F = S_F = 3$, $(R_F) = (\boldsymbol{v}_1,\boldsymbol{v}_2,\boldsymbol{v}_3)$, $T_F = 0$, $N_F = 12$ (**a**), $N_F = 9$ (**b**), limb topology $\underline{Pa}^{ss}\perp Pa\perp^{||}P$ (**a**) and $\underline{Pa}\perp Pa^{cs}\perp^{||}P\perp^{\perp}R^*\perp^{||}R^*$ (**b**)

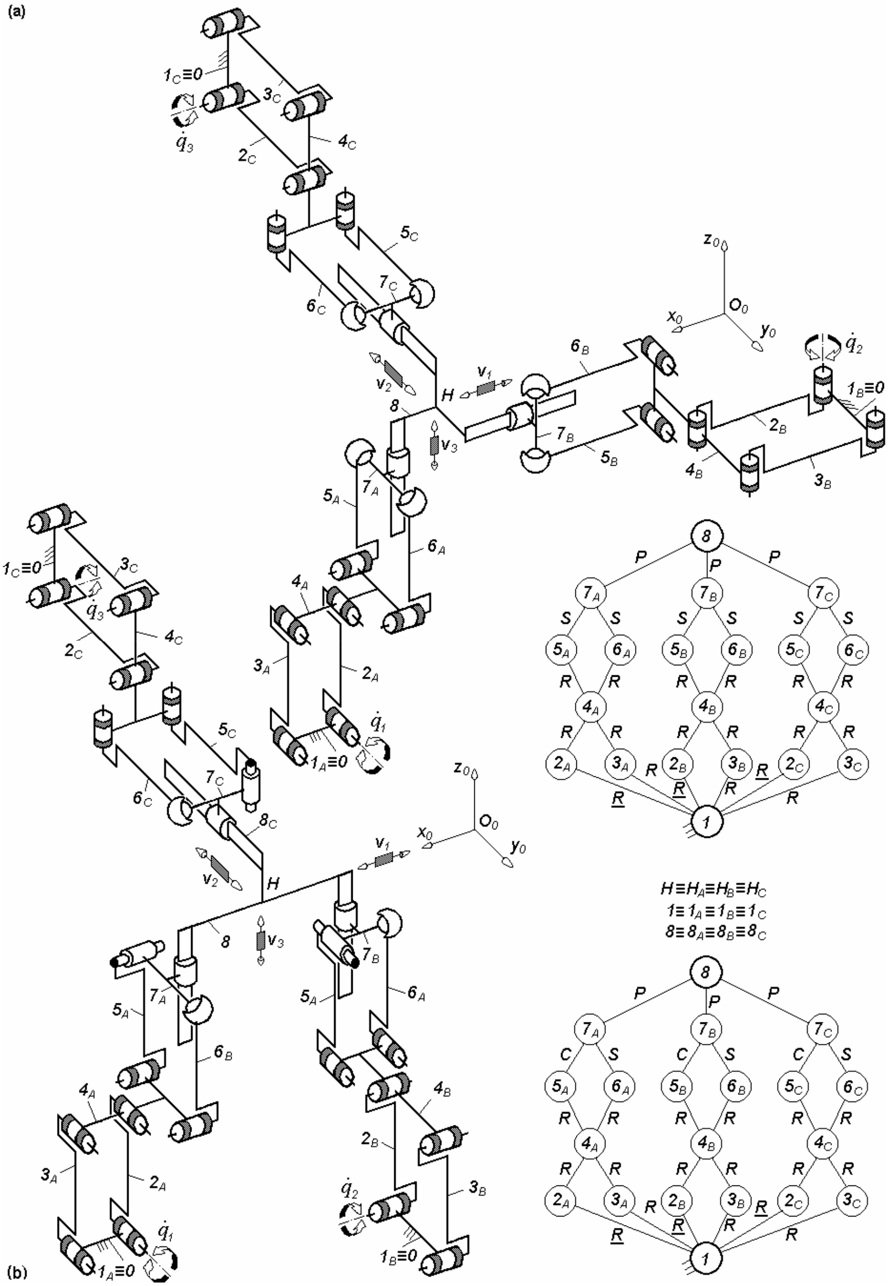


**Fig. 5.55.** Overconstrained TPMs with uncoupled motions of types $3\text{-}\underline{Pa}Pa^{ss}P$ (**a**) and $3\text{-}\underline{Pa}Pa^{cs}P$ (**b**) defined by $M_F = S_F = 3$, $(R_F) = (\boldsymbol{v}_1, \boldsymbol{v}_2, \boldsymbol{v}_3)$, $T_F = 0$, $N_F = 12$ (**a**), $N_F = 15$ (**b**), limb topology $\underline{Pa} \perp Pa^{ss} \perp^{\perp} P$ (**a**) and $\underline{Pa} \perp Pa^{cs} \perp^{\perp} P$ (**b**)

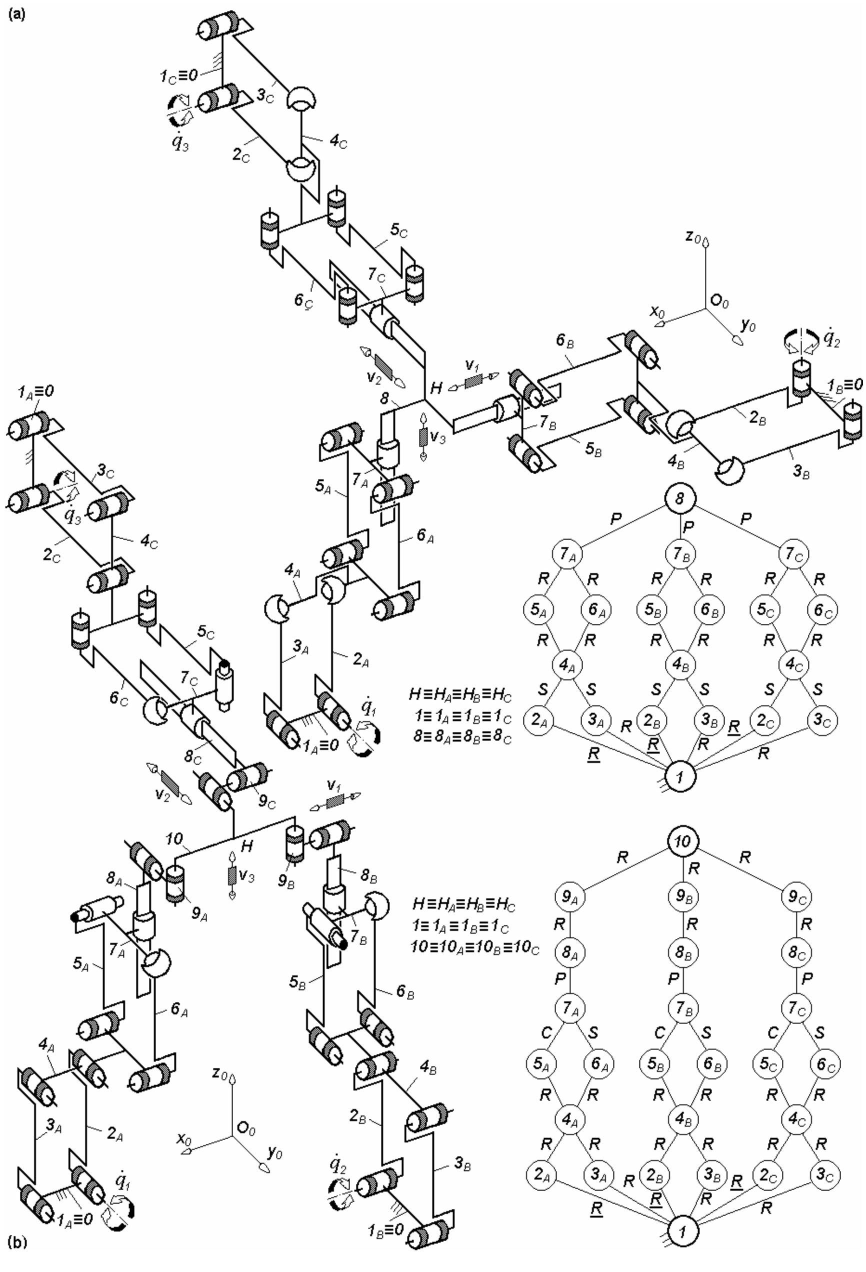


**Fig. 5.56.** Overconstrained TPMs with uncoupled motions of types *3-<u>Pa</u>*$^{ss}$*PaP* (**a**) and *3-<u>Pa</u>Pa*$^{cs}$*PR*R** (**b**) defined by $M_F = S_F = 3$, $(R_F) = (\mathbf{v}_1, \mathbf{v}_2, \mathbf{v}_3)$, $T_F = 0$, $N_F = 12$ (**a**), $N_F = 9$ (**b**), limb topology $\underline{Pa}^{ss} \perp Pa \perp^{\perp} P$ (**a**) and $\underline{Pa} \perp Pa^{cs} \perp^{\perp} P \perp^{\perp} R^* \perp^{\parallel} R^*$(**b**)

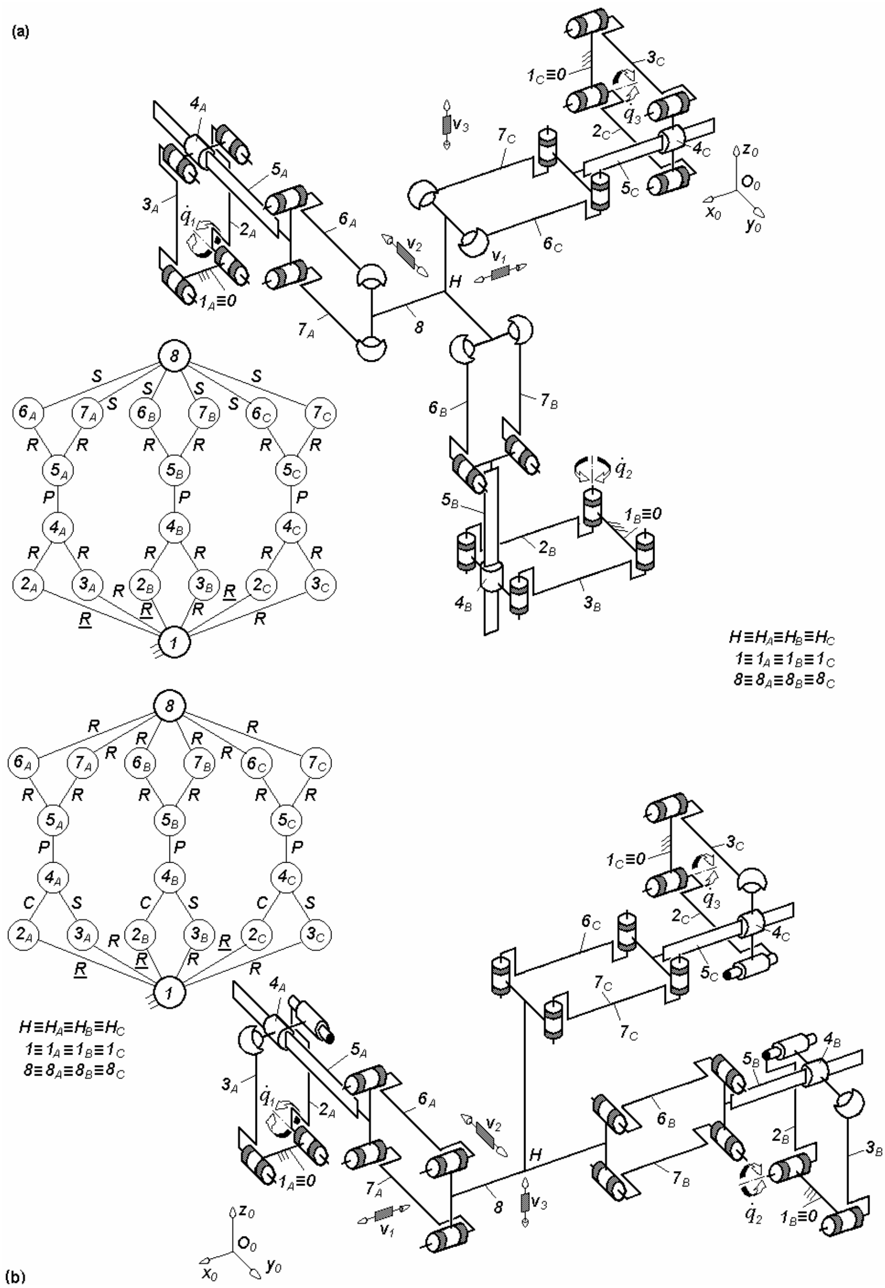


**Fig. 5.57.** Overconstrained TPMs with uncoupled motions of types *3-*$\underline{Pa}PPa^{ss}$ (**a**) and *3-*$\underline{Pa}^{cs}PPa$ (**b**) defined by $M_F = S_F = 3$, $(R_F) = (\boldsymbol{v}_1, \boldsymbol{v}_2, \boldsymbol{v}_3)$, $T_F = 0$, $N_F = 12$ (**a**), $N_F = 15$ (**b**), limb topology $\underline{Pa}||P \perp Pa^{ss}$ (**a**) and $\underline{Pa}^{cs}||P \perp Pa$ (**b**)

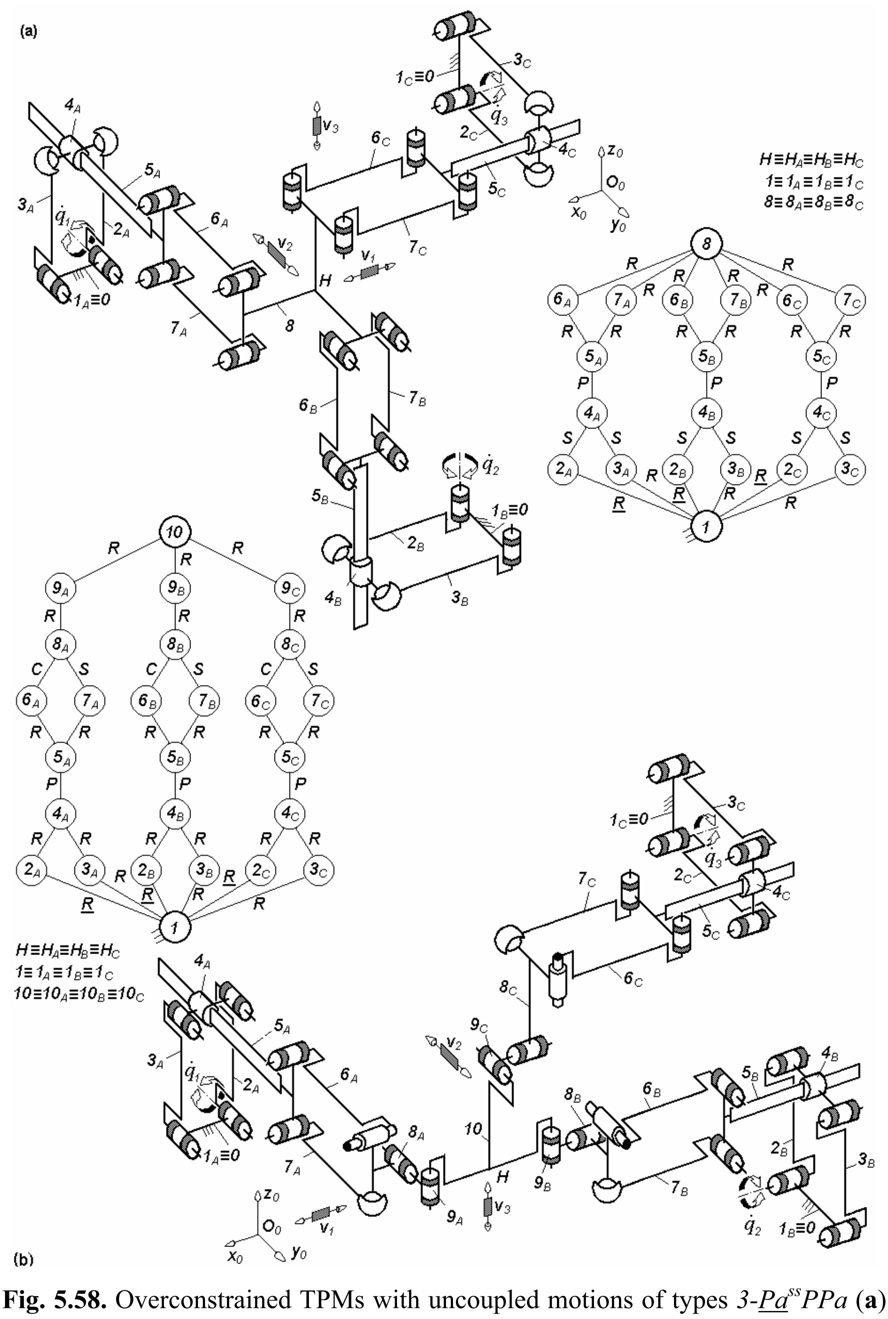

**Fig. 5.58.** Overconstrained TPMs with uncoupled motions of types $3\text{-}\underline{Pa}^{ss}PPa$ (**a**) and $3\text{-}\underline{Pa}PPa^{cs}R^*R^*$ (**b**) defined by $M_F = S_F = 3$, $(R_F) = (\boldsymbol{v}_1, \boldsymbol{v}_2, \boldsymbol{v}_3)$, $T_F = 0$, $N_F = 12$ (**a**), $N_F = 9$ (**b**), limb topology $\underline{Pa}^{ss}||P \perp Pa$ (**a**) and $\underline{Pa}||P \perp Pa^{cs} \perp^{||} R^* \perp^{\perp} R^*$ (**b**)

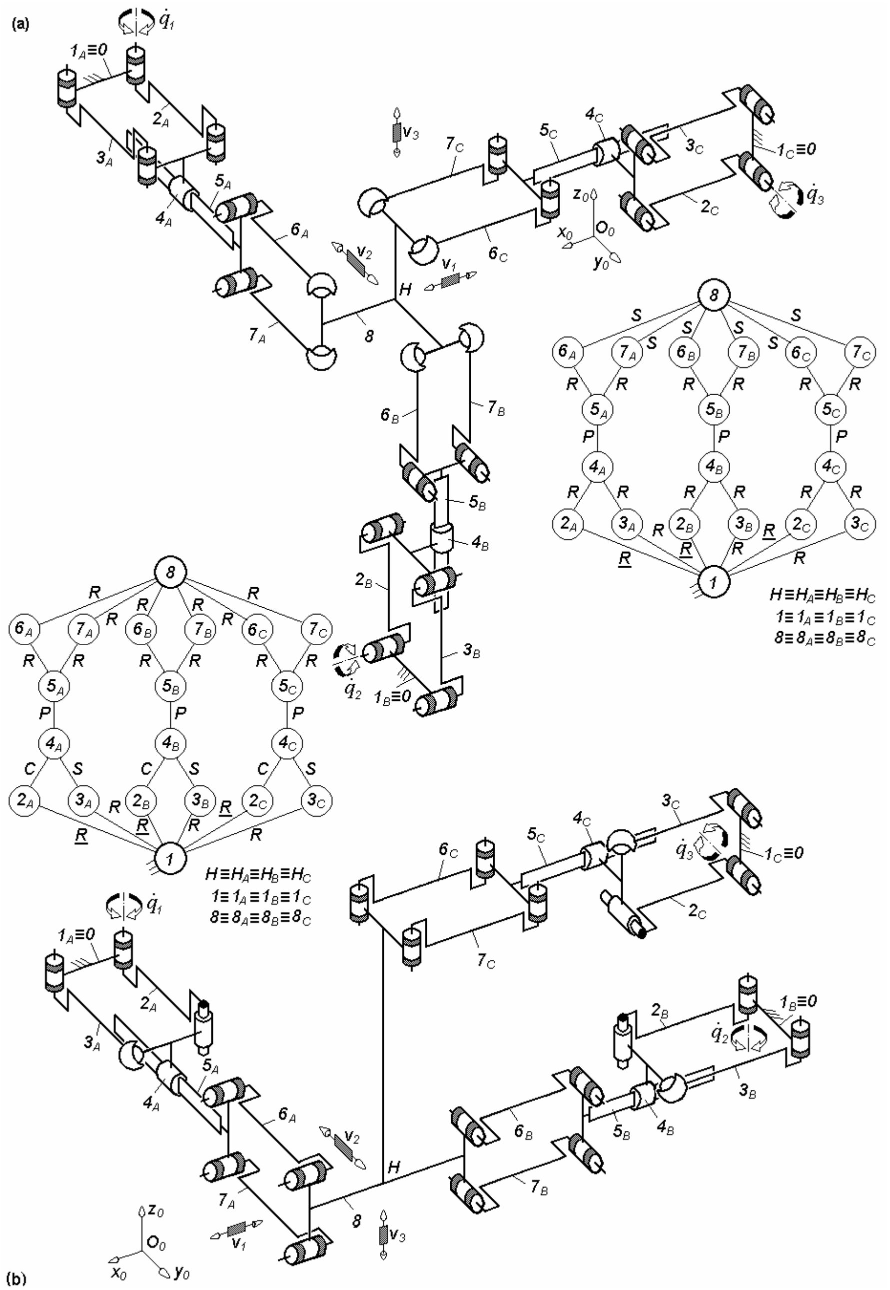


**Fig. 5.59.** Overconstrained TPMs with uncoupled motions of types *3-<u>Pa</u>PPa*$^{ss}$ (**a**) and *3-<u>Pa</u>*$^{cs}$*PPa* (**b**) defined by $M_F = S_F = 3$, $(R_F) = (\boldsymbol{v}_1, \boldsymbol{v}_2, \boldsymbol{v}_3)$, $T_F = 0$, $N_F = 12$ (**a**), $N_F = 15$ (**b**), limb topology $\underline{Pa} \perp P \perp^{\perp} Pa^{ss}$ (**a**) and $\underline{Pa}^{cs} \perp P \perp^{\perp} Pa$ (**b**)

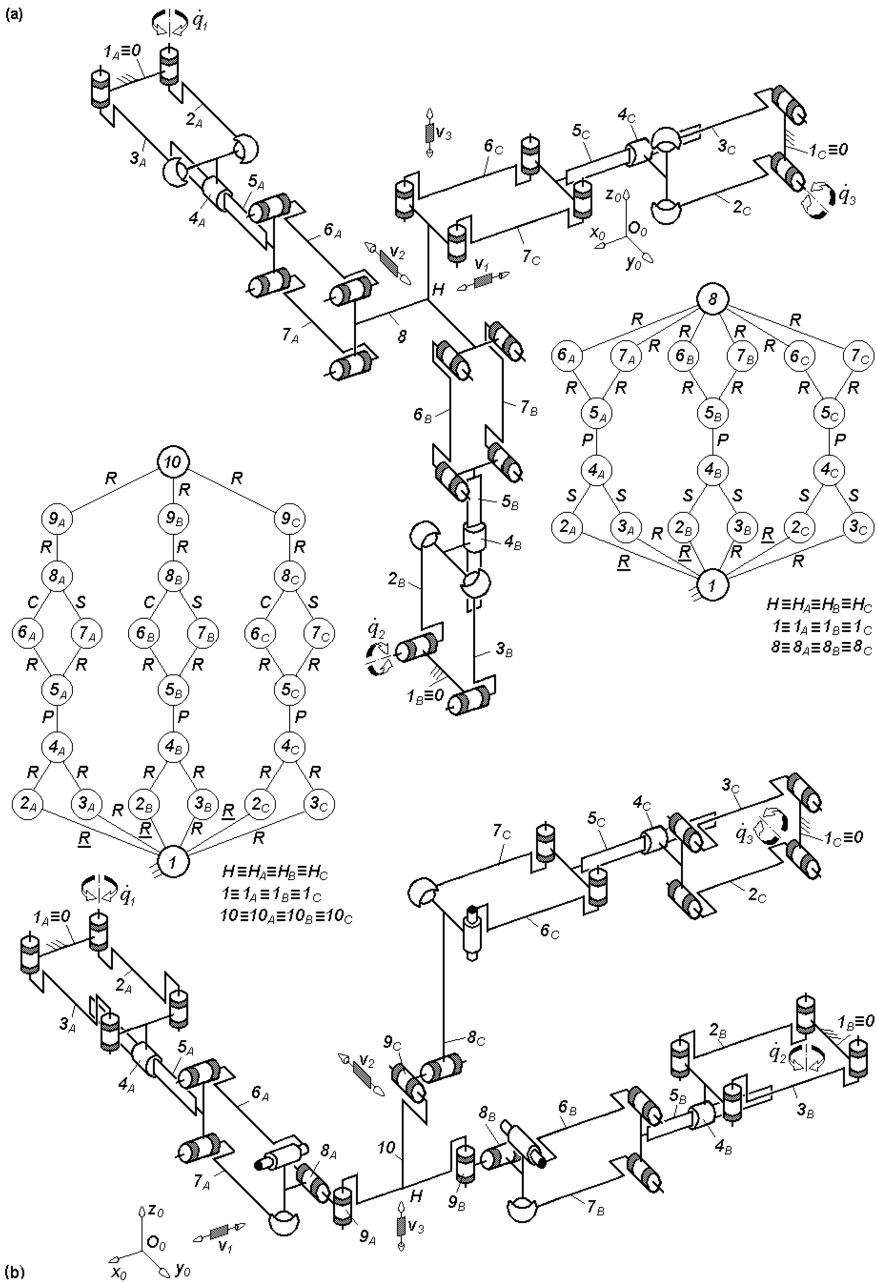

**Fig. 5.60.** Overconstrained TPMs with uncoupled motions of types *3-$\underline{Pa}^{ss}$PPa* (**a**) and *3-$\underline{Pa}$PPa$^{cs}$R*R** (**b**) defined by $M_F = S_F = 3$, $(R_F) = (\boldsymbol{v}_1, \boldsymbol{v}_2, \boldsymbol{v}_3)$, $T_F = 0$, $N_F = 12$ (**a**), $N_F = 9$ (**b**), limb topology $\underline{Pa}^{ss} \perp P \perp^{\perp} Pa$ (**a**) and $\underline{Pa} \perp P \perp^{\perp} Pa^{cs} \perp^{\parallel} R^* \perp^{\perp} R^*$ (**b**)

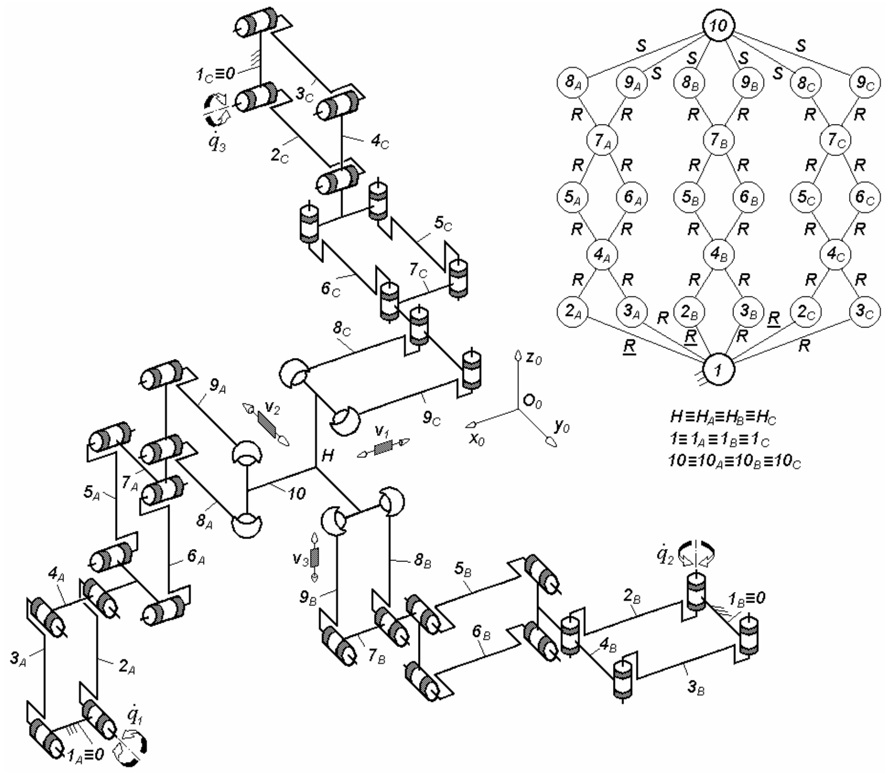


**Fig. 5.61.** *3-<u>Pa</u>PaPa*$^{ss}$-type overconstrained TPM with uncoupled motions and rotating actuators mounted on the fixed base, defined by $M_F = S_F = 3$, $(R_F) = (\boldsymbol{v}_1, \boldsymbol{v}_2, \boldsymbol{v}_3)$, $T_F = 0$, $N_F = 21$, limb topology $\underline{Pa} \perp Pa||Pa^{ss}$

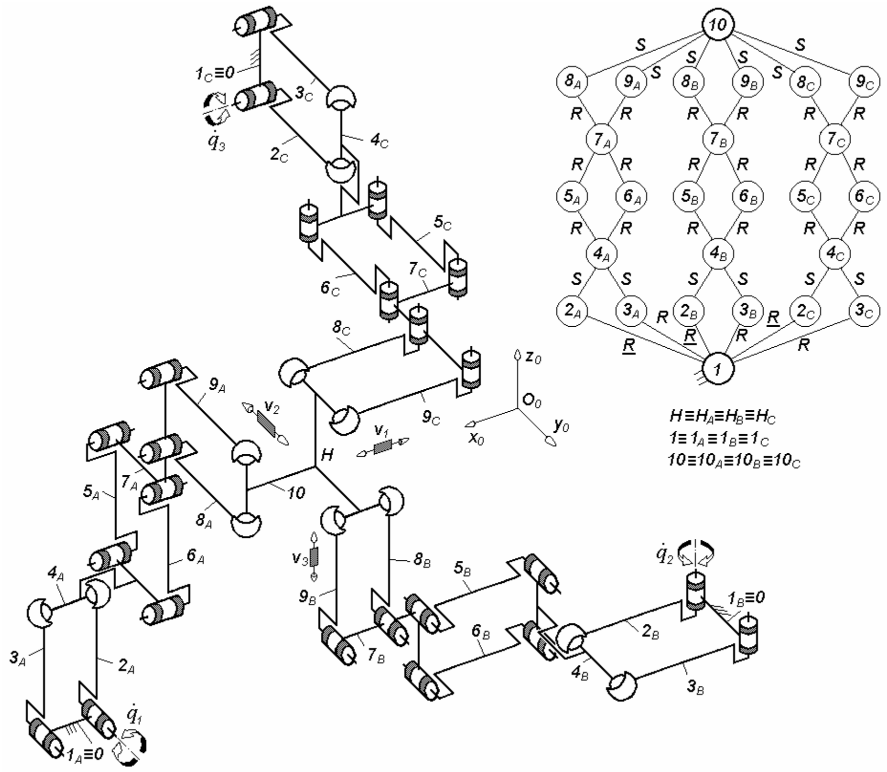


**Fig. 5.62.** *3-<u>Pa</u>$^{ss}$PaPa$^{ss}$*-type overconstrained TPM with uncoupled motions and rotating actuators mounted on the fixed base, defined by $M_F = S_F = 3$, $(R_F) = (\boldsymbol{v}_1, \boldsymbol{v}_2, \boldsymbol{v}_3)$, $T_F = 0$, $N_F = 9$, limb topology <u>*Pa*</u>$^{ss} \perp Pa||Pa^{ss}$

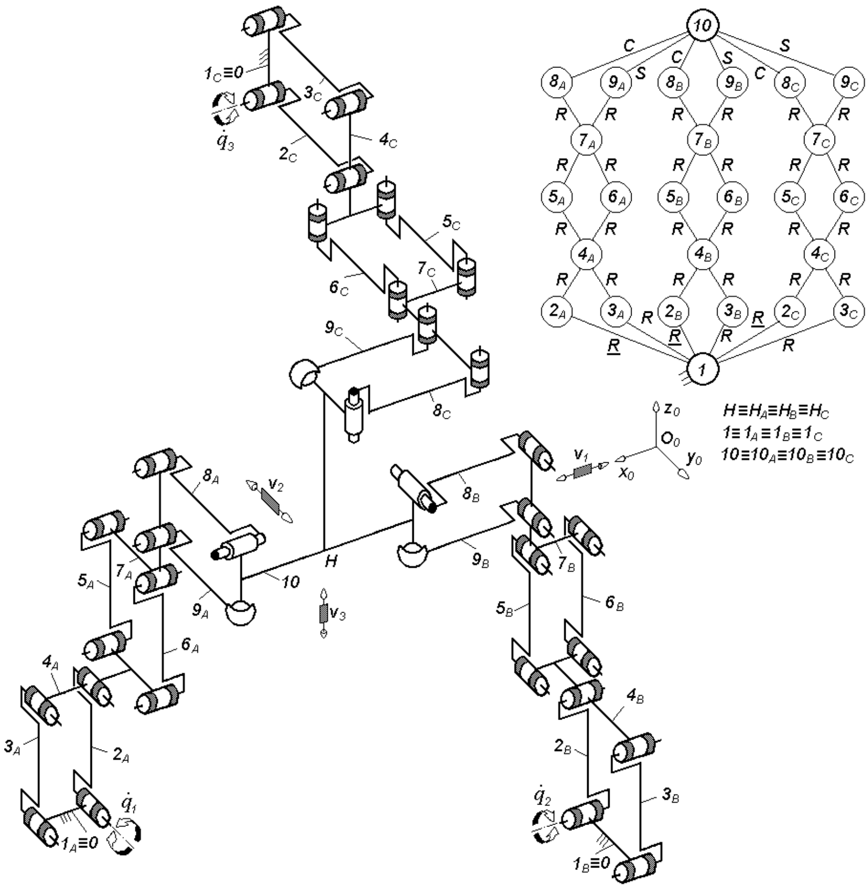


**Fig. 5.63.** *3-PaPaPa*$^{cs}$-type overconstrained TPM with uncoupled motions and rotating actuators mounted on the fixed base, defined by $M_F = S_F = 3$, $(R_F) = (\boldsymbol{v}_1, \boldsymbol{v}_2, \boldsymbol{v}_3)$, $T_F = 0$, $N_F = 24$, limb topology $\underline{Pa} \perp Pa || Pa^{cs}$

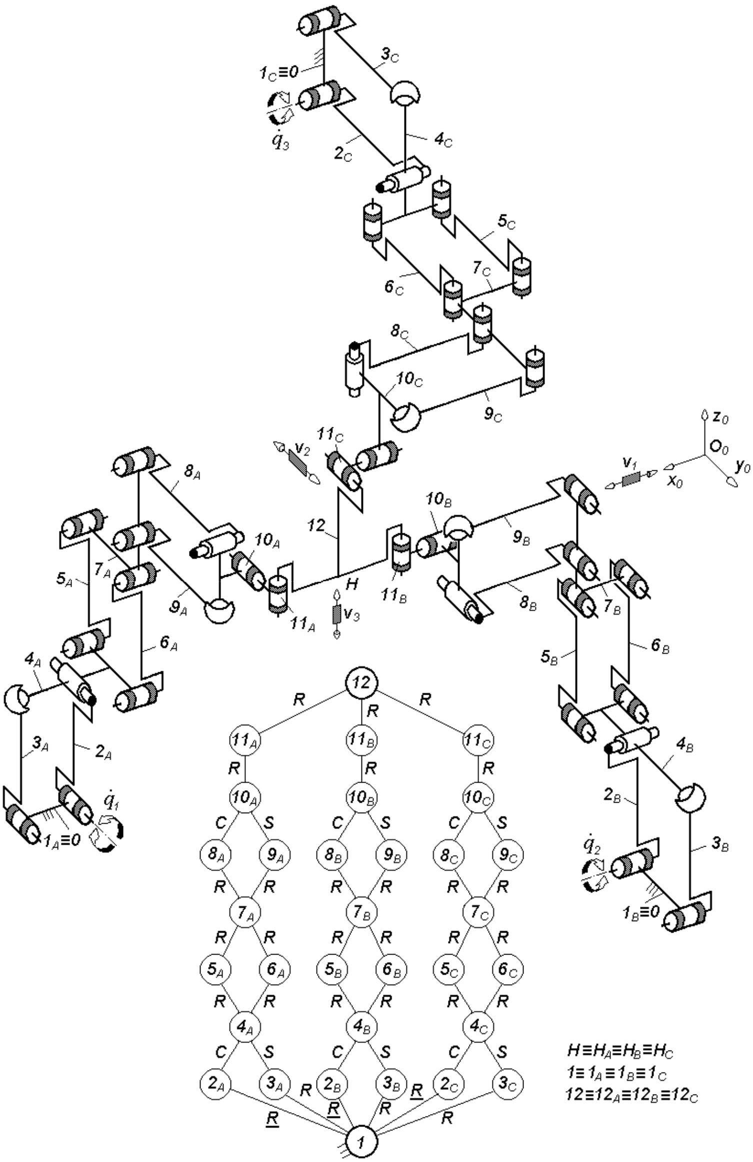


**Fig. 5.64.** 3-$\underline{Pa}^{cs}PaPa^{cs}R^*R^*$-type overconstrained TPM with uncoupled motions and rotating actuators mounted on the fixed base, defined by $M_F = S_F = 3$, $(R_F) = (\mathbf{v}_1, \mathbf{v}_2, \mathbf{v}_3)$, $T_F = 0$, $N_F = 9$, limb topology $\underline{Pa}^{cs} \perp Pa||Pa^{cs} \perp^{||} R^* \perp^{\perp} R^*$

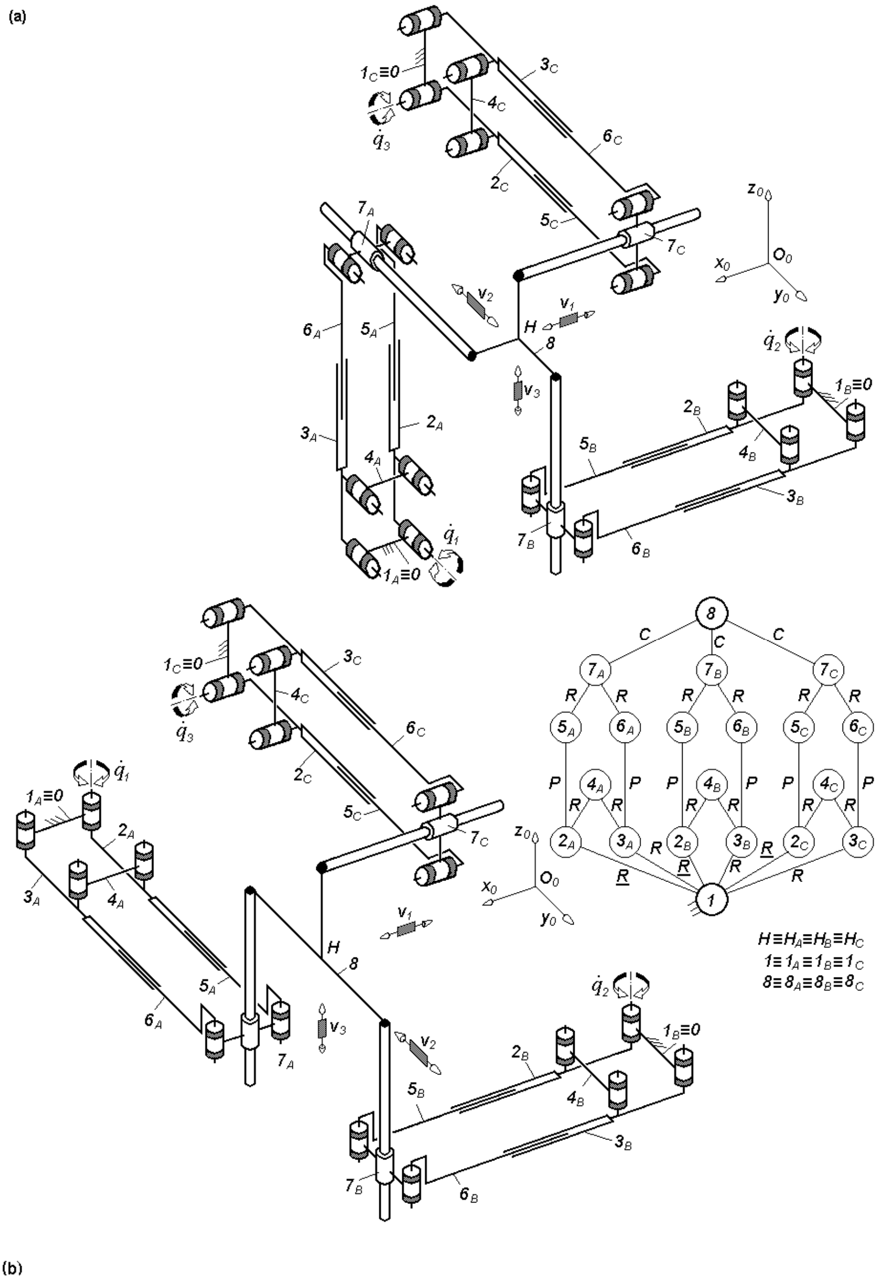


**Fig. 5.65.** *3-$\underline{Pa}Pa^tC^*$*-type overconstrained TPMs with uncoupled motions and rotating actuators mounted on the fixed base, defined by $M_F = S_F = 3$, $(R_F) = (\mathbf{v}_1, \mathbf{v}_2, \mathbf{v}_3)$, $T_F = 0$, $N_F = 21$, limb topology $\underline{Pa}||Pa^t||C^*$

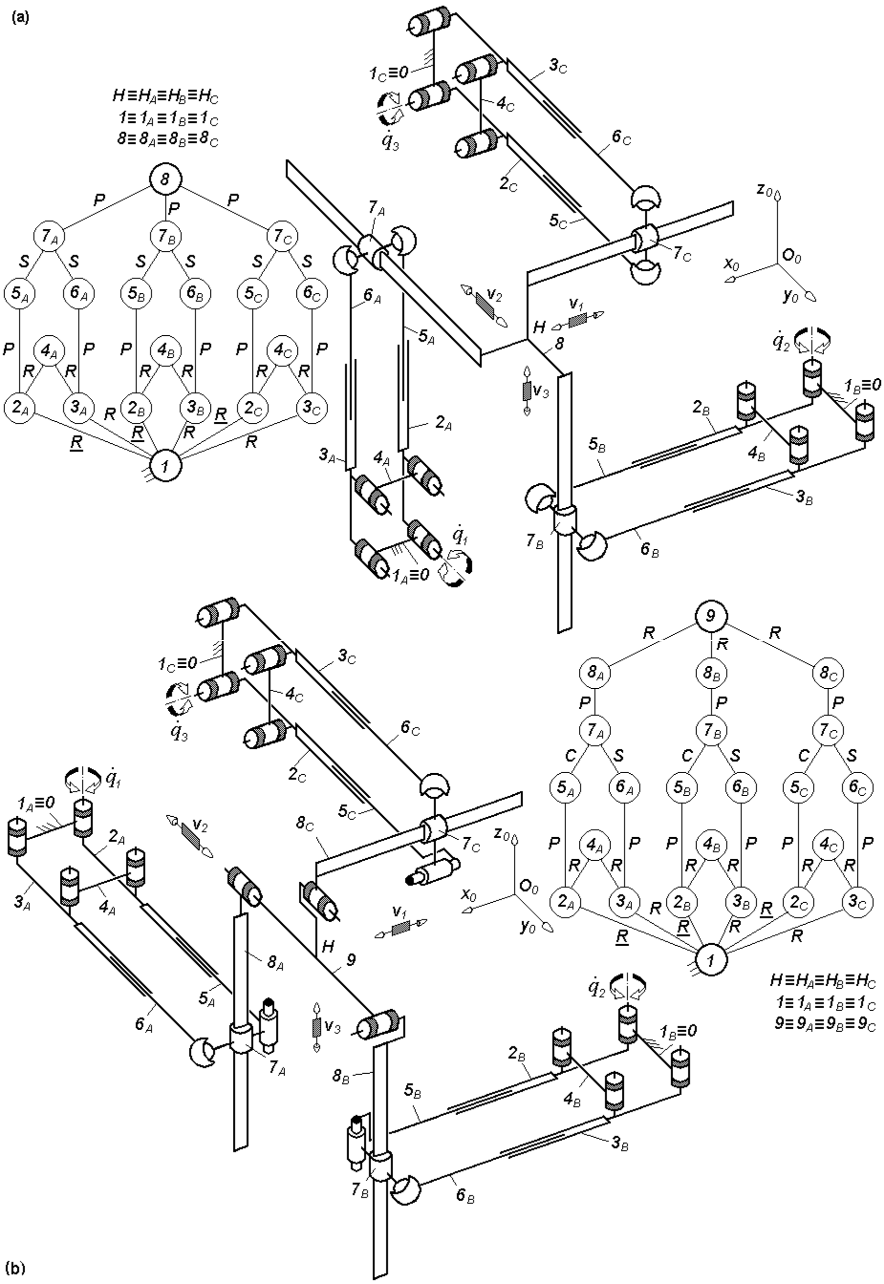


**Fig. 5.66.** Overconstrained TPMs with uncoupled motions of types $3\text{-}\underline{Pa}Pa^{tss}P$ (**a**) and $3\text{-}\underline{Pa}Pa^{tcs}PR^{*}$ (**b**) defined by $M_F = S_F = 3$, $(R_F) = (\boldsymbol{v}_1, \boldsymbol{v}_2, \boldsymbol{v}_3)$, $T_F = 0$, $N_F = 12$, limb topology $\underline{Pa}||Pa^{tss}||P$ (**a**) and $\underline{Pa}||Pa^{tcs}||P \perp^{\perp} R^{*}$ (**b**)

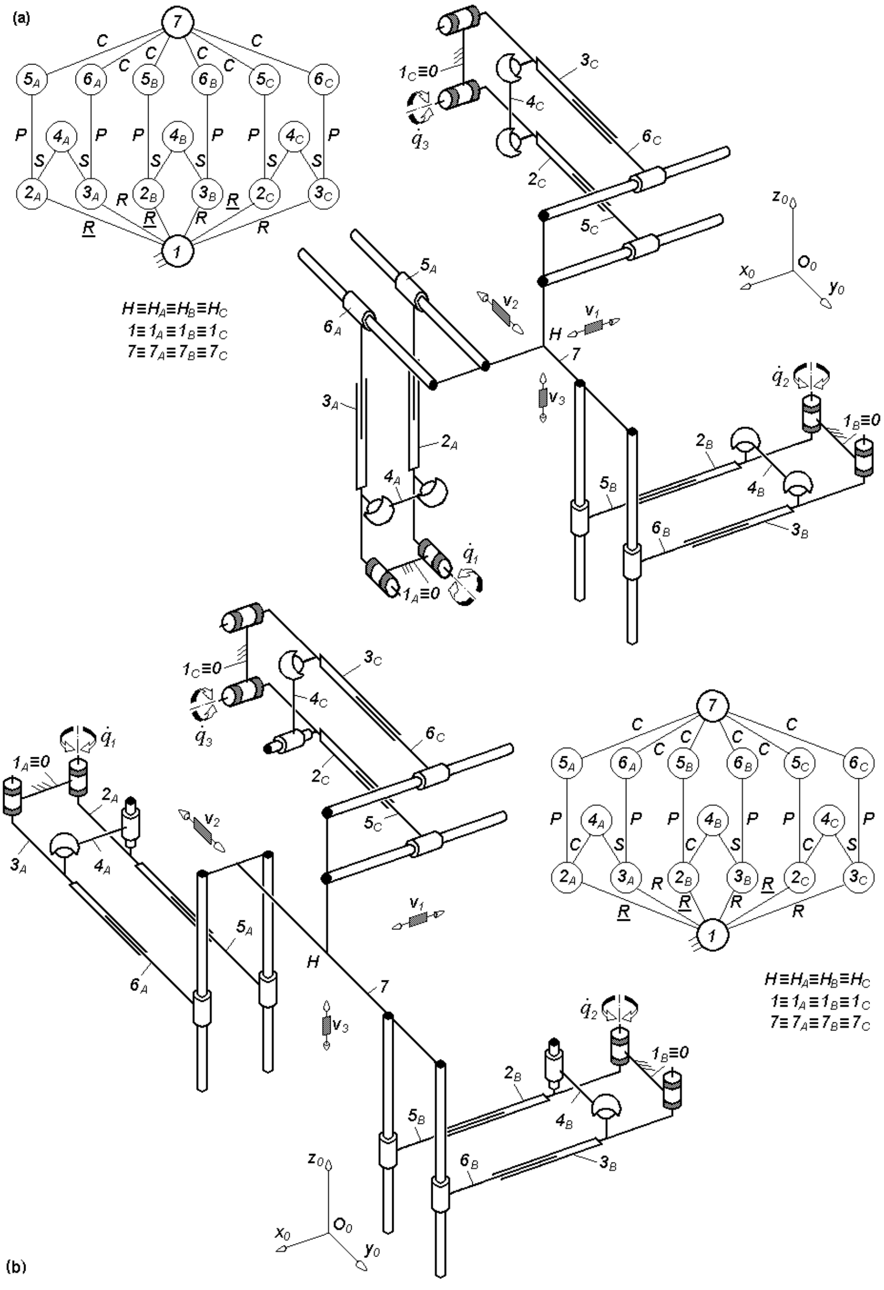


**Fig. 5.67.** Overconstrained TPMs with uncoupled motions of types $3\text{-}\underline{Pa}^{ss}Pa^{tcc}$ (**a**) and $3\text{-}\underline{Pa}^{cs}Pa^{tcc}$ (**b**) defined by $M_F = 6$ (**a**) $M_F = 3$ (**b**) $S_F = 3$, $(R_F) = (\boldsymbol{v}_1, \boldsymbol{v}_2, \boldsymbol{v}_3)$, $T_F = 3$, $T_F = 0$ (**b**), $N_F = 12$, limb topology $\underline{Pa}^{ss}||Pa^{tcc}$ (**a**) and $\underline{Pa}^{cs}||Pa^{tcc}$ (**b**)

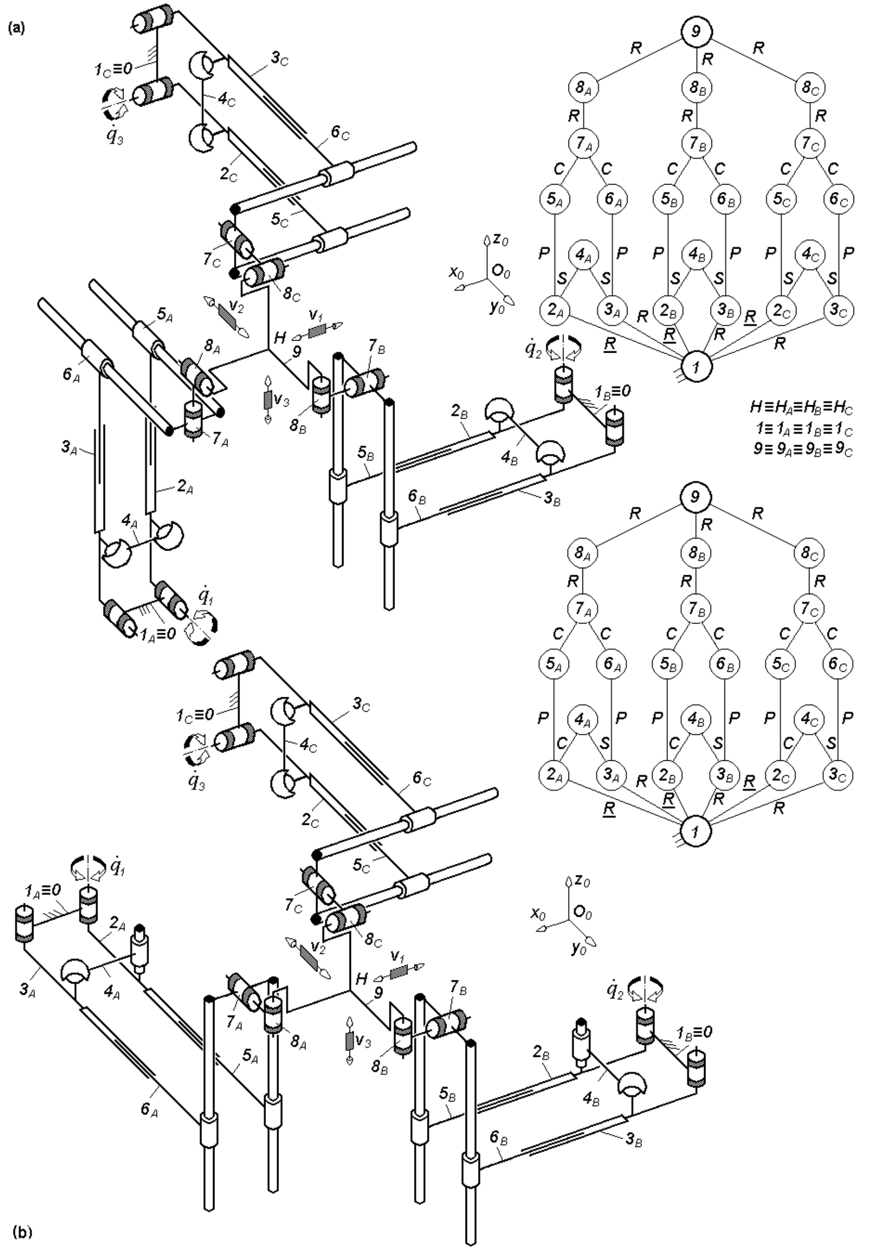


**Fig. 5.68.** Overconstrained TPMs with uncoupled motions of types $3\text{-}\underline{Pa}^{ss}Pa^{tcc}R^{*}R^{*}$ (**a**) and $3\text{-}\underline{Pa}^{cs}Pa^{tcc}R^{*}R^{*}$ (**b**) defined by $M_F = 6$ (**a**) $M_F = 3$ (**b**) $S_F = 3$, $(R_F) = (\boldsymbol{v}_1, \boldsymbol{v}_2, \boldsymbol{v}_3)$, $T_F = 3$ (**a**), $T_F = 0$ (**b**), $N_F = 6$, limb topology $\underline{Pa}^{ss}||Pa^{tcc} \perp R^{*} \perp^{||} R^{*}$ (**a**) and $\underline{Pa}^{cs}||Pa^{tcc} \perp R^{*} \perp^{||} R^{*}$ (**b**)

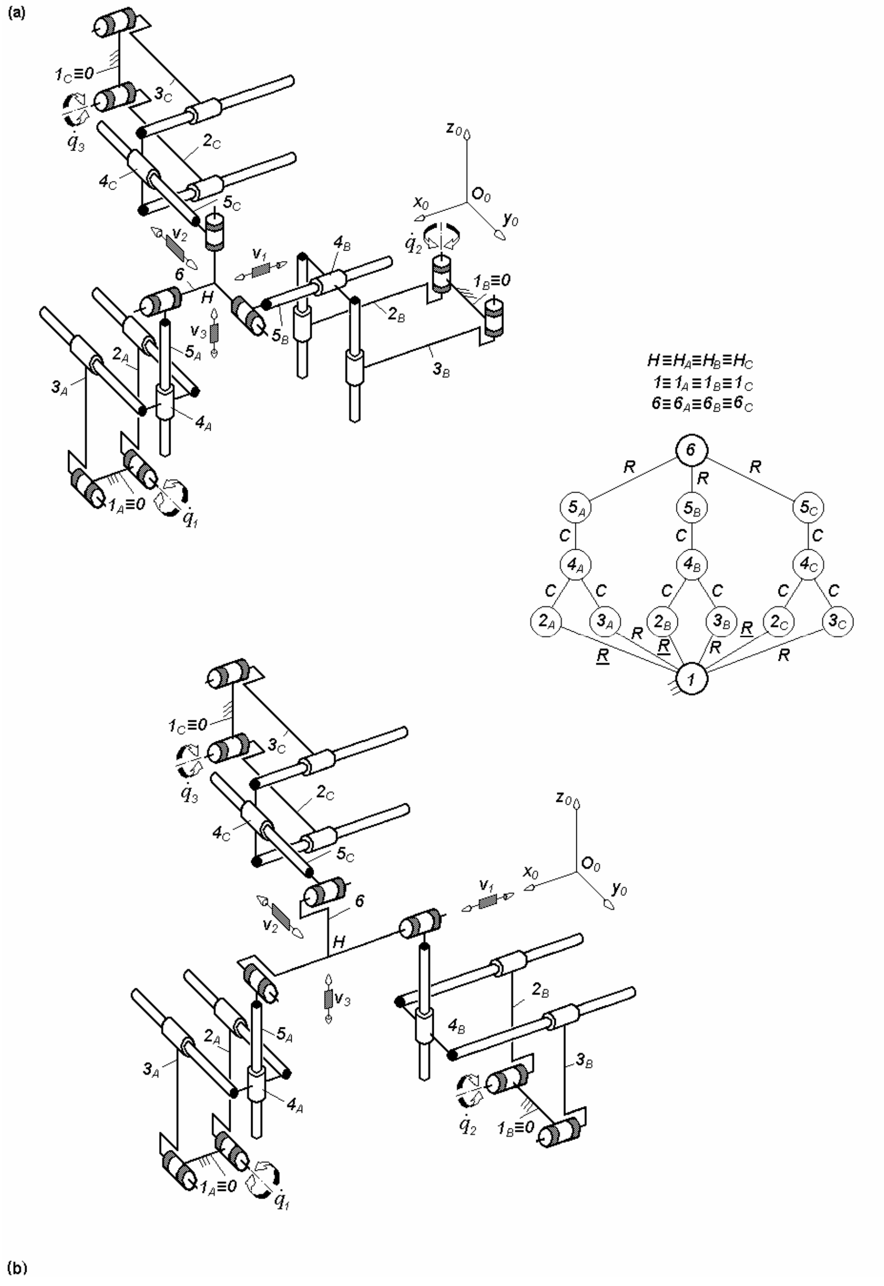


**Fig. 5.69.** *3-$\underline{Pa}^{cc}C^*R^*$*-type *o*verconstrained TPMs with uncoupled motions defined by $M_F = S_F = 3$, $(R_F) = (\boldsymbol{v}_1, \boldsymbol{v}_2, \boldsymbol{v}_3)$, $T_F = 0$, $N_F = 6$, limb topology $\underline{Pa}^{cc} \perp C^* \perp R^*$

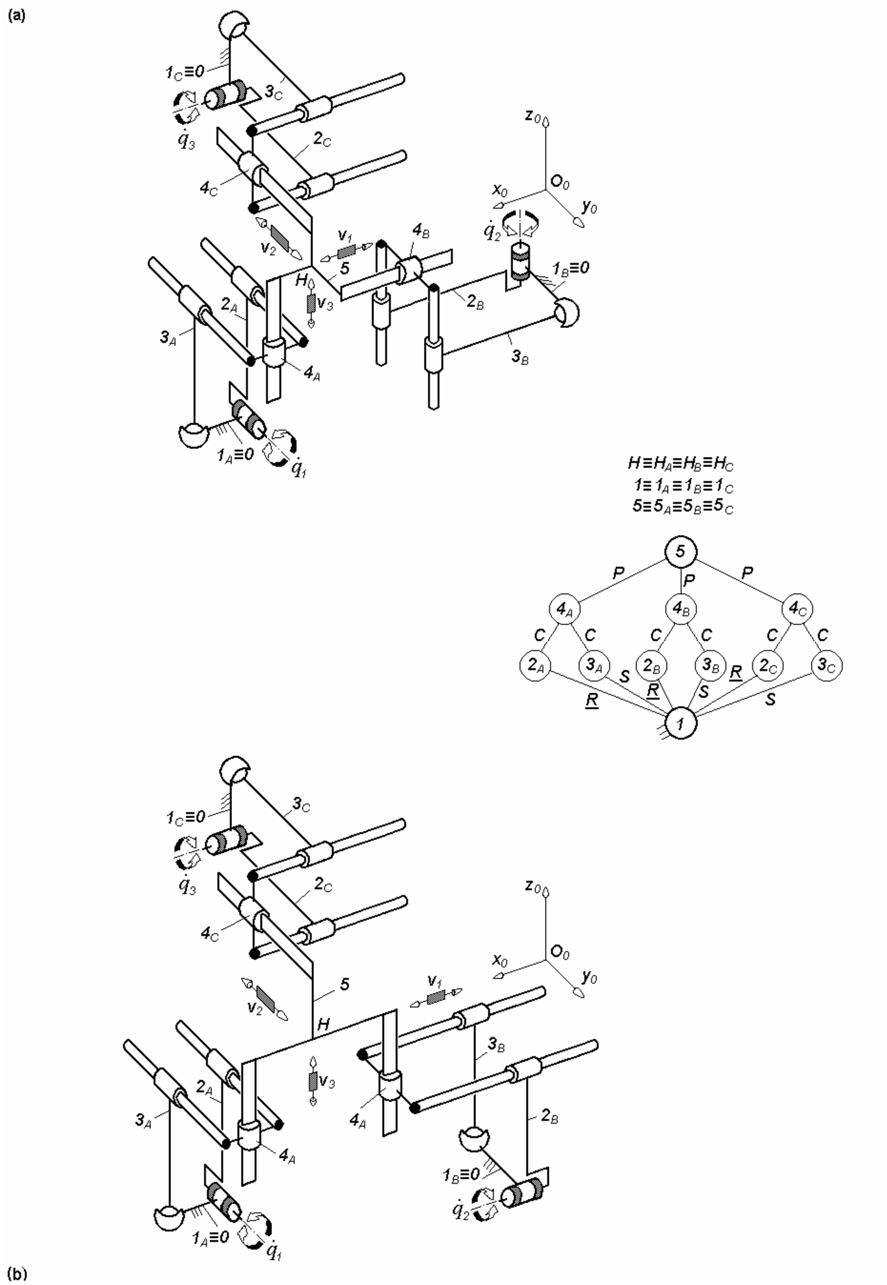


**Fig. 5.70.** *3-*$\underline{Pa}^{ccs}P$-type *o*verconstrained TPMs with uncoupled motions defined by $M_F = S_F = 3$, $(R_F) = (\boldsymbol{v}_1, \boldsymbol{v}_2, \boldsymbol{v}_3)$, $T_F = 0$, $N_F = 6$, limb topology $\underline{Pa}^{ccs} \perp P$

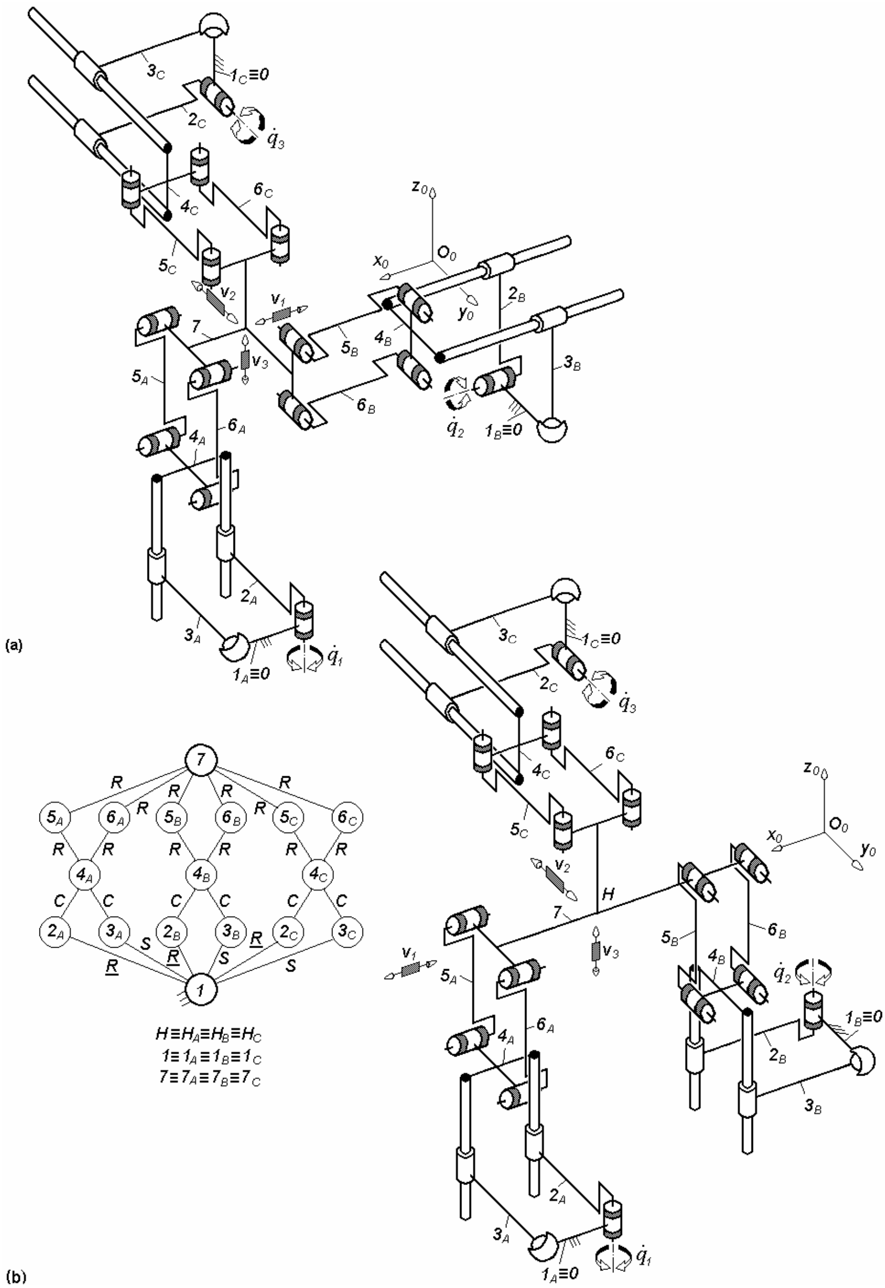


**Fig. 5.71.** $3$-$\underline{Pa}^{ccs}Pa$-type *o*verconstrained TPMs with uncoupled motions defined by $M_F = S_F = 3$, $(R_F) = (\boldsymbol{v}_1, \boldsymbol{v}_2, \boldsymbol{v}_3)$, $T_F = 0$, $N_F = 15$, limb topology $\underline{Pa}^{ccs} \perp Pa$

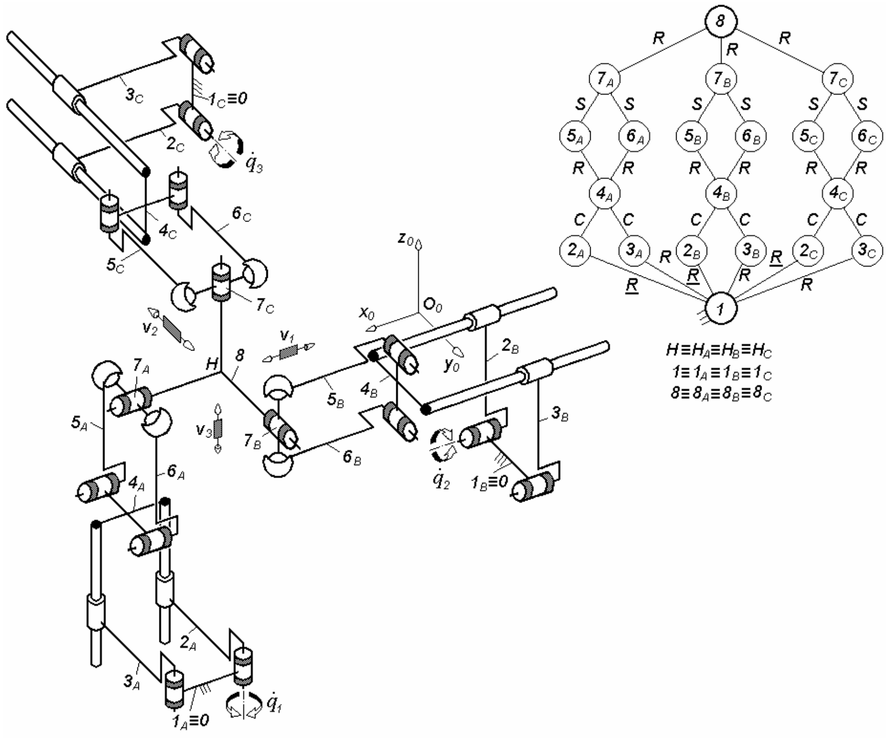


**Fig. 5.72.** *3-$\underline{Pa}^{cc}Pa^{ss}R$**-type overconstrained TPM with uncoupled motions defined by $M_F = S_F = 3$, $(R_F) = (\boldsymbol{v}_1, \boldsymbol{v}_2, \boldsymbol{v}_3)$, $T_F = 0$, $N_F = 6$, limb topology $\underline{Pa}^{cc} \perp Pa^{ss} || R^*$

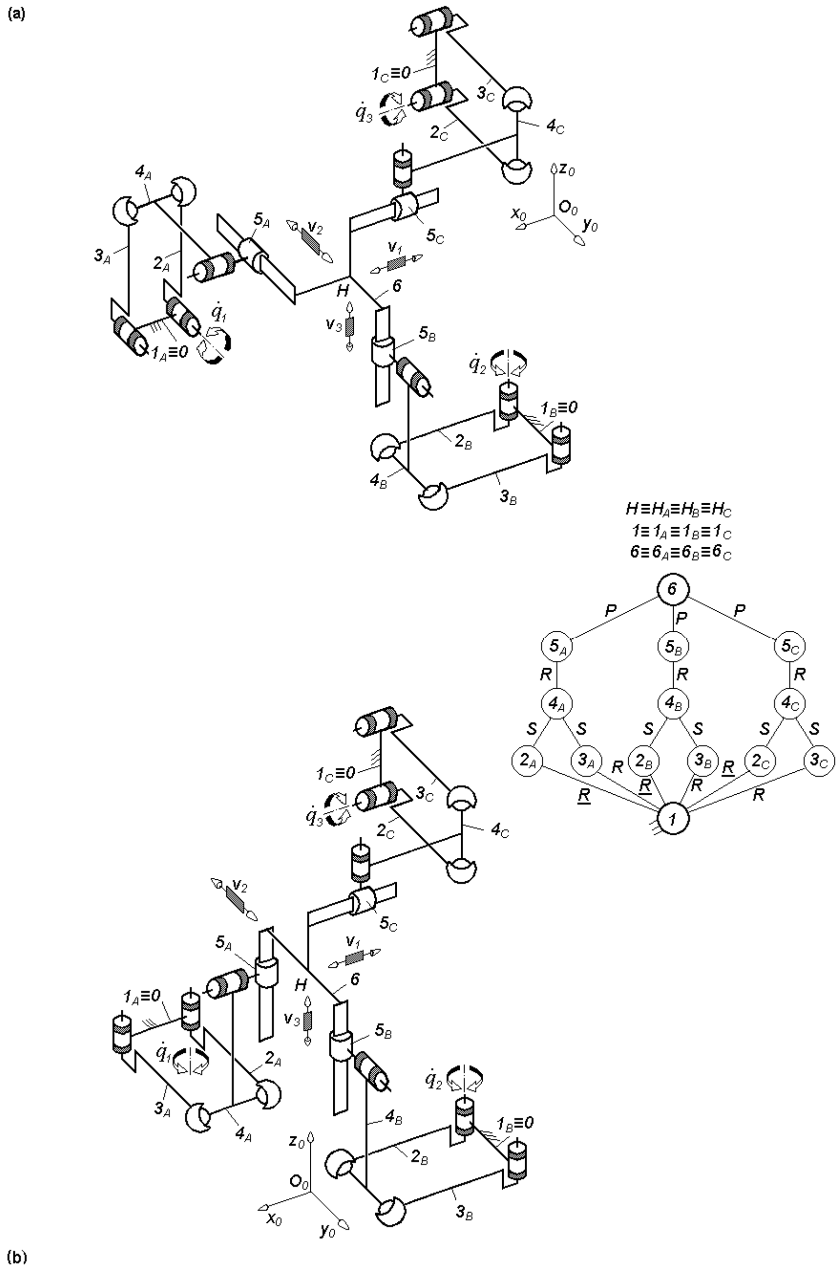


**Fig. 5.73.** *3-$\underline{Pa}^{ss}RP$*-type overconstrained TPMs with uncoupled motions defined by $M_F = S_F = 3$, $(R_F) = (\boldsymbol{v}_1, \boldsymbol{v}_2, \boldsymbol{v}_3)$, $T_F = 0$, $N_F = 3$, limb topology $\underline{Pa}^{ss} \perp R \perp^{\parallel} P$

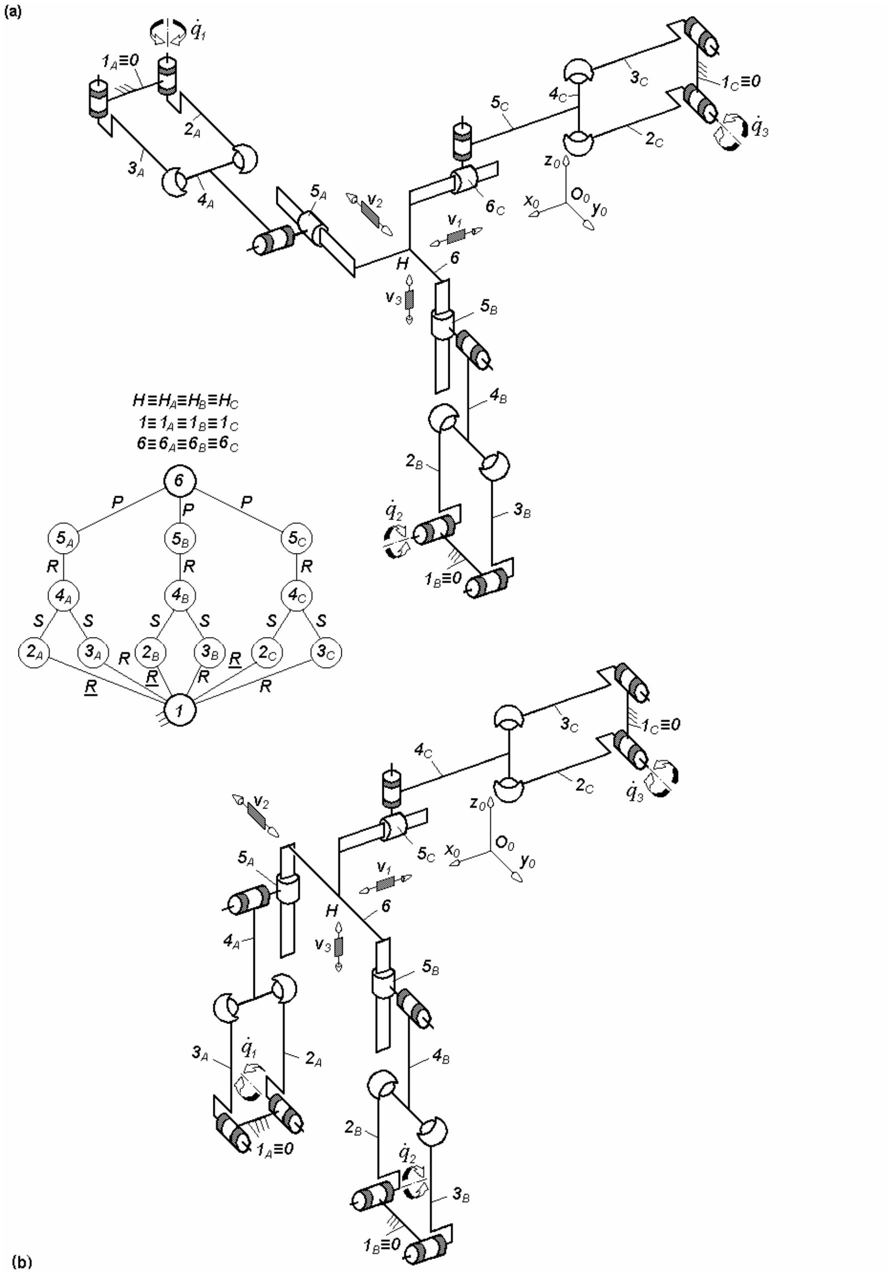


**Fig. 5.74.** *3-$\underline{Pa}^{ss}RP$*-type overconstrained TPMs with uncoupled motions defined by $M_F = S_F = 3$, $(R_F) = (\mathbf{v}_1, \mathbf{v}_2, \mathbf{v}_3)$, $T_F = 0$, $N_F = 3$, limb topology $\underline{Pa}^{ss} \perp R \perp^{\perp} P$

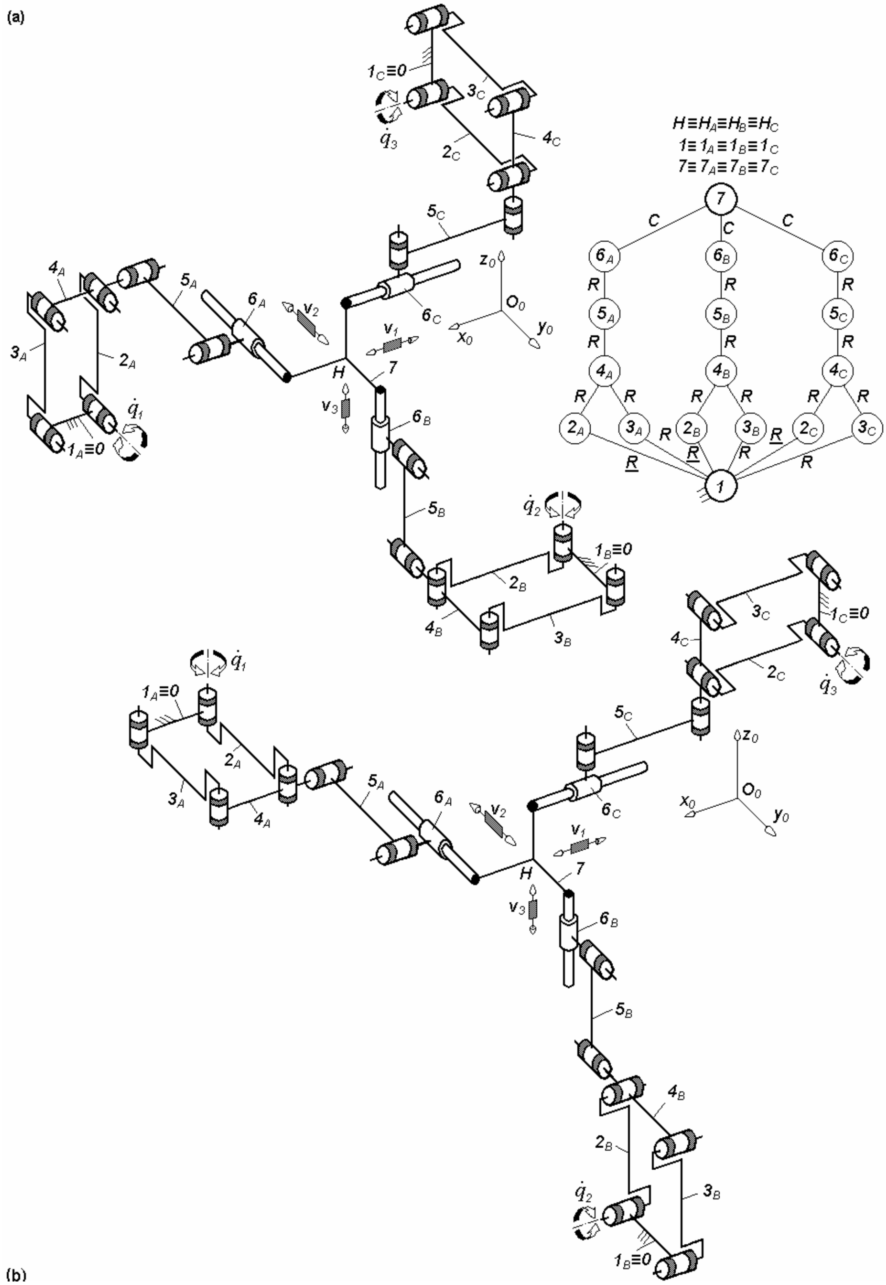


**Fig. 5.75.** *3-PaRRC**-type overconstrained TPMs with uncoupled motions defined by $M_F = S_F = 3$, $(R_F) = (\boldsymbol{v}_1, \boldsymbol{v}_2, \boldsymbol{v}_3)$, $T_F = 0$, $N_F = 9$, limb topology $\underline{Pa} \perp R||R \perp^{\perp} C^*$

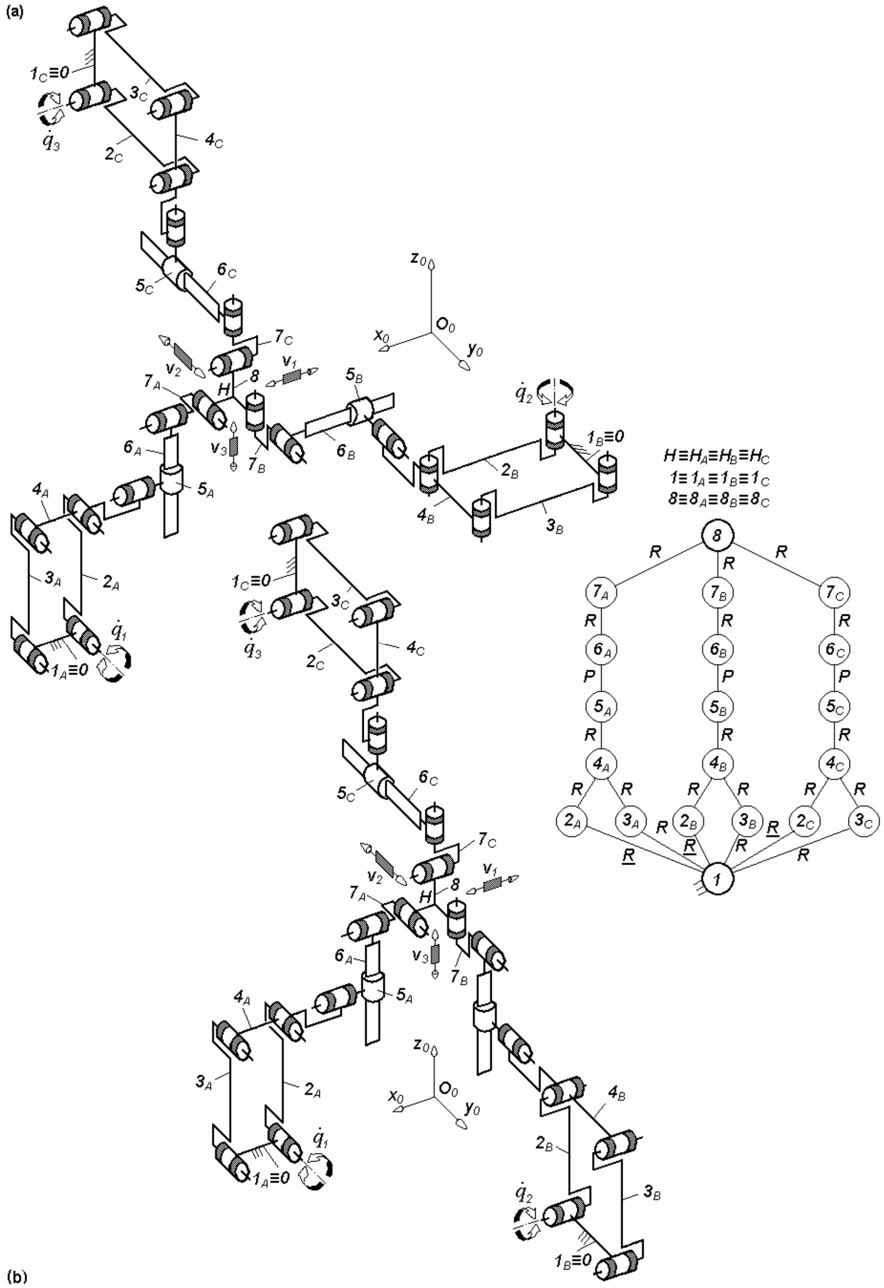


**Fig. 5.76.** *3-<u>Pa</u>RPRR**-type overconstrained TPMs with uncoupled motions defined by $M_F = S_F = 3$, $(R_F) = (\boldsymbol{v}_1, \boldsymbol{v}_2, \boldsymbol{v}_3)$, $T_F = 0$, $N_F = 9$, limb topology $\underline{Pa}\perp R\perp P\perp^{\parallel}R\perp R^*$

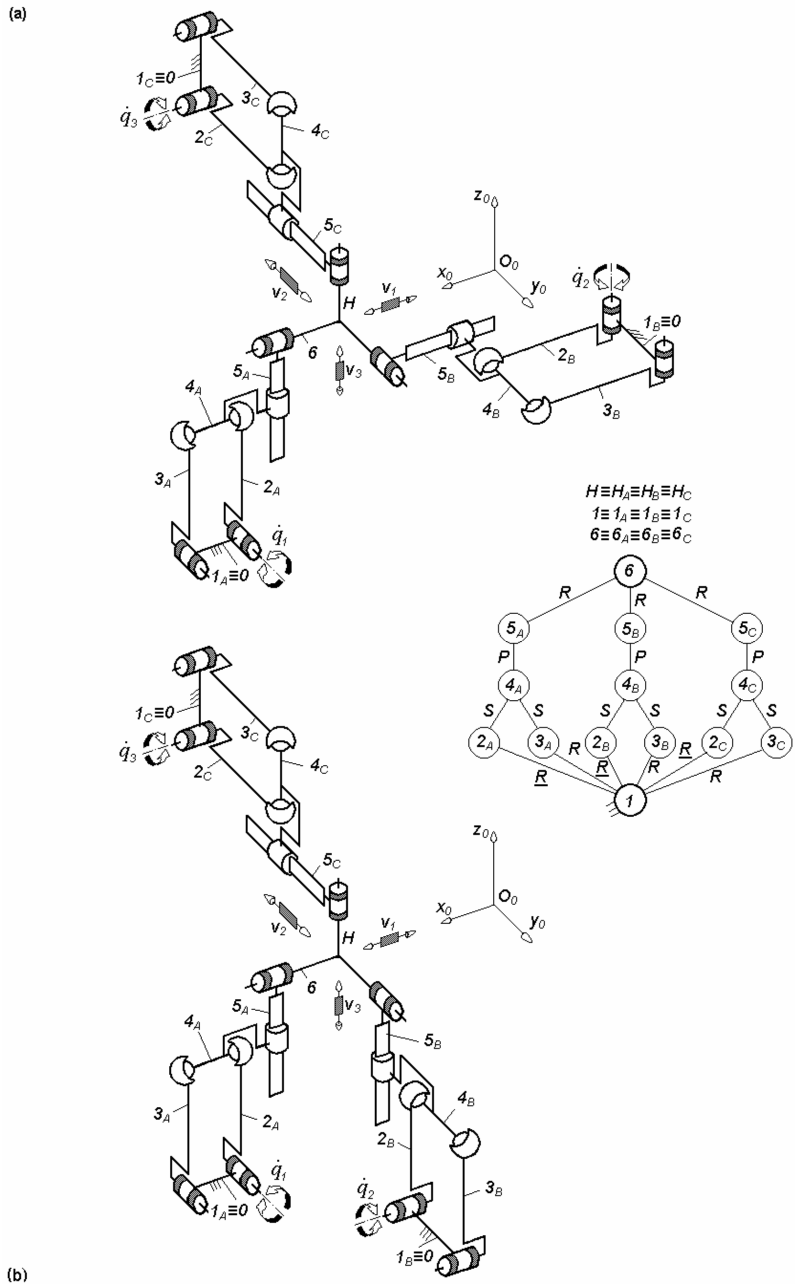


**Fig. 5.77.** $3\text{-}\underline{Pa}^{ss}PR$-type overconstrained TPMs with uncoupled motions defined by $M_F = S_F = 3$, $(R_F) = (\boldsymbol{v}_1, \boldsymbol{v}_2, \boldsymbol{v}_3)$, $T_F = 0$, $N_F = 3$, limb topology $\underline{Pa}^{ss}\text{-}P \perp^{\perp} R$

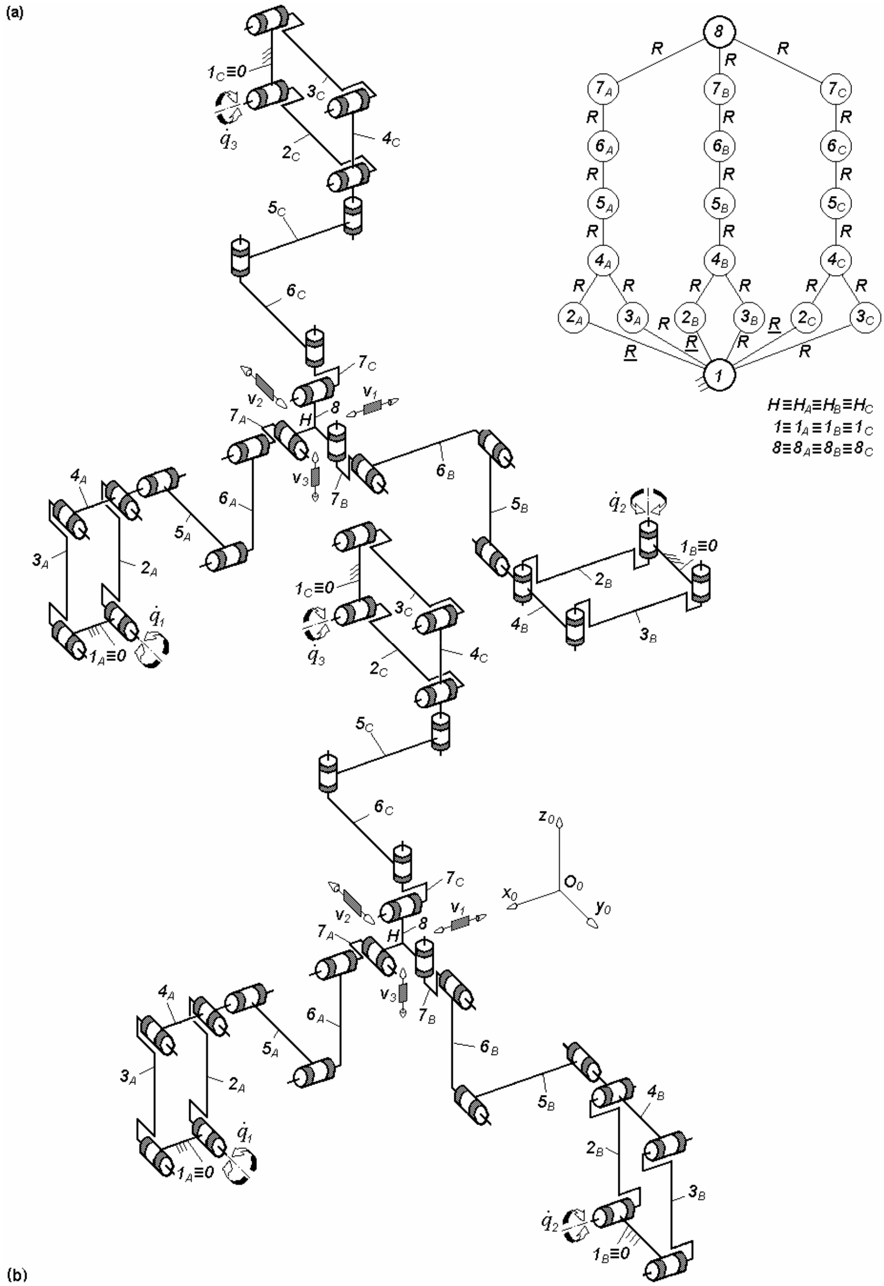


**Fig. 5.78.** *3-PaRRRR**-type overconstrained TPMs with uncoupled motions defined by $M_F = S_F = 3$, $(R_F) = (\boldsymbol{v}_1, \boldsymbol{v}_2, \boldsymbol{v}_3)$, $T_F = 0$, $N_F = 9$, limb topology $\underline{Pa} \perp R||R||R \perp R*$

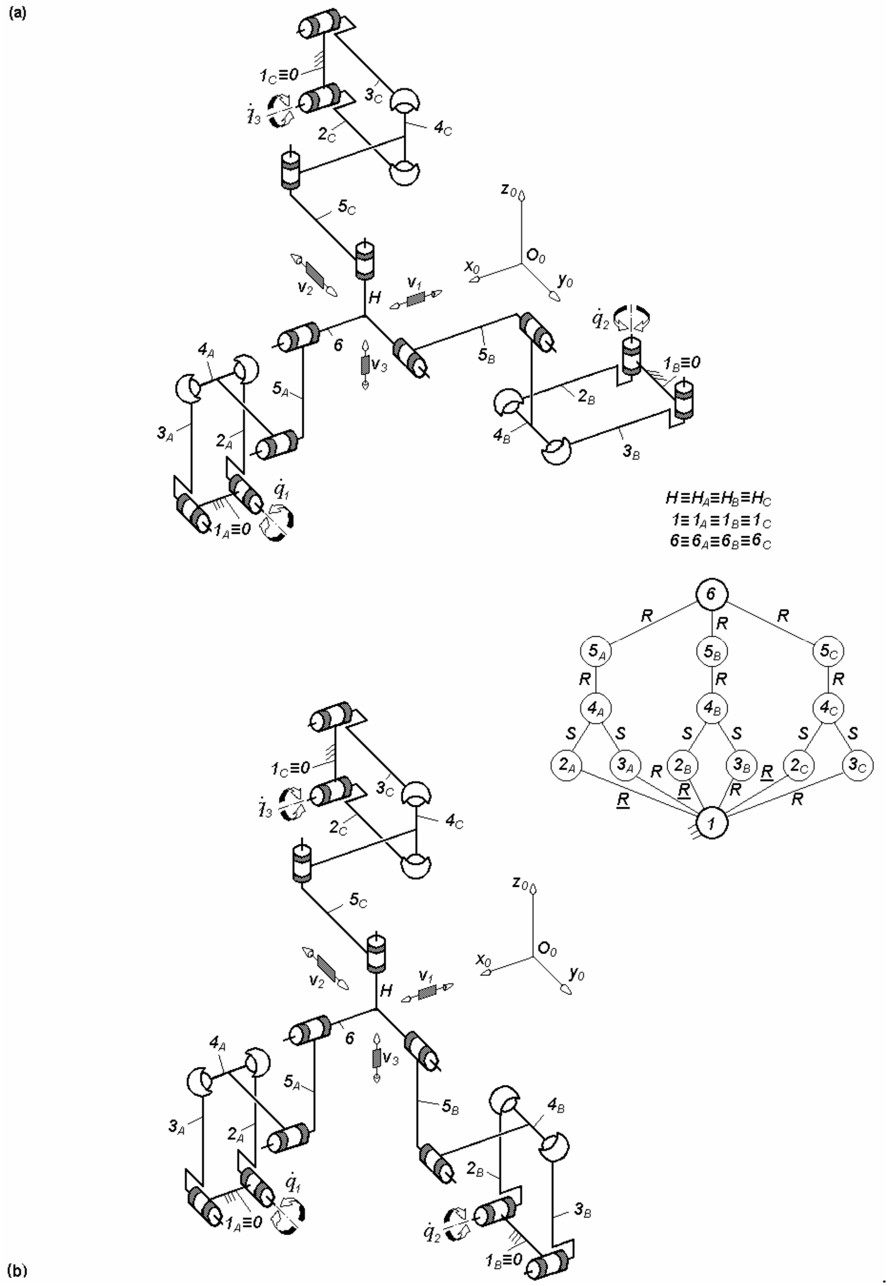


**Fig. 5.79.** *3-$\underline{Pa}^{ss}RR$*-type overconstrained TPMs with uncoupled motions defined by $M_F = S_F = 3$, $(R_F) = (\mathbf{v}_1, \mathbf{v}_2, \mathbf{v}_3)$, $T_F = 0$, $N_F = 3$, limb topology $\underline{Pa}^{ss} \perp R||R$

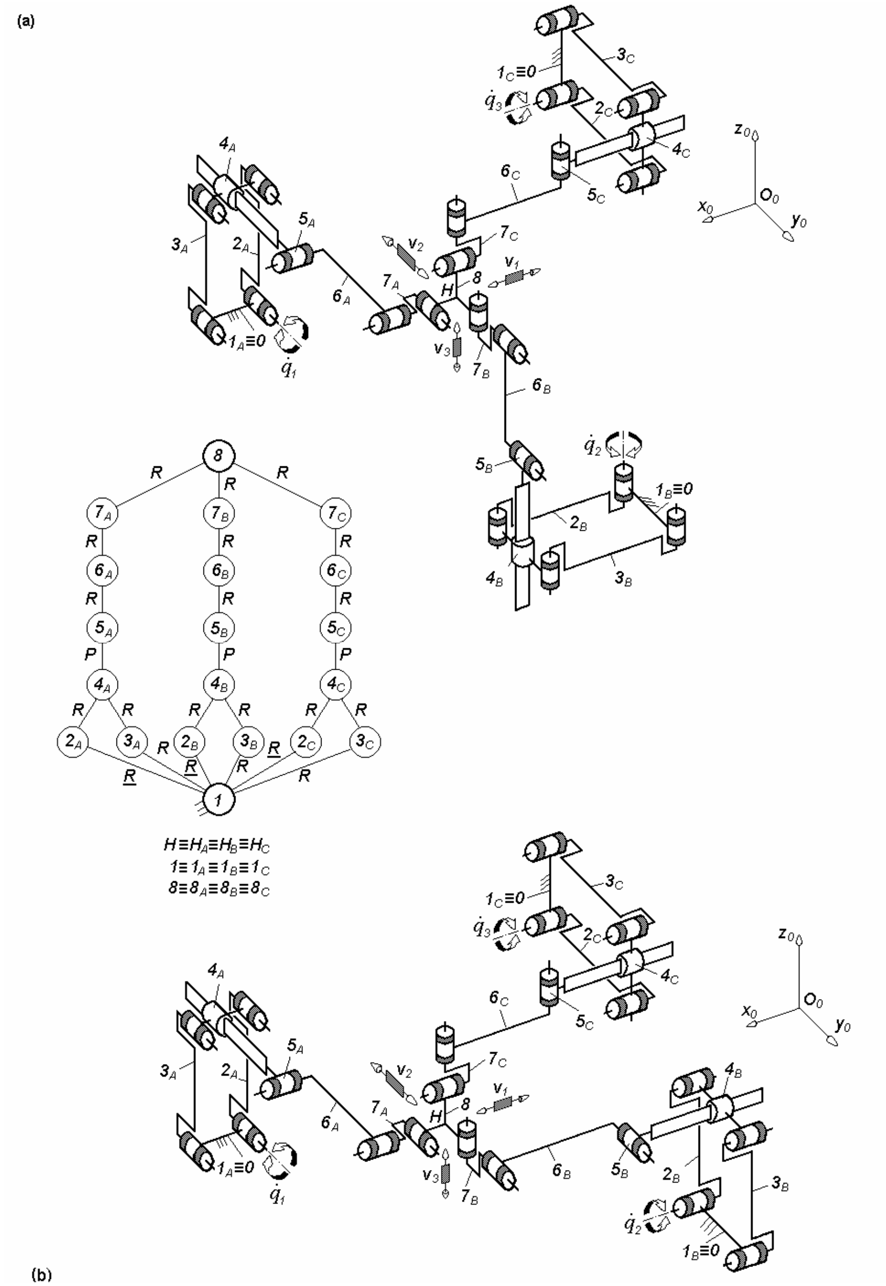


**Fig. 5.80.** *3-<u>Pa</u>PRRR**-type overconstrained TPMs with uncoupled motions defined by $M_F = S_F = 3$, $(R_F) = (\boldsymbol{v}_1, \boldsymbol{v}_2, \boldsymbol{v}_3)$, $T_F = 0$, $N_F = 9$, limb topology $\underline{Pa}||P \perp R||R \perp R^*$

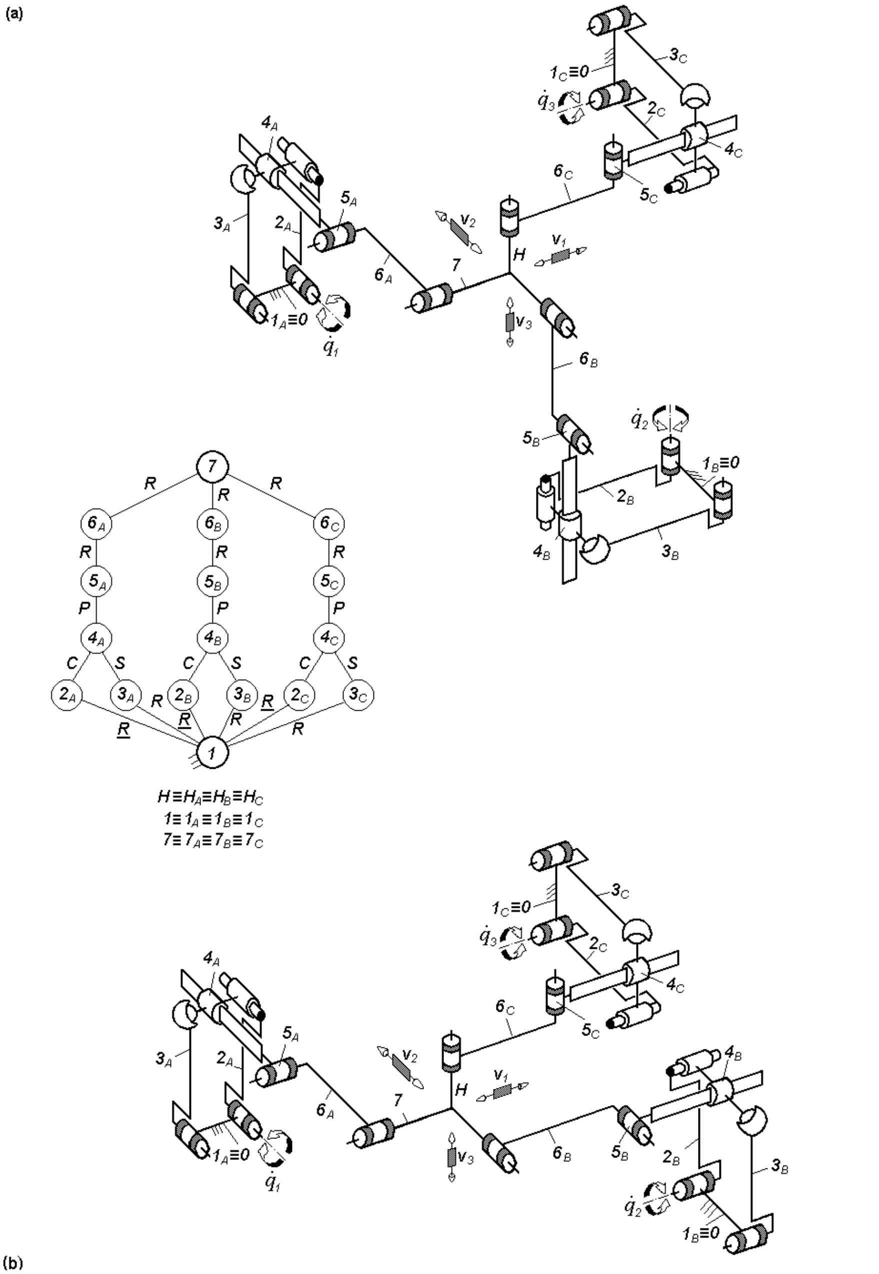


**Fig. 5.81.** *3-$\underline{Pa}^{cs}PRR$*-type overconstrained TPMs with uncoupled motions defined by $M_F = S_F = 3$, $(R_F) = (\mathbf{v}_1, \mathbf{v}_2, \mathbf{v}_3)$, $T_F = 0$, $N_F = 3$, limb topology $\underline{Pa}^{cs}||P \perp R||R$

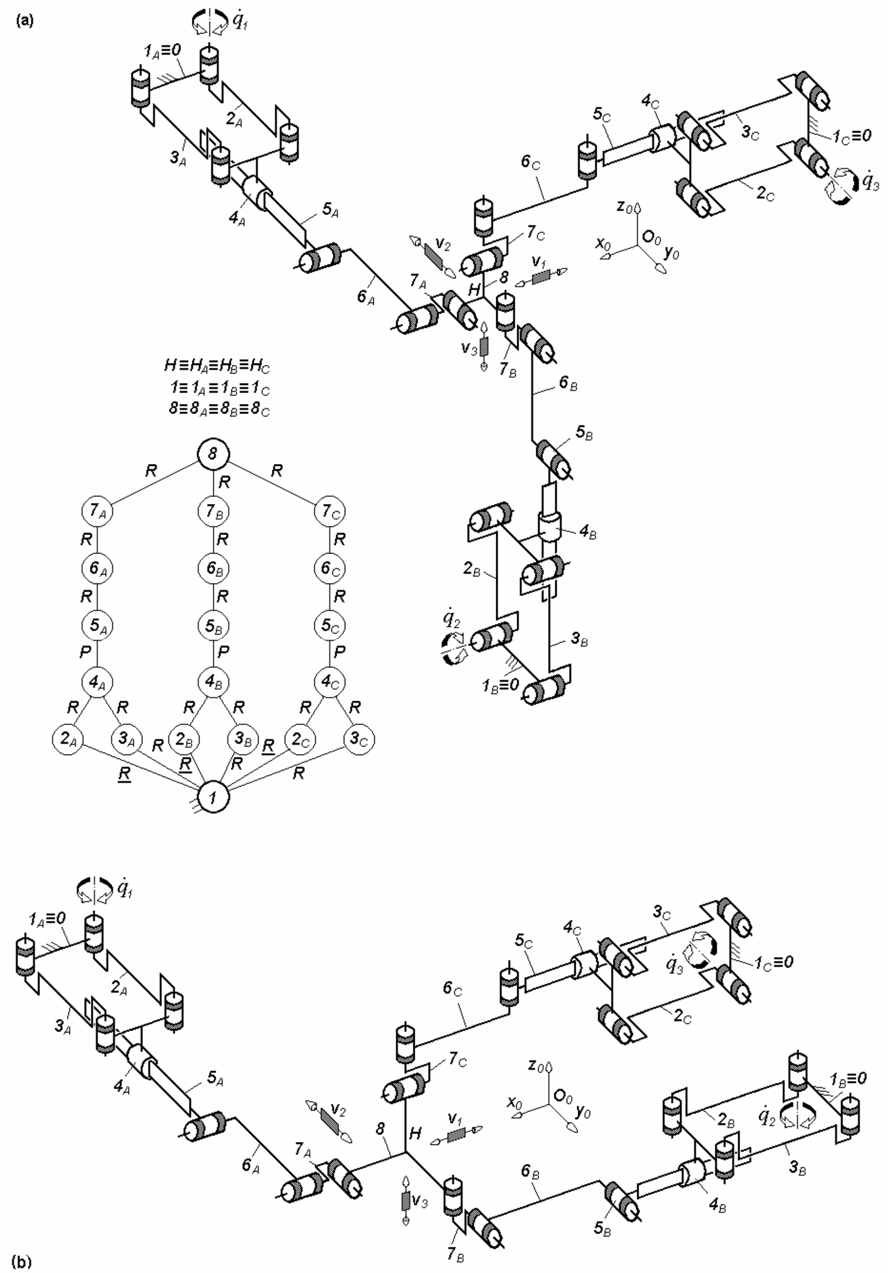


**Fig. 5.82.** *3-<u>Pa</u>PRRR**-type overconstrained TPMs with uncoupled motions defined by $M_F = S_F = 3$, $(R_F) = (\mathbf{v}_1,\mathbf{v}_2,\mathbf{v}_3)$, $T_F = 0$, $N_F = 9$, limb topology $\underline{Pa}\perp P\perp^{\perp} R||R\perp R^*$

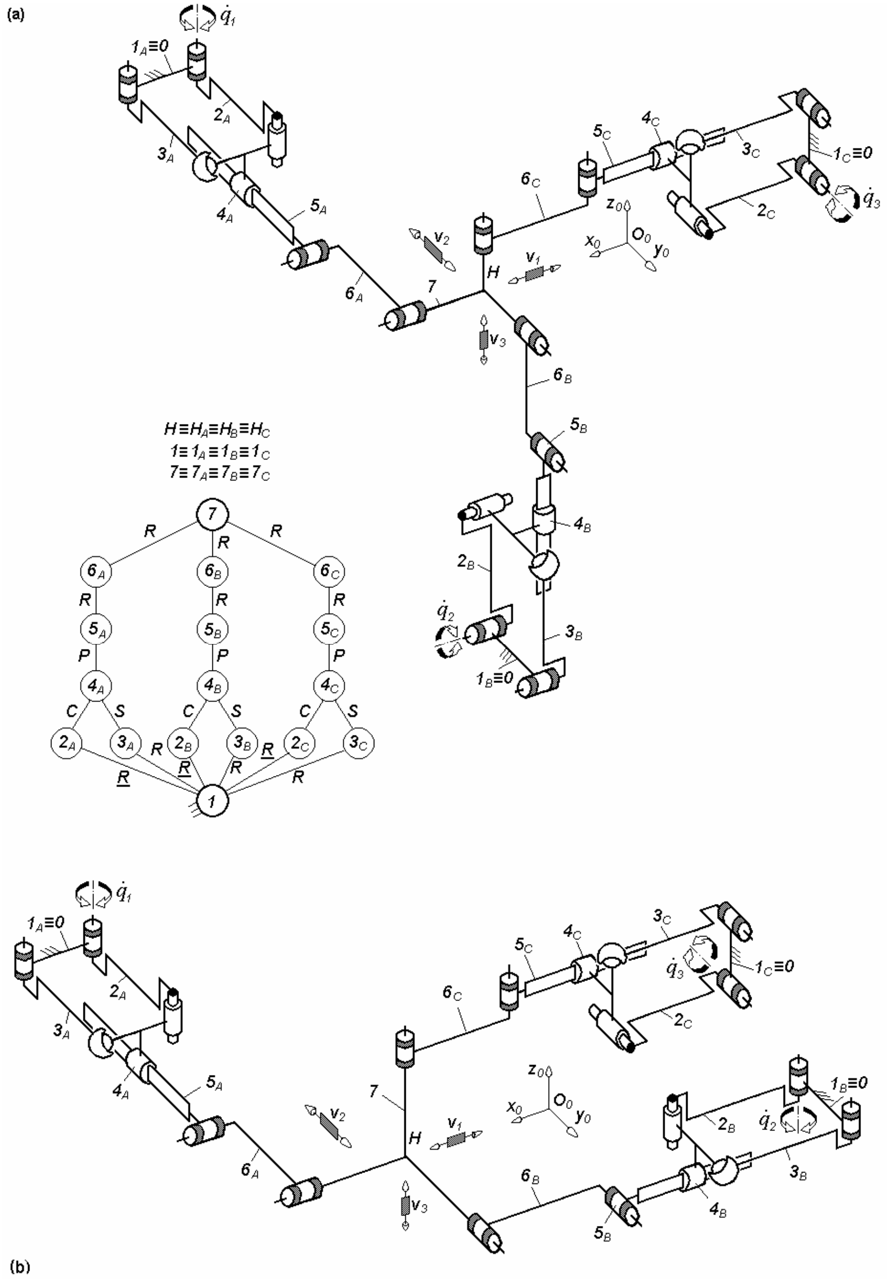


**Fig. 5.83.** *3-$\underline{Pa}^{cs}PRR$*-type overconstrained TPMs with uncoupled motions defined by $M_F = S_F = 3$, $(R_F) = (\boldsymbol{v}_1, \boldsymbol{v}_2, \boldsymbol{v}_3)$, $T_F = 0$, $N_F = 3$, limb topology $\underline{Pa}^{cs} \perp P \perp^{\perp} R||R$

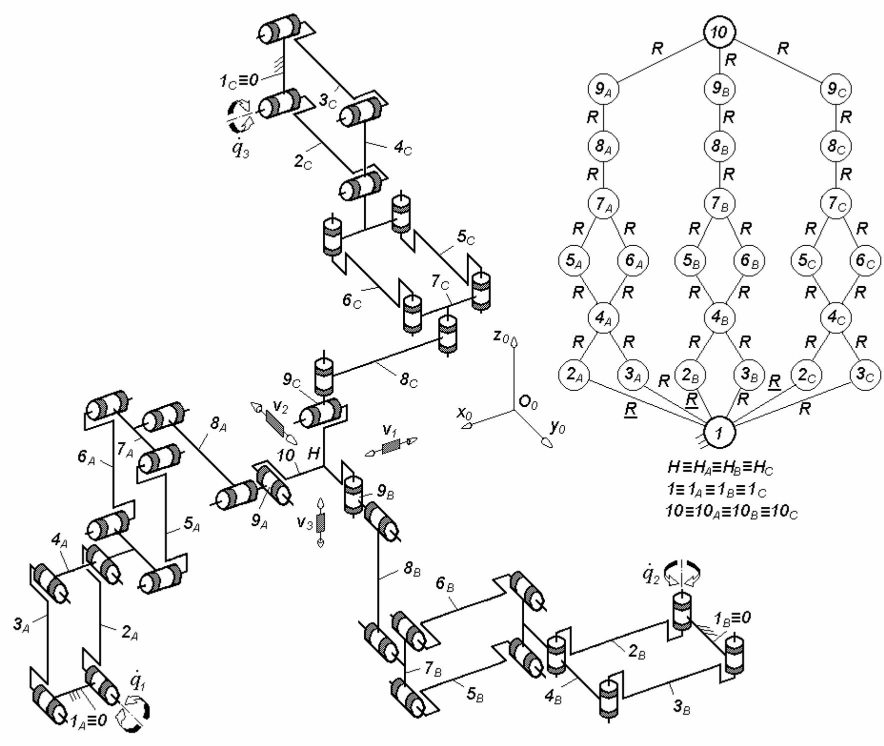

**Fig. 5.84.** *3-PaPaRRR**-type overconstrained TPMs with uncoupled motions defined by $M_F = S_F = 3$, $(R_F) = (\mathbf{v}_1, \mathbf{v}_2, \mathbf{v}_3)$, $T_F = 0$, $N_F = 18$, limb topology $\underline{Pa} \perp Pa||R||R \perp^{\perp} R^*$

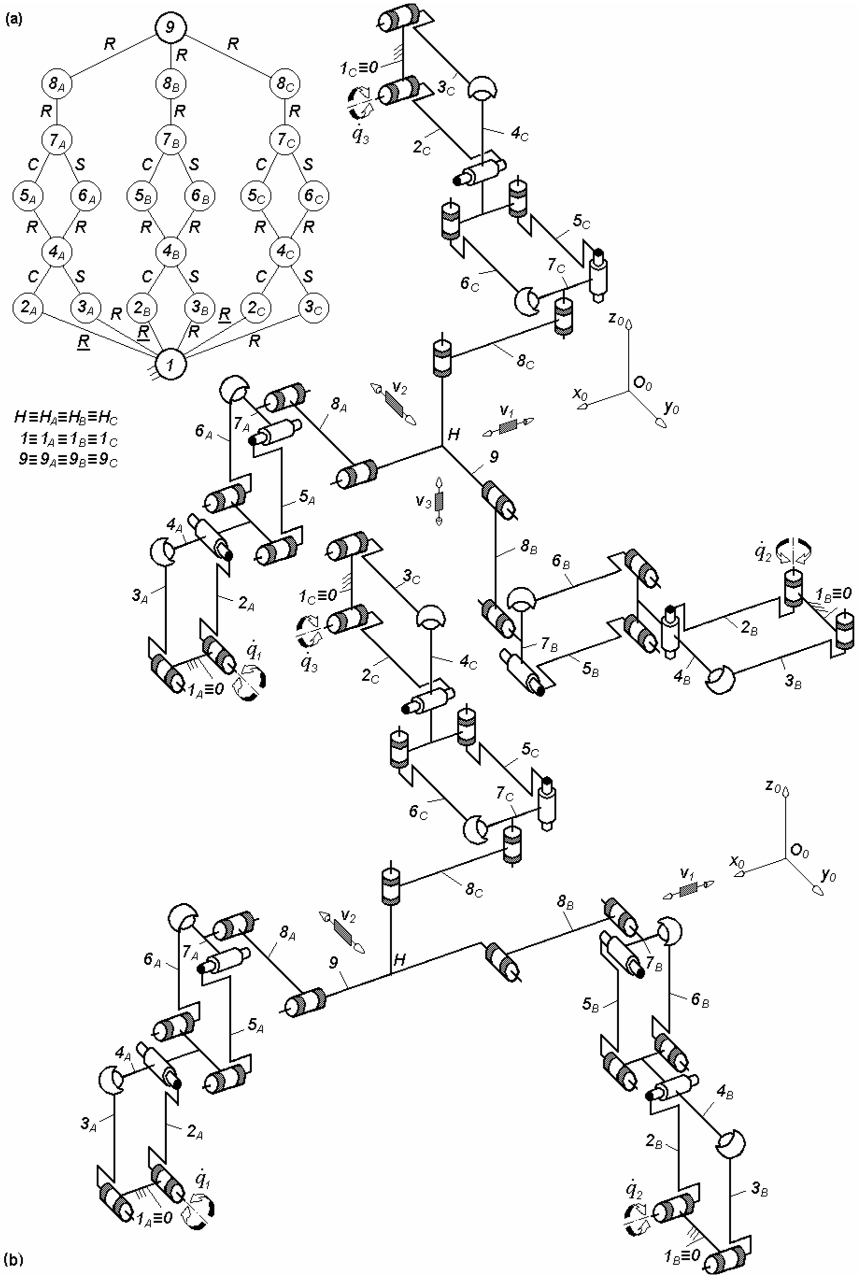


**Fig. 5.85.** *3-*$\underline{Pa}^{cs}Pa^{cs}RR$-type overconstrained TPMs with uncoupled motions defined by $M_F = S_F = 3$, $(R_F) = (\boldsymbol{v}_1, \boldsymbol{v}_2, \boldsymbol{v}_3)$, $T_F = 0$, $N_F = 3$, limb topology $\underline{Pa}^{cs} \perp Pa^{cs} || R || R$

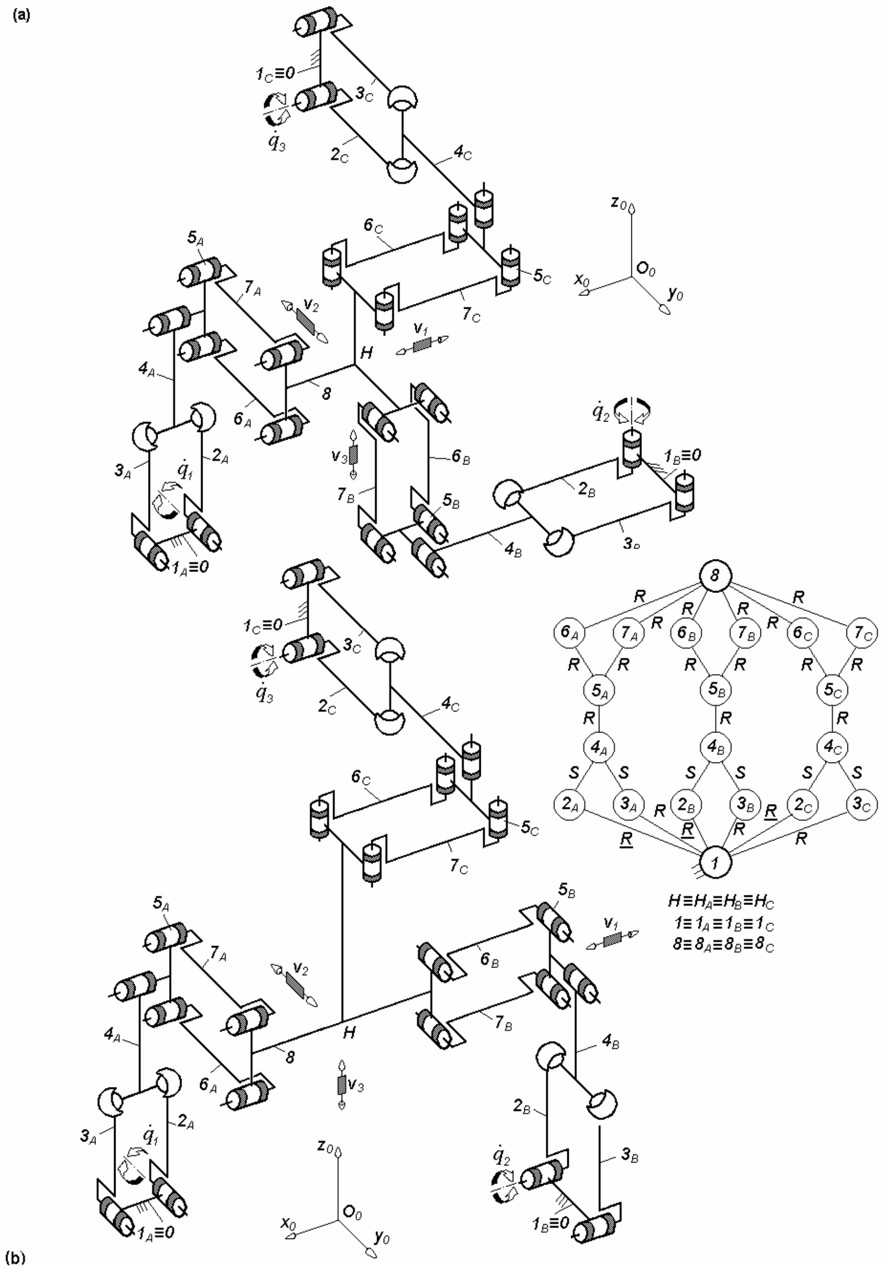


**Fig. 5.86.** *3-*$\underline{Pa}^{ss}$*RPa*-type overconstrained TPMs with uncoupled motions defined by $M_F = S_F = 3$, $(R_F) = (\boldsymbol{v}_1, \boldsymbol{v}_2, \boldsymbol{v}_3)$, $T_F = 0$, $N_F = 12$, limb topology $\underline{Pa}^{ss} \perp R||Pa$

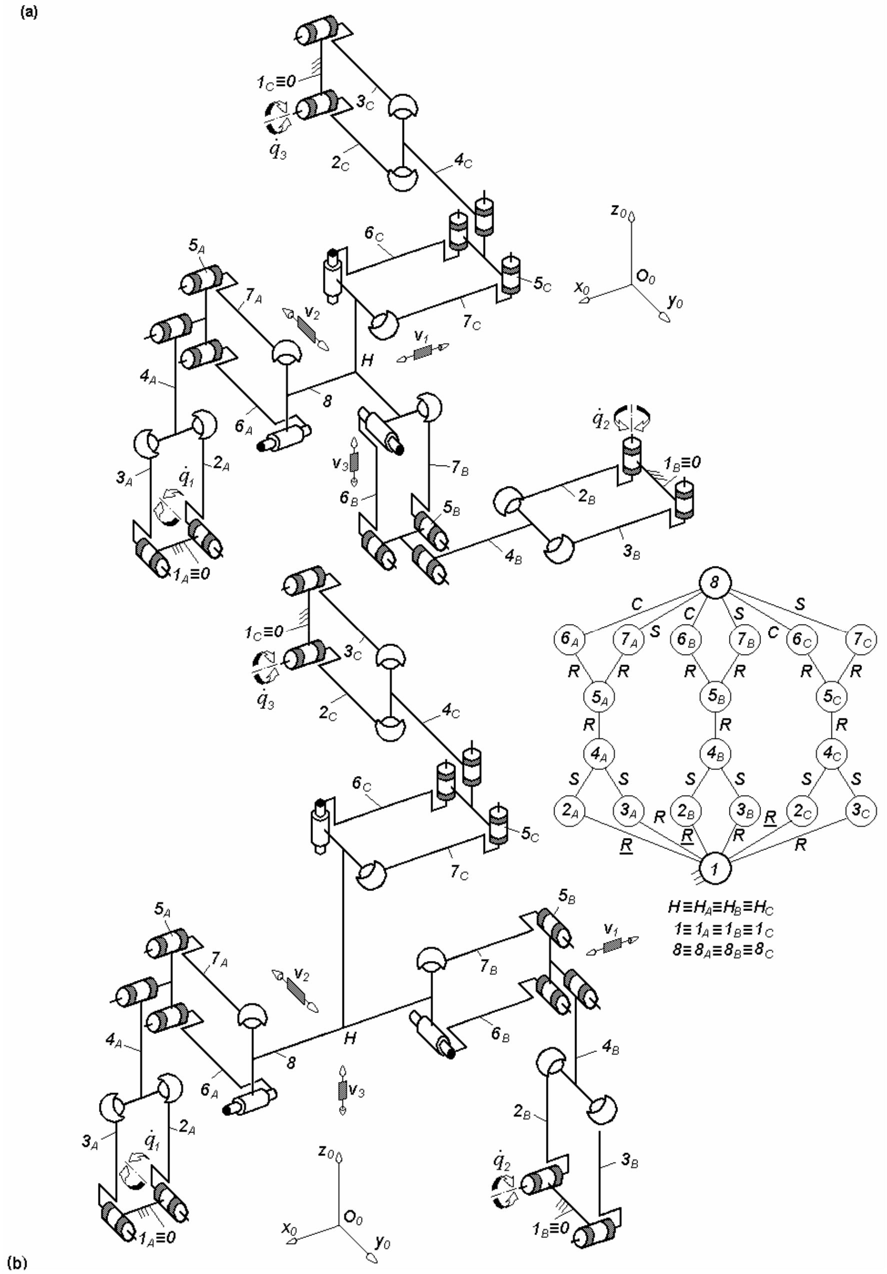


**Fig. 5.87.** *3-*$\underline{Pa}^{ss}RPa^{cs}$-type overconstrained TPMs with uncoupled motions defined by $M_F = S_F = 3$, $(R_F) = (\boldsymbol{v}_1, \boldsymbol{v}_2, \boldsymbol{v}_3)$, $T_F = 0$, $N_F = 3$, limb topology $\underline{Pa}^{ss} \perp R||Pa^{cs}$

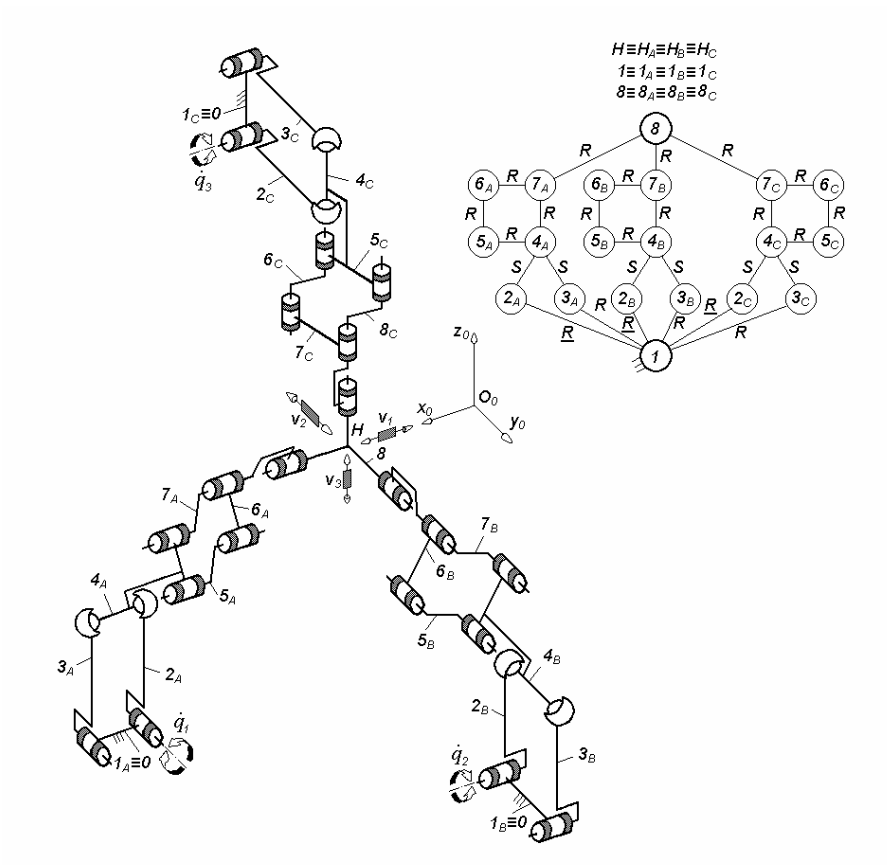

**Fig. 5.88.** *3-*$\underline{Pa}^{ss}$*RbR*-type overconstrained TPMs with uncoupled motions defined by $M_F = S_F = 3$, $(R_F) = (\mathbf{v}_1, \mathbf{v}_2, \mathbf{v}_3)$, $T_F = 0$, $N_F = 12$, limb topology $\underline{Pa}^{ss} \perp Rb||R$

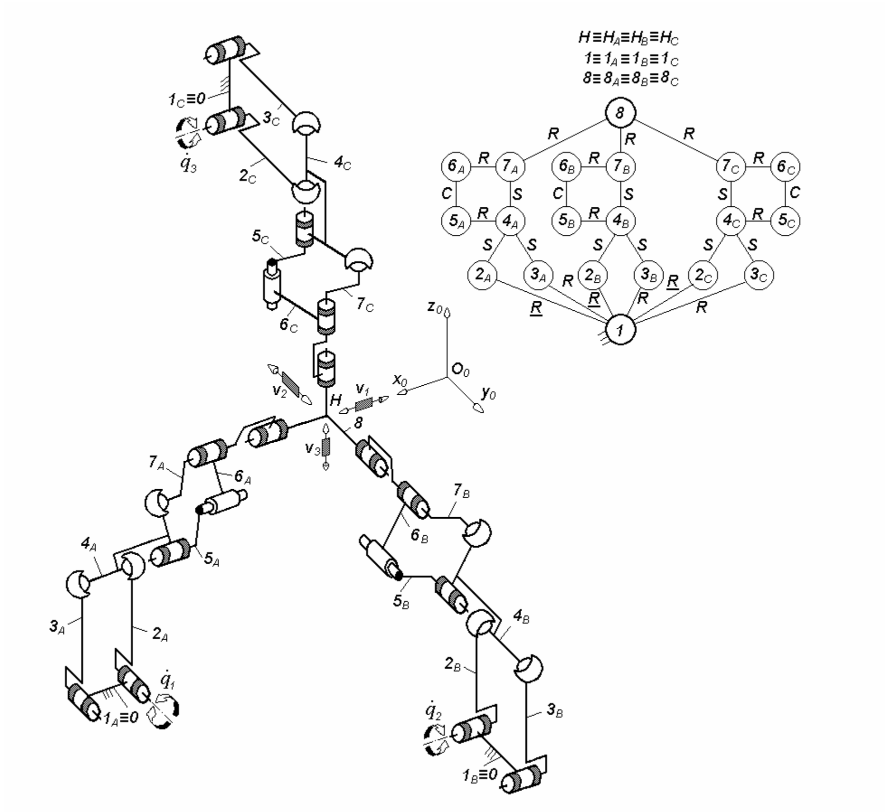

**Fig. 5.89.** $3\text{-}\underline{Pa}^{ss}Rb^{cs}R$-type overconstrained TPMs with uncoupled motions defined by $M_F = S_F = 3$, $(R_F) = (\boldsymbol{v}_1, \boldsymbol{v}_2, \boldsymbol{v}_3)$, $T_F = 0$, $N_F = 3$, limb topology $\underline{Pa}^{ss} \perp Rb^{cs}||R$

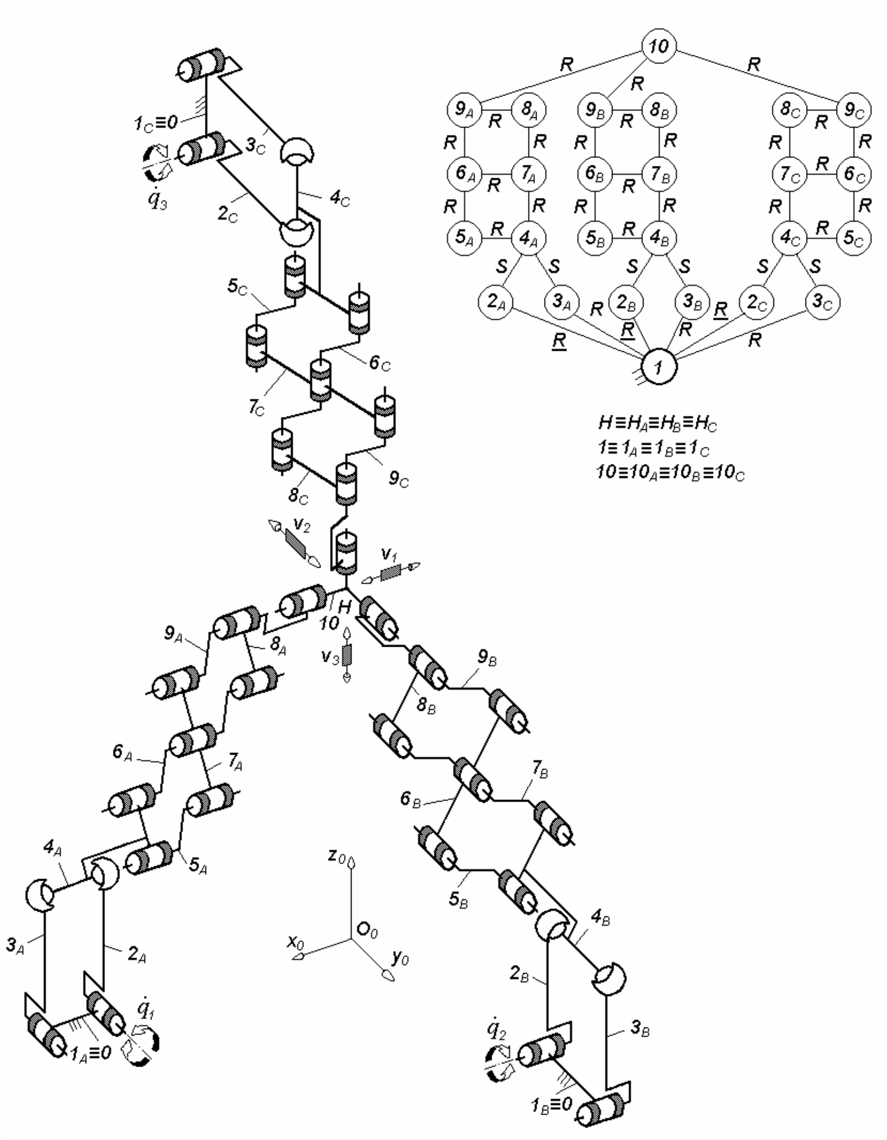


**Fig. 5.90.** *3-*$\underline{Pa}^{ss}$*RbRbR*-type overconstrained TPMs with uncoupled motions defined by $M_F = S_F = 3$, $(R_F) = (\boldsymbol{v}_1, \boldsymbol{v}_2, \boldsymbol{v}_3)$, $T_F = 0$, $N_F = 21$, limb topology $\underline{Pa}^{ss} \perp Rb||Rb||R$

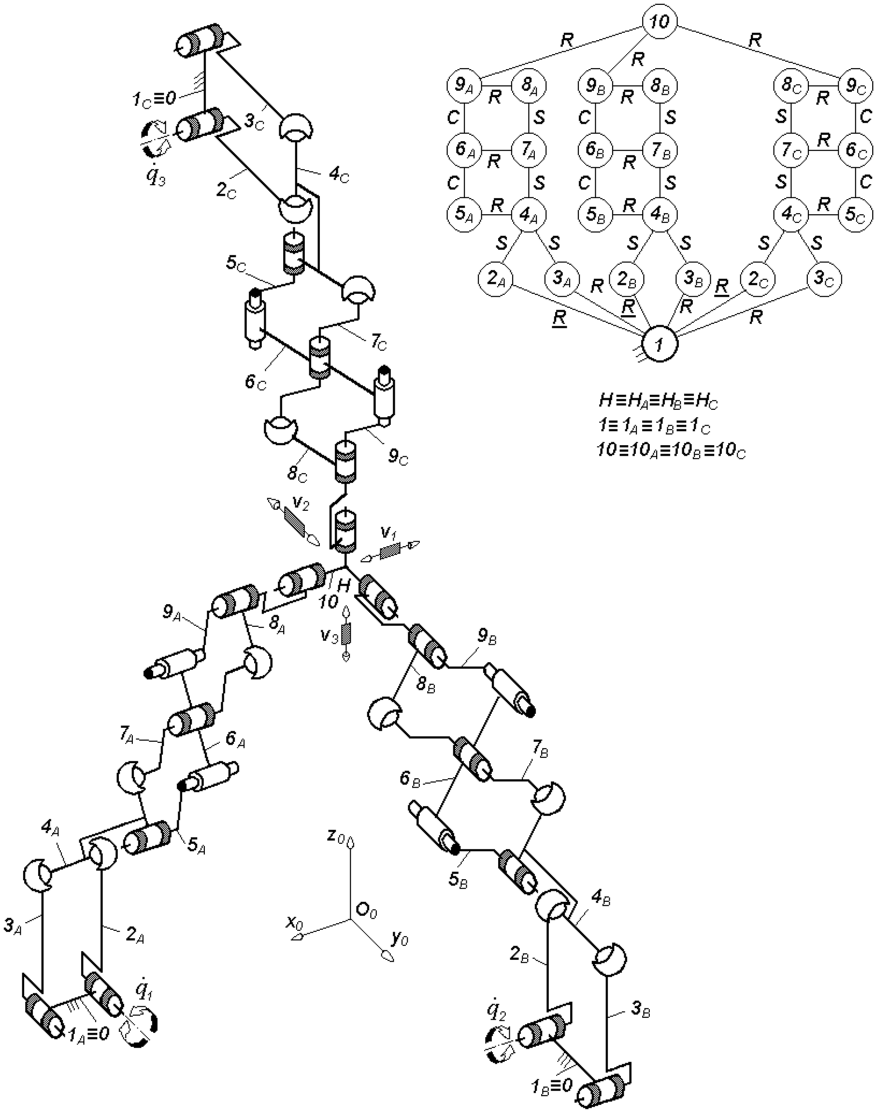


**Fig. 5.91.** $3\text{-}\underline{Pa}^{ss}Rb^{cs}Rb^{cs}R$-type overconstrained TPMs with uncoupled motions defined by $M_F = S_F = 3$, $(R_F) = (\boldsymbol{v}_1, \boldsymbol{v}_2, \boldsymbol{v}_3)$, $T_F = 0$, $N_F = 3$, limb topology $\underline{Pa}^{ss} \perp Rb^{cs}||Rb^{cs}||R$

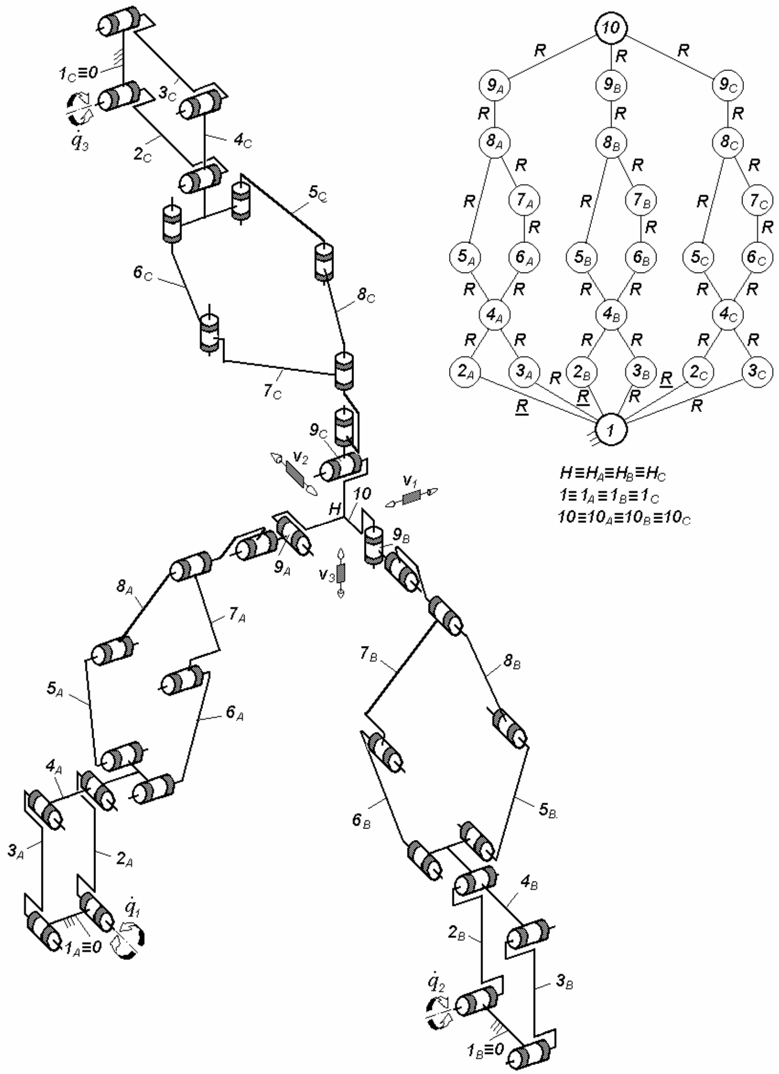

**Fig. 5.92.** *3-<u>Pa</u>Pn2RR**-type overconstrained TPMs with uncoupled motions defined by $M_F = S_F = 3$, $(R_F) = (\mathbf{v}_1, \mathbf{v}_2, \mathbf{v}_3)$, $T_F = 0$, $N_F = 18$, limb topology $\underline{Pa} \perp Pn2 || R \perp R^*$

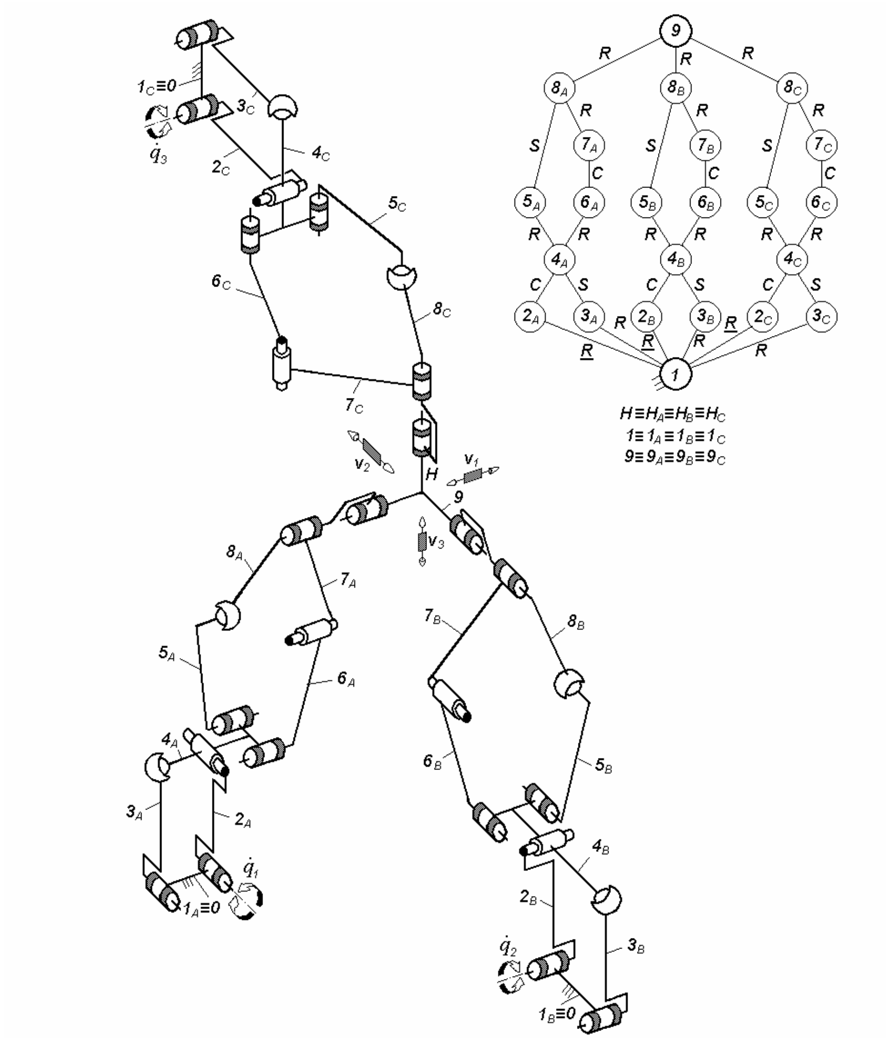


**Fig. 5.93.** *3-<u>Pa</u>$^{cs}$Pn2$^{cs}$R*-type overconstrained TPMs with uncoupled motions defined by $M_F = S_F = 3$, $(R_F) = (\boldsymbol{v}_1, \boldsymbol{v}_2, \boldsymbol{v}_3)$, $T_F = 0$, $N_F = 3$, limb topology <u>Pa</u>$^{cs} \perp Pn2^{cs}||R$

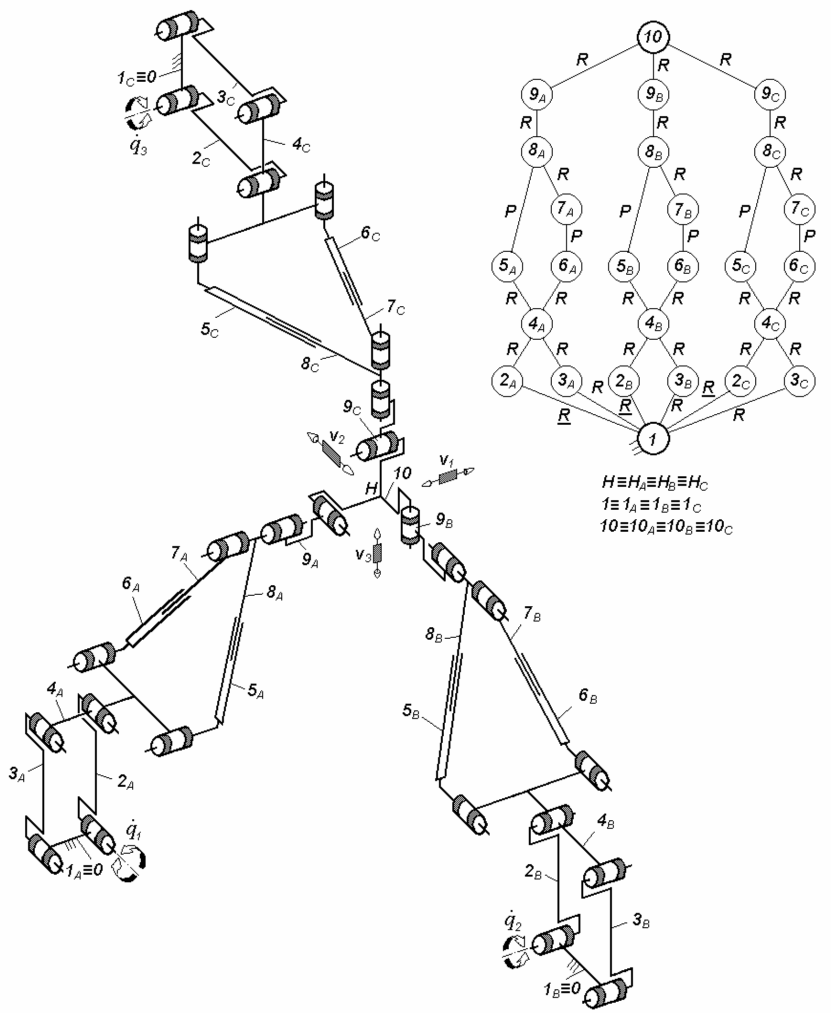


**Fig. 5.94.** *3-PaPn2RR**-type overconstrained TPMs with uncoupled motions defined by $M_F = S_F = 3$, $(R_F) = (\boldsymbol{v}_1, \boldsymbol{v}_2, \boldsymbol{v}_3)$, $T_F = 0$, $N_F = 18$, limb topology $\underline{Pa} \perp Pn2 || R \perp R*$

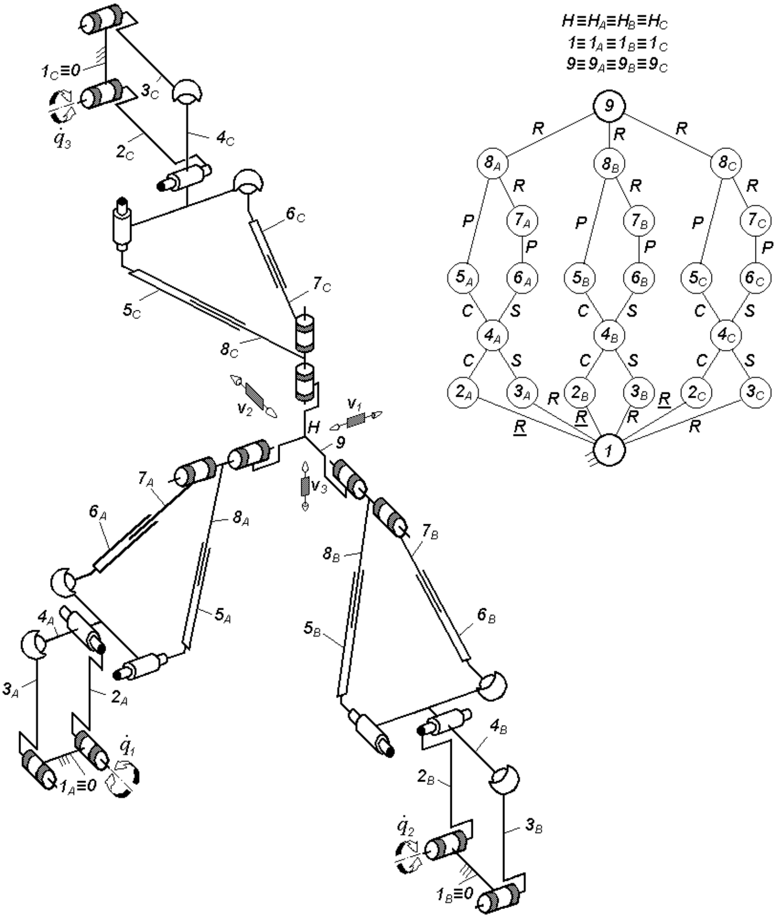


**Fig. 5.95.** $3\text{-}\underline{Pa}^{cs}Pn2^{cs}R$-type overconstrained TPMs with uncoupled motions defined by $M_F = S_F = 3$, $(R_F) = (\boldsymbol{v}_1, \boldsymbol{v}_2, \boldsymbol{v}_3)$, $T_F = 0$, $N_F = 3$, limb topology $\underline{Pa}^{cs} \perp Pn2^{cs}||R$

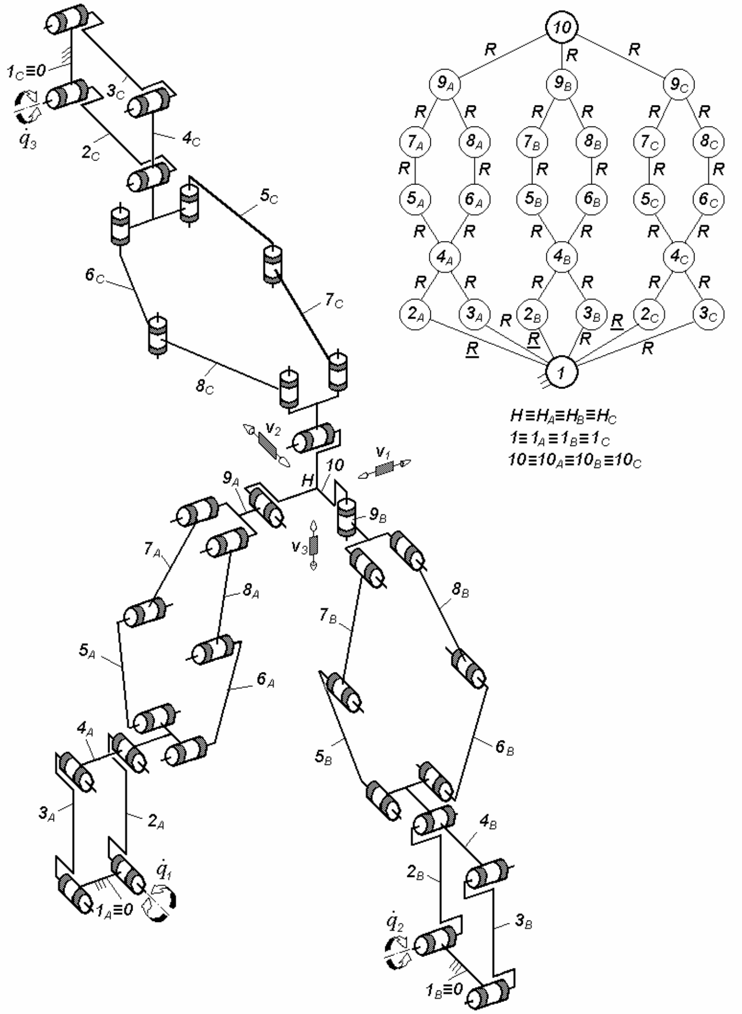


**Fig. 5.96.** *3-PaPn3R**-type overconstrained TPMs with uncoupled motions defined by $M_F = S_F = 3$, $(R_F) = (\boldsymbol{v}_1, \boldsymbol{v}_2, \boldsymbol{v}_3)$, $T_F = 0$, $N_F = 18$, limb topology $\underline{Pa} \perp Pn3 \perp R^*$

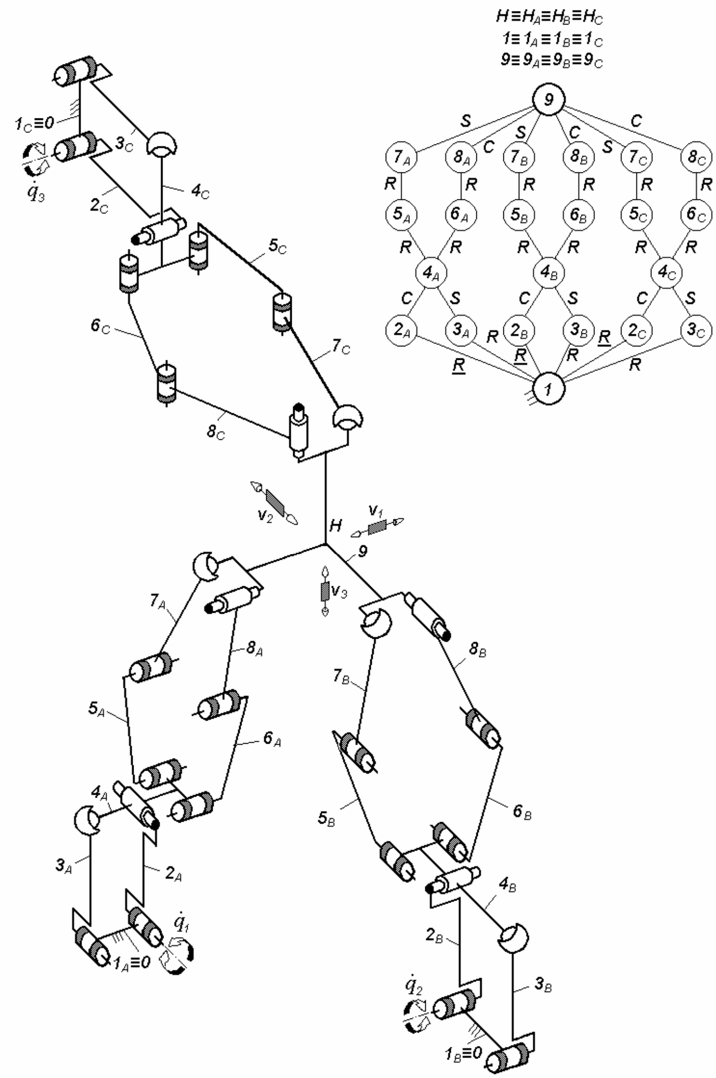


**Fig. 5.97.** $3\text{-}\underline{Pa}^{cs}Pn3^{cs}$-type overconstrained TPMs with uncoupled motions defined by $M_F = S_F = 3$, $(R_F) = (\boldsymbol{v}_1, \boldsymbol{v}_2, \boldsymbol{v}_3)$, $T_F = 0$, $N_F = 3$, limb topology $\underline{Pa}^{cs} \perp Pn3^{cs}$

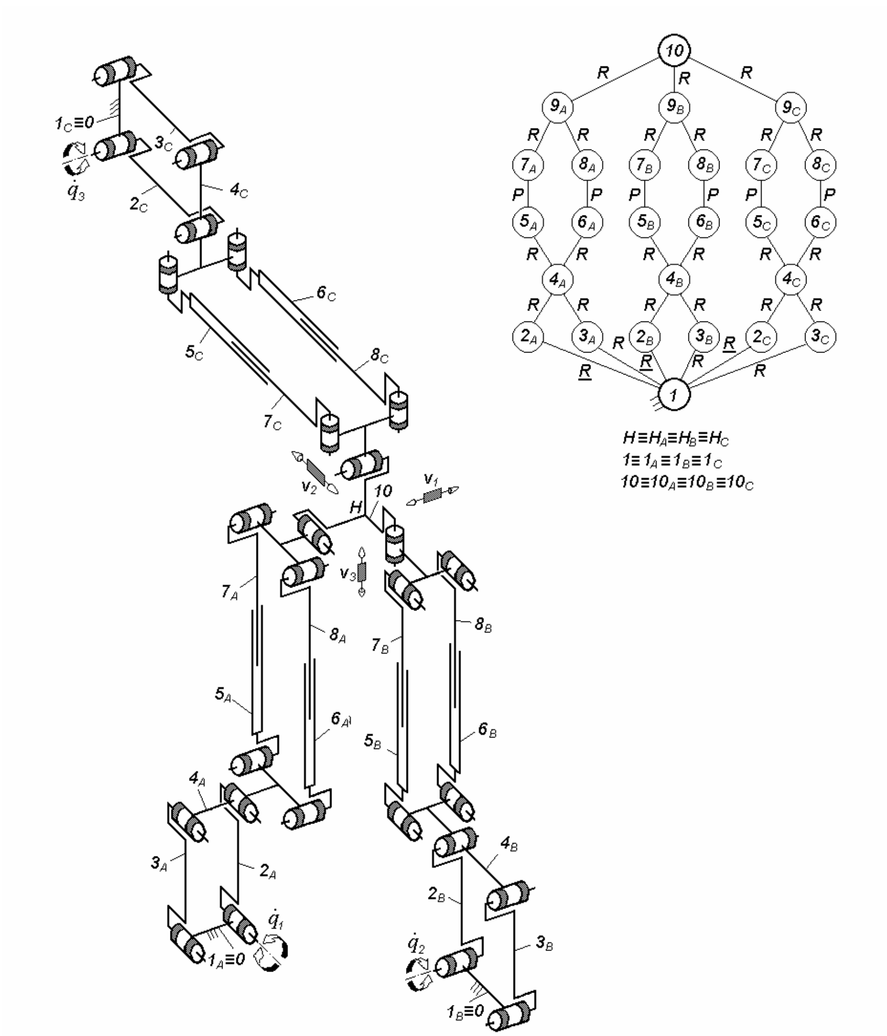


**Fig. 5.98.** *3-PaPn3R**-type overconstrained TPMs with uncoupled motions defined by $M_F = S_F = 3$, $(R_F) = (\mathbf{v}_1, \mathbf{v}_2, \mathbf{v}_3)$, $T_F = 0$, $N_F = 18$, limb topology $\underline{Pa} \perp Pn3 \perp R^*$

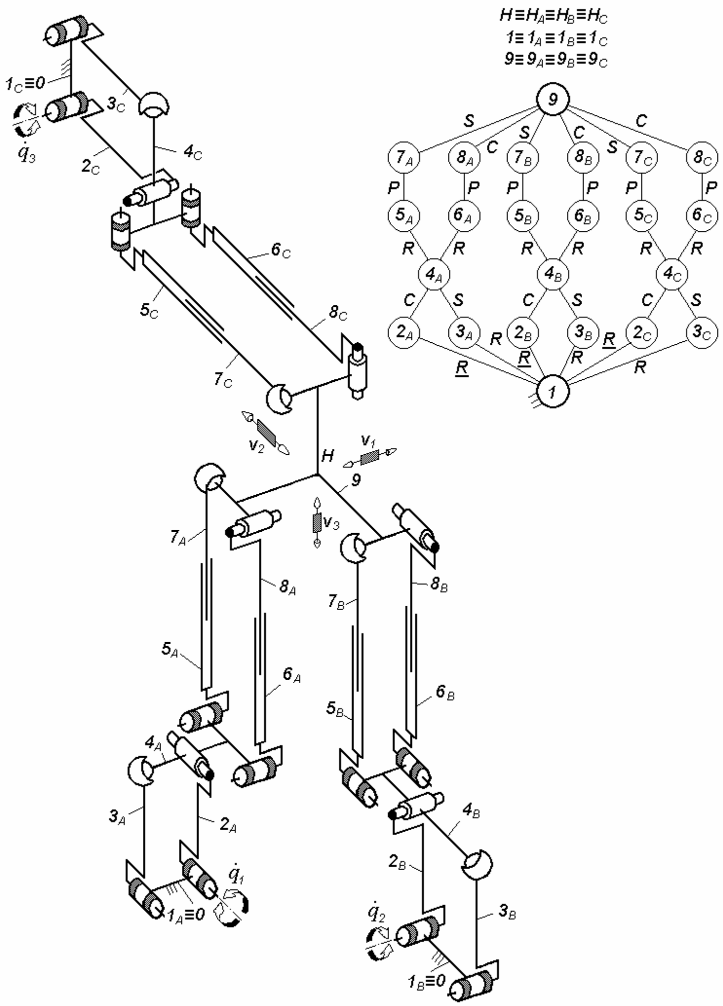


**Fig. 5.99.** *3-*<u>*Pa*</u>$^{cs}$*Pn3*$^{cs}$-type overconstrained TPMs with uncoupled motions defined by $M_F = S_F = 3$, $(R_F) = (\boldsymbol{v}_1, \boldsymbol{v}_2, \boldsymbol{v}_3)$, $T_F = 0$, $N_F = 3$, limb topology <u>*Pa*</u>$^{cs} \perp Pn3^{cs}$

(a)

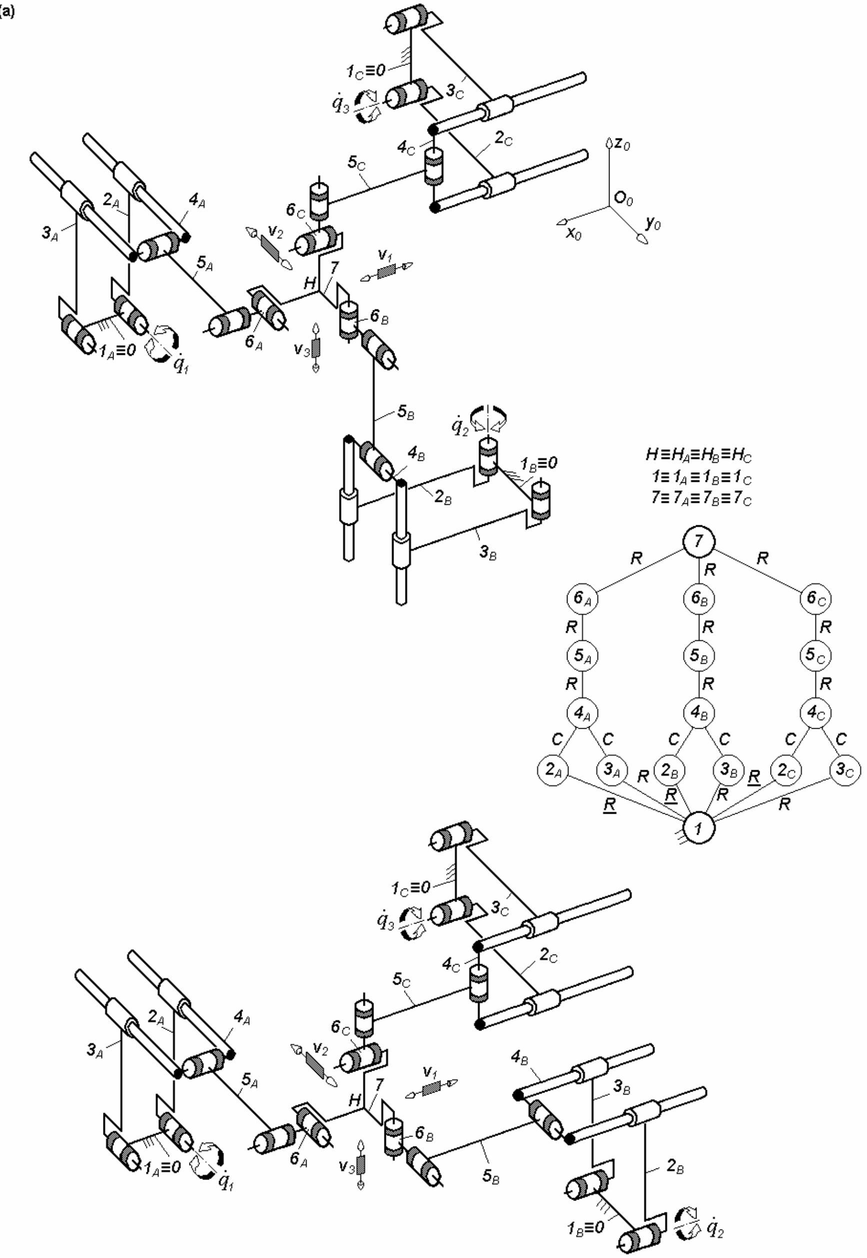


(b)

**Fig. 5.100.** *3-Pa^cc RRR**-type overconstrained TPMs with uncoupled motions defined by $M_F = S_F = 3$, $(R_F) = (\boldsymbol{v}_1, \boldsymbol{v}_2, \boldsymbol{v}_3)$, $T_F = 0$, $N_F = 6$, limb topology $\underline{Pa}^{cc} \perp R || R \perp R^*$

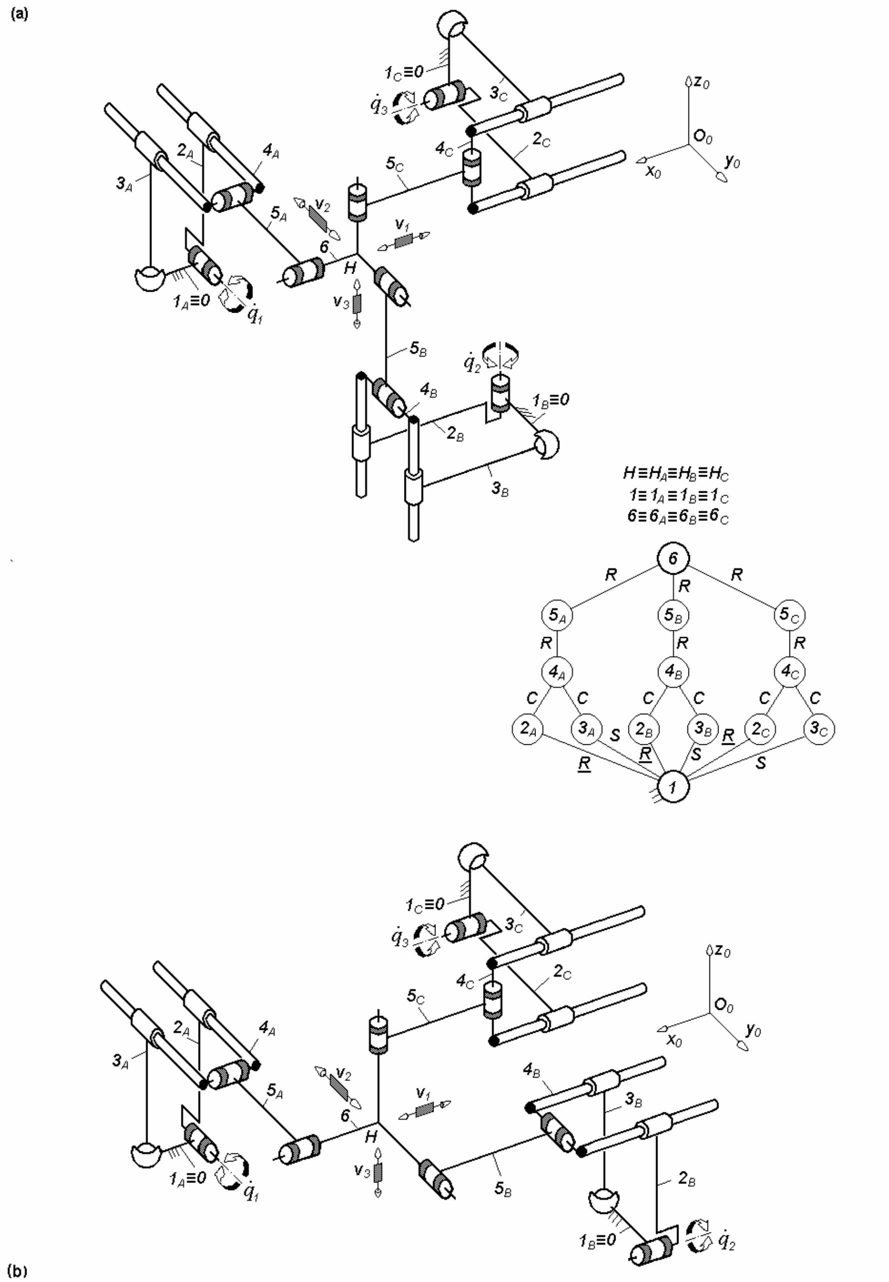


**Fig. 5.101.** *3-*$\underline{Pa}^{scc}RR$-type overconstrained TPMs with uncoupled motions defined by $M_F = S_F = 3$, $(R_F) = (\mathbf{v}_1, \mathbf{v}_2, \mathbf{v}_3)$, $T_F = 0$, $N_F = 3$, limb topology $\underline{Pa}^{scc} \perp R||R$

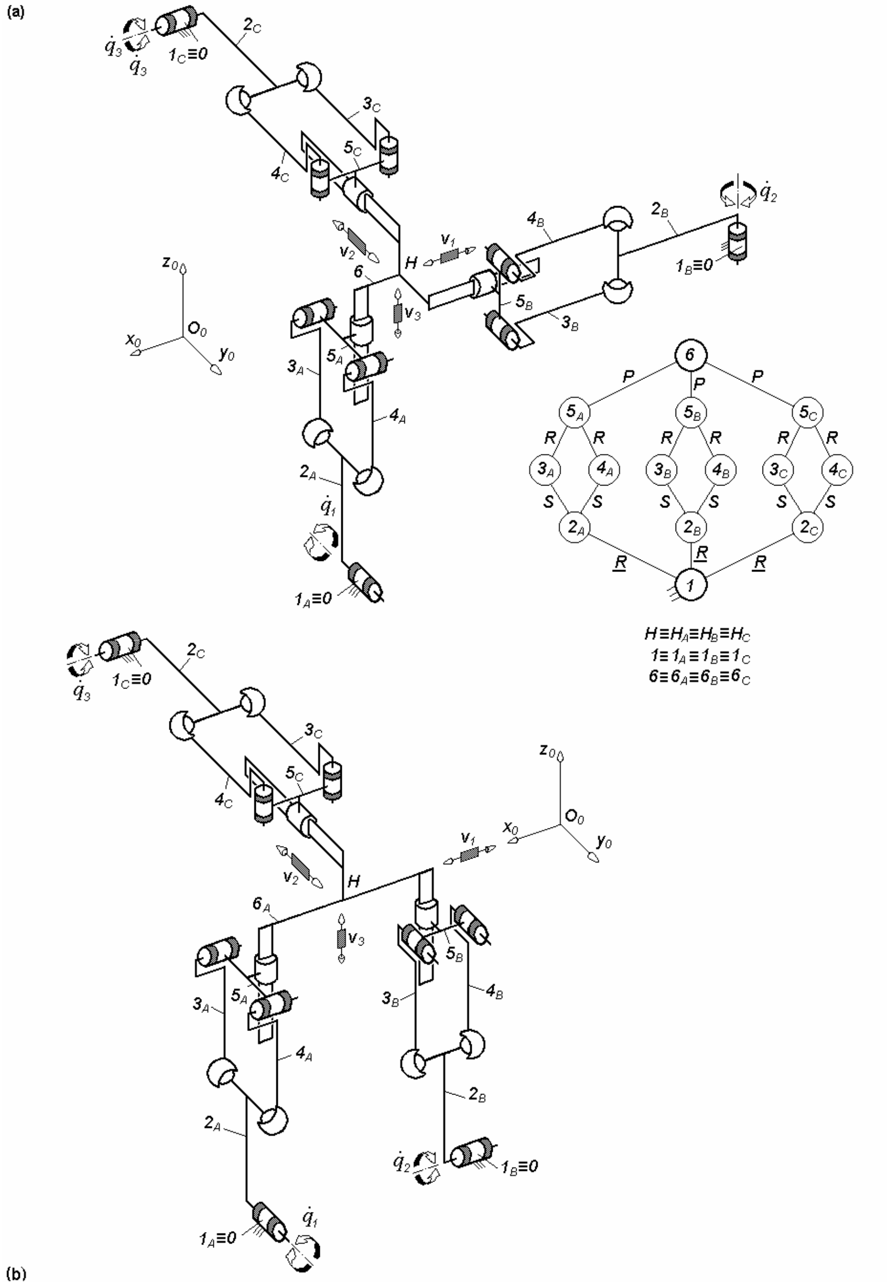


**Fig. 5.102.** *3-$\underline{R}Pa^{ss}P$*-type overconstrained TPMs with uncoupled motions defined by $M_F = S_F = 3$, $(R_F) = (\mathbf{v}_1, \mathbf{v}_2, \mathbf{v}_3)$, $T_F = 0$, $N_F = 3$, limb topology $\underline{R} \perp Pa^{ss} \perp P$

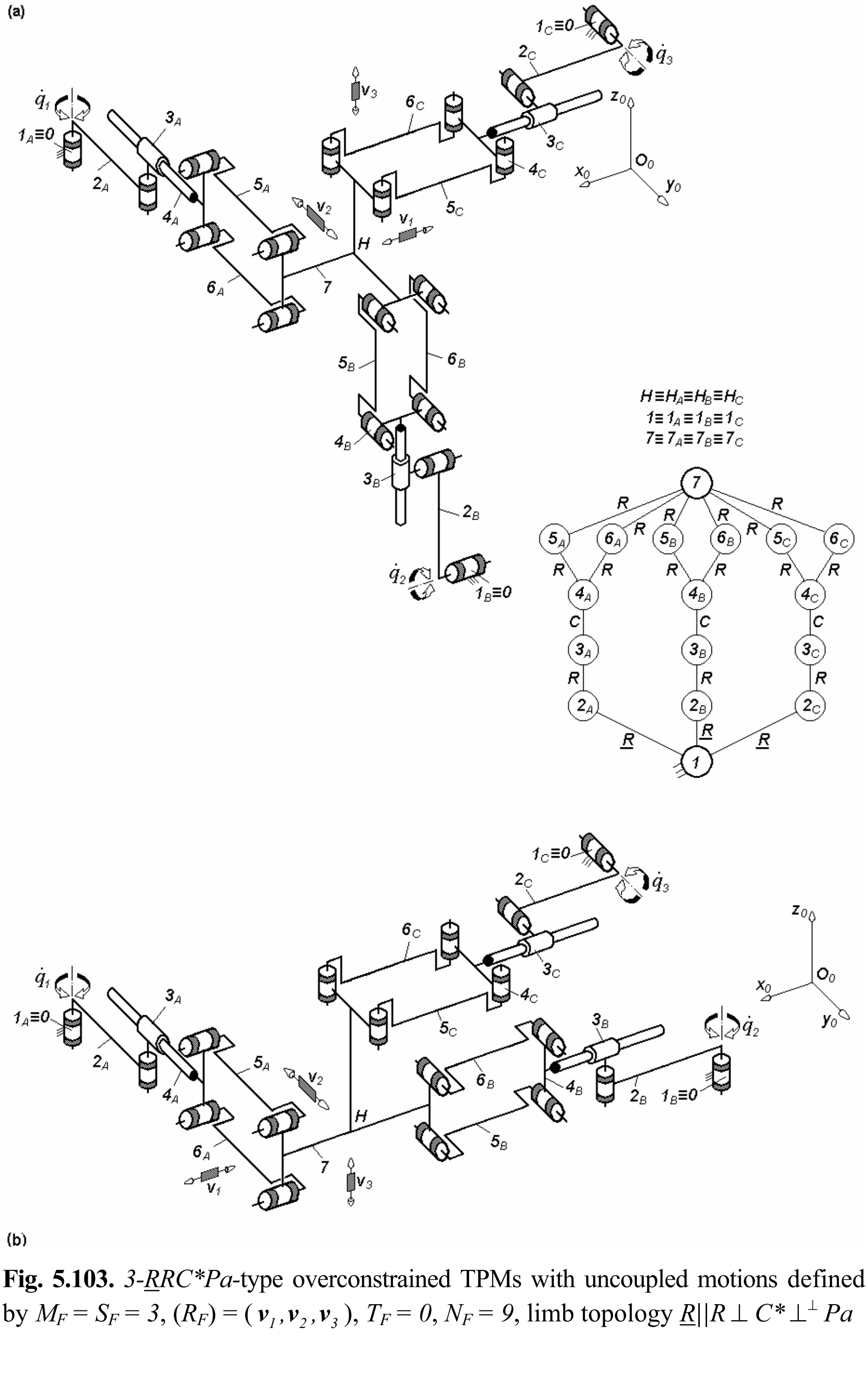


**Fig. 5.103.** *3-<u>R</u>RC*Pa*-type overconstrained TPMs with uncoupled motions defined by $M_F = S_F = 3$, $(R_F) = (\boldsymbol{v}_1, \boldsymbol{v}_2, \boldsymbol{v}_3)$, $T_F = 0$, $N_F = 9$, limb topology $\underline{R}||R \perp C^* \perp^{\perp} Pa$

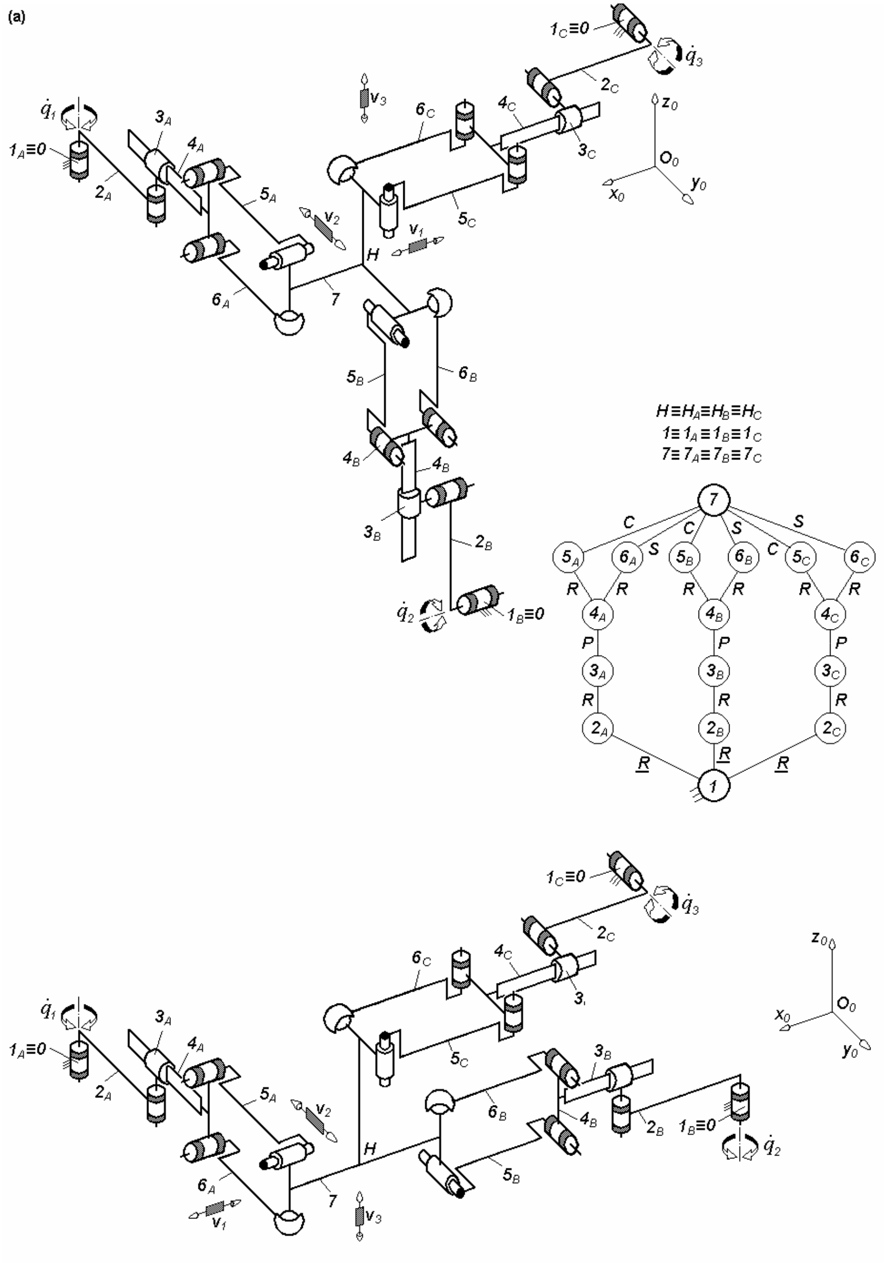


**Fig. 5.104.** *3-$\underline{R}RPPa^{cs}$*-type overconstrained TPMs with uncoupled motions defined by $M_F = S_F = 3$, $(R_F) = (\boldsymbol{v}_1, \boldsymbol{v}_2, \boldsymbol{v}_3)$, $T_F = 0$, $N_F = 3$, limb topology $\underline{R}||R \perp P \perp^{\perp} Pa^{cs}$

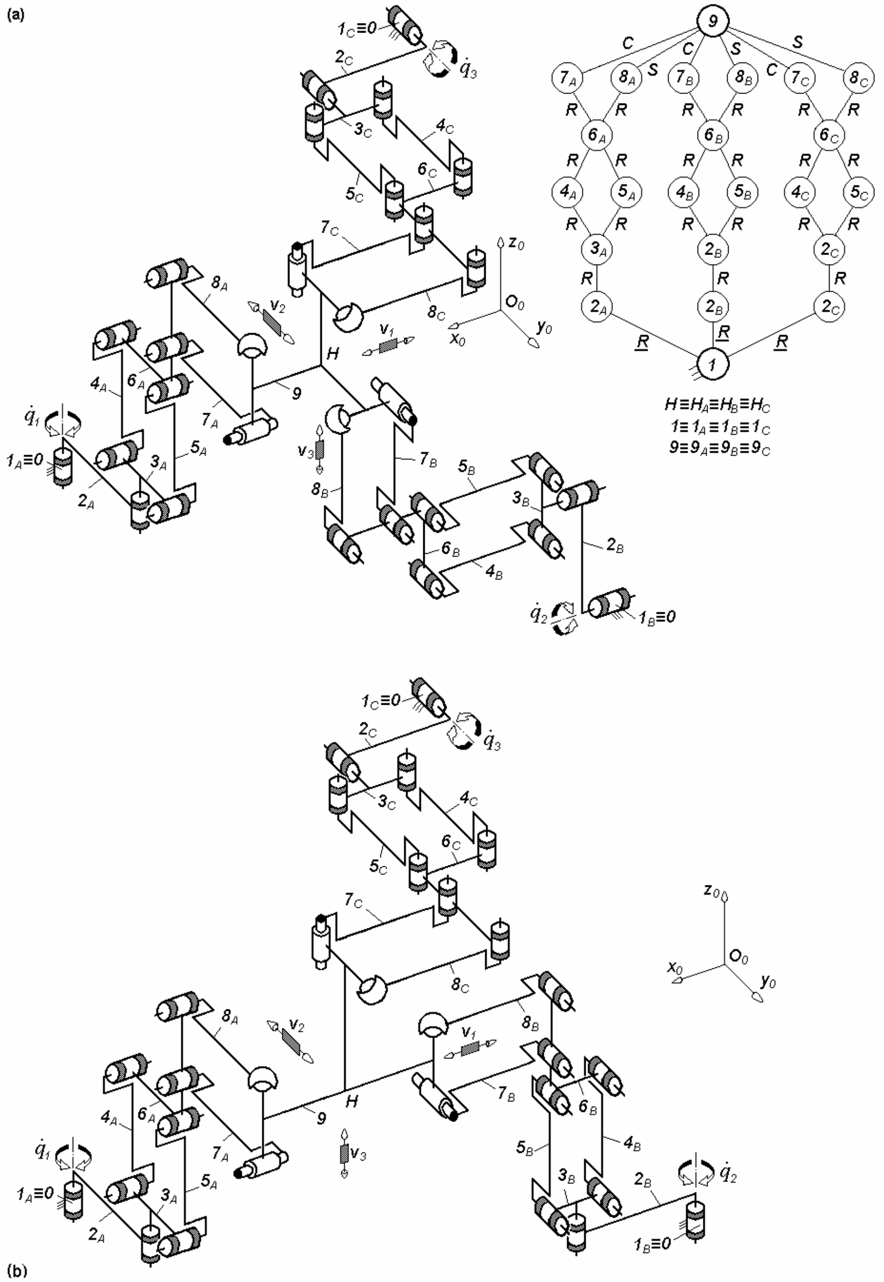


**Fig. 5.105.** *3-*$\underline{R}$*RPaPa*$^{cs}$-type overconstrained TPMs with uncoupled motions defined by $M_F = S_F = 3$, $(R_F) = (\boldsymbol{v}_1, \boldsymbol{v}_2, \boldsymbol{v}_3)$, $T_F = 0$, $N_F = 12$, limb topology $\underline{R}||R \perp Pa||Pa^{cs}$

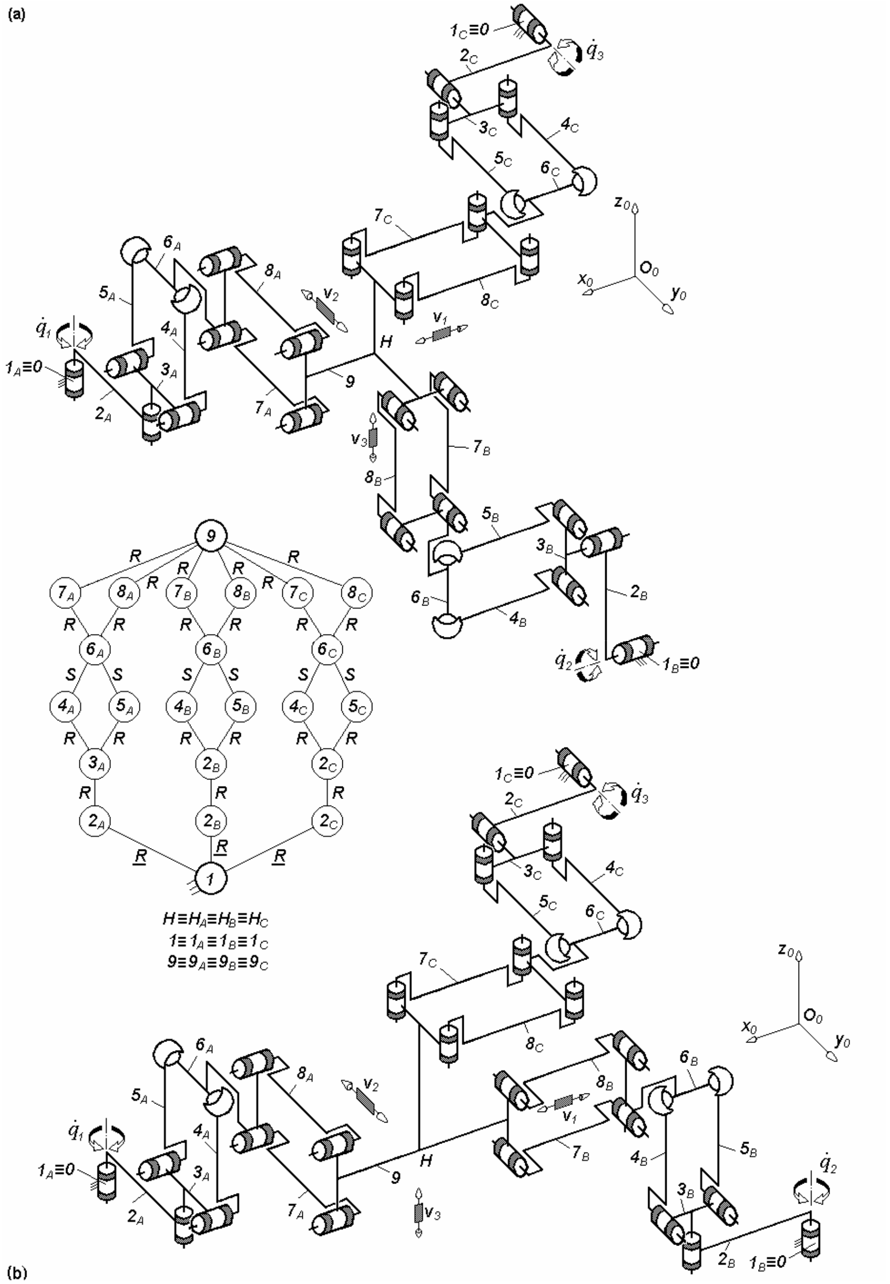


**Fig. 5.106.** *3-$\underline{R}RPa^{ss}Pa$*-type overconstrained TPMs with uncoupled motions defined by $M_F = S_F = 3$, $(R_F) = (\boldsymbol{v}_1, \boldsymbol{v}_2, \boldsymbol{v}_3)$, $T_F = 0$, $N_F = 9$, limb topology $\underline{R}||R \perp Pa^{ss}||Pa$

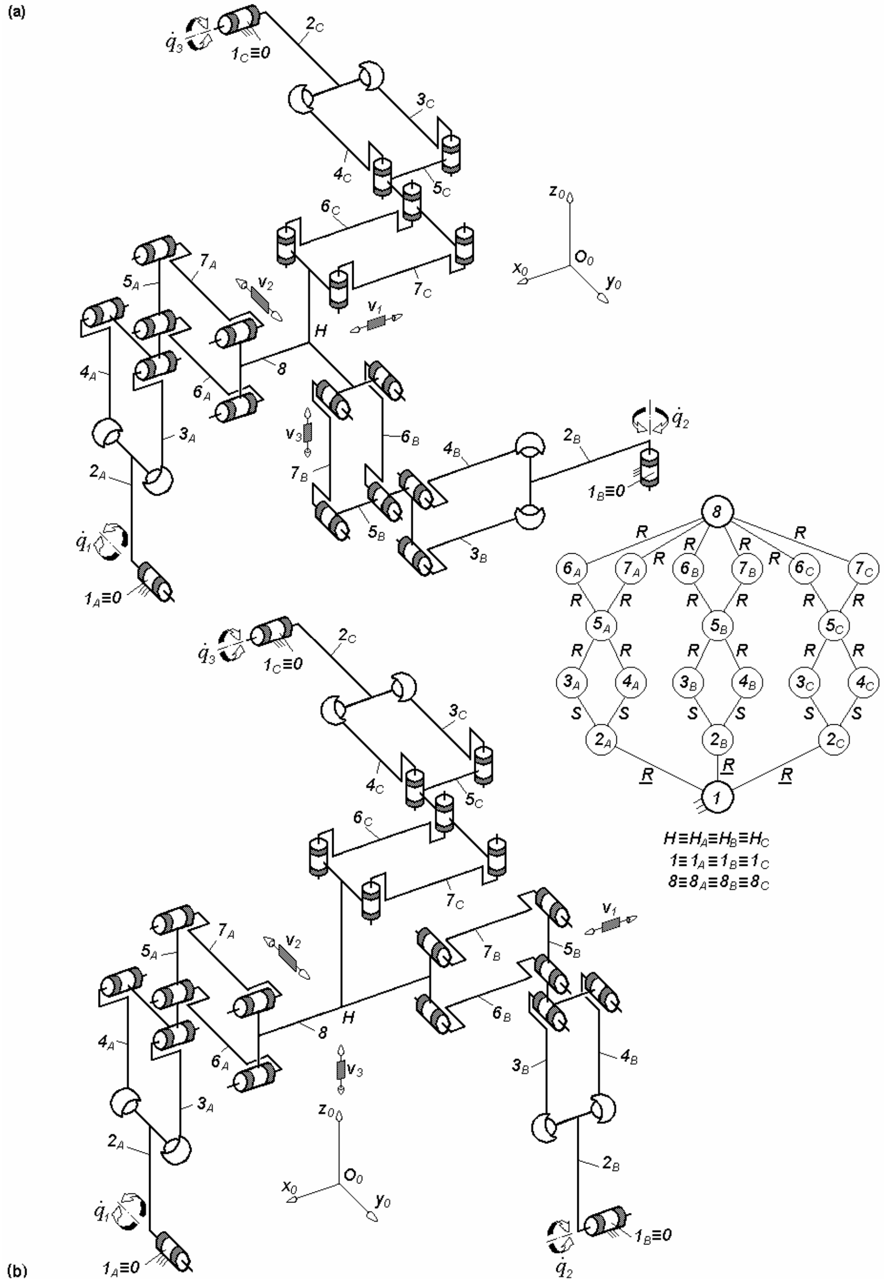


**Fig. 5.107.** *3-$\underline{R}Pa^{ss}Pa$-type* overconstrained TPMs with uncoupled motions defined by $M_F = S_F = 3$, $(R_F) = (\boldsymbol{v}_1, \boldsymbol{v}_2, \boldsymbol{v}_3)$, $T_F = 0$, $N_F = 12$, limb topology $\underline{R} \perp Pa^{ss} || Pa$

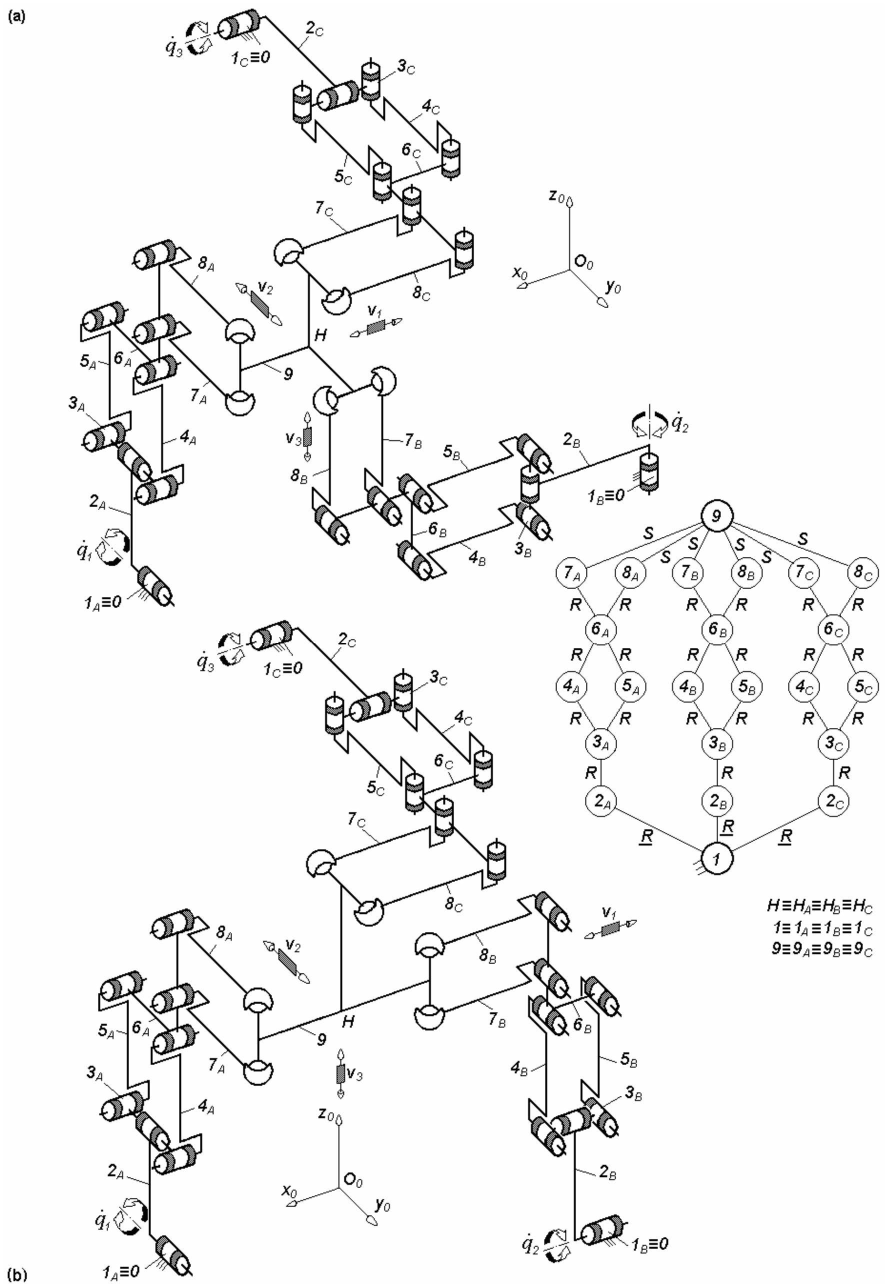

**Fig. 5.108.** *3-$\underline{R}$RPaPa$^{ss}$*-type overconstrained TPMs with uncoupled motions defined by $M_F = S_F = 3$, $(R_F) = (\boldsymbol{v}_1, \boldsymbol{v}_2, \boldsymbol{v}_3)$, $T_F = 0$, $N_F = 12$, limb topology $\underline{R}||R \perp Pa||Pa^{ss}$